Fire behaviour, spalling and residual durability of concrete made with recycled concrete aggregates

Bruno Fernandes

Université de Pau et des Pays de l'Adour
École Doctorale des Sciences Exactes et leurs Applications

Thèse présentée pour obtenir le grade de
Docteur en Génie Civil

Bruno Fernandes

Fire behaviour, spalling and residual durability of concrete made with recycled concrete aggregates

Thèse soutenue le 21 juin 2022 devant le jury composé de:

Martin CYR	Université de Toulouse	Rapporteur
João Paulo Correia RODRIGUES	Universidade de Coimbra	Rapporteur
Fabienne ROBERT	CERIB	Examinatrice
Jean-Michel TORRENTI	Université Gustave Eiffel	Examinateur
Hélène CARRÉ	UPPA	Directrice de thèse
Céline PERLOT	UPPA	Co-encadrante de thèse
Christian LA BORDERIE	UPPA	Co-encadrant de thèse
Jean-Christophe MINDEGUIA	Université de Bordeaux	Co-encadrant de thèse

Esta tese é dedicada a memória da minha avó,
Irma Maria Cardoso Alberti.

This thesis is dedicated to the memory of my grandmother,
Irma Maria Cardoso Alberti.

Acknowledgements

Doing a PhD abroad was one of the biggest challenges that I have ever faced, and I would like to acknowledge everyone who, in one way or another, helped me to reach this important step in my life.

First, I would like to thank my thesis director, Hélène Carré, not only for the opportunity, but also for her guidance, support and dedication throughout all these years. She always motivated me and helped me in all aspects of my work and life in France. I would also like to express my gratitude to all my co-advisors. Céline Perlot, for the support and guidance; Jean-Christophe Mindeguia, for the dedication and inspiration, even at a distance; and Christian La Borderie, for his spot-on guidance and expertise.

I thank the reviewers, Martin Cyr and João Paulo Correia Rodrigues, and the jury members, Jean-Michel Torrenti and Fabienne Robert. Their comments, suggestions and scientific exchanges improved the quality of my work. And speaking about my work, I would like to express my gratitude to the Région Nouvelle-Aquitaine, for funding my PhD as a part of the RECYFEU project. I would also like to thank the industrial partners of the project, Groupe Cassous (Guyenne Environnement and AQIO) and Groupe Garandeau. Last, I would like to thank Yannick Anguy and Cécile Gaborieau from the I2M laboratory, for all the support and contribution to the microstructural analysis.

This work would not be possible without the hard work of different interns during these years. I want to thank Michel Khodeir, not only for his dedication, but also for his kindness and friendship. In addition, I would like to express my gratitude to Florian Laborde, Mahamat Abdellatif, Tristan Hermet and Sibylle Gouhier. I would also like to show my appreciation for Olivier Nouailletas and Mehdi Tchaaouaou, who were always available for assistance in the lab.

Speaking about SIAME laboratory, I would like to thank all the team, colleagues and friends I have spent these years with. I want to give two special thanks. The first is to Ana Dabés, for all the kindness, support and company during these three years. The second one is to Rafik Abdallah for his brotherhood, support and all the time spent exchanging knowledge, coffee and fire-related dramas. I would also like to thank all the support of Caroline Hanin, who was always there to solve any bureaucratic problem. Besides the friends from university, France also brought me new friends (Eva, Joel, Vitor and Humberto) and "new old friends" (Carla and Igor). I want to thank all the support, trips and moments.

But speaking about friends, I would like to express my gratitude to some that, even not in person, helped me in many ways during these three years. First, Natalia Manzo and Anderson Pires, who helped me even before this journey began, with support, company and friendship. Also, I would like to thank other friends I met during my masters and, in one way or another, helped me during my journey until here (Sarah, Gustavo, Ricardo and Isabela). And for sure, I could not forget to thank Luiz Vieira, who, even if he never was my advisor, gave me guidance and support that were crucial to my life and career. Finally, this PhD would not be possible without the support from the Vaz family (Ednéia, Juliana and Mateus).

I also want to express my gratitude to other family and friends from Brazil who gave me the strength and courage to be here. My grandpa, Cris, Beto, Vera, Ivone, Clarice, Quellen, Ilse, Lourenço, Vicente, Jerusa, Delio, Fernanda, Augusto and many others. A special thanks to my father, Walmor Luiz Fernandes, for the support, guidance and motivation. And finally, to my mother, Neuza Alberti, for all the love, kindness and support throughout my life. Thank you for everything you did for me!

Lastly, I thank everyone who fights for free and quality education. I was extremely privileged during my journey, and this PhD could not be possible without the support of the public school, governmental scholarships and free education. A praise for everyone who fights for social justice and reducing inequalities.

Muito Obrigado!
Merci Beaucoup!
Thank You!

Abstract

In the last decades, the use of recycled concrete aggregates (RCA) has proven to be a possible solution for making concrete with less environmental impact. This concrete has shown similar properties to conventional concrete and can reach an adequate performance. However, its broader application depends on a better understanding of its fire behaviour, a critical factor for structures. Concrete made with RCA presents specific properties that may lead to a particular behaviour (higher porosity, water content and different interfaces). Within this context, the present work had the aim to do a comprehensive evaluation of the fire and high temperature behaviour of concrete made with RCA. First, different concrete mixes made with RCA have been designed. These mixes had different replacement rates (from 0 % to 100 %) and different replacement methods (direct replacement and strength-based replacement). The latter was designed to achieve the same performance (compressive strength and slump) as concrete made with natural aggregates (NA). Then, a comprehensive experimental campaign on elevated temperature behaviour was done. The first campaign was on the residual thermomechanical properties. The concrete mixes were heated and, after cooling, subjected to mechanical, thermal and microstructural evaluations. The second campaign was on fire spalling behaviour. In this, concrete prisms were exposed to the standard fire curve (ISO 834-1) and uniaxial loading. An additional spalling campaign was also made to evaluate the effect of water content profiles on the spalling risk. Finally, post-heating durability after heating and cooling was evaluated in the light of performance-based approaches. Results show that RCA affects concrete's thermal and mechanical properties after high temperatures, but the reduction was similar to what was observed in concrete made with NA. An even closer behaviour was observed if concrete made with RCA was optimised. From the fire tests, it was seen that concrete made with RCA exhibited a higher spalling degree than concrete made with NA, and this is associated with the physical properties of concrete, particularly water content. The results from the complementary campaign confirmed that spalling was strongly sensitive to the water content and the drying profile. The drying of the concrete samples reduced the risk of spalling in all studied mixes. Lastly, exposure to high temperatures resulted in a decrease in all durability parameters for all studied concretes. The addition of RCA reduced the performance, but, as in the case of residual thermomechanical properties, this decrease can be reduced with a proper mix optimisation. This study provided an overview of the behaviour of concrete made with RCA after exposure to elevated temperatures. The results herein presented may serve as a reference for different aspects of the fire behaviour of concrete structures made with RCA.

Keywords: Recycled concrete aggregates, high temperature, mechanical properties, thermal properties, durability, transfer properties, spalling, water content

Résumé

Au cours des dernières décennies, l'utilisation de granulats de béton recyclés (GRB) s'est avérée être une bien adapte pour fabriquer du béton avec un moindre impact environnemental. Ces bétons présentent des propriétés similaires à celles des bétons conventionnels et peuvent atteindre de bonnes performances. Cependant, son utilisation plus courante nécessite une meilleure compréhension de son comportement au feu, un paramètre critique pour les structures. Le béton à base de GRB présente des propriétés spécifiques qui peuvent conduire à un comportement différent (porosité plus élevée, teneur en eau et interfaces différentes). Dans ce contexte, l'étude présentée avait pour objectif d'effectuer une évaluation complète du comportement au feu et à haute température du béton fabriqué avec des GRB. Tout d'abord, différents mélanges de béton à base de GRB ont été conçus. Ces mélanges avaient différents taux de remplacement (de 0 % à 100 %) et différentes méthodes de remplacement (remplacement direct et remplacement basé sur la résistance). Le deuxième mode de substitution avait pour but d'atteindre les mêmes performances (résistance à la compression et affaissement) que le béton fabriqué avec granulats naturel (GN). Ensuite, une campagne expérimentale sur le comportement à haute température a été réalisée. La première campagne a porté sur les propriétés thermomécaniques résiduelles. Les mélanges de béton ont été chauffés et, après refroidissement, soumis à des essais pour déterminer les propriétés mécaniques, thermiques et microstructurelles. La deuxième campagne portait sur le risque d'écaillage au feu. Des prismes de béton ont été exposés à un chauffage feu standard (ISO 834-1) et à un chargement de compression uniaxiale. Une campagne d'essais au feu supplémentaire a également été réalisée pour évaluer l'effet des profils de teneur en eau sur le risque d'écaillage. Pour finir, la durabilité après chauffage et refroidissement a été évaluée via l'approche performantielle. Les résultats montrent que bétons à base de GRB voient leurs propriétés thermiques et mécaniques du béton diminuées après exposition à haute température, mais la réduction était similaire à celle observée dans le béton fabriqué avec des GN. Un comportement encore plus proche a été observé si le béton fabriqué avec GRB était optimisé. Les essais au feu ont montré que le béton fabriqué avec des GRB présentait un degré d'écaillage plus élevé que le béton fabriqué avec des GN, ce qui est associé aux propriétés physiques du béton, en particulier sa teneur en eau. Les résultats de la campagne complémentaire ont confirmé que le risque d'écaillage était fortement lié à la teneur en eau. En effet, le séchage a réduit le risque d'écaillage dans tous les mélanges étudiés. Enfin, l'exposition à des températures élevées a entraîné une diminution de tous les paramètres de durabilité pour tous les bétons étudiés. L'ajout de RCA a réduit les performances, mais, comme dans le cas des propriétés thermomécaniques résiduelles, cette diminution peut être atténuée avec une optimisation appropriée du mélange. Cette étude a donné un aperçu du comportement du béton fabriqué avec des GRB après exposition à haute température. Les résultats présentés ici peuvent servir de référence pour différents aspects du comportement au feu des structures en béton fabriquées avec des GRB.

Mots-Clés: granulats de béton recyclés, haute température, propriétés mécaniques, propriétés thermiques, durabilité, propriétés de transfert, écaillage, teneur en eau

Table of Contents

List of Figures

List of Tables

Chapter 01

Introduction

This PhD deals with the behaviour of concrete made with recycled concrete aggregates (RCA) exposed to elevated temperatures. It is structured as a compilation of journal and extended conference papers manuscripts. This initial chapter introduces the research background and motivation for the thesis. Given the thesis's nature and structure (compilation of papers), the research background also includes a brief literature review on concrete made with RCA and the behaviour of concrete at elevated temperatures. After, the research project aims and objectives are presented. Lastly, the thesis layout and the relation between the proposed papers and chapters are given.

1.1 Research background, motivation and literature review

1.1.1 Concrete and environmental considerations

Concrete is the most used construction material in the world [1], and its consumption is more than twice that of all other building materials [2]. Each year, more than 10 billion tonnes are produced [3] and the rate of consumption of concrete will undoubtedly increase until 2050 due to population growth and urbanisation [1]. Concrete popularity comes from its versatility, affordability, durability, mechanical properties, and structural performance [2, 4]. At the same time, concrete has one of the highest environmental impacts in terms of emission of greenhouse gases, use of natural resources and waste production [1–3].

For a typical residential building, construction-related emissions come mainly from reinforced concrete, with concrete by itself being responsible for up to 38 % of CO_2 emissions [1]. In typical commercially produced concrete mixes, cement and aggregates represent the majority of CO_2 emissions. The first is responsible for up to 70 %. At the same time, the production and transport of sand and aggregates are responsible for almost 20 % of concrete CO_2 emissions (for one cubic metre) [1]. Cement industry per itself is responsible up to 5 % of total CO_2 emissions, considered the major responsible for greenhouse effect [5].

Concrete production also requires the use of non-renewable resources, using a high quantity of raw materials, including sand, stone and water [6]. It is estimated that the industry consumes 40 % of raw materials (stone, gravel and sand), 40 % of total energy and 16 % of water [7]. In terms of aggregate use, worldwide consumption is up to 48.3 billion tones per year and a increase rate of 5 % is expected annually [8, 9]. Considering the current infrastructure growth, it is expected that the demand for natural resources will further increase.

Another big concern of the concrete industry is waste production (Fig. 1.1). In the European Union, the total amount of waste generated in 2014 was 2.5 billion tonnes, of which 34.7 % were from construction and demolition waste (C&DW) [10]. It is estimated that concrete corresponds to one-third of C&DW [11, 12]. The most common method of disposal of these materials is still landfilling, which is now banned from public policies in Europe [3, 13, 14].

Hence, reducing the environmental impact of concrete production is necessary to reach more sustainable development. One of the promising strategies is the reuse and recycling of construction and demolition waste. Regarding concrete waste, the primary approach is to use recycled concrete aggregates (RCA) as a replacement for natural aggregates (NA) for concrete production. The RCA is an aggregate made from concrete debris usually composed of two different materials: natural aggregate and attached (or adhered) mortar (AM). The use of this aggregate to produce new concrete (Recycled Aggregate Concrete or RAC) can help reduce the amount of waste produced and sent to landfills, reduce the scarcity of raw materials and reduce CO_2 associated to aggregate transportation [15–18].

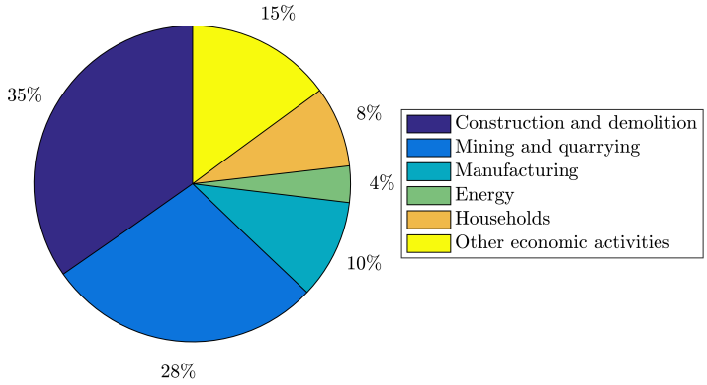

Figure 1.1: Waste generation by economical activities - 2014 (adapted from Eurostat [10])

1.1.2 Concrete made with RCA

The reuse of construction and demolition waste to make new concrete has gained popularity in the last years [19]. Especially in academic research, a great effort was made to understand the aggregate's behaviour, how it might influence the structural performance of concrete and how its use will contribute to reducing the environmental impact [14, 20]. Some countries and institutions also provide standards and guidelines addressing the use of RCA for the production of concrete. In the European context, in order to produce a concrete made with RCA, aggregates specifications should follow EN 12620:2013 [21], the concrete composition should follow EN 206:2013 [22] and execution should follow EN 13670:2009 [23]. Lastly, in French context, the national project RECYBETON further developed the feasibility of using RCA in concrete, showing that the usual requirements of strucutral concrete can be achieved using RA, even for high replacement rates [24].

The recycling procedure of RCA consists of turning the demolition waste into recycled aggregates. Given the usual miscellaneous nature of waste debris, the RCAs may contain different materials and contaminants, such as glass, wood, paper, bituminous particles and steel [4, 16]. The recycling procedure of RA includes different stages, such as demolition, crushing, material separation (screening), removal of contaminants, and sieving [4, 5]. The different components and configurations of the recycling procedure will affect the type, quantity and quality of the recycled aggregate [25]. Significantly, the crushing processes will have a crucial influence on RCAs, given that they affect the detachment of different mineral phases attached to the aggregates [18]. Other advanced processing techniques (ultrasonic, thermal treatments, nitric acid solution, for example) can help to improve aggregates quality [4]. In addition to these processes, the quality of parent concrete also plays a crucial role in the final behaviour of RCAs [17].

In the case of recycled concrete aggregates, the main difference from NA is that RCAs are composed of two different materials: the old natural aggregate and the attached (or adhered) mortar (AM). The fractions and the interactions between these elements control the properties of the RCA [5]. However, the

AM content is the principal responsible for the worsening of most properties of the RCA [26, 27]. The research done so far shows that recycled aggregates are more heterogeneous, porous and less dense than natural aggregates and, as a consequence, RCA presents high water absorption and low strength when compared to NA [4, 28, 29].

Finally, concrete made with RCA has more phases than an ordinary concrete (Fig. 1.2). In the case of a mix with both NA and RCA, concrete is composed of RCA (old natural aggregate and old cement paste), NA and (new) cement paste. Hence, RACs presents three interfacial transition zones (ITZ): between old aggregate and old cement paste, between new cement paste and the RCA (new paste/old paste and/or new paste/old NA), and between NA and new cement paste [30].

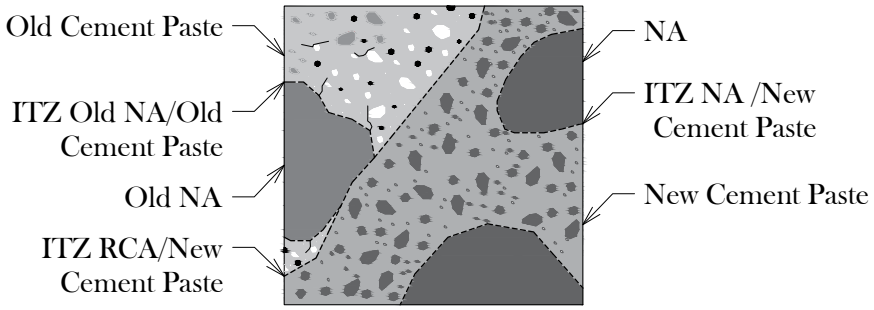

Figure 1.2: Scheme of RCA mesostructure

This difference in the composition, along with the worse properties of RCA, can harm the concrete properties, influencing practical aspects, such as mixing methods, to microstructure and properties [29, 31]. Indeed, one of the main concerns when using RCA in concrete is the high water absorption. This property, along with the high heterogeneity of RCA, makes the correct determination of mixing water a complex task [16, 32]. The fast and higher absorption affects the effective water/binder (w/b) ratio of concrete, which influences the fresh and hardened behaviour of concrete [33] and the bond between paste and aggregates.

Different technical methods have been proposed to prevent the decrease in fresh and hardened properties. The most prevalent techniques are saturation and pre-wetting (or pre-humidification), where the aggregates are added to the mix in a saturated or nearly saturated state [28, 33]. However, this kind of approach may lead to a decrease in compressive strength [16]. Mixing water compensation, when aggregates are used in dry conditions and extra water is added to the mix, is also proposed [33]. Other mixing procedures, such as the Two-Stage Mixing Approach and other enveloping methods, were also proposed. In these methods, the concept is based on the filling of RCA pores, which may improve the ITZs and the final compressive strength [16, 33]. In any case, a standard method is not defined and dealing with the higher water absorption of RCA is one of the major concerns in the industrial production of RAC [33].

Regarding the microstructure of RAC, the two new ITZs also have a crucial role in this new concrete, promoting changes in the concrete properties [28, 30]. In the case of RCA, the ITZ formation is strongly affected by the water exchanges

between the aggregate and the cement paste [16]. The higher porosity and cracking of the old ITZ (old paste/old NA) increase the water demand, reducing water for hydration and making the new ITZ (new paste/RCA) more open and loose [28, 34]. At the same time, some authors also state that this extra water can help the hydration process, promoting internal curing and densification of ITZ at longer ages [28]. In general, the quality of the ITZ depends on the surface characteristics of aggregates, chemical bonding, absorption, and the saturation state of aggregates [35].

As stated before, the higher water absorption affects the free water of concrete, thus, affecting the workability of concrete. Besides water absorption, the shape and texture of aggregates can also affect the fresh behaviour of the mix [28, 31, 36]. In general, concrete with RCA has lower slump values as the percentage of RCA increases [5, 26]. The approaches mentioned above to compensate higher water absorption should be applied to present a competitive slump and overcome this behaviour. Another approach is using water-reducing admixtures to guarantee the required workability without significantly changing the w/b ratio [36]. Previous works also observed that, even though similar workability can be obtained, concrete made with RCA tends to present slightly higher bleeding [36]. Another parameter that is affected is fresh density since the substitution of NA by RCA may reduce it up to 5 % [36].

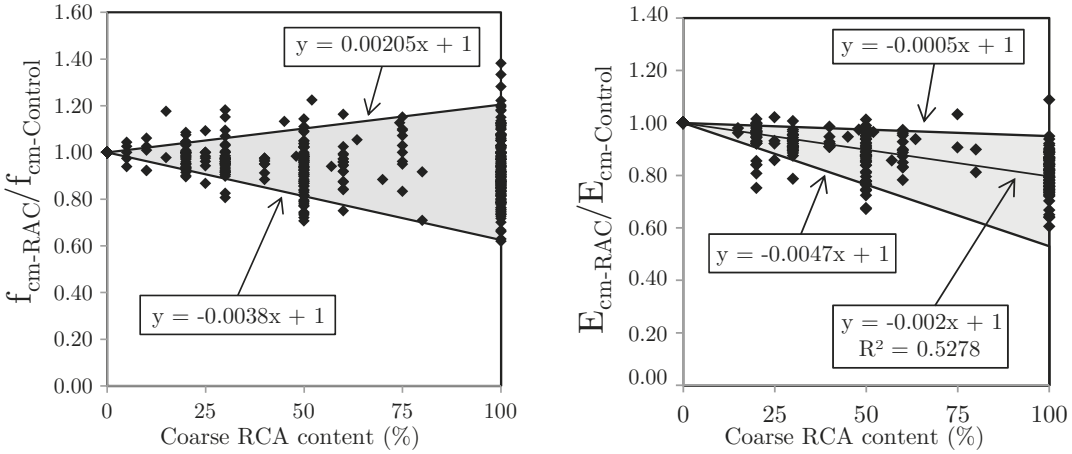

(a) compressive strength (b) elastic modulus

Figure 1.3: Mechanical properties with the increase in RCA content (adapted from Silva et al. [37, 38])

The use of RCA also has a strong influence on all mechanical properties, from compressive strength to fatigue behaviour. The main one, the compressive strength, has been deeply studied by several researchers [16, 37]. In general, if RCA content increases, the compressive strength decreases, but this drop will depend on factors related to the type, origin and quality of aggregate [37]. Silva et al. [37] compiled the results from 65 publications that studied different types of recycled aggregates. Fig. 1.3a shows the variation of relative compressive strength with the increase of coarse RCA content, together with upper and lower

limits of 95 % confidence interval. A variation can be observed in the results, but a general decrease trend is verified. With 100 % of RCA, compressive strength may range from 0.62 to 1.2 times the value of concrete with NA.

Similar behaviour is also observed in the case of elastic modulus, flexural and tensile splitting strength [5]. Again, the quantity, size, type and quality of recycled aggregate affect the evolution of these properties with RCA content [38, 39]. Fig. 1.3b shows the evolution of elastic modulus with replacement rate, compiled by Silva et al. [38]. With 100 % of RCA, the relative elastic modulus varies from 0.53 to 1.05 times the value of concrete made with NA. Tensile behaviour was also compiled and analysed by Silva et al. [39], which verified that the splitting tensile strength of RAC (100 % of RCA) was around 0.88 times the value of concrete made with NA. Further analysis on other mechanical properties (shrinkage, stress-strain, creep, fatigue) can be found in previous works [4, 16, 20].

Another concern in the use of RCA in concrete is durability. Again, the presence of attached mortar affects the overall performance. Indeed, the higher quantity of mortar leads to higher porosity and water absorption, which may reduce the durability of concrete made with RCA [16, 40]. Besides this, the different ITZs also affect the durability properties. Guo et al. [40] compiled the main results related to the durability of recycled aggregate concrete (Fig. 1.4).

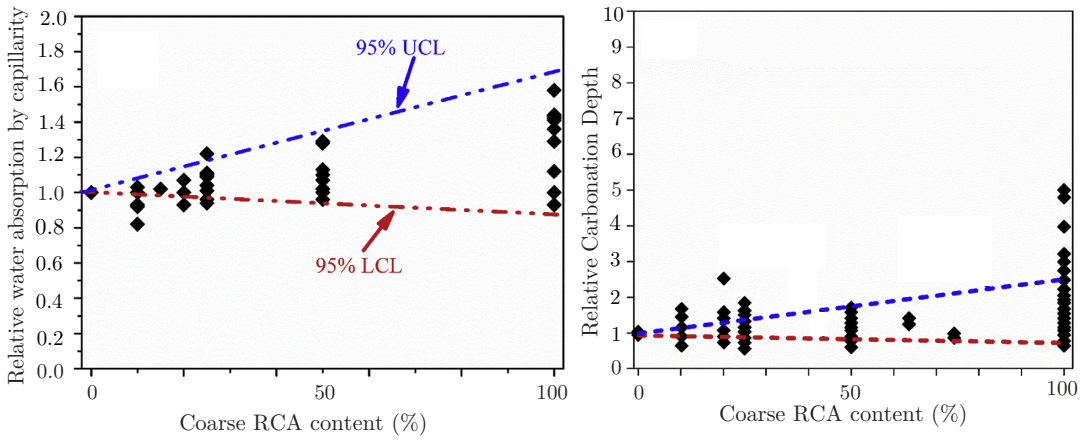

(a) water absorption (b) carbonation depth

Figure 1.4: Durability of concrete made with RCA (adapted from Guo et al. [40])

Fig. 1.4a shows the effect of coarse RCA content on concrete water absorption by immersion. Authors indicate that RAC specimens can have a water absorption 1.7 times higher than ordinary concrete. Fig. 1.4b shows the carbonation depth with replacement rate and indicates that these concretes can have depths 2.5 times higher. However, some measures can be taken to minimise RCA's negative effect. The use of mineral admixtures (fly ash and slag, for example) and the reduction of the water/binder ratio can help to achieve equivalent resistances to carbonation penetration, and chloride diffusion [16, 40, 41]. Other studies on durability properties, such as freezing-thawing and alkali-silica reaction, can be

found elsewhere [16, 40].

Even though the use of RCA implies specific properties and concerns, previous research shows that concrete made with RCA may have similar properties to conventional concrete and can reach the desired structural performance, even for high replacement rates [24]. Although significant work has been done in the past years, there are still open issues that prevent the widespread use of RCA [42]. One of these is related to the high-temperature behaviour of concrete made with RCA, the scope of this present thesis.

1.1.3 Concrete made with NA at elevated temperatures

Before studying the behaviour of concrete made with RCA, it's fundamental to describe the behaviour of concretes made with NA at elevated temperatures. Understanding of the elevated temperature behaviour of concrete is fundamental since fire safety it's a critical factor in the design of concrete structures. The current knowledge of the behaviour of these concretes is quite known. Under heating, several physicochemical changes occur, resulting in the deterioration of the material's mechanical properties depending on the temperature range.

The first transformations are related to the slow capillary water loss associated with water evaporation, from 20 °C to 80 °C [43, 44]. From 80 °C to 100 °C, the first concrete hydration product (ettringite) starts dehydrating and decomposing [45, 46]. Also at this stage, the water physically bonded in aggregates and cement matrix evaporates, increasing capillary porosity and microcracking [44, 47]. From 100 °C to 200 °C, concrete loses more water (bonded and capillary), and calcium silicate hydrates (C-S-H) start to dehydrate and disintegrate, forming αC_2S [46].

In addition, between 120 °C and 300 °C, cement gel layers starts to moving closer, increasing van der Waals forces [48, 49]. This movement may lead to an increase in the strength up to 300 °C. At this temperature, hydration of unhydrated cement grains may also occur, which also may lead to a constant or increase in strength [50]. Up to 350 °C, water loss is almost complete, and C-S-H continues to disintegrate, increasing microcracks, and porosity in the cement paste [46]. It is noteworthy that above 300 °C concrete starts to have some significant loss of strength and stiffness [50].

After 400 °C and up to 600 °C, portlandite (CH) decomposes, further contributing to microcracking in the cement paste [44, 46]. Also, siliceous aggregates containing quartz (e.g. sand) transform at 573 °C [43, 46], inducing cracking on the surrounding cement paste. From 600 °C to 800 °C, a second phase of decomposition of C-S-H undergoes [43, 51]. From 800 °C to 1200 °C, the dehydrated phases starts to melt, along with an intense microcracking at 1200 °C [43, 46]. The aggregates, depending on mineralogical composition, starts to melt at temperatures higher than 1000 °C [43, 46].

In addition to these physicochemical changes, heating leads to a difference in deformations between cement paste and aggregate – what is often called "the thermal mismatch". When heated, cement paste first expands but rapidly after 100 °C, it shrinks due to dehydration, while most of the aggregates used in

concrete expand [52, 53]. This differential strain can lead to thermal-induced stresses that may induce microcracks in the ITZ, contributing to the degradation of mechanical properties [54]. Fig. 1.5 shows an example of the cracking in the concrete after exposure to 600 °C, both at the material scale and at the microstructure scale.

(a) specimen (adapted from Mindeguia et al. [55])

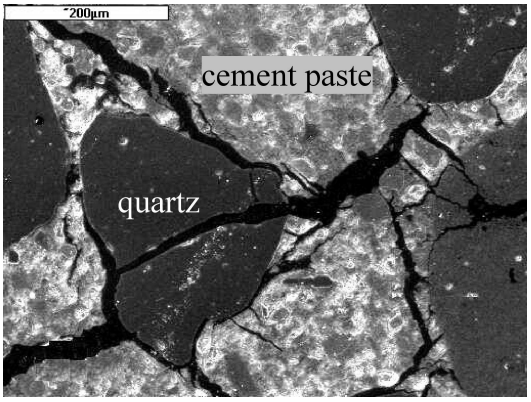

(b) microstructure (adapted from Hager [43])

Figure 1.5: Concrete after exposure to 600 °C (heated with no external mechanical load)

The abovementioned transformations result in several changes in the properties of concrete. These properties, from mechanical to thermal properties, are fundamental parameters to understand, describe and predict the behaviour of concrete at elevated temperatures. High temperature mechanical properties of concrete made with NA have been deeply studied for the last decades. As pointed out by previous studies [50, 56, 57], different parameters may affect the measured properties. These parameters range from mixture proportions (e.g., w/b ratio, curing conditions, aggregate type and size, additions, and admixtures) to test parameters (hot/residual states, stressed/unstressed conditions, specimen size, heating rate and exposure time).

In relation to mechanical properties, compressive strength, modulus of elasticity, tensile strength and stress-strain response are fundamental. Kodur [56] compiled and compared experimental results with standard recommendations. Fig. 1.6 shows the evolution of relative (ratio between high and room temperature properties) compressive strength and elastic modulus with temperature. Regarding compressive strength, up to 300 °C, compressive strength values show small decay and, in some cases, constant or even increase. From 300 °C to 800 °C, strength decreases linearly and, after 800 °C, almost all compressive strength is lost [50]. Elastic modulus and tensile strength also face strong reduction as temperature increases, and in this case, the reduction rate is almost linear since room temperature [50]. Regarding stress-strain response, with the increase in temperature, curves become flattered, and strain at peak stress increases [50].

Concrete made with RCA at elevated temperatures has also been a research subject in the last decade. In general, the behaviour shows similarities to the

behaviour of ordinary concrete made with NA. However, the exact influence of the RCA and its content is still lacking. Contradictory results have been found in previous works related to the impact of the replacement rate on its properties after exposure to high temperatures. Some authors [58–63] pointed out that increasing the replacement rate can improve the relative mechanical properties compared to the behaviour of concrete made with NA. On the opposite, other authors verified similar [42, 64, 65] or even a slightly worse [66–69] behaviour as replacement increases. This is usually attributed to different factors, such as the higher initial porosity of RCA, the possible weaker and thicker ITZ, and microcracking.

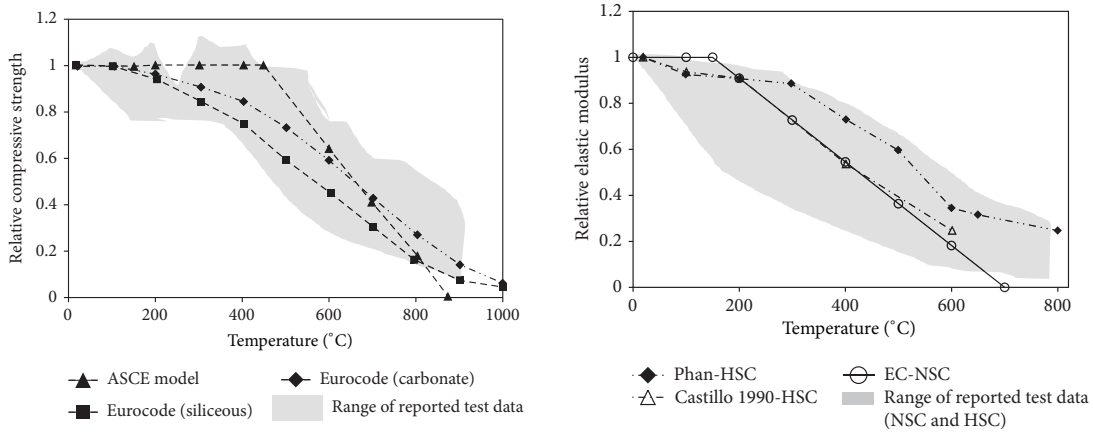

(a) compressive strength

(b) elastic modulus

Figure 1.6: Relative mechanical properties versus temperature (adapted from Kodur [56])

1.1.4 Fire spalling

Another important aspect of the behaviour of concrete at elevated temperatures is the spalling during fire. This phenomenon consists on a violent or nonviolent detachment of concrete fragments from structures exposed to fire [53, 70]. Spalling can seriously affect the performance of the concrete structures, reducing thermal insulation, exposing the steel rebars directly to fire and reducing the load-bearing capacity [71, 72] (Fig. 1.7). Despite the numerous experimental and numerical studies, some uncertainties remain, especially regarding spalling prediction.

Fire spalling is affected by thermal, hydric, chemical and mechanical mechanisms. Spalling usually occurs by the coupled action of some of these mechanisms (thermo-hydro and thermo-mechanical), i.e., a combination of pore pressure, compression stresses (induced by thermal action and loading), and cracking [53]. Lately, another type of mechanism (thermo-chemical spalling) has also been proposed.

The two first mechanisms (thermo-hydro and thermo-mechanical) are behind the most common theories about spalling in concrete [70, 73]. The first, the thermo-hydro mechanism, is related to the pore pressure build-up driven by water

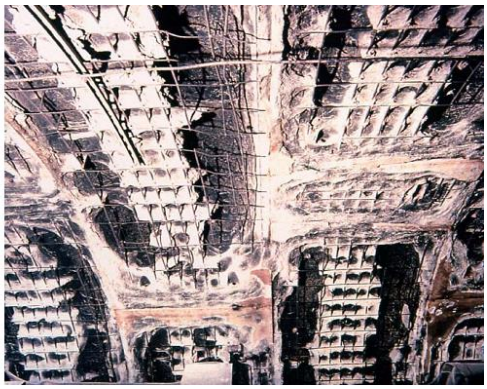

(a) Fire damage to concrete of Channel Tunnel indicating severe spalling

(b) Exposed surface of slabs after fire test (Mindeguia et al. [55])

Figure 1.7: Examples of spalling of concrete

transport and vaporisation. When concrete heats, vapour will escape from the concrete towards the heated surface. Also, another part of the vapour will move towards the inner core of concrete (nonheated). This vapour that goes inside the concrete will condensate due to the thermal gradients. This condensation will lead to a saturation of the pores in a zone located a few centimetres from the exposed side. This zone, the so-called 'moisture-clog', will block further vapour movements, increasing pore pressure. As temperature increases, these pore pressure will rise, and if the stresses due to this pore pressure overcome the tensile strength of concrete, spalling may occur [50, 70, 72, 74, 75].

The thermo-mechanical mechanism is related to the thermal-gradient-induced thermal stresses and/or restrained thermal dilation [70]. The heating of concrete leads to a high thermal gradient, which will induce bi-axial compressive stresses parallel to the heated surface. Subsequently, heating will induce tensile stress perpendicular to the same surface. When these high stresses (compressive ones) exceed concrete strength, spalling may occur [50, 72, 73]. The last mechanism, thermo-chemical spalling, is is related to the decomposition of calcium hydroxide, and the rehydration of calcium oxide [70].

In the case of concrete made with RCA, little is known about spalling risk of these concretes. The addition of RCA tends to increase concrete's porosity and permeability, which may facilitate vapour migration, thus reducing spalling risk [76]. At the same time, these aggregates also induce high water content in concrete, which also strongly affects the spalling risk. Spalling was observed in some previous works [76–79], and the water content was indicated as one of the main contributors to the phenomena. In any case, a systematic evaluation of the spalling risk of concrete made with RCA is still missing.

1.1.5 Post-heating durability

Durability can be defined as the capacity of structures to meet the requirements of serviceability, strength and stability during all the service life [80]. Concrete structures should resist different environmental, chemical and physical actions

to achieve these durability requirements [2]. Various approaches can be used to determine the durability of concrete. Usually, most of them are linked with the measurement of the transport properties of concrete. These properties are linked with the ability of concrete to resist (or facilitate) the ingress of fluids or ions [81]. Different methods can be used to measure the permeability, capillary suction/absorption, and porosity to characterise concrete pore structure and connectivity [81]. Other methods, simulating exposure to the aggressive environments, such as chloride penetration tests and accelerated carbonation, can also be used [81].

This requisite is also valid in the case of post-fire scenarios, especially when the building is not too structurally damaged. In these situations, a post-fire diagnosis of material is required. After exposure to fire, concrete residual behaviour should be assessed regarding all its properties, including its remaining durability properties. Understanding the remaining durability is crucial for defining repair, strengthening, and maintenance strategies. However, several gaps are observed within the current knowledge of concrete post-heating durability properties [82]. In addition, these issues are often overlooked in standards and codes related to the fire behaviour of concrete structures [82]. Hence, it is crucial to develop studies and strategies to assess the residual durability of concrete structures.

As described in the previous section, exposing concrete to high temperatures induces several physicochemical changes that damage hydration products, increase porosity and promote cracking. Most of these physical and chemical changes are irreversible and could affect concrete durability [83]. The decay of durability properties due to heating has been verified in some previous works [82, 83]. These works indicate that properties such as porosity, water absorption, chloride, and carbonation can be affected even at temperatures lower than 300 °C [82, 84, 85]. Fig. 1.8 shows the chloride and accelerated carbonation resistance of three types of ordinary concretes with NA. It can be seen that, after 300 °C, all mixes show less than 50 % of their room temperature property.

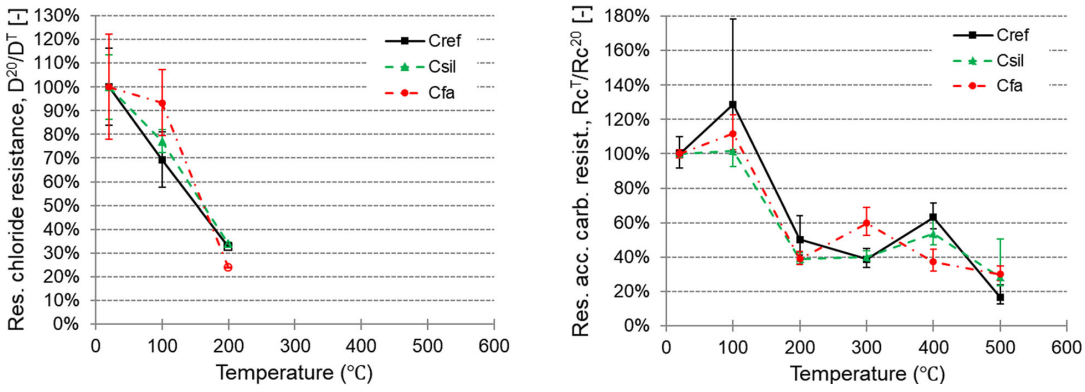

(a) chloride resistance (b) accelerated carbonation resistance

Figure 1.8: Relative durability properties versus temperature (adapted from Monteiro and Vieira [82])

No specific study in post-heating durability of RCA was verified, but some works showed this reduction in durability [86–90]. These works showed the

increase of porosity after exposure to elevated temperatures [86–88]. Authors pointed out a better behaviour than NA [86], due to a better thermal compatibility between the phases in RAC. In contrast, another study [88] indicates a worsening in porosity due to the decomposition of hydration products from the cement mortar in RAC. Water absorption also significantly increases after exposure to elevated temperatures [86]. Residual chloride permeability was also evaluated [89, 90], and it was seen that the permeability increases with RCA content.

1.1.6 Concluding remarks

The use of RCA is a promising approach for producing more sustainable concrete. At the same time, it can reduce the amount of C&DW and reduces natural resource depletion. Even though the use of RCA affects concrete fresh and hardened properties, concrete made with RCA can reach an equivalent performance to concrete made with NA. Some points still need to be addressed to widespread the use of this concrete in the industry, especially for complete replacement. One of them is the behaviour at elevated temperatures, as in the case of a fire situation.

When concrete is heated, several physicochemical occur within the material, resulting in deterioration of all properties. The extent of this damage is related to different factors, and among them, the material properties play a fundamental role. Seeing the particular properties of concrete made with RCA (higher porosity, water absorption, and different ITZs), the replacement of NA with RCA may result in a specific thermomechanical behaviour. Works adressed the thermomechanical behaviour of concrete made with RCA, but further investigation is needed.

Another fundamental aspect of concrete at elevated temperatures is fire spalling. This phenomenon can be very harmful to the safety of concrete structures. Despite extensive research, uncertainties regarding the phenomenon remain, even for concrete made with NA. The spalling risk of concrete made of RCA is almost unknown. The phenomenon was observed in some previous works, but no systematic study addressed the spalling risk.

Finally, besides residual thermal and mechanical behaviour, post-heating durability is also affected by fire and should be evaluated for a proper assessment. Limited attention has been given to this topic, especially to concrete made with RCA. It is fundamental to examine the changes in transfer properties and the ingress of aggressive agents to understand the effect of heating on the durability of these concretes with RCA.

1.2 Research aims and objectives

This PhD is part of the RECYFEU project, conducted by four different partners: two universities (*Université de Pau et des Pays de l'Adour* and *Université de Bordeaux*) and two industrial partners (*Groupe Cassous* and *Groupe Garandeau*).

The project aims to (i) valorise the use of RCA in the Nouvelle Aquitaine Region and (ii) evaluate the high-temperature behaviour of these sustainable concretes.

Based on the project aims and the knowledge gaps, the following objectives were drawn:

- Develop mixes and characterise the behaviour of concrete made with RCA with different coarse replacement rates and different target strengths.
- Characterise the thermomechanical behaviour of the proposed mixes, evaluating the residual mechanical, thermal and microstructural properties.
- Evaluate the spalling sensitivity of concrete made with RCA.
- Evaluate through a performance-based approach the post-heating durability of concrete (with and without coarse RCA).

1.3 Thesis layout and scientific contributions

The manuscript is divided into eight chapters (Fig. 1.9). As highlighted before, this PhD is structured as a compilation of papers (coloured chapters in Fig. 1.9). Hence, five of the eight initial chapters have a manuscript structure.

Chapter 1 (current chapter) introduces the fundamental concepts of the present thesis, from the environmental impact to the fire behaviour of concrete made with RCA. Besides this brief literature review, the project aim and objectives are presented. Lastly, the structure of the thesis and the scientific contributions are presented.

Chapter 2 presents **Paper I** (published). This chapter is a state-of-art review of the high-temperature behaviour of concrete made with RCA. It first addresses the mechanical and thermal properties, compiling and discussing the influence of RCA on these parameters. It also deals with the spalling, medium and full-scale tests on structures made from these concretes. Lastly, the post-heating microstructure is also reviewed.

Chapter 3 is an overview of the methodology related to the mix design and sample preparation. The materials and their properties are presented. The mix properties, including the design method and mixing procedure, are presented. The fresh and hardened properties of all the mixes are shown and analysed. Finally, an overview of the test samples is given.

Chapter 4 refers to the manuscript of **Paper II** (to be submitted). This chapter evaluates the thermomechanical properties of concrete made with RCA. To this, residual mechanical and thermal properties were evaluated for different mixes. Microstructural analyses were also made for some of the mixes.

Chapter 5 is a compilation of the manuscript of **Paper III** (published) and **Paper IV** (submitted). This chapter evaluates the fire spalling risk of concrete made with RCA. First, a fire spalling screening test was done in several concrete mixes made with RCA and NA. Then, the effect of the water content profile on the fire spalling risk was investigated. Post-heating parameters (depth and volume) were evaluated using digital photogrammetry.

Chapter 6 refers to the manuscript of **Paper V** (to be submitted). This chapter evaluates the post-heating durability of three different mixes. Transport properties and resistance to aggressive environmental analyses were done after and before exposure to elevated temperatures. A performance-based approach was used for the durability assessment of these mixes.

Chapter 7 is the closure of the PhD thesis. A coupled analysis of all the evaluated parameters is done. In addition, it summarises the main conclusions of the PhD and gives recommendations for future work.

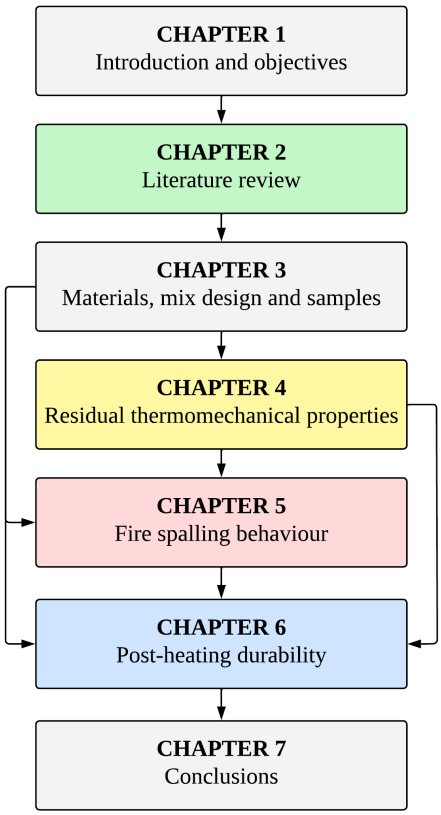

Figure 1.9: Thesis structure

The papers related to the chapters are listed below:

Paper I Fernandes, B.; Carré, H.; Mindeguia, J-C.; Perlot, C.; La Borderie, C. *Effect of elevated temperatures on concrete made with recycled concrete aggregates - An overview.* Journal of Building Engineering. (`https://doi.org/10.1016/j.jobe.2021.103235`)

Paper II Fernandes, B.; Carré, H.; Gaborieau, C.; Mindeguia, J-C.; Perlot, C.; Anguy, Y.; La Borderie, C. *Residual thermomechanical properties of concrete made with recycled concrete aggregates after exposure to high temperatures.* To be submitted.

Paper III Fernandes, B.; Carré, H.; Mindeguia, J-C.; Perlot, C.; La Borderie, C. *Spalling behaviour of concrete made with recycled concrete ag-*

gregates. Construction and Building Materials. (https://doi.org/10.1016/j.conbuildmat.2022.128124)

Paper IV Fernandes, B.; Carré, H.; Mindeguia, J-C.; Perlot, C.; La Borderie, C. *Experimental investigation on the effect of water content profile on fire spalling*. Submitted to the 7th International Workshop on Concrete Spalling due to Fire Exposure, Berlin, Germany.

Paper V Fernandes, B.; Khodeir, M.; Perlot, C.; Carré, H.; Mindeguia, J-C.; La Borderie, C. *Durability of concrete made with recycled concrete aggregates after exposure to elevated temperatures*. To be submitted.

Besides the **Papers I-V**, the author also wrote and contributed to other conference papers during the PhD. **A** presents results related to **Chapter 4** of the thesis. **Paper B** presents the initial work conducted in **Chapter 5** of the PhD. Lastly, in **Paper C**, the author contributes with the same methodology used in **Chapter 5**.

Paper A Fernandes, B.; Gaborieau, C.; Carré, H.; Mindeguia, J-C.; Perlot, C.; Anguy, Y.; La Borderie, C.; Anguy, Y. *Microstructure of concrete made with recycled concrete aggregates after exposure to elevated temperatures*. In 15èmes JEMP, Strasbourg, France.

Paper B Fernandes, B.; Carré, H.; Mindeguia, J-C.; Perlot, C.; La Borderie, C. *Fire spalling sensitivity of concrete made with recycled concrete aggregates (RCA)*. In *fib* ICCS2021: 3rd International Conference on Concrete Sustainability, Prague, Czech Republic.

Paper C Sultangaliyeva, F.; Fernandes, B.; Carré, H.; Pimienta, P.; La Borderie, C.; Roussel, N. *Experimental contribution to the optimization of the choice of polypropylene fibers in concrete for its thermal stability*. In 6th International Workshop on Concrete Spalling due to Fire Exposure, Sheffield, United Kingdom.

References

[1] G. Habert, S. Miller, V. John, J. Provis, A. Favier, A. Horvath, et al. "Environmental impacts and decarbonization strategies in the cement and concrete industries". In: *Nature Reviews Earth & Environment* 1.11 (2020), pp. 559–573.

[2] J. de Brito and N. Saikia. *Recycled Aggregate in Concrete*. Springer-Verlag London, 2013, p. 448. DOI: 10.1007/978-1-4471-4540-0.

[3] C. Meyer. "The greening of the concrete industry". In: *Cement and Concrete Composites* 31.8 (2009), pp. 601–605. DOI: 10.1016/j.cemconcomp.2008.12.010.

[4] M. Behera, S. K. Bhattacharyya, A. K. Minocha, R. Deoliya, and S. Maiti. "Recycled aggregate from C&D waste & its use in concrete - A breakthrough towards sustainability in construction sector: A review". In: *Construction and Building Materials* 68 (2014), pp. 501–516. DOI: 10.1016/j.conbuildmat.2014.07.003.

[5] M. Pepe. *A Conceptual Model for Designing Recycled Aggregate Concrete for Structural Applications*. 1st ed. Springer Theses. Springer International Publishing, 2015.

[6] J. Xiao. *Recycled Aggregate Concrete Structures*. Springer-Verlag Berlin Heidelberg, 2018, p. 632. DOI: 10.1007/978-3-662-53987-3_16.

[7] M. K. Dixit, J. L. Fernández-Solís, S. Lavy, and C. H. Culp. "Identification of parameters for embodied energy measurement: A literature review". In: *Energy and Buildings* 42.8 (2010), pp. 1238–1247. DOI: 10.1016/j.enbuild.2010.02.016.

[8] V. W. Tam, M. Soomro, and A. C. J. Evangelista. "A review of recycled aggregate in concrete applications (2000–2017)". In: *Construction and Building materials* 172 (2018), pp. 272–292.

[9] B. Wang, L. Yan, Q. Fu, and B. Kasal. "A comprehensive review on recycled aggregate and recycled aggregate concrete". In: *Resources, Conservation and Recycling* 171 (2021), p. 105565.

[10] Eurostat. *Energy, transport and environment indicators. 2018 Edition*. 2018, p. 232.

[11] S. Böhmer, G. Moser, C. Neubauer, M. Peltoniemi, E. Schachermayer, M. Tesar, et al. *Aggregates case study*. Tech. rep. 2008, p. 282.

[12] B. Qi, J. Gao, F. Chen, and D. Shen. "Evaluation of the damage process of recycled aggregate concrete under sulfate attack and wetting-drying cycles". In: *Construction and Building Materials* 138 (2017), pp. 254–262. DOI: 10.1016/j.conbuildmat.2017.02.022.

[13] F. de Larrard and H. Colina. "Introduction". In: *Concrete Recycling: Research and Practice*. Ed. by F. de Larrad and H. Colina. CRC Press, 2019, pp. 1–4.

[14] N. Tošić, S. Marinković, T. Dašić, and M. Stanić. "Multicriteria optimization of natural and recycled aggregate concrete for structural use". In: *Journal of Cleaner Production* 87.1 (2015), pp. 766–776. DOI: 10.1016/j.jclepro.2014.10.070.

[15] M. Amario, C. S. Rangel, M. Pepe, and R. D. Toledo Filho. "Optimization of normal and high strength recycled aggregate concrete mixtures by using packing model". In: *Cement and Concrete Composites* 84 (2017), pp. 83–92. DOI: 10.1016/j.cemconcomp.2017.08.016.

[16] H.-b. Le and Q.-b. Bui. "Recycled aggregate concretes – A state-of-the-art from the microstructure to the structural performance". In: *Construction and Building Materials* 257 (2020), p. 119522. DOI: 10.1016/j.conbuildmat.2020.119522.

[17] M. Nedeljković, J. Visser, B. Šavija, S. Valcke, and E. Schlangen. "Use of fine recycled concrete aggregates in concrete: A critical review". In: *Journal of Building Engineering* 38 (2021), p. 102196.

[18] Y. A. Villagrán-Zaccardi, A. T. Marsh, M. E. Sosa, C. J. Zega, N. De Belie, and S. A. Bernal. "Complete re-utilization of waste concretes–Valorisation pathways and research needs". In: *Resources, Conservation and Recycling* 177 (2022).

DOI: 10.1016/j.resconrec.2021.105955.

[19] C. Shi, Y. Li, J. Zhang, W. Li, L. Chong, and Z. Xie. "Performance enhancement of recycled concrete aggregate - A review". In: *Journal of Cleaner Production* 112 (2016), pp. 466–472. DOI: 10.1016/j.jclepro.2015.08.057.

[20] R. V. Silva, J. De Brito, and R. K. Dhir. "Prediction of the shrinkage behavior of recycled aggregate concrete: A review". In: *Construction and Building Materials* 77 (2015), pp. 327–339. DOI: 10.1016/j.conbuildmat.2014.12.102.

[21] *Aggregates for concrete*. Comité Européen de Normalisation. Brussels, 2013.

[22] *Concrete. Specification, performance, production and conformity*. Comité Européen de Normalisation. Brussels, 2013.

[23] *Execution of concrete structures*. Comité Européen de Normalisation. Brussels, 2009.

[24] F. de Larrard and H. Colina. "Conclusion". In: *Concrete Recycling: Research and Practice*. Ed. by F. de Larrad and H. Colina. CRC Press, 2019, pp. 544–545.

[25] M. Hiete. "Waste management plants and technology for recycling construction and demolition (C&D) waste: state-of-the- art and future challenges". In: *Handbook of recycled concrete and demolition waste*. Ed. by F. Pacheco-Torgal, V. Tam, J. Labrincha, Y. Ding, and J. de Brito. Woodhead Publishing, 2013, pp. 53–75.

[26] L. Butler. "Evaluation of Recycled Concrete Aggregate Performance in Structural Concrete". PhD thesis. University of Waterloo, 2012, p. 433.

[27] S. Rémond, J. M. Mechling, E. Garcia-Diaz, R. Lavaud, R. Trauchessec, and B. Cazacliu. "Characterisation of Recycled Concrete Aggregates". In: *Concrete Recycling: Research and Practice*. Ed. by F. de Larrad and H. Colina. CRC Press, 2019, pp. 33–61.

[28] M. B. Leite and P. J. Monteiro. "Microstructural analysis of recycled concrete using X-ray microtomography". In: *Cement and Concrete Research* 81 (2016), pp. 38–48. DOI: 10.1016/j.cemconres.2015.11.010.

[29] M. S. de Juan and P. A. Gutiérrez. "Study on the influence of attached mortar content on the properties of recycled concrete aggregate". In: *Construction and Building Materials* 23.2 (2009), pp. 872–877. DOI: 10.1016/j.conbuildmat.2008.04.012.

[30] M. Pepe, R. D. Toledo Filho, E. A. Koenders, and E. Martinelli. "Alternative processing procedures for recycled aggregates in structural concrete". In: *Construction and Building Materials* 69 (2014), pp. 124–132. DOI: 10.1016/j.conbuildmat.2014.06.084.

[31] M. Etxeberria, E. Vázquez, A. Marí, and M. Barra. "Influence of amount of recycled coarse aggregates and production process on properties of recycled aggregate concrete". In: *Cement and Concrete Research* 37.5 (2007), pp. 735–742. DOI: 10.1016/j.cemconres.2007.02.002.

[32] M. Joseph, L. Boehme, Z. Sierens, and L. Vandewalle. "Water absorption variability of recycled concrete aggregates". In: *Magazine of Concrete Research* 67.11 (2015), pp. 592–597. DOI: 10.1680/macr.14.00210.

[33] L. Ferreira, J. de Brito, and M. Barra. "Influence of the pre-saturation of recycled coarse concrete aggregates on concrete properties". In: *Magazine of Concrete Research* 63.8 (2011), pp. 617–627. DOI: 10.1680/macr.2011.63.8.617.

[34] C. S. Poon, Z. H. Shui, and L. Lam. "Effect of microstructure of ITZ on compressive strength of concrete prepared with recycled aggregates". In: *Construction and Building Materials* 18.6 (2004), pp. 461–468. DOI: 10.1016/j.conbuildmat.2004.03.005.

[35] T. Le, G. Le Saout, E. Garcia-Diaz, D. Betrancourt, and S. Rémond. "Hardened behavior of mortar based on recycled aggregate: Influence of saturation state at macro- and microscopic scales". In: *Construction and Building Materials*

141 (2017), pp. 479–490. DOI: 10.1016/j.conbuildmat.2017.02.035.

[36] R. V. Silva, J. de Brito, and R. K. Dhir. "Fresh-state performance of recycled aggregate concrete: A review". In: *Construction and Building Materials* 178 (2018), pp. 19–31. DOI: 10.1016/j.conbuildmat.2018.05.149.

[37] R. V. Silva, J. De Brito, and R. K. Dhir. "The influence of the use of recycled aggregates on the compressive strength of concrete: A review". In: *European Journal of Environmental and Civil Engineering* 19.7 (2014), pp. 825–849. DOI: 10.1080/19648189.2014.974831.

[38] R. V. Silva, J. De Brito, and R. K. Dhir. "Establishing a relationship between modulus of elasticity and compressive strength of recycled aggregate concrete". In: *Journal of Cleaner Production* 112 (2016), pp. 2171–2186.

[39] R. V. Silva, J. D. Brito, and R. K. Dhir. "Tensile strength behaviour of recycled aggregate concrete". In: *Construction and Building Materials* 83 (2015), pp. 108–118. DOI: 10.1016/j.conbuildmat.2015.03.034.

[40] H. Guo, C. Shi, X. Guan, J. Zhu, Y. Ding, T. C. Ling, et al. "Durability of recycled aggregate concrete – A review". In: *Cement and Concrete Composites* 89 (2018), pp. 251–259. DOI: 10.1016/j.cemconcomp.2018.03.008.

[41] S. C. Kou and C. S. Poon. "Enhancing the durability properties of concrete prepared with coarse recycled aggregate". In: *Construction and Building Materials* 35 (2012), pp. 69–76. DOI: 10.1016/j.conbuildmat.2012.02.032.

[42] J. Vieira, J. Correia, and J. De Brito. "Post-fire residual mechanical properties of concrete made with recycled concrete coarse aggregates". In: *Cement and Concrete Research* 41.5 (2011), pp. 533–541.

[43] I. Hager. "Behaviour of cement concrete at high temperature". In: *Bulletin of the Polish Academy of Sciences: Technical Sciences* 61.1 (Jan. 2013), pp. 1–10. DOI: 10.2478/bpasts-2013-0013.

[44] M. C. Alonso and U. Schneider. "Degradation Reactions in Concretes Exposed to High Temperatures". In: *Physical Properties and Behaviour of High-Performance Concrete at High Temperature*. Springer, 2019, pp. 5–40.

[45] M. Castellote, C. Alonso, C. Andrade, X. Turrillas, and J. Campo. "Composition and microstructural changes of cement pastes upon heating, as studied by neutron diffraction". In: *Cement and Concrete Research* 34.9 (2004), pp. 1633–1644. DOI: 10.1016/S0008-8846(03)00229-1.

[46] P. Pimienta, M. C. Alonso, R. Jansson McNamee, and J.-C. Mindeguia. "Behaviour of high-performance concrete at high temperatures: some highlights". In: *RILEM Technical Letters* 2.2017 (2017), p. 45. DOI: 10.21809/rilemtechlett.2017.53.

[47] E. Annerel and L. Taerwe. "Revealing the temperature history in concrete after fire exposure by microscopic analysis". In: *Cement and Concrete Research* 39.12 (2009), pp. 1239–1249. DOI: 10.1016/j.cemconres.2009.08.017.

[48] D. J. Naus. *The effect of elevated temperature on concrete materials and structures - A literature review*. Tech. rep. 2005.

[49] M. Malik, S. K. Bhattacharyya, and S. V. Barai. "Thermal and mechanical properties of concrete and its constituents at elevated temperatures : A review". In: *Construction and Building Materials* 270 (2021), p. 121398. DOI: 10.1016/j.conbuildmat.2020.121398.

[50] Q. Ma, R. Guo, Z. Zhao, Z. Lin, and K. He. "Mechanical properties of concrete at high temperature-A review". In: *Construction and Building Materials* 93 (2015), pp. 371–383. DOI: 10.1016/j.conbuildmat.2015.05.131.

[51] G. F. Peng and Z. S. Huang. "Change in microstructure of hardened cement paste subjected to elevated temperatures". In: *Construction and Building Materials* 22.4 (2008), pp. 593–599.

[52] *fib Bulletin 46: Fire design of concrete structures — structural behaviour and assessment*. Tech. rep. Lausanne, Swiss, 2008, p. 209.

[53] G. A. Khoury. "Effect of fire on concrete and concrete structures". In: *Progress in Structural Engineering and Materials* 2.4 (2000), pp. 429–447. DOI: 10.1061/41016(314)299.

[54] Z. H. Deng, H. Q. Huang, B. Ye, H. Wang, and P. Xiang. "Investigation on recycled aggregate concretes exposed to high temperature by biaxial compressive tests". In: *Construction and Building Materials* 244 (2020), p. 118048. DOI: 10.1016/j.conbuildmat.2020.118048.

[55] J.-C. Mindeguia, P. Pimienta, H. Carré, and C. La Borderie. "On the influence of aggregate nature on concrete behaviour at high temperature". In: *European Journal of Environmental and Civil Engineering* 16.2 (2012), pp. 236–253. DOI: 10.1080/19648189.2012.667682.

[56] V. Kodur. "Properties of Concrete at Elevated Temperatures". In: *ISRN Civil Engineering* 2014 (2014), pp. 1–15. DOI: 10.1155/2014/468510.

[57] V. Kodur, S. Banerji, and R. Solhmirzaei. "Test methods for characterizing concrete properties at elevated temperature". In: *Fire and Materials* September (2019), pp. 1–15. DOI: 10.1002/fam.2777.

[58] C. Zega and A. Di Maio. "Recycled concrete exposed to high temperatures". In: *Magazine of Concrete Research* 58.10 (2006), pp. 675–682.

[59] C. J. Zega and A. A. Di Maio. "Recycled concrete made with different natural coarse aggregates exposed to high temperature". In: *Construction and building materials* 23.5 (2009), pp. 2047–2052.

[60] S. R. Sarhat and E. G. Sherwood. "Residual mechanical response of recycled aggregate concrete after exposure to elevated temperatures". In: *Journal of Materials in Civil Engineering* 25.11 (2013), pp. 1721–1730.

[61] S. C. Kou, C. S. Poon, and M. Etxeberria. "Residue strength, water absorption and pore size distributions of recycled aggregate concrete after exposure to elevated temperatures". In: *Cement and concrete composites* 53 (2014), pp. 73–82.

[62] Y. Wang, F. Liu, L. Xu, and H. Zhao. "Effect of elevated temperatures and cooling methods on strength of concrete made with coarse and fine recycled concrete aggregates". In: *Construction and Building Materials* 210 (2019), pp. 540–547. DOI: 10.1016/j.conbuildmat.2019.03.215.

[63] H. Zhao, F. Liu, and H. Yang. "Residual compressive response of concrete produced with both coarse and fine recycled concrete aggregates after thermal exposure". In: *Construction and Building Materials* 244 (2020), p. 118397. DOI: 10.1016/j.conbuildmat.2020.118397.

[64] H. Zhao, Y. Wang, and F. Liu. "Stress–strain relationship of coarse RCA concrete exposed to elevated temperatures". In: *Magazine of Concrete Research* 69.13 (2017), pp. 649–664.

[65] H. Yang, H. Zhao, and F. Liu. "Residual cube strength of coarse RCA concrete after exposure to elevated temperatures". In: *Fire and Materials* 42.4 (2018), pp. 424–435.

[66] G. Chen, Y. He, H. Yang, J. Chen, and Y. Guo. "Compressive behavior of steel fiber reinforced recycled aggregate concrete after exposure to elevated temperatures". In: *Construction and Building Materials* 71 (2014), pp. 1–15.

[67] J. Gales, T. Parker, D. Cree, and M. Green. "Fire performance of sustainable recycled concrete aggregates: mechanical properties at elevated temperatures and current research needs". In: *Fire Technology* 52.3 (2016), pp. 817–845.

[68] F. U. A. Shaikh. "Mechanical properties of concrete containing recycled coarse aggregate at and after exposure to elevated temperatures". In: *Structural Concrete* 19.2 (2018), pp. 400–410.

[69] J. B. da Silva, M. Pepe, and R. D. Toledo Filho. "High temperatures effect on mechanical and physical performance of normal and high strength recycled aggregate concrete". In: *Fire Safety Journal* 117.August (2020). DOI: 10.1016/j.firesaf.2020.103222.

[70] J.-C. Liu, K. H. Tan, and Y. Yao. "A new perspective on nature of fire-induced spalling in concrete". In: *Construction and Building Materials* 184 (2018), pp. 581–590. DOI: 10.1016/j.conbuildmat.2018.06.204.

[71] J. C. Mindeguia, P. Pimienta, A. Noumowé, and M. Kanema. "Temperature, pore pressure and mass variation of concrete subjected to high temperature - Experimental and numerical discussion on spalling risk". In: *Cement and Concrete Research* 40.3 (2010), pp. 477–487. DOI: 10.1016/j.cemconres.2009.10.011.

[72] J.-C. Mindeguia, H. Carré, P. Pimienta, and C. La Borderie. "Experimental discussion on the mechanisms behind the fire spalling of concrete". In: *Fire and Materials* 39.7 (2014), pp. 619–635. DOI: 10.1002/fam.2254.

[73] E. W. H. Klingsch. "Explosive spalling of concrete in fire". PhD thesis. ETH Zurich, 2014, p. 252.

[74] G. Shorter and T. Harmathy. "Discussion on the fire resistance of prestressed concrete beams". In: *Proceedings of the Institution of Civil Engineers* 20.2 (1961), pp. 313–315.

[75] T. Harmathy. "Effect of moisture on the fire endurance of building elements". In: *Moisture in materials in relation to fire tests*. ASTM International, 1965, pp. 74–95.

[76] P. Pliya, D. Cree, H. Hajiloo, A.-L. Beaucour, M. Green, and A. Noumowé. "High-Strength Concrete Containing Recycled Coarse Aggregate Subjected to Elevated Temperatures". In: *Fire Technology* (2019), pp. 1–18.

[77] F. Robert, A.-L. Beaucour, and H. Colina. "Behavior Under Fire". In: *Concrete Recycling: Research and Practice*. Ed. by F. De Larrard and H. Colina. CRC Press, 2019. Chap. 13, p. 13.

[78] Z. Chen, J. Zhou, P. Ye, and Y. Liang. "Analysis on Mechanical Properties of Recycled Aggregate Concrete Members after Exposure to High Temperatures". In: *Applied Sciences* (2019). DOI: 10.3390/app9102057.

[79] P. Pliya, H. Hajiloo, S. Romagnosi, D. Cree, S. Sarhat, and M. F. Green. "The compressive behaviour of natural and recycled aggregate concrete during and after exposure to elevated temperatures". In: *Journal of Building Engineering* 38.June 2020 (2021), p. 102214. DOI: 10.1016/j.jobe.2021.102214.

[80] A. E. Richardson. "Strength and durability of concrete using recycled aggregates (RAs)". In: *Handbook of recycled concrete and demolition waste*. Ed. by F. Pacheco-Torgal, V. Tam, J. Labrincha, Y. Ding, and J. de Brito. Woodhead Publishing, 2013, pp. 330–348.

[81] H. Beushausen, R. Torrent, and M. G. Alexander. "Performance-based approaches for concrete durability: State of the art and future research needs". In: *Cement and Concrete Research* 119.January 2018 (2019), pp. 11–20. DOI: 10.1016/j.cemconres.2019.01.003.

[82] A. Valente Monteiro and M. Vieira. "Effect of elevated temperatures on the residual durability-related performance of concrete". In: *Materials and Structures/Materiaux et Constructions* 54.6 (2021), pp. 13–15. DOI: 10.1617/s11527-021-01824-5.

[83] S. A. Memon, S. F. A. Shah, R. A. Khushnood, and W. L. Baloch. "Durability of sustainable concrete subjected to elevated temperature – A review". In: *Construction and Building Materials* 199 (2019), pp. 435–455. DOI: 10.1016/j.conbuildmat.2018.12.040.

[84] C.-S. Poon, S. Azhar, M. Anson, and Y.-L. Wong. "Comparison of the strength and durability performance of normal-and high-strength pozzolanic concretes at elevated temperatures". In: *Cement and concrete research* 31.9 (2001), pp. 1291–1300.

[85] H. Carré, C. Perlot, A. Daoud, M. J. Miah, and B. Aidi. “Durability of ordinary concrete after heating at high temperature”. In: *Key Engineering Materials*. Vol. 711. Trans Tech Publ. 2016, pp. 428–435.

[86] S. C. Kou, C. S. Poon, and M. Etxeberria. “Residue strength, water absorption and pore size distributions of recycled aggregate concrete after exposure to elevated temperatures”. In: *Cement and Concrete Composites* 53 (2014), pp. 73–82. DOI: 10.1016/j.cemconcomp.2014.06.001.

[87] C. Laneyrie, A.-L. Beaucour, M. F. Green, R. L. Hebert, B. Ledesert, and A. Noumowe. “Influence of recycled coarse aggregates on normal and high performance concrete subjected to elevated temperatures”. In: *Construction and Building Materials* 111 (2016), pp. 368–378.

[88] D. Xuan, B. Zhan, and C. S. Poon. “Thermal and residual mechanical profile of recycled aggregate concrete prepared with carbonated concrete aggregates after exposure to elevated temperatures”. In: *Fire and Materials* 42.1 (2017), pp. 134–142.

[89] Z. Ma, G. Ba, and Z. Duan. “Effects of High Temperature and Cooling Pattern on the Chloride Permeability of Concrete”. In: *Advances in Civil Engineering* 2019 (2019).

[90] Z. Ma, M. Liu, Q. Tang, C. Liang, and Z. Duan. “Chloride permeability of recycled aggregate concrete under the coupling effect of freezing-thawing, elevated temperature or mechanical damage”. In: *Construction and Building Materials* 237 (2020), p. 117648. DOI: 10.1016/j.conbuildmat.2019.117648.

Chapter 02

Effect of elevated temperatures on concrete with recycled concrete aggregates - a review

This chapter is based on the paper *Effect of elevated temperatures on concrete made with recycled concrete aggregates - an overview*, published in the *Journal of Building Engineering*. It is a state-of-art review of the behaviour of concrete made with RCA at high temperatures. Particular focus is given to mechanical and thermal properties, which are compiled and discussed to identify critical aspects and particularities of RCA on these properties. In addition, spalling, fire behaviour and microstructure of heated concrete with RCA are also discussed. This chapter gives an overview of the specific research topic, paving the way for the experimental works conducted in the thesis.

Fernandes, B.; Carré, H.; Mindeguia, J-C.; Perlot, C.; La Borderie, C. *Effect of elevated temperatures on concrete made with recycled concrete aggregates - An overview.* Journal of Building Engineering. (https://doi.org/10.1016/j.jobe.2021.103235)

2.1 Introduction

Since the last century, the construction industry is facing a huge problem concerning the depletion of natural resources concomitantly to the massive production of construction and demolition wastes (C&DW). Concrete is the most used construction material in the world [1] and for this reason, it plays an important role in the environmental impact of the construction industry. It is estimated that the construction industry depletes 40 % of raw materials (stone, gravel and sand), 40 % of total energy and 16 % of water [2]. In terms of waste, C&DW represent almost 35 % of all waste in Europe [3] and concrete corresponds to one-third of this value [4]. The most common method of disposal of these materials is still landfilling, which is avoided by public policies in Europe [5, 6].

Aiming to reach sustainable development, it is essential that the construction sector, especially the concrete industry, reduces its environmental impact. One of the possible approaches is the recycling and reusing of C&DW wastes in new construction. During the last decades, the usage of recycled concrete aggregates (RCA) as a replacement for natural aggregates (NA) for producing concrete has shown a great potential to promote ecological efficiency. This solution can reduce the amount of waste produced and sent to landfills, help to solve the depletion of the natural resources, and reduce the impact of production and transportation of aggregates [7, 8].

Employing RCA to produce Recycled Aggregates Concrete (RAC) has gained popularity in research recently. A significant amount of this research focuses on understanding how recycled aggregates influence the mechanical and durability performances of concrete. The main difference between RCA to natural aggregates is that RCA is composed of two different materials: natural aggregate and attached (or adhered) mortar (AM). The concrete made with RCA is a compound of natural aggregate (NA), old natural aggregate, new cement paste and old cement paste. Consequently, three interfacial transition zones (ITZ) are observed: between old aggregate and old cement paste, between new mortar paste and the RCA, and between NA and new cement paste [9].

Recycled aggregates are generally more heterogeneous, porous and less dense than NA. Consequently, RCA presents higher water absorption and lower strength [10, 11]. Hence, these recycled concrete aggregates impact fresh and hardened properties [8]. However, the problems mentioned above have not represented significant drawbacks in the use of RCA into new concretes. RAC may have similar properties to conventional concrete and can reach the desired structural performance, even for high replacement rates [12].

Although significant work has been done in the past years, there are still open issues that prevent the widespread use of RCA [13]. One of these is related to the fire behaviour of concrete made with RCA. This paper aims to provide a comprehensive and updated report about high temperature behaviour of concrete made with recycled concrete aggregates. Firstly, mechanical and thermal properties at elevated temperatures are discussed. Then, spalling, medium and full-scale experiments are presented. Additionaly, microstructure related properties are addressed. Lastly, conclusions and research needs are presented.

2.2 Behaviour of concrete made with natural aggregate at elevated temperatures – a brief review

Before presenting the studies on concrete made with RCA, this section summarizes the main concepts about the high temperature behaviour of concretes made with natural aggregates. When concrete is under heat, several physicochemical changes occur, resulting in the changing of thermo-mechanical properties of the material.

The first reactions that occur are related to the slow capillary water loss associated with a water expansion, from 20 °C to 80 °C [14, 15]. From 80 °C to 100 °C, ettringite dehydrates and decomposes [14]. At this stage, the water physically bonded in aggregates and cement matrix evaporates, increasing capillary porosity and microcracking [15]. From 100 °C to 200 °C, concrete starts losing water and C-S-H (calcium silicate hydrate) of the cement paste starts to dehydrate and decompose, forming αC_2S [14]. Also, between 120 °C and 300 °C, cement gel layers starts to moving closer, increasing van der Waals forces [16, 17]. This may lead to an increase in the strength up to 300 °C. At this temperature, hydration of unhydrated cement grains may also occur, which also may lead to a constant or increase in strength [18]. At 350 °C, water loss becomes more intense and C-S-H continues to decompose, increasing porosity and microcracks [14]. At this point, above 300 °C, concrete starts to have some significant loss of strength and stiffness [18].

After 400 °C and up to 600 °C, CH (portlandite) decomposes, contributing to microcracking in the cement paste [14, 15]. Also, siliceous aggregates containing quartz transform at 573 °C [14, 19]. From 600 °C to 800 °C, a second phase of the C-S-H decomposition undergoes [15, 19]. At this phase, most of the compressive strength has been lost [18]. From 800 °C to 1200 , the dehydrated phases start to melt, with an intense microcracking at 1200 °C [14, 19]. Aggregates also start to melt with temperatures higher than 1000 °C, dependending on mineralogical composition [14, 19].

In addition to phase changes and reactions, heating leads to a thermal mismatch between cement paste and aggregates, as the cement paste shrinks, while most of the aggregates used in concrete expand [20, 21]. This differential strain can lead to thermal-induced stresses that might originate microcracks in the ITZ and the cement paste, contributing to the degradation of mechanical properties [22]. Since aggregates occupy 60 % to 80 % of the volume of the concrete, the selection of the aggregate affects the thermal stability of concrete at high temperatures [22, 23]. Razafinjato et al. [23] studied a wide range of petrographic types of siliceous and calcareous aggregates. They concluded that the thermal behaviour of the aggregates depends on their mineralogical and chemical compositions. The petrographic origin of these aggregates also influences the behaviour of heated concrete [24].

Another relevant aspect of the behaviour of concrete at elevated temperatures is spalling due to fire exposure. This phenomenon consists of a sudden

detachment of concrete fragments from structures exposed to fire. Spalling can seriously affect the structures' performance, reducing thermal insulation, exposing the steel rebars directly to fire and then reducing the load-bearing capacity [25]. The phenomenon is not yet fully understood, however, previous studies reveal that material, geometry and environmental parameters (such as heating rate and external loading) influence the phenomenon. Among material parameters, transport properties (e.g., permeability, porosity, and water content) appear to affect the mechanism behind spalling [26, 27].

Given the influence of material properties on the high temperature behaviour of concrete, it seems that concrete made with recycled concrete aggregates may behave differently than concrete made with natural aggregates in these extreme conditions. Moreover, the higher porosity, higher water absorption, the different interfacial transition zones and the thermal expansion behaviour of RCA may lead to distinctive behaviour at high temperatures.

2.3 Mechanical properties of concrete made with RCA at elevated temperatures

The mechanical properties are fundamental parameters for understanding and predicting the behaviour of concrete structures at elevated temperatures. Studies concerning the behaviour of concrete made with RCA evaluated different properties, such as compressive strength, elastic modulus, tensile strength, and stress-strain relationship. Table 2.1 presents a chronological summary of the works used in this review. A relevant aspect concerning the determination of mechanical properties at high temperatures is the lack of standardized test proceedings, even for concrete made with NA. As pointed out by previous studies [18, 28, 29], the different parameters related to testing conditions, procedures, and mix properties affect the results. The compiled results presented herein come from a wide range of diffferent test parameters and mix properties. The following sections aim to perform an in-depth discussion related to these parameters.

Table 2.1: Summary of research on the mechanical properties at high temperatures of concrete made with RCA

Author	Replacement Rate		High Temperature Parameters				Experiments
	Coarse Aggregate (%)	Fine Aggregate (%)	Test type	Rate/Curve (°C/min)	Temp. (°C)	Exposure time (h)	
Zega & Di Maio [30]	75	-	Residual	n.s.	500 °C	1; 4	CS; EM; UPV; DME
Zega & Di Maio [31]	75	-	Residual	n.s.	500 °C	1	CS; EM; UPV; DME
Vieira et al. [13]	20; 50; 100	-	Residual	ISO 834	400-800 °C	1	CS; STS; EM
Sarhat & Sherwood [32]	25; 50; 75; 100	-	Residual	n.s.	250-750 °C	1	CS; STS; EM
Xiao et al. [33]	30; 50; 70; 100	-	Residual	ISO 834	200-800 °C	2	CS; FS
Chen et al. [34]	100	-	Residual	2.5	200-600 °C	1	CS; EM; SS
Kou et al. [35]	50; 100	-	Residual	5	300-800 °C	4	CS; STS
Gales et al. [36]	30; 100	-	Hot	2	500-560 °C	2	CS; EM; SS; P
Laneyrie et al. [37]	100	-	Residual	0.5	150-750 °C	2	CS; STS; DME
Liu et al. [38]	30; 50	-	Residual	5	100-800 °C	4	CS; EM; SS
Yang et al. [39]	50; 100	-	Residual	n.s.	200-400 °C	n.s.	SHE
Meng et al. [40]	30; 70; 100	-	Residual	n.s.	200-500 °C	1	TR
Shaikh [41]	50; 100	-	Hot/Residual	8	600-800 °C	1	CS; EM
Xuan et al. [42]	20; 40; 60; 80; 100	-	Residual	10	200-600 °C	2	CS; EM; SS
Yang et al. [39]	30; 50; 70; 100	-	Residual	n.s.	300-500 °C	6	CS; EM; SS
Zhao et al. [43]	25; 50; 75; 100	-	Residual	12	200-800 °C	3	CS: EM; SS
Bui et al. [44]	100	-	Residual	5	500 °C	1	CS; EM. SS; UPV
Chen et al. [45]	30; 50; 70; 100	-	Residual	10	200-800 °C	1	CS; EM; SS
Khaliq [46]	100	-	Hot/Residual	5	100-800 °C	2.50	CS; EM; SS; STS
Xie et al. [47]	100	-	Residual	5	200-800 °C	2	CS; EM; SS
Yang et al. [48]	25; 50; 75; 100	-	Residual	10	200-800 °C	3	CS; STS
Abed et al. [49]	25; 50	-	Residual	ISO 834	100-800 °C	2	CS; FS
Pliya et al. [50]	15; 30	-	Hot	1.5	500 °C	1	CS; DIC, SEM
Salahuddin et al. [51]	30; 60; 100	-	Residual	3	200-600 °C	1	CS; UPV; ML
Wang et al. [52]	100	50; 100	Residiual	12	200-800 °C	3	CS; STS
Yang et al. [53]	50; 100	-	Hot	7 - 9	300-800 °C	2	CS; EM; SS
Abed et al. [54]	25; 50	-	Residual	ISO 834	100-800 °C	2	CS; FS
Abed et al. [55]	25; 50	-	Residual	ISO 834	100-800 °C	2	CS; FS; UPV
Deng et al. [22]	50; 100	-	Residual	10	200-400 °C	1	BI
Varona et al. [56]	25; 50; 100		Residual	7-7.5	350-850 °C	2	CS
Wang et al. [57]	100	-	Residual	5	200-800 °C	2	TPB
Zhao et al. [58]	100	50; 100	Hot	12	200-800 °C	3	CS; EM; SS
Silva et al. [59]	50; 100	-	Residual	2	150-650 °C	1	CS; EM; SS ; STS
Pliya et al. [60]	30	30	Hot/Residual	2	150-450 °C	2	CS; EM; DIC; SEM

n.s. = not specified
CS = Compressive Strength; EM=Elasticity Modulus; UPV = Ultrasonic Pulse Velocity; DME = Dynamic Modulus of Elasticity;
STS = Splitting Tensile Strength; FS=Flexural Strength; SS=Stress-Strain Curve; P=Poisson; SHE=Shear Strength; TR=Triaxial Loading Test;
BI = Biaxial Loading Test; TPB = Three-Point Bending

2.3.1 Compressive strength

Fig.2.1 depicts the data collected regarding the compressive strength of RAC at elevated temperatures in terms of relative compressive strength as a function of temperature. The relative compressive strength consists of the ratio between strength at elevated temperatures and strength at ambient temperature (${f_{cu}}^T/f_{cu}$). The results depicted in Fig. 2.1 present no differences regarding mixture proportions nor test conditions. The only differences are related to the testing modality, i.e., hot or residual tests. Further in this section a discussion regarding both types of tests is provided.

Despite the great variability in the results, two different stages can be identified, especially in the residual data. In the first stage, from room temperature up to 300 °C, the compressive strength deviates approximately 20 % from its initial value, with individual data presenting either decrease or increase of strength. The second stage ranges from 300 °C to 800 °C, when the compressive strength starts do decrease prominently. This general trend is very similar to conventional concrete behaviour [18, 29]. The second stage ranges from 300 °C to 800 °C, when the compressive strength decreases prominently. Such a decreasing trend is also observed in the conventional concrete, as pointed out by [18, 29]. The hot dataset presents a more linear decrease trend. However, due to the reduced number of hot tests, one cannot assert whether its variability is lower than the variability obtained from the residual tests.

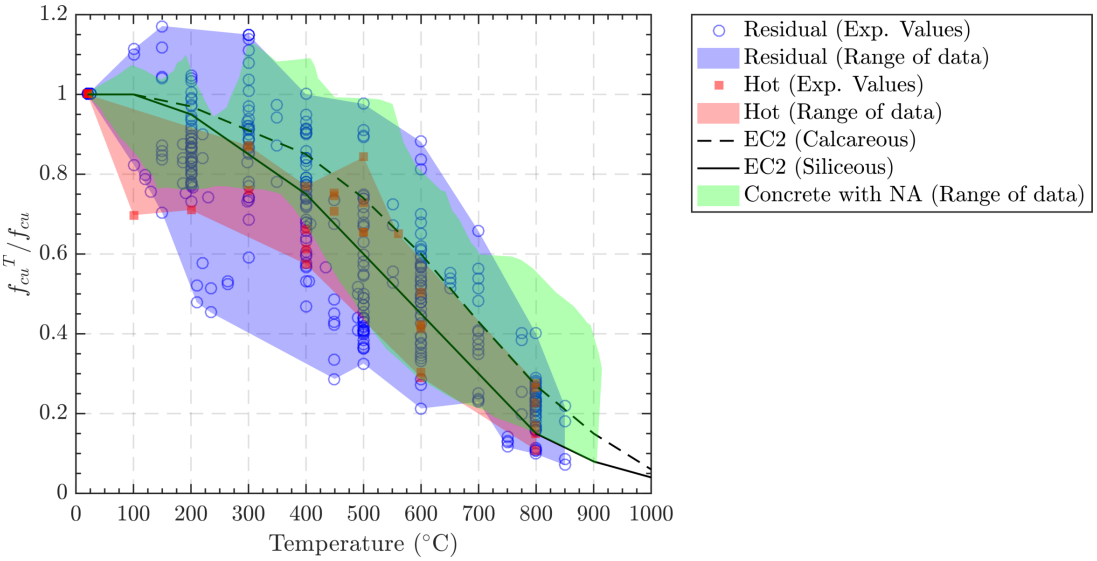

Figure 2.1: Relative compressive strength of concrete made with RCA at elevated temperatures (residual experimental data from [13, 30–35, 37, 38, 41, 43–48, 51, 52, 56, 58, 59], hot data from [36, 41, 46, 50, 53] and concrete made with NA data from Kodur [28])

Fig. 2.1 also depicts a comparison between the compiled data and the curves for siliceous and calcareous concrete provided by Eurocode 2 [61]. The curves provided in the Eurocode are the ones used to determine the fire resistance of

structures. The high scattering in the experimental results does not allow to draw easily a general conclusion. However, it is noticeable that a significant amount of experimental values are lower than the code previsions. Hence, using the Eurocode 2 [61] for evaluating the fire resistance of structures with RAC may be unreliable. For this reason, particular attention should be paid when using these previsions and complementary curves, adapted for RCA, could be added to Eurocode 2.

The variability in the results is not an exclusivity of concrete with RCA. Different studies [18, 28, 62] point out similar dispersions related to the ordinary and high strength concrete properties at high temperature. This variation in the results can be attributed to different factors, suchs as testing conditions (e.g., heating rate, hot or residual, sizes, curing, cooling) and material parameters (e.g., moisture, composition, age) [28, 29].

The first material parameter that raises questions is the presence of RCA itself. It is relevant to know how the presence of recycled aggregates affect the mechanical properties when compared to ordinary concrete made with NA. To depict this difference, the compressive dataset was also compared to results of concrete made with NA. The comparison was made with a set of experimental results (green cloud in Fig.2.1), extracted from the review paper of Kodur [28]. For higher temperatures (from 700 °C), concretes with NA tend to present higher values. Although no clear conclusion can be drawn from Fig.2.1, one notices a significant variability in the RAC data, particularly under 500 °C. Such dispersion in data suggests that the design process should be stricter for concrete made with RCA.

From comparing the works available in the literature, it is verified that different authors obtained contradictory results and drew distinctive conclusions. A first group of works [34, 36, 41, 59] stated that concrete made with RCA presented lower relative compressive strength than concrete made with NA after exposure to high temperatures. The authors also reported that the compressive strength reduces as the RCA content increases. Chen et al. [34] attributed the weak behaviour (top right of Fig.2.2) to the high porosity of RCA. Gales et al. [36] observed similar behaviour in hot tests and asserted that worse performances were associated with three factors: (i) weak ITZ between the old cement paste on the RCA and the new cement paste; (ii) weaker strength at elevated temperatures of the RCA; (iii) possible microcracking in the RCA. Likewise, Shaikh [41] stated that the compressive strength reduction is due to weaker RCA and the greater size of the ITZ's in RCA. Silva et al. [59], on the other hand, attributed this behaviour to the higher total amount of mortar in these mixtures.

A second group of authors [13, 37, 43, 48, 60] reported that the concrete made with RCA presented similar performance of conventional concrete. Fig.2.2 (bottom left) depicts the results obtained by Zhao et al. [43]. These works [13, 37, 43, 48, 60] did not provide a clear relationship between the compressive strength degradation and the replacement rate. Also, the authors provided no explanations regarding this behaviour.

Finally, a last group of works observed an increase of the relative residual mechanical properties of concrete made with RCA [30–33, 35, 46, 49, 52, 54, 56, 58].

One of the evolution is presented in Fig.2.2 (top left). The main reason for this improvement, according to different authors [30–32, 35], is better compatibility of the coefficient of thermal expansion between recycled aggregates and the cement paste, which reduces micro and macrocracking in the interface and the cement paste. The compressive strength also increased with the increase of fine RCA (0/5 fraction) quantities, as observed by [52, 58]. The authors also attributed the gains in the behaviour to a better match between thermal expansions.

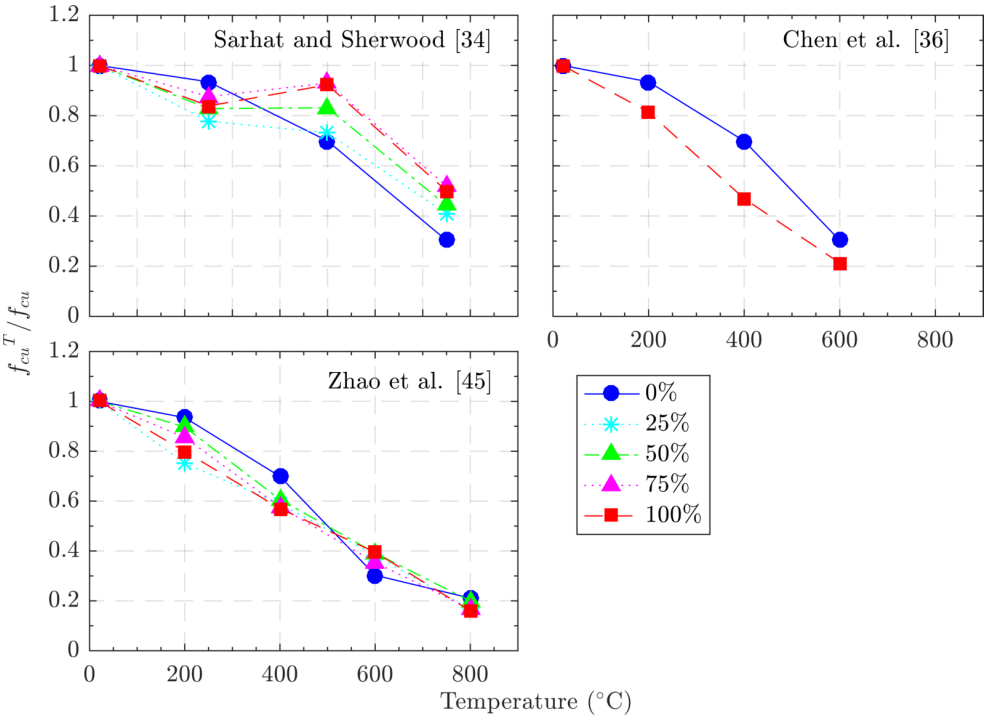

Figure 2.2: Relative compressive strength of concrete made with RCA for different replacement rates

It is also relevant to disclose that the composition of the recycled aggregates may also affect the compressive strength. Laneyrie et al. [37] studied two different recycled concrete aggregates: one produced in a laboratory with controlled properties and one obtained from an industrial source. The concrete made with RCA from industry presented a more significant decrease in strength. The authors [37] stated that this behaviour was related to the presence of flammable non-cementitious impurities (*e.g.*, bituminous, plastic, wood). As the material burns, additional cracks and pores are created in the matrix.

The water/cement ratio may also influence the compressive strength at high temperatures of concrete. Such influence was first studied by Zega and Di Maio [30, 31]. Both works pointed out that for concrete made with RCA with a low w/c ratio, the reduction of relative residual compressive strength was less significant. The authors [30, 31] attributed this to the fact that the interface between old mortar and new mortar was better in the case of low w/c; hence, thermal expansion between the materials (new paste and RCA) is closer.

Laneyrie et al. [37] also studied the effects of varying the w/c ratio (0.3 and 0.6) in compressive strength for two different concretes made with RCA (industrial and laboratory-produced aggregates) subjected to high temperatures. Relative residual values were similar for both cases, yet the authors did not comment on this similarity. Likewise, Yang et al. [48] observed that different w/c ratios make insignificant differences in the compressive strength. Lastly, Silva et al. [59] studied concretes with the same RCA content and different strengths (C25 and C65). They observed similar behaviour for both concretes, with an increase of compressive strength at 150 °C, followed by a decrease up to 650 °C. The main difference was a more relevant increase of compressive strength for C25 concrete when compared to C65. The authors did not provide reasons for this behaviour.

Some studies also addressed the effect of mineral additions as partial replacement of cement. For concrete made with NA, previous studies reported that fly ash and slag can improve its resistance at high temperature, while silica fume seems to worsen the performance [18].

Kou et al. [35] evaluated the addition of fly ash and ground granulated blast furnace slag. They reported an improvement in the compressive strength of concrete made with RCA and mineral additions, up to 300 °C. After 500 °C, however, the concrete suffered significant deterioration. Bui et al. [44] evaluated four different mineral additions: fly ash, waste paper sludge ash, silica fume and metakaolin. The results revealed that mineral additions improved the relative residual compressive strength of heated RAC. The use of waste fly ash, cellular concrete powder and perlite powder as replacement for cement in self-compacting concrete with RCA was studies by Abed et al. [49, 54]. The authors state that adoption of 15 % of any of the waste materials with 25 % of RCA replacement improve concrete performance. Lastly, some studies [34, 41] verified the effects of adding fibres to the concrete with RCA, whereas Xie et al. [47] added fly ash and fibres. Authors reported that fibres improved the residual mechanical properties of heated RCA.

Concerning the testing parameters, two of them stand out: heating rate and type of test. Regarding the heating rate, strong thermal gradients may take place in concrete samples due to their low thermal diffusivity [63]. This kind of thermal gradients induces a structural behaviour in the sample and should be avoided when determining material properties. Moreover, it is important to guarantee a homogeneous temperature distribution inside the specimen. In that context, RILEM recommendation [64] limits the heating rate up to 4 °C/min, depending on the specimen size. Regardless of the type of mechanical test, hot or residual tests can be carried out. For hot tests, concrete specimens are loaded at elevated temperatures. On the other hand, in residual tests, loads are applied after cooling the samples. The first type of test helps to understand the behaviour of concrete structures during a fire and the second one is more related to the post-fire assessment and repair of concrete structures [65].

Fig.2.3 presents the influence of the heating rate and the type of mechanical tests in the relative compressive strength of RAC. Fig.2.3a depicts the relative compressive strengths obtained from low heating rates (up to 5 °C/min), whereas

Fig.2.3b portrays the compressive strengths obtained from high heating heating rates - including ISO 834-1 [66] fire curve. Addtionally, the dataset depicted in Fig.2.3a was obtained from [34–38, 44, 46, 47, 50, 51], whereas the dataset depicted in Fig.2.3b was obtained from [13, 30–33, 41, 43, 45, 48, 52, 53, 56, 58]. It is clear that the data distribution varies between both datasets, especially for residual values. Lastly, the dataset obtained from low heating rates presents a two-phase behaviour, with some works showing a slightly increase of strength for temperatures up to 300 °C.

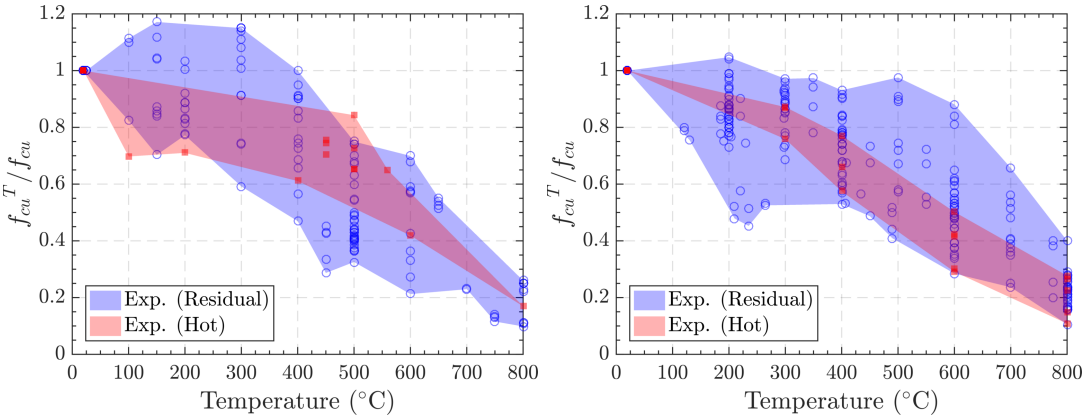

(a) low heating rates ($\leq 5\,°C/min$) (b) high heating rates ($> 5\,°C/min$)

Figure 2.3: Relative compressive strength of concrete made with RCA at high temperatures

The influences of the type of mechanical test (i.e., hot or residual tests) are also studied by a few authors [41, 43, 46, 53, 60], whose results are plotted in Fig.2.4. The small amount of works, however, does not allow one to draw specific conclusions. Some authors [41, 43, 46, 53, 60] studied specifically the influence of the type of testing, and some of their results are plotted in Fig.2.4. A clear difference in trends is observed, which allows one to assert that the obtained results are contradictory. Shaikh [41] observed that relative compressive strengths from residual tests are higher than hot ones, regardless of the temperature (top left on Fig.2.4). The author [41] stated that this behaviour is associated with the rehydration of hydration products after cooling, which may reduce porosity.

Khaliq [46], on the other hand, observed a different behaviour. In his study, residual tests values are higher for temperature up to 200 °C. From 200 °C up to 800 °C, the results obtained from residual tests become lower than the results obtained from the hot test (top right on Fig.2.4). Zhao et al. [43], and Yang et al. [53] reported similar results to Khaliq [46]. Namely, for high temperatures, the relative values obtained from the hot tests outperform the ones obtained from the residual test. Contrarily, for low temperatures, the results obtained from the residual test outperform the ones obtained from hot tests. It is worthwhile mentioning that the results from Zhao et al. [43], and Yang et al. [53] are presented together on the bottom left of Fig.2.4 as they come from the same research project, having the same test mix and testing conditions. The lower values of hot samples for the lowest temperatures, as observed in Kahliq [46], might be related

to a higher internal vapour pressure due to free water evaporation, as stated by Ma et al. [18] for concrete with NA. On the other hand, for high temperatures, lower values of residual tests may be explained by additional mechanical damage due to cooling of concrete [18].

Pliya et al. [60] studied the effect of residual/hot testing and also the effect of different pre-loading (40 % and 70 %) during hot tests. Same rate of 2 °C/min was used in all the tests. Authors stated that hot values, regardless of the pre-load, were always higher than residual ones. They attributed this behaviour to additional thermal stresses due to the cooling phase. The influence of the cooling method was also studied in the works of Yang et al. [48] and Wang et al. [52]. Both studies evaluated the differences between natural and water cooling by spraying cold water for 30 minutes. They concluded that water cooling resulted in a more significant decrease of compressive strength, especially for temperatures below 600 °C. Yang et al. [48] and Wang et al. [52] stated that lower values of normalized compressive strength might be related to the severe thermal shock induced by water cooling.

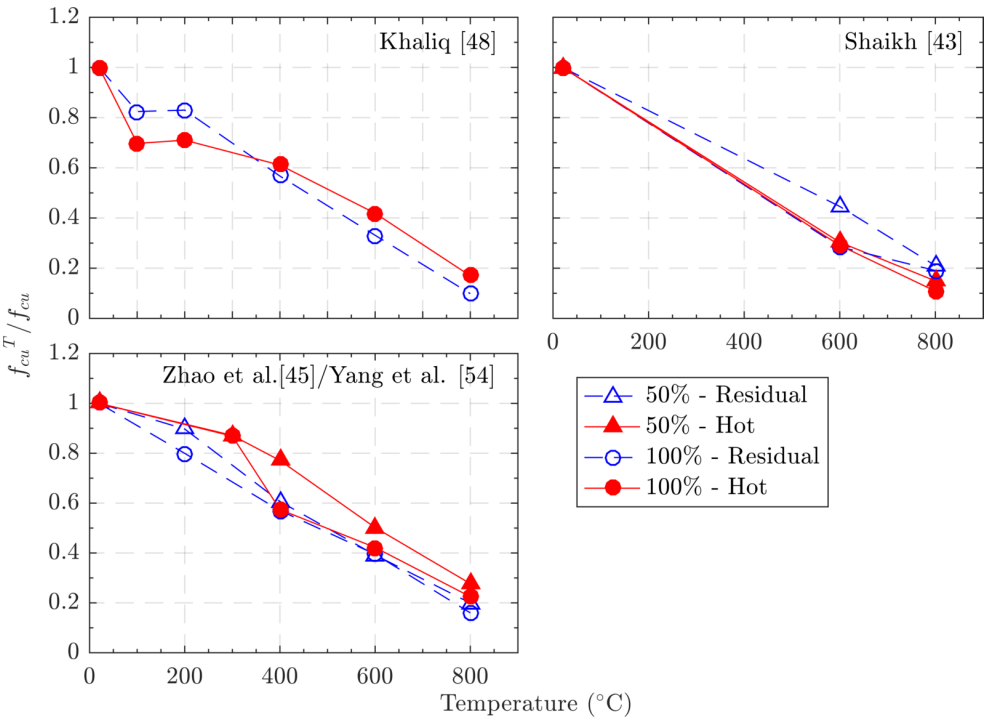

Figure 2.4: Hot and residual relative compressive strength of concrete made with RCA (percentage refers to the evaluated replacement rate)

2.3.2 Elastic modulus

Fig. 2.5a depicts the variation of the relative static elastic modulus as a function of the temperature. The relative static elastic modulus consists of the ratio between the elastic modulus at elevated temperatures and the elastic modulus at ambient temperature ($E_c{}^T / E_c$). No distinction of mixtures was made and

results were presented in two groups: residual tests [13, 30–32, 34, 38, 43, 45–47, 59] and hot tests [36, 41, 46, 50, 53]. Similarly to the compressive strength case, the results present a significant scattering of data, especially for residual tests. In general, the elastic modulus decreases almost linearly between room temperatures - and this behaviour is more prominent with hot tests.

The linear decrease of elastic modulus is very similar to those observed in concrete made with NA [18, 28], as observed in Fig.2.5b. This figure depicts the experimental results obtained by [28] from hot and residual tests for concrete made with NA in the green shaded area. The grey shaded area represents the both hot and residual tests for concrete made with RCA. Remarkably, the RCA dataset is almost entirely inside the range of concrete with NA. For these reasons, it is possible to assert that the behaviour of both types of concrete is similar. However, the behaviour is not identical as differences can be found between 23 °C and 500 °C, as RAC presents higher relative static elastic modulus. Additionally, [13, 44, 53, 59] highlighted that the decrease of elastic modulus was more significant than in compressive strength. Vieira et al. [13] attributed that to the high level of cracking observed in the heated samples.

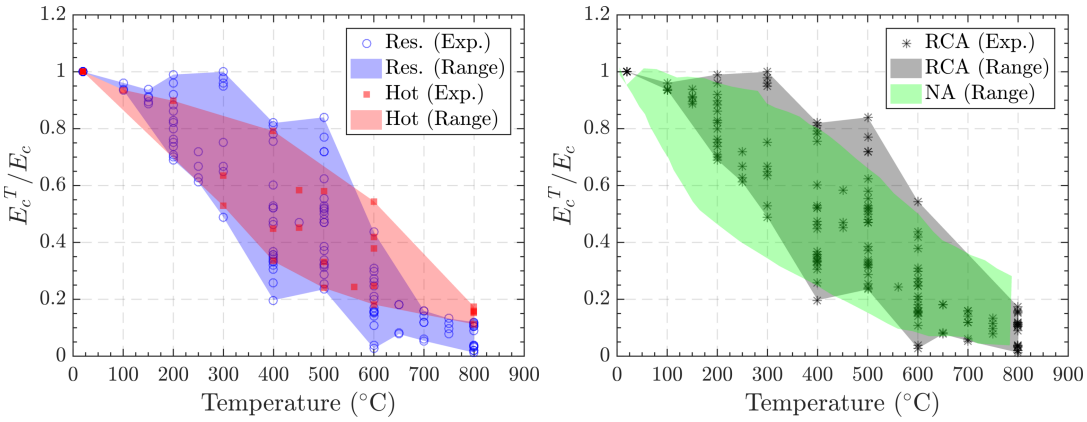

(a) all experimental values (b) comparision with NA

Figure 2.5: Relative modulus of elasticity of concrete made with RCA at elevated temperatures

In general, the factors that influence elastic modulus are very similar to those affecting compressive strength. Some works [13, 32, 43, 53] stated that the replacement rate makes little difference in the residual elastic modulus . Like the case of compressive strength, however, contradictory conclusions are observed in the literature. Shaikh et al. [41] observed a worse performance of RAC when compared to concrete with NA. They associated these results to the pre-existing microcracks in the RCA. Allegedly, These microcracks induced damages during heating, which reduced the load capacity and increased deformation, resulting in lower elastic modulus. Bui et al. [44] also observed worse behaviour for RAC. They attributed this to the old mortar in the RCA, which had higher deformability than the NA. Lastly, Khaliq [46] reported better elastic modulus retention in high strength RAC samples. The author [46] attributed this behaviour to the lesser deterioration in the microstructure of RA-HSC due to the higher perme-

ability given by the RCA.

The use of fine RCA (0/5 fraction) also showed some increase in the elastic modulus, as observed by Zhao et. al [58]. According to their work, mixes with 50 % of fine RCA might improve the residual stiffness after exposure to high temperatures. Similar phenomenon was also observed by Pliya et al. [60] which verified that RAC with 30 % of fine RCA presented less damage. Authors attributed these results to the higher porosity of RAC, which might ease the thermal and hydrous transfer and consequently reduce the damage of this material.

2.3.3 Tensile strength

The tensile strength of concrete is significantly lower than compressive strength. For this reason this property is often neglected. At high temperatures, however, such property becomes relevant as the cracking and spalling phenomenons are related to tensile stresses [28]. In the literature, the tensile properties of concrete are usually determined by splitting test. Direct tension tests on concrete made with RCA at elevated temperatures are not reported in the literature. Fig.2.6a depicts the temperature dependence of the relative splitting tensile strength [13, 32, 35, 37, 46, 48, 52, 59]. The relative splitting tensile strength consists of the ratio between the splitting tensile strength at elevated temperatures and the value at ambient temperature (${f_t}^T/f_t$). No distinctions regarding mix proportions and testing procedures were made. The only study giving hot values is highlighted [46]. As the case of the other mechanical properties, wide variability of results is observed.

Fig.2.6b depicts a comparison with experimental results of concrete made with NA (extracted from Kodur [28]) and Eurocode 2 [61] provisions. Remarkably, the Eurocode 2 [61] provisions are more conservative than the experimental measurements. The analyses regarding the splitting tensile strength must be cautious, as the amount of available data is scarce. Additionally, similarly to the elastic modulus, the deterioration of the tensile strength property is more significant than the decrease in the compressive strength. The main reason for this behaviour is the higher sensitivity of tensile strength to thermal micro and macro-cracks [13, 37, 48, 52]. Comparing the experimental dataset (green and grey clouds in Fig.2.6b) of concrete made with RCA and NA, a higher variation of RAC results is verified. In general, relative splitting tensile strengths for concrete made with RCA exceeded the results obtained for conventional concrete. Lastly, although the experimental results presented its maximum at 300 °C, Kou et al. [35] did not provide any specific explanation addressing this behaviour.

However, the general higher tensile strength values for RAC were not always the case in the literature. Similarly to the previous commented concrete properties, contradictory results are reported in the literature. Whereas some works [13, 48, 52] pointed out that the replacement rate did not significantly affect splitting tensile behaviour, other authors [37, 46, 59] related slightly worse behaviour when compared to concrete made with NA. Laneyrie et al. [37] attribute the deterioration in behaviour to the higher number of interfaces, which might in-

crease the development of cracks. According to Silva et al. [59], this behaviour is due to the higher amount of mortar in the concrete made with RCA. Contrarily, Sarhat and Sherwood [32] obtained different results. They observed an increase in the relative splitting tensile strength as the replacement rate increased. They attributed this behaviour to the low performance of the reference concrete with NA obtained from river gravel. Kou et al. [35] also observed some increase in the residual splitting tensile strength. They attributed this to the lower quantity of cracks around RCA (experimentally observed).

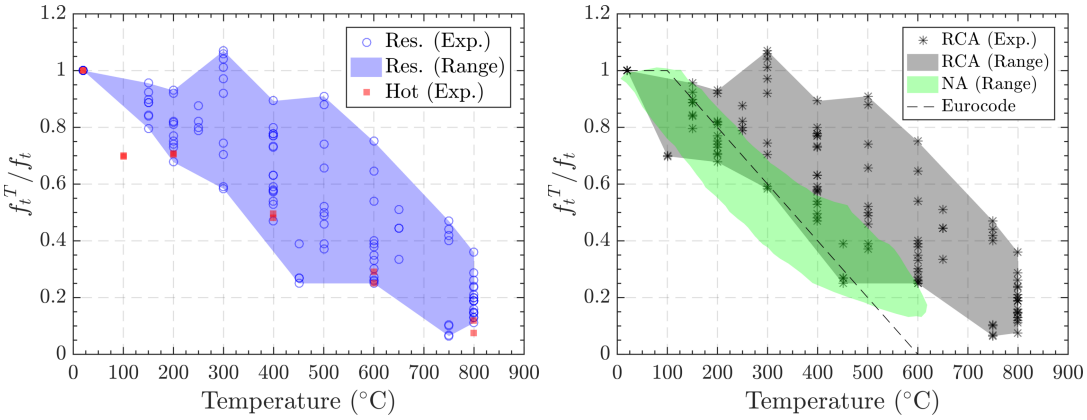

(a) all experimental values (b) comparision with NA and Eurocode 2

Figure 2.6: Relative splitting tensile strength of concrete made with RCA at elevated temperatures

Once again, Laneyrie et al. [37] highlighted the influence regarding the quality of the aggregates. Since they used industrial RCA in their concrete, their results presented weak tensile strengths due to the melting and burning of impurities, which left additional voids and cracks. Laneyrie et al. [37] also assessed the strength of concrete and pointed out that high strength concretes (i.e., with low w/c ratio) exhibited lower deterioration of the properties due to a better match between interfaces. Yang et al. [48], however, evaluated different w/c ratios and concluded that it made no difference in the relative residual splitting tensile strength.

2.3.4 Stress-strain relationship in compression

The stress-strain relationship expresses the mechanical response of concrete under an increasing compression load. The resulting curves are commonly used as an input to mathematical models to determine the fire resistance of concrete structures [28, 62]. Usually, stress-strain curves allow to determine compressive strength, elasticity modulus and peak strain. Many studies [34, 36, 38, 39, 42–47, 53, 58, 59] evaluated the stress-strain relationship of concrete made with RCA at elevated temperatures. In general, the shape and the differences caused by the temperature are very similar for both the RAC and concretes made with NA [18, 28]. As the temperature increase, stress-strain curves flatten, the peak stresses reduce, the slopes decrease and the strains at peak stresses increase. Fig.2.7

depicts this behaviour by presenting stress-strain curves obtained by Yang et al. [53].

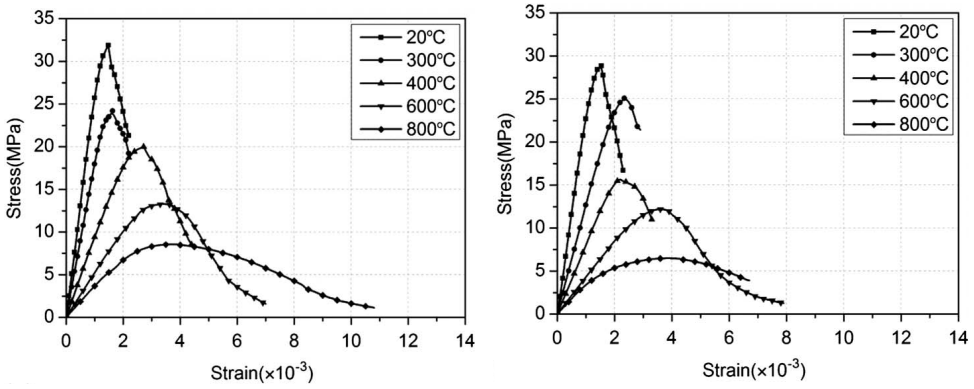

Figure 2.7: Stress-strain curves of concrete after heating: (a) concrete made with NA (b) concrete made with a 100 % replacement rate (adapted from Yang et al. [53])

Gales et al. [36] were the first ones to present hot stress-strain curves for concrete made with RCA. Strain properties were measured with digital image correlation (DIC), but only the ascending branch was recorded. The temperature dependency of the ascending branch was similar to ordinary concrete. In this study, concrete made with a higher replacement rate presented a lower slope and higher peak strain at elevated temperatures. Khaliq [46] also compared hot and residual stress-strain responses. To measure strains, LVDTs were attached to compression platens. The author concluded that high strength concrete made with RCA was more ductile than concrete made with NA, notably above 400 °C. Additionaly, Khaliq [46] comments that this behaviour is due to the high temperature dilatation and microstructure damage when compared with NA-HSC. Regarding the effect of the type of test, residual test samples presented a more ductile behaviour when compared with hot tests.

Zhao et al. [43] compared normalized (relative) curves and found out that concrete made with RCA registered lower energy absorption capacities when compared with concrete made with NA. Yang et al. [39] tested different replacement rates and did not observe significant differences for the stress-strain curves. Zhao et al. [58] evaluated the influence of fine RCA (0.15-4.75) in the stress-strain response of concrete and stated that the inclusion of fine RCA had an insignificant impact on the behaviour. Lastly, the addition of steel fibres in concrete made with RCA improves the high temperature mechanical behaviour, increasing the energy absorption capacity, as observed by Chen et al. [34], and the stiffness, as reported by Xie et al. [47].

2.3.5 Other mechanical properties

Different mechanical properties were studied in several works. For instance, Gales et al. [36] determined the Poisson's coefficient at hot state employing digital

image correlation (DIC) measurements of transverse and longitudinal strains. According to their research, For ambient temperature, the property is not affected by the presence of RCA. At 500 °C, however, the Poisson's ratio depends on the recycled aggregate content. Compared with ambient temperature, the Poisson's ratio increased for NA and for the mix with 30 % of replacement. For concrete with 100 % of RCA, the Poisson's ratio decreased with temperature. The authors suggested that the Poisson's ratio was dependent on the type of aggregate and the behaviour of the different ITZ inside the concrete.

Pliya et al. [60] also used DIC to measure thermal strains of concrete specimens under transient temperature tests. Different replacement rates (0 % and 30 % of both fine and coarse RCA) were exposed to high temperatures under different sustained pre-loading (40 % and 70 %). The authors [60] stated that the deformation depended on the pre-loading. Besides, it was observed that with 70 % of pre-loading, the transient thermal strains neutralize the effect of free thermal expansion, reversing the total strains from expansion to contraction. They also verified that thermal strains of concrete with NA were higher than concrete with RCA.

The deformation properties of heated RAC were also evaluated by Zhao et al. [67]. The authors assessed the free thermal strain for different replacement rates. In general, as the temperature increases, the thermal expansion increases. An abrupt increase at 500 °C was verified, related to the quartz transformation of siliceous aggregates. Zhao et al. [67] also observed that beyond 500 °C, thermal expansion significantly increases for concrete made with 50 % of RCA. They attribute this behaviour to the microcracking caused by the non-uniform thermal stresses between the two coarse aggregates (NA and RCA), as it did not for concretes with replacement rates of 0 % and 100 %.

Flexural behaviour of concrete made with RCA was first studied by Xiao et al. [33]. The authors observed that residual flexural strength gradually decreases with the increase of temperature and the effect of the replacement rate is not very significant. The property was also evaluated by Abed et al. [49, 54]. They verified the effect of replacement rate, cement-replacement materials and time in self-compacting concrete with RCA. The authors verified that residual flexural strength increased with the increase of RCA content, due to strong ITZ between aggregates and mortar and also due to the better thermal compatibility. The use of waste material (fly ash and perlite powder) as a replacement to cement also presented a little improvement, depending on the replacement rate.

Meng et al. [40] studied the triaxial compressive properties of concrete made with RCA at high temperatures. The triaxial stress state is usually occurs in concretes during accidental loads (shock, fire, earthquake), in reinforced concrete with spiral hoops or concrete inside steel stubes. When triaxial stress are applied, the residual compressive strength of the material increases due to the limitation of cracks and deformations by the confining stress. The authors [40] stated that, up to 400 °C, the triaxial strength of RAC specimens was not influenced by temperature. From this temperature on, the triaxial strength starts to decline. It is worthwhile mentioning that the deterioration of the triaxial strength is less severe than uniaxial compressive strength. Deng et al. [22] studied the biaxial

behaviour. They evaluated different stress ratios, different replacement rates, and different temperatures. The main conclusions were that the biaxial compressive strength decreased as the replacement rate increased. They asserted that this behaviour is associated with initial cracking presented in the RCA.

Shear behaviour of RAC at elevated temperature was evaluated by Yang et al. [68]. Authors evaluated residual shear properties after exposure to temperatures up to 400 °C. Their results revealed that shear modulus and peak secant shear modulus quickly decrease when exposed to high temperatures. Yang et al. [68] also pointed out that the replacement rate had minimal effect on the shear strength, although peak strain slightly increased. Fracture properties of concrete made with RCA, silica fume and fibres were evaluated by Wang et al. [57]. Three-point bending tests were performed on notched beams after heating. Wang et al. [57] concluded that concrete made with only RCA presented worse fracture properties. The addition of silical fume and steel fibres, however, improved this behaviour.

Lastly, some studies [30, 31, 44, 51] made some qualitative evaluations of mechanical properties of concrete made with RCA, such as ultrasonic pulse velocity (UPV). Zega and Di Maio [30, 31] reported that concrete made with RCA presented a lower reduction of UPV values at high temperatures than concrete made with NA. They attributed this behaviour to the better bond in the aggregate-mortar interface. Bui et al. [44] evaluated the effect of adding mineral admixtures and found that it did not affect UPV values. Authors [44] also reported that increase of the cement content improved UPV values of RAC at 500 °C. Abed et al. [55] evaluated the UPV of self-compacting concrete made with RCA with different replacement rates and cement replacement materials. The authors state that the incorporation of both waste materials improved the residual UPV, due to denser ITZ and better bond between mortar-mortar. Correlations with density, flexural strength and compressive strength were also given.

2.4 Thermal properties

Thermal properties govern the temperature diffusion inside the concrete; hence, these properties dictate the behaviour of concrete during heating (e.g., during a fire). Usually, thermal properties are defined in terms of thermal conductivity, specific heat and density. Thermal conductivity is the property related to heat conduction and is highly affected by moisture, porosity, and permeability. At room temperature, for concrete made with NA, thermal conductivity ranges between 1.4 and 3.6 W/mK. For concrete made with RCA, two works [37, 67] addressed this behaviour. They observed that thermal conductivity decreases as temperature increases. This decrease is higher up to 400 °C due to the intense loss of free and pore water in concrete in that range of temperature [67].

Laneyrie et al. [37] evaluated thermal conductivity using the hot disc method and revealed that, up to 900 °C, concrete made with RCA presented less thermal conductivity than concrete made with NA. They also reported that ordinary strength mixes made with RCA had 10 % lower thermal conductivity when compared with the high strength mixes. Zhao et al. [67] used a hot wire method to

evaluate thermal conductivity. Fig.2.8a depicts a comparison between the results from Zhao et al. [67], Laneyrie et al. [37], Eurocode 2 [61] and ASCE models . The results obtained by Zhao et al. [67] are similar to the ones from Laneyrie et al. [37] but are slightly higher than ones obtained from the models values [1]. The authors [67] also showed that increasing RCA content reduces thermal conductivity.

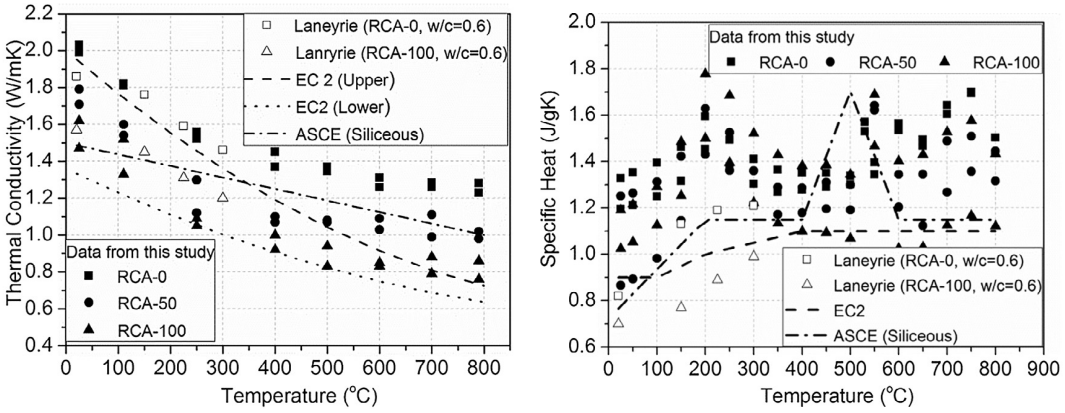

(a) Thermal Conductivity (b) Specific Heat

Figure 2.8: Thermal properties of concrete made with RCA [67]: comparison of experimental results [37, 67] and code models

Aiming to measure the specific heat of concrete made with RCA, Laneyrie et al. [37] employed hot disc method, whereas Zhao et al. [67] opted for the differential scanning calorimeter. The specific heat depends mainly on the physical and chemical transformations that occur in the concrete when heated. Beside, specific heat is highly affected by moisture content and w/b ratio [28, 62]. Laneyrie et al. [37] showed that specific heat of RAC slightly increased as temperature increased. Zhao et al. [67], however, obtained less clear results, revealing relevant discrepancies between different studies, as depicted in Fig.2.8b. Disparities were also observed while evaluating the influence of the replacement rate. Zhao et al. [67] concluded that coarse RCA did not significantly influence the specific heat of concrete at elevated temperatures. Additionally, the specific heat of RAC is, in general, higher than the specific heat obtained from EC2 and ASCE models.

Density evolution as function of the temperature was studied by Bui et al. [44], who recorded values at fresh state, 20 °C, 100 °C and 500 °C. At high temperatures, concrete made with RCA presented greater loss of density than concrete made with NA, due to the higher porosity of RCA. Density evolution is mainly driven by the mass loss due to water departure from the material, and mass loss of concrete made with RCA was also evaluated in literature [37, 45–47, 51]. In general, as RCA presents higher water content, concrete made with RCA will also present more significant mass losses than concrete with NA; hence a

[1]Corrigendum: Care should be taken when comparing experimental results with Eurocode 2 models. The lattter was obtained through inverse calibration and not using any experimental set-up to determine thermal properties of materials. Indeed, the final objective of the EC2 models is to predict the temperatures inside concrete members

more significant decrease of density as temperature increases.

2.5 Medium, full-scale and fire spalling tests

Usually, medium and full-scale fire tests consist of evaluating the behaviour of different concrete members subjected to a standard heating curve (e.g., ISO 834-1 [66]). Often called fire resistance tests, these tests aim to check the load bearing capacity, integrity and thermal insulation of concrete members during rapid heating. In addition to fire resistance tests, experiments concerning spalling, bond between RAC and steel rebars, and impact behaviour were observed in the literature.

Dong et al. [69] performed fire tests on columns made from RAC (100 % replacement) and concrete made with NA. The columns were subjected to ISO 834-1 [66] fire curve with a constant axial load. All tested columns failed due to large axial deformations. Dong et al. [69] reported that for the same compressive strength (C30), the fire resistance performance of concrete made with RCA (100 % replacement) was higher (118 min) than columns made of concrete made with NA (78 min) [2]. They attributed this to the higher moisture content of concrete made with RCA, which may dissipate heat through water evaporation (lower temperatures in cross-section were measured in concrete with RCA).

Within the French project "Recybeton", Robert et al. [70] carried out fire resistance tests on two RAC reinforced beams. One beam was made with 30 % of coarse aggregates and the other with 30 % of coarse and 30 % fine replacement. Beams were tested under ISO 834-1 [66] standard fire curve for 60 minutes. A comparison between the experimental bending moments and the bending moments assessed according to Eurocode 2 part 1-2 [61] revealed that experimental bending moments were higher than code previsions.

Robert et al. [70] also tested slabs to verify spalling and thermal diffusion within the thickness of slabs. Similarly to the prior experiments, two reference slabs and two slabs of concrete made with RCA (one with 30 % of coarse aggregates and the other with 30 % of coarse and 30 % fine replacement) were tested. All slabs were subjected to the ISO 834-1 [66] fire curve. As depicted in Fig.2.9, superficial and localized spalling was observed only in the slabs containing RCA. The authors [70] state that the spalling extent was not detrimental to the stability of the slabs. Additionally, Robert et al. [70] attributed the phenomenon to the high water content of RAC slabs.

Chen et al. [71] evaluated the mechanical behaviour of reinforced concrete and steel-reinforced concrete (i.e., composite) short columns and beams after exposure to elevated temperature. All the studied elements consisted of RAC with different replacement rates. The samples were initially heated inside an electrical furnace, then cooled and subjected to axial and three-point bending

[2] Corrigendum: Care should be taken when analyzing these results. Although the compared concretes have similar strengths, they have significant differences in cement and filler content. Indeed, the NA concrete used in the column that fails at 78 min had a low amount of cement - under the standards commonly used in Europe. Hence, any comparison of the fire resistance of these two concretes should also consider these parameters.

tests. The authors [71] verified a significant reduction in the bearing capacity of RAC short columns. They also reported that the shear properties deteriorated more significantly than flexural properties in their experiments. Additionally, Chen et al. [71] observed spalling in all samples heated up to 800 °C.

Pliya et al. [50] tested spalling sensitivity of high strength concrete made with NA and RCA (0 %, 15 % and 30 % replacement rate). To evaluate spalling, authors placed cylinder samples in a furnace and submitted them to a heating rate of 10 °C/min. The authors [50] reported progressive and explosive spalling, characterized by the sudden disintegration of all samples (i.e., either with or without RCA). It is worth noting that this heating rate is lower than the one expected during a real fire. Pliya et al. [60] reported a similar phenomenon in another study, in which they applied 70 % pre-loading when the surface temperature reached 150 °C.

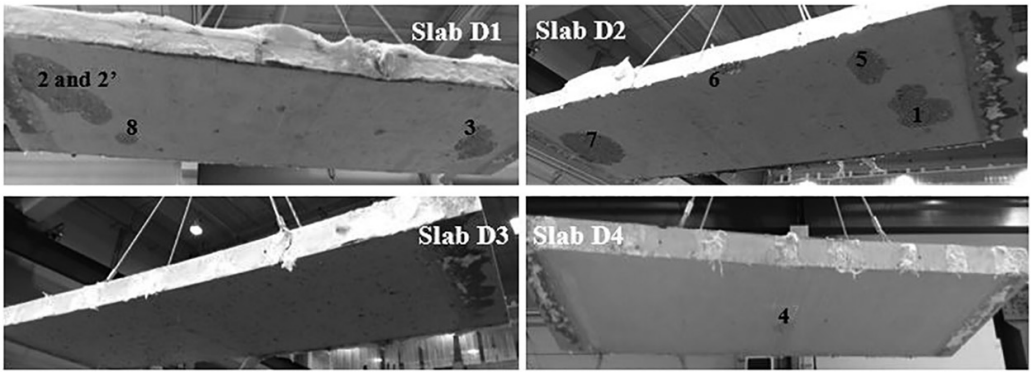

Figure 2.9: Slabs after ISO 834-1 [66] fire test: D1 and D2 are concrete with RCA; D3 and D4 are concrete with NA (adapted from Robert et al.[70])

Another aspect evaluated at elevated temperatures was the bond behaviour between concrete made with RCA and steel rebars. Yang et al. [68] evaluated post-heating bond for different replacement rates (0 % to 100 %) up to 500 °C. Results revealed that increasing RCA replacement increases the relative bond strength after temperature. The authors [68] stated that this increase can be associated with the similar elasticity modulus between RCA and cement paste, the better matching of thermal expansion and the higher moisture content.

The high temperature behaviour of recycled aggregate concrete-filled steel tubes (RACFST) was also studied [72–75]. This use is associated with the fact that RAC presents lower mechanical properties. Hence, confining them with steel tubes might overcome this drawback. Most of the authors [72, 73, 76] observed that RAC specimens presented inferior mechanical properties, such as compressive strength, composite (concrete and steel) elastic modulus, and larger deformations. In general, increasing the replacement rate leads to the degradation of concrete properties. They attribute this behaviour to the lower fire resistance of RAC when compared to NAC [76].

2.6 Microstructure of heated concrete made with RCA

In addition to mechanical and thermal properties, microstructure properties were also evaluated after heating. The experiments helped to understand the behaviour of concrete during heating and characterize the residual performance of concrete after cooling. The RAC microstructure was studied either by employing optical microscopy [42] or by applying scanning electron microscopy (SEM) [36, 46, 47, 50, 59].

SEM analysis by Gales et al. [36] focused on the ITZ of concretes made with different replacement rates after exposure to high temperature (500 °C/ with a heating rate of 2 °C/min) and mechanical load. The concrete made with 100 % replacement rate presented several microcracks at the interface between RCA and new mortar, which Gales et al. [36] attributed to thermal stresses. To support this affirmation, they studied the microstructure of samples submitted to mechanical load only (i.e., the samples were not heated) and noticed no cracks in the ITZ. Similarly, the heated specimens of concrete with NA did not showed cracks in the interface, indicating that RAC presented interfaces more prone to cracking. Additionally, Pliya et al. [50] evaluated ITZ of high-strength concrete (HSC) made with RCA with replacements rates of 15 % and 30 %. In both cases, microcracks were observed at the interface and in the new cement paste.

SEM observations made by Xie et al. [47] showed that at 200 °C, the microstructure of concrete made with RCA is almost unchanged. At 400 °C, however, hydration products tend to loosen and at 600 °C, C-S-H morphology starts to transform and CH starts to dehydrate. Finally, at 800 °C, cracks and voids are observed. Similar observations were done by Khaliq [46], who verified a loss of filling compounds due to dehydration.

Silva et al. [59] used SEM images to support their assumption that the decrease of physical properties of concrete (water absorption, mass loss, and density) after exposure to elevated temperature was related to the increase of the total mortar amount (new and attached mortar). Aiming to prove their point, Silva et al. [59] utilized the post-heating SEM observations depicted in Fig.2.10. As Fig.2.10 portrays, the higher porosity of RCA and the different interfaces led to bigger crack openings during the heating process.

Xuan et al. [42] used optical microscopy to evaluate mesocracks at the interfaces and in the mortar of concretes made with NA, RCA, and with carbonated RCA, after a thermal exposure of 600 °C. The idea behind using carbonated RCA relies on the reaction between CO_2 and the hydration products of cement in concrete. Such reactions produces $CaCO_3$, which might precipitate in pores and densify the microstructure [77]. The authors [42] observed that by using RCA and carbonated RCA, the mesocracks at the interface aggregate-mortar dissapeared, whereas the width of mesocracks in the mortar after heating decreased. They asserted that the thermal damage of concrete with NA is higher than concrete with RCA after heating up to 600 °C.

The porosity of concrete made with RCA was evaluated by means of water porosimetry [37] and mercury intrusion porosimetry (MIP) [35, 42]. Laneyrie et

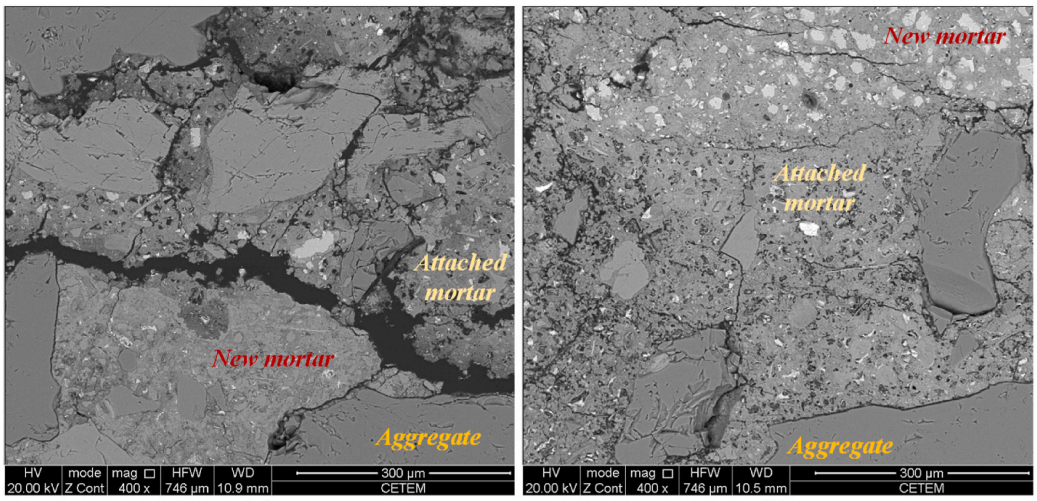

Figure 2.10: SEM images of concrete made with RCA after exposure to 650 °C: C25 (left) and C65 (right) (adapted from Silva et al.[59])

al. [37] pointed out that water porosity did not change significantly up to 300 °C. From this temperature on, a slight increase was observed. MIP results from Kou et al. [35] revealed that, at room temperature, concrete made with RCA was more porous than concrete made with NA. After heating up to 500 °C and 800 , however, conventional concrete presented increases in porosity and average pore diameter. According to Kou et al. [35], the initial porosity of RAC prevented the build-up of vapour pressure, reduce internal cracks, and improves the thermal compatibility between new mortar and old mortar (attached mortar).On the other hand, Xuan et al. [42] found out that RAC at 600 °C presented more porosity than concrete made with NA and carbonated RCA. They attributed this behaviour to the decomposition of hydration products from the cement mortar in RAC.

Capillary absorption, directly related to porosity, was also studied in previous research. Kou et al. [35] investigated capillary water absorption and found results that agree with MIP, i.e., a relative residual water absorption coefficient that was higher for RAC up to 500 °C. At 800 °C this behaviour shifted, as concrete made with NA presented a higher water absorption.

2.7 Summary and Conclusions

Based on this literature study, some highlights on the behaviour of concrete made with RCA at elevated temperatures can be drawn:

- All the mechanical properties deteriorate as temperature increases, similarly to concrete with NA. Relative residual compressive strength presented different phases - up to 300 °C, some properties remain quite constant and from this level up to 800 °C, all properties start to decrease significantly. For elastic modulus and splitting tensile strength decrease almost linearly

as temperature increases. For stress-strain curves, in general, increasing the temperature causes the curves to flatten.

- The influence of the RCA and the replacement rate on mechanical properties is not well defined. Some works reported a possible increase of the relative residual properties as replacement rate increases. Other results pointed out that the replacement rate makes no significant difference or is even slightly worse. The inferior mechanical behaviour of concrete made with RCA relies upon the peculiar porous microstructure of the RCA and the weaker interfacial transition zones. In contrast, the studies which observed superior behaviour attributed this to the better match of thermal expansion between RCA and cement paste.

- Test conditions, such as heating rate and test modality (residual/hot), influence the measurements of mechanical properties. Additionally, the results found in the literature were also contradictory, as some authors pointed out that residual tests resulted in higher values, whereas others indicated the opposite. Standardized specifications and test protocols are needed to develop reliable outcomes.

- As temperature increases, the thermal conductivity decreases and specific heat presents miscellaneous results. In general, the use of RCA has no significant influence on thermal properties.

- Full-scale tests were performed on slabs, and localized spalling was observed. The authors reported no significant influence on the structural behaviour was noticed. Additionally, full-scale tests were also performed on columns of concrete made with RCA. The results revealed better fire resistance ratings than concrete made with NA [3]. Beams of concrete made with RCA were also tested, and experimental bending moments before collapse were higher than code previsions.

- Microstructural observations pointed out that concrete made with RCA presented ITZs more brittle than concrete made with NA. SEM observations of concrete made with RCA also revealed dehydration of concrete hydrates. Additionally, some works reported that even if RAC presents high porosity, the increase of relative residual porosity is lower comparing with concrete made with NA. Similar behaviour was observed for the relative residual water absorption.

2.8 Research needs

Based on this literature review, the following research needs and recommendations are proposed:

[3]Corrigendum: As commented, care should be taken when analyzing the fire resistance results. The work [69] from which these conclusions were drawn compared concretes with similar strengths but significant differences in cement content.

- Only a limited amount of works measured the mechanical properties at the hot state. Understanding the material behaviour at the hot state is crucial for predicting its performance during an actual fire.
- Deformation properties are another fundamental aspect to understand the concrete behaviour at high temperatures. Moreover, understanding the total strain of concrete made with RCA during heating is crucial to develop realistic computations. The deformation properties comprise the free thermal strain, the elastic strain, and the transient thermal strain.
- The spalling behaviour of concrete made with RCA should be studied more deeply, as it is fundamental for understanding the fire behaviour of concrete structures. Although some works reported spalling in concrete made with RCA (either normal or high-strength), it is yet to be found whether this behaviour is related to the aggregates or other parameters, e.g., the dense microstructure of HSC or water content. The effect of different replacement rates on spalling extent should also be studied.
- More full-scale fire tests are needed. Previous works related a similar behaviour between RAC and concrete made with NA, however, further research with different structural members and testing parameters are needed.
- No numerical modelling of concrete made with RCA at high temperatures was found in the literature. Mesoscale models, including the different phases of concrete made with RCA, should be used for thermo-mechanical simulations.
- Further microstructural observations are needed for an in-depth understanding of the post-fire behaviour of RAC. X-ray diffraction (XRD), differential thermal analysis (DTA), X-ray computed tomography would improve the knowledge regarding the behaviour and the differences between concrete made with RCA and NA at high temperatures.

References

[1] G. Habert, S. Miller, V. John, J. Provis, A. Favier, A. Horvath, et al. "Environmental impacts and decarbonization strategies in the cement and concrete industries". In: *Nature Reviews Earth & Environment* 1.11 (2020), pp. 559–573.

[2] M. K. Dixit, J. L. Fernández-Solís, S. Lavy, and C. H. Culp. "Identification of parameters for embodied energy measurement: A literature review". In: *Energy and Buildings* 42.8 (2010), pp. 1238–1247. DOI: 10.1016/j.enbuild.2010.02.016.

[3] Eurostat. *Energy, transport and environment indicators. 2018 Edition*. 2018, p. 232.

[4] S. Böhmer, G. Moser, C. Neubauer, M. Peltoniemi, E. Schachermayer, M. Tesar, et al. *Aggregates case study*. Tech. rep. 2008, p. 282.

[5] F. de Larrard and H. Colina. "Introduction". In: *Concrete Recycling: Research and Practice*. Ed. by F. de Larrad and H. Colina. CRC Press, 2019, pp. 1–4.

[6] N. Tošić, S. Marinković, T. Dašić, and M. Stanić. "Multicriteria optimization of natural and recycled aggregate concrete for structural use". In: *Journal of Cleaner Production* 87.1 (2015), pp. 766–776. DOI: 10.1016/j.jclepro.2014.10.070.

[7] M. Amario, C. S. Rangel, M. Pepe, and R. D. Toledo Filho. "Optimization of normal and high strength recycled aggregate concrete mixtures by using packing model". In: *Cement and Concrete Composites* 84 (2017), pp. 83–92. DOI: 10.1016/j.cemconcomp.2017.08.016.

[8] H.-b. Le and Q.-b. Bui. "Recycled aggregate concretes – A state-of-the-art from the microstructure to the structural performance". In: *Construction and Building Materials* 257 (2020), p. 119522. DOI: 10.1016/j.conbuildmat.2020.119522.

[9] R. Wang, N. Yu, and Y. Li. "Methods for improving the microstructure of recycled concrete aggregate : A review". In: *Construction and Building Materials* 242 (2020), p. 118164. DOI: 10.1016/j.conbuildmat.2020.118164.

[10] M. Behera, S. K. Bhattacharyya, A. K. Minocha, R. Deoliya, and S. Maiti. "Recycled aggregate from C&D waste & its use in concrete - A breakthrough towards sustainability in construction sector: A review". In: *Construction and Building Materials* 68 (2014), pp. 501–516. DOI: 10.1016/j.conbuildmat.2014.07.003.

[11] R. V. Silva, J. De Brito, and R. K. Dhir. "Properties and composition of recycled aggregates from construction and demolition waste suitable for concrete production". In: *Construction and Building Materials* 65 (2014), pp. 201–217. DOI: 10.1016/j.conbuildmat.2014.04.117.

[12] F. de Larrard and H. Colina. "Conclusion". In: *Concrete Recycling: Research and Practice*. Ed. by F. de Larrad and H. Colina. CRC Press, 2019, pp. 544–545.

[13] J. Vieira, J. Correia, and J. De Brito. "Post-fire residual mechanical properties of concrete made with recycled concrete coarse aggregates". In: *Cement and Concrete Research* 41.5 (2011), pp. 533–541.

[14] P. Pimienta, M. C. Alonso, R. Jansson McNamee, and J.-C. Mindeguia. "Behaviour of high-performance concrete at high temperatures: some highlights". In: *RILEM Technical Letters* 2.2017 (2017), p. 45. DOI: 10.21809/rilemtechlett.2017.53.

[15] M. C. Alonso and U. Schneider. "Degradation Reactions in Concretes Exposed to High Temperatures". In: *Physical Properties and Behaviour of High-Performance Concrete at High Temperature*. Springer, 2019, pp. 5–40.

[16] D. J. Naus. *The effect of elevated temperature on concrete materials and structures - A literature review*. Tech. rep. 2005.

[17] M. Malik, S. K. Bhattacharyya, and S. V. Barai. "Thermal and mechanical properties of concrete and its constituents at elevated temperatures : A review". In: *Construction and Building Materials* 270 (2021), p. 121398. DOI: 10.1016/j.conbuildmat.2020.121398.

[18] Q. Ma, R. Guo, Z. Zhao, Z. Lin, and K. He. "Mechanical properties of concrete at high temperature-A review". In: *Construction and Building Materials* 93 (2015), pp. 371–383. DOI: 10.1016/j.conbuildmat.2015.05.131.

[19] I. Hager. "Behaviour of cement concrete at high temperature". In: *Bulletin of the Polish Academy of Sciences: Technical Sciences* 61.1 (Jan. 2013), pp. 1–10. DOI: 10.2478/bpasts-2013-0013.

[20] *fib Bulletin 46: Fire design of concrete structures — structural behaviour and assessment*. Tech. rep. Lausanne, Swiss, 2008, p. 209.

[21] G. A. Khoury. "Effect of fire on concrete and concrete structures". In: *Progress in Structural Engineering and Materials* 2.4 (2000), pp. 429–447. DOI: 10.1061/41016(314)299.

[22] Z. H. Deng, H. Q. Huang, B. Ye, H. Wang, and P. Xiang. "Investigation on recycled aggregate concretes exposed to high temperature by biaxial compressive tests". In: *Construction and Building Materials* 244 (2020), p. 118048. DOI: 10.1016/j.conbuildmat.2020.118048.

[23] R. Niry, A.-l. Beaucour, R. L. Hebert, B. Ledesert, R. Bodet, and A. Noumowe. "High temperature behaviour of a wide petrographic range of siliceous and calcareous aggregates for concretes". In: *Construction and Building Materials* 123 (2016), pp. 261–273. DOI: 10.1016/j.conbuildmat.2016.06.097.

[24] R. Niry Razafinjato. "Comportement des bétons à haute température : influence de la nature du granulat". PhD thesis. Université de Cergy-Pontoise, 2015, p. 320.

[25] J.-C. Mindeguia, H. Carré, P. Pimienta, and C. La Borderie. "Experimental discussion on the mechanisms behind the fire spalling of concrete". In: *Fire and Materials* 39.7 (2014), pp. 619–635. DOI: 10.1002/fam.2254.

[26] M. Maier, A. Saxer, K. Bergmeister, and R. Lackner. "An experimental fire-spalling assessment procedure for concrete mixtures". In: *Construction and Building Materials* 232 (2020), p. 117172. DOI: 10.1016/j.conbuildmat.2019.117172.

[27] M. Maier, M. Zeiml, and R. Lackner. "On the effect of pore-space properties and water saturation on explosive spalling of fire-loaded concrete". In: *Construction and Building Materials* 231 (2020), p. 117150. DOI: 10.1016/j.conbuildmat.2019.117150.

[28] V. Kodur. "Properties of Concrete at Elevated Temperatures". In: *ISRN Civil Engineering* 2014 (2014), pp. 1–15. DOI: 10.1155/2014/468510.

[29] V. Kodur, S. Banerji, and R. Solhmirzaei. "Test methods for characterizing concrete properties at elevated temperature". In: *Fire and Materials* September (2019), pp. 1–15. DOI: 10.1002/fam.2777.

[30] C. Zega and A. Di Maio. "Recycled concrete exposed to high temperatures". In: *Magazine of Concrete Research* 58.10 (2006), pp. 675–682.

[31] C. J. Zega and A. A. Di Maio. "Recycled concrete made with different natural coarse aggregates exposed to high temperature". In: *Construction and building materials* 23.5 (2009), pp. 2047–2052.

[32] S. R. Sarhat and E. G. Sherwood. "Residual mechanical response of recycled aggregate concrete after exposure to elevated temperatures". In: *Journal of Materials in Civil Engineering* 25.11 (2013), pp. 1721–1730.

[33] J. Xiao, Y. Fan, and M. Tawana. "Residual compressive and flexural strength of a recycled aggregate concrete following elevated temperatures". In: *Structural Concrete* 14.2 (2013), pp. 168–175.

[34] G. Chen, Y. He, H. Yang, J. Chen, and Y. Guo. "Compressive behavior of steel fiber reinforced recycled aggregate concrete after exposure to elevated temperatures". In: *Construction and Building Materials* 71 (2014), pp. 1–15.

[35] S. C. Kou, C. S. Poon, and M. Etxeberria. "Residue strength, water absorption and pore size distributions of recycled aggregate concrete after exposure to elevated temperatures". In: *Cement and concrete composites* 53 (2014), pp. 73–82.

[36] J. Gales, T. Parker, D. Cree, and M. Green. "Fire performance of sustainable recycled concrete aggregates: mechanical properties at elevated temperatures and current research needs". In: *Fire Technology* 52.3 (2016), pp. 817–845.

[37] C. Laneyrie, A.-L. Beaucour, M. F. Green, R. L. Hebert, B. Ledesert, and A. Noumowe. "Influence of recycled coarse aggregates on normal and high performance concrete subjected to elevated temperatures". In: *Construction and Building Materials* 111 (2016), pp. 368–378.

[38] Y. Liu, W. Wang, Y. F. Chen, and H. Ji. "Residual stress-strain relationship for thermal insulation concrete with recycled aggregate after high temperature exposure". In: *Construction and Building Materials* 129 (2016), pp. 37–47.

[39] H. Yang, L. Lv, Z. Deng, and W. Lan. "Residual compressive stress-strain relation of recycled aggregate concrete after exposure to high temperatures". In: *Structural Concrete* 18.3 (2017), pp. 479–486.

[40] E. Meng, Y. Yu, J. Yuan, K. Qiao, and Y. Su. "Triaxial compressive strength experiment study of recycled aggregate concrete after high temperatures". In: *Construction and Building Materials* 155 (2017), pp. 542–549.

[41] F. U. A. Shaikh. "Mechanical properties of concrete containing recycled coarse aggregate at and after exposure to elevated temperatures". In: *Structural Concrete* 19.2 (2018), pp. 400–410.

[42] D. Xuan, B. Zhan, and C. S. Poon. "Thermal and residual mechanical profile of recycled aggregate concrete prepared with carbonated concrete aggregates after exposure to elevated temperatures". In: *Fire and Materials* 42.1 (2017), pp. 134–142.

[43] H. Zhao, Y. Wang, and F. Liu. "Stress–strain relationship of coarse RCA concrete exposed to elevated temperatures". In: *Magazine of Concrete Research* 69.13 (2017), pp. 649–664.

[44] N. K. Bui, T. Satomi, and H. Takahashi. "Effect of mineral admixtures on properties of recycled aggregate concrete at high temperature". In: *Construction and Building Materials* 184 (2018), pp. 361–373.

[45] Z. Chen, J. Chen, F. Ning, and Y. Li. "Residual properties of recycled concrete after exposure to high temperatures". In: *Magazine of Concrete Research* (2018), pp. 1–13.

[46] W. Khaliq et al. "Mechanical and physical response of recycled aggregates high-strength concrete at elevated temperatures". In: *Fire safety journal* 96 (2018), pp. 203–214.

[47] J. Xie, Z. Zhang, Z. Lu, and M. Sun. "Coupling effects of silica fume and steel-fiber on the compressive behaviour of recycled aggregate concrete after exposure to elevated temperature". In: *Construction and Building Materials* 184 (2018), pp. 752–764.

[48] H. Yang, H. Zhao, and F. Liu. "Residual cube strength of coarse RCA concrete after exposure to elevated temperatures". In: *Fire and Materials* 42.4 (2018), pp. 424–435.

[49] M. Abed and R. Nemes. "The impact of time on the heat resistance of self-compacting high- performance concrete incorporated with recycled martials". In: *Journal of Thermal Analysis and Calorimetry volume* 138 (2019), pp. 35–45. DOI: 10.1007/s10973-019-08263-z.

[50] P. Pliya, D. Cree, H. Hajiloo, A.-L. Beaucour, M. Green, and A. Noumowé. "High-Strength Concrete Containing Recycled Coarse Aggregate Subjected to Elevated Temperatures". In: *Fire Technology* (2019), pp. 1–18.

[51] H. Salahuddin, A. Nawaz, A. Maqsoom, T. Mehmood, et al. "Effects of elevated temperature on performance of recycled coarse aggregate concrete". In: *Construction and Building Materials* 202 (2019), pp. 415–425.

[52] Y. Wang, F. Liu, L. Xu, and H. Zhao. "Effect of elevated temperatures and cooling methods on strength of concrete made with coarse and fine recycled concrete aggregates". In: *Construction and Building Materials* 210 (2019), pp. 540–547. DOI: 10.1016/j.conbuildmat.2019.03.215.

[53] H. Yang, H. Zhao, and F. Liu. "Compressive Stress-Strain Relationship of Concrete Containing Coarse Recycled Concrete Aggregate at Elevated Temperatures". In: *Journal of Materials in Civil Engineering* 31.9 (2019), pp. 1–8. DOI: 10.1061/(ASCE)MT.1943-5533.0002851.

[54] M. Abed, R. Nemes, D. Ph, É. Lubl, and D. Ph. "Performance of Self-Compacting High- Performance Concrete Produced with Waste Materials after Exposure to Elevated Temperature". In: *Journal of Materials in Civil Engineering* 32.2008 (2020), pp. 1–10. DOI: 10.1061/(ASCE)MT.1943-5533.0002989.

[55] M. Abed and J. D. Brito. "Evaluation of high-performance self-compacting concrete using alternative materials and exposed to elevated temperatures by non-destructive testing". In: *Journal of Building Engineering* 32 (2020), p. 101720. DOI: 10.1016/j.jobe.2020.101720.

[56] F. B. Varona, F. Baeza-brotons, A. J. Tenza-abril, and F. J. Baeza. "Residual Compressive Strength of Recycled Aggregate Concretes after High Temperature Exposure". In: *Materials* (2020).

[57] J. Wang, J. Xie, J. He, M. Sun, J. Yang, and L. Li. "Combined use of silica fume and steel fibre to improve fracture properties of recycled aggregate concrete exposed to elevated temperature". In: *Journal of Material Cycles and Waste Management* 22.3 (2020), pp. 862–877. DOI: 10.1007/s10163-020-00990-y.

[58] H. Zhao, F. Liu, and H. Yang. "Residual compressive response of concrete produced with both coarse and fine recycled concrete aggregates after thermal exposure". In: *Construction and Building Materials* 244 (2020), p. 118397. DOI: 10.1016/j.conbuildmat.2020.118397.

[59] J. B. da Silva, M. Pepe, and R. D. Toledo Filho. "High temperatures effect on mechanical and physical performance of normal and high strength recycled aggregate concrete". In: *Fire Safety Journal* 117.August (2020). DOI: 10.1016/j.firesaf.2020.103222.

[60] P. Pliya, H. Hajiloo, S. Romagnosi, D. Cree, S. Sarhat, and M. F. Green. "The compressive behaviour of natural and recycled aggregate concrete during and after exposure to elevated temperatures". In: *Journal of Building Engineering* 38.June 2020 (2021), p. 102214. DOI: 10.1016/j.jobe.2021.102214.

[61] *Design of concrete structures - Part 1-2: General rules - Structural fire design*. Comité Européen de Normalisation. Brussels, 2004, p. 99.

[62] M. Abid, X. Hou, W. Zheng, and R. R. Hussain. "High temperature and residual properties of reactive powder concrete – A review". In: *Construction and Building Materials* 147.519 (2017), pp. 339–351. DOI: 10.1016/j.conbuildmat.2017.04.083.

[63] M. Colombo and R. Felicetti. "New NDT techniques for the assessment of fire-damaged concrete structures". In: *Fire Safety Journal* 42.6-7 (2007), pp. 461–472. DOI: 10.1016/j.firesaf.2006.09.002.

[64] R. T. C. 2.-H. U. schneider@ tuwien. ac. at. "Recommendation of RILEM TC 200-HTC: mechanical concrete properties at high temperatures—modelling and applications: Part 2: Stress–strain

relation". In: *Materials and Structures* 40 (2007), pp. 855–864.

[65] D. Cree, M. Green, and A. Noumowé. "Residual strength of concrete containing recycled materials after exposure to fire: A review". In: *Construction and Building Materials* 45 (2013), pp. 208–223. DOI: 10.1016/j.conbuildmat.2013.04.005.

[66] *Fire-resistance tests — Elements of building construction — Part 1: General requirements*. International Organization for Standardization. Geneva, 1999.

[67] H. Zhao, F. Liu, and H. Yang. "Thermal properties of coarse RCA concrete at elevated temperatures". In: *Applied Thermal Engineering* 140 (2018), pp. 180–189.

[68] H. Yang, Y. Qin, Y. Liao, and W. Chen. "Shear behavior of recycled aggregate concrete after exposure to high temperatures". In: *Construction and Building Materials* 106 (2016), pp. 374–381.

[69] H. Dong, W. Cao, J. Bian, and J. Zhang. "The fire resistance performance of recycled aggregate concrete columns with different concrete compressive strengths". In: *Materials* 7.12 (2014), pp. 7843–7860.

[70] F. Robert, A.-L. Beaucour, and H. Colina. "Behavior Under Fire". In: *Concrete Recycling: Research and Practice*. Ed. by F. De Larrard and H. Colina. CRC Press, 2019. Chap. 13, p. 13.

[71] Z. Chen, J. Zhou, P. Ye, and Y. Liang. "Analysis on Mechanical Properties of Recycled Aggregate Concrete Members after Exposure to High Temperatures". In: *Applied Sciences* (2019). DOI: 10.3390/app9102057.

[72] Y. Yang and R. Hou. "Experimental behaviour of RACFST stub columns after exposed to high temperatures". In: *Thin-Walled Structures* 59 (2012), pp. 1–10.

[73] W. Liu, W. Cao, J. Zhang, R. Wang, and L. Ren. "Mechanical behavior of recycled aggregate concrete-filled steel tubular columns before and after fire". In: *Materials* 10.3 (2017), p. 274.

[74] W. Li, Z. Luo, C. Wu, V. W. Tam, W. H. Duan, and S. P. Shah. "Experimental and numerical studies on impact behaviors of recycled aggregate concrete-filled steel tube after exposure to elevated temperature". In: *Materials & Design* 136 (2017), pp. 103–118.

[75] W. Li, Z. Luo, C. Wu, and W. H. Duan. "Impact performances of steel tube-confined recycled aggregate concrete (STCRAC) after exposure to elevated temperatures". In: *Cement and Concrete Composites* 86 (2018), pp. 87–97.

[76] W. Li, Z. Luo, Z. Tao, W. H. Duan, and S. P. Shah. "Mechanical behavior of recycled aggregate concrete-filled steel tube stub columns after exposure to elevated temperatures". In: *Construction and Building Materials* 146 (2017), pp. 571–581.

[77] D. Xuan, B. Zhan, and C. S. Poon. "Assessment of mechanical properties of concrete incorporating carbonated recycled concrete aggregates". In: *Cement and Concrete Composites* 65 (2016), pp. 67–74. DOI: 10.1016/j.cemconcomp.2015.10.018.

Chapter 03

Materials, mix design and samples overview

This section presents the materials and methods related to the mix design of concrete made with RCA. This chapter specifies the general behaviour of concrete made with RCA, detailing the materials, mixture procedures, fresh properties, and hardened properties at 28 days. This chapter also gives an overview of all tests and samples produced during the project. Given the thesis structure, the remaining specific experimental procedures (residual properties and fire tests) will be described in their respective chapters (Chapters 04 to 07).

3.1 Materials

The materials used in this project are cement, filler, fine aggregates (sand), coarse aggregates (natural aggregates and recycled concrete aggregates), superplasticizer and water. All of them were supplied by the partner companies of the project. The following sections present all materials' descriptions and properties.

3.1.1 Cement

The cement used in this research was a CEM II/A-L 42.5R, produced by the Eqiom company at La Rochelle (France). It has a specific strength of 54 MPa at 28 days, a density of 3010 kg/m^3 and a specific surface of 4700 cm^2/g. The cement is composed of clinker (91 %), limestone (8 %) and secondary constituents (1 %). Table 3.1 presents its chemical composition.

Table 3.1: Cement chemical composition

Property/Element	Weight (%)
Ignition loss	4.2
Insoluble residue	0.6
SiO_2	18.4
Al_2O_3	4.5
Fe_2O_3	3.5
CaO	62.9
MgO	2
SO_3	2.6
K_2O	0.8
Na_2O	0.22
S^-	0.01
Cl^-	0.02
CaO free	1.3
Na_2O eq. active	0.75

3.1.2 Filler

A limestone filler (Omya Betocarb HP-SC) was used. This filler presents a density of 2700 kg/m^3 and a specific surface of 4330 cm^2/g. Its fine content (less than 63 µm) is 79 %.

3.1.3 Superplasticizer

A polycarboxylate-based superplasticizer (SIKA ViscoCrete Tempo-483) was used in the mixes. It has a density of 1065 kg/m^3 and a dry content of 30 %.

3.1.4 Aggregates

This study used alluvial sand obtained from Passirac (France) as fine aggregates. The sand fraction is 0/4 mm and presents a fineness modulus of 3.10. Natural aggregates were made from diorite (Genouillac, France) and divided into two fractions, 4/10 and 10/20. Both sand and coarse aggregates were extracted and produced by the Groupe Garandeau. Recycled concrete aggregates were crushed and screened near Bordeaux (France) by the recycling company Guyenne Environnement (Groupe Cassous). They were divided into the same fractions as NA. Grading curves of fine and coarse aggregates are presented in Fig. 3.1.

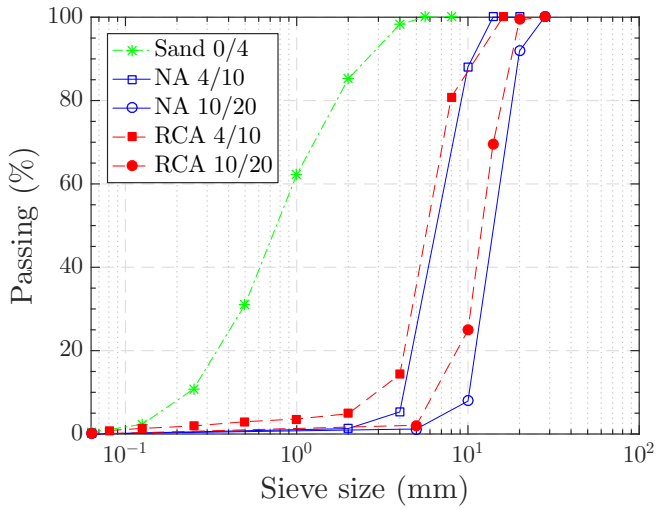

Figure 3.1: Grading curves of sand, natural and recycled coarse aggregates

Physical properties of aggregates(NA, RCA and sand) were measured by the supplier and partner company (Groupe Garandeau). Density, water absorption and LA coefficient were measured according to EN 1097-2:2010 [1] and EN 1097-6:2013 [2]. Table 3.2 presents all obtained results. As expected, RCA presented higher water absorption and a lower LA coefficient, mainly due to adhered mortar.

Table 3.2: Aggregate properties

Property	Sand	Natural aggregate		Recycled aggregate	
Grading Size	0/4	4/10	10/20	4/10	10/20
Density (kg/m^3)	2650	2820	2840	2570	2590
Water absorption (%)	0.35	0.92	0.81	5.60	4.52
LA coefficient (%)	-	16	16	30	36

Since RCA were obtained from a recycling plant, they presented some impurities related to demolition wastes, such as wood, plastic, brick and bituminous materials. A manual sorting was done to quantify these impurities, following EN 933-11:2009 [3]. Before manual sorting, a quartering process was done, following the NF EN 932-1 [4] and the NF EN 932-2 [5]. Then the manual sorting was

conducted, separating the aggregates into the different sub-classes proposed by EN 933-11:2009 [3]. Table 3.3 presents the results from this classification. Considering the NF EN 206/CN:2014 [6] classification, the aggregates used in this project were Type 3 due to the high quantity of bituminous grains

Table 3.3: RCA constituents

Aggregate Fraction	Constituents (% of mass)*					
	Rc	Ru	Rb	Ra	Rg	X
RCA 4/10	73.3	24.0	0.5	2.1	-	0.1
RCA 10/20	76.8	18.6	0.5	3.8	0.1	0.2

*Rc is concrete grains; Ru is natural stones; Rb is ceramic elements; Ra is bituminous grains; Rg is glass and X is other materials (wood, plastics, steel, papers and others)

3.2 Mix design

The design of mixtures was planned based on the partner company's current approaches and standard requisitions. The mixes were divided into three categories: reference, direct replacement (DR) and strength-based replacement (SBR).

The first one refers to concrete made with NA. It was designed to meet NF EN 206/CN:2014 [6] durability requirements for the XD3 exposure class. It refers to corrosion induced by chlorides with cyclic wetting and drying. This class is one of the most used in the company and also refers to car parking slabs. Hence, following NF EN 206/CN:2014 [6] specifications, the reference concrete was designed considering a maximum water/cement (w/c) ratio of 0.5, a compressive strength class of C35/45 and a minimum cement content of 350 kg/m^3. For slump, the partner company specifies a minimum of 150 mm.

In direct replacement (DR) mixes, NA were replaced by RCA in volume, without any changes in other constituents. Replacement rates for this mix were chosen based on RECYBETON [7] French project recommendations, which, for XD3 exposure classe, allows maximum replacement rates of 20 % and 40 %. Additional replacement rates of 10 % and 100 % were also studied for DR mixes. For strength-based replacement (SBR) mixes, cement paste was adjusted besides aggregate replacement to obtain the same performance (compressive strength at 28 days) as the reference concrete (made with NA). For these mixes, replacement rates of 40 % and 100 % were studied.

The mix design of SBR mixes was done using BetonLab Software [8]. This software runs simulations based on the Compressible Packing Model (CPM), developed by De Larrard [9]. This method describes the packing density obtained by a particular granular mixture, considering all the interactions between grains [10, 11]. To this, BetonLab requires the introduction of different materials properties, ranging from granulometry to different semi-empirical coefficients. Especially, the aggregates coefficients p and q describe their contribution to concrete compressive strength and are fundamental among the parameters.

In this project, p and q parameters were determined based on compressive strength results of reference and DR mixes. Usual p and q values were chosen and then manually adjusted to obtain approximately the same compressive strength observed in the trial mixes. It is noteworthy that among the factors, p is the one that affects more the compressive strength. After calibration of p and q values, SBR mixes were designed. First, the w/c ratio was adjusted for each replacement rate to achieve the same compressive strength of the reference mix. Then, cement content and water were adjusted to achieve target consistency (defined as between 180 mm and 190 mm). This adjustment in cement paste was made while keeping the w/c constant. Trial mixes were done to verify and adjust the superplasticizer content. Fig 3.2 presents the performance results of the calibration, with the points indicating the average experimental values and the lines representing the BetonLab predictions after adjustments. Further details of properties will be given in Section 3.4.

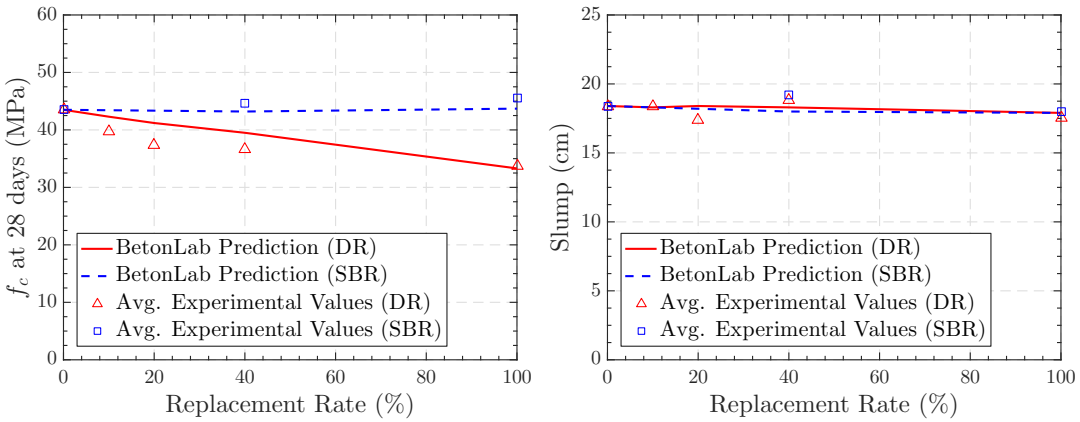

(a) compressive strength (b) slump

Figure 3.2: Results from calibration with BetonLab [8]

Table 3.4 presents the mixture proportions for all studied mixes. It is noteworthy that each experimental campaign used different replacement rates, i.e., not all of them were used for all experiments. In any case, further details are given in in Section 3.5 and each chapter/paper.

Table 3.4: Mix proportions (in kg/m^3, SP in % of cement mass)

Material	Mix						
	NA	RCA-10-DR	RCA-20-DR	RCA-40-DR	RCA-100-DR	RCA-40-SBR	RCA-100-SBR
Cement	350	350	350	350	350	368	420
Filler	60	60	60	60	60	60	60
Sand	804.3	804.3	804.3	804.3	804.3	787.1	799.8
NA 4/10	331.7	298.5	265.3	199.0	-	207.2	-
NA 10/20	711.1	640.0	568.9	426.7	-	447.5	-
RCA 4/10	-	30.2	60.5	120.9	302.3	114.7	291.5
RCA 10/20	-	64.9	129.7	259.4	648.5	248.1	630.3
Water	175	175	175	175	175	172	168
SP	0.9	0.9	0.9	0.9	0.9	0.9	0.9

3.3 Mixing procedure

When using RCA, one of the main concerns comes from their high water absorption (close to 5 % [12]). Indeed this property may affect the workability of concrete, even when moisture adjustments are made to the mixes [13]. Previous works proposed different methodologies [11, 14] to prevent the decrease in fresh properties. Saturation, pre-wetting (or pre-humidification), mixing and compensation methods were proposed, but there is no standardized approach. Aiming for a method that can be reproduced in the concrete plant of the partner company, it was chosen to work with wet-aggregates in all mixes. To this, all aggregates (sand, NA and RCA) were first pre-wetted for a specific time (wetting time) using a perforated soaker hose. This perforated hose was placed on each big bag containing the aggregates. After the wetting time, the aggregates were covered with a plastic sheet (resting time). Before casting, the moisture content of aggregates was measured to adjust the water quantity of concrete mixes.

The pre-conditioning approach was tested with different wetting and resting times: 1 hour of wetting (1h), 3 hours of wetting (3h), 1 hour of wetting and 2 hours of resting (1h+2h), and 1 hour of wetting and 3 hours of resting (1h+3h). Fig. 3.3a presents the results for all used aggregates. The water content was measured with the frying pan method (the same used in the company). Results indicate that all the procedures induced water content higher than absorption for all aggregates. Finally, it was chosen to work with 1 hour of wetting and 3 hours of resting since it produced values closer to the saturation state. The results of water content measured with the pan were also compared with the oven-dried method (Fig. 3.3b), specified in NF EN 1097-5 [15]. Results show that water content is similar when measured by both ways.

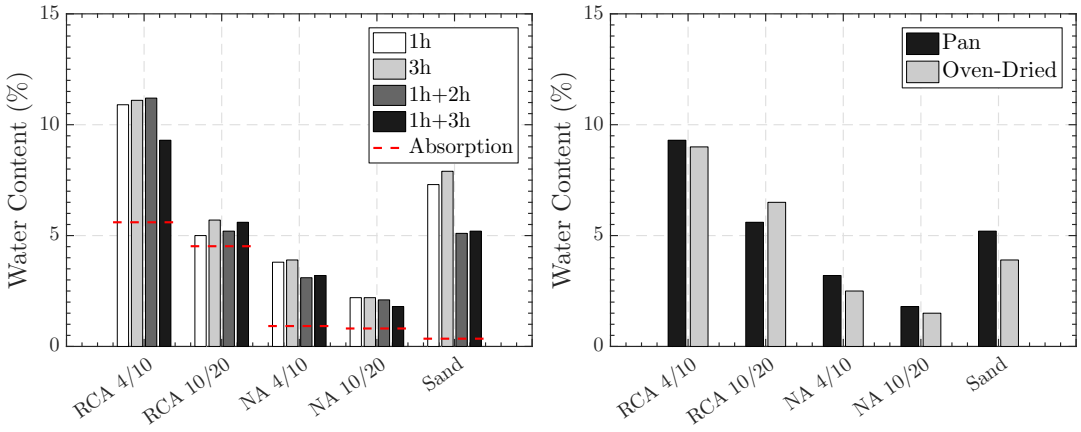

(a) wetting approach comparison (b) measurement method comparision

Figure 3.3: Effect of pre-conditioning methods of aggregates on their water content

Preliminary castings were done using the wetting procedure, measuring the water content and correcting the mixing water. However, during these initial studies, a significant variation was observed in workability and compressive

strength, even for the same mixes. Fig 3.4 presents the results obtained with concrete made with NA and RCA (RCA-100-DR) casted at different days. As seen in the figure, concrete mixes showed relevant variations in properties, despite the fact that the same wetting, measuring and corrections were made. At the same time, the relation between slump and compressive strength is obvious in these trials.

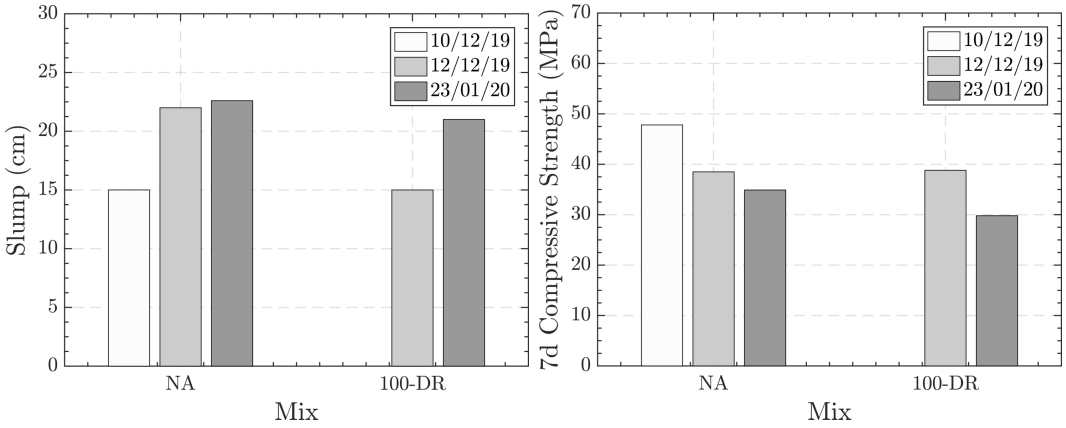

(a) slump (b) 7 days compressive strength

Figure 3.4: Effect of pre-conditioning methods of aggregates on their water content

Two hypotheses for this variation were investigated. The first one was the method (frying pan) used to measure the water content of the aggregates before the casting. To verify the method's precision, the water content values obtained with frying pan were compared with the water content measured with the drying oven at 80 °C. Table 3.5 presents the differences between measurement. Even though oven-dried aggregates present higher water content, the difference is insignificant. The other hypothesis was the water content difference within the height of the container used to store the aggregates. To verify this, the water content of the sand was measured at different depths (0, 10 and 20 cm depth). Table 3.6 presents the different water content at each depth. Results show some variation, but again, at a lower scale.

Material	Water Content (%)	
	Pan	Oven-Dried
RCA 4/10	9	9.2
RCA 10/20	6.5	7
NA 4/10	2.5	2.6
Sand	3.8	4.2

Table 3.5: Measurement method

Material	Water Content (%)
Sand at the top	4.5
Sand at 10 cm	4.4
Sand at 20 cm	4.2

Table 3.6: Height difference

Given the source of slump and strength variation was not clear, a different approach for the mixing procedure was studied. Given the relation between slump and strength, it was chosen with the slump as an indicator of performance.

However, it was necessary first to determine the reference performance in terms of slump and strength. And to this, NA RCA mixes with dried aggregates followed by a highly controlled water content were cast.

For concrete made with NA, the reference was cast with all aggregates fully dried (at 80 °C). The water corresponding to the aggregates' absorption was added together with mixing water. For concrete made with 100 % of RCA, the cast was done following Recybeton recommendations [16]. RCAs were initially dried and then pre-humidified. The pre-humidification of RCA consisted in, before casting, aggregates were placed inside a sealed container, and the quantity of water corresponding to water absorption plus 1 % was added to the aggregates. The container was rolled to homogenization and rested horizontally for 2 hours. After this, the concrete was cast. Fig. 3.5 presents the results from these two reference mixes (black line). It's noteworthy that all mixes were cast with the same amount of superplasticizer.

With the performance reference established, mixes with the wet aggregates were cast to verify the protocol. First, the aggregates were wetted using the abovementioned approach (perforated soaker hose). Then, before casting, the water content of these wet aggregates was measured and adjusted in the mixing water. Then, the slump was verified to check if the performance was the same as the reference mix. After, more water was usually be added to this mix to correct to have the desired slump. Fig. 3.5 also presents the results from trial mixes cast with this approach - (wet aggregates, in blue). The results indicate that the proposed approach gives values close to the reference mixes, both in terms of slump and compressive strength. Hence the method was chosen for the following studies. More details about the mechanical properties and the consistency of the method are given in Section 3.4.

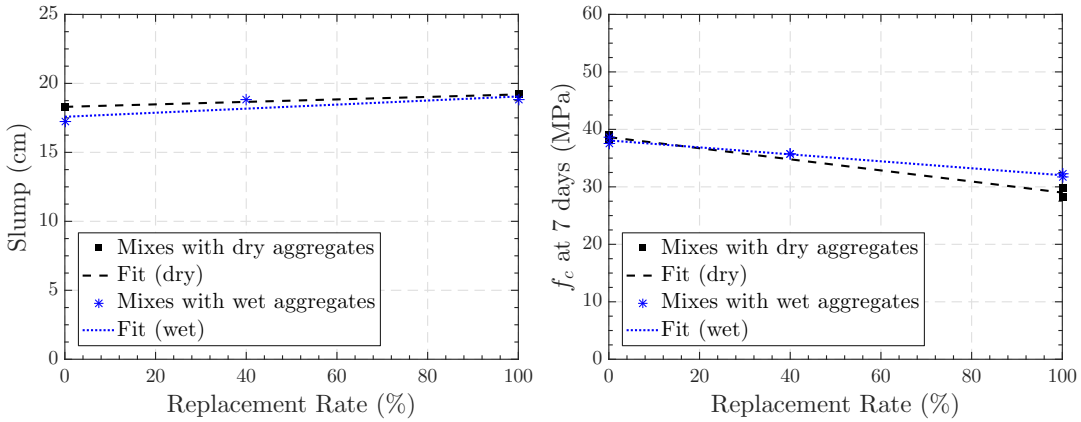

(a) Slump (b) Compressive Strength

Figure 3.5: Results from mixes with dry and wet aggregates

Finally, the mixing procedure was the same for all mixes. First, aggregates and cement were mixed for 2 minutes. Then, water and superplasticizer were added and mixed for 2 minutes. Then, a first slump (following NF EN 12350-2 [17]) measurement was done. Then the water was corrected if the slump was far to the slump of reference mixes (between 180 mm and 190 mm). Table 3.7

presents the mixing water needed in each one of the castings made during the PhD lifespan. The variation was expected since it was not possible to fully take into account the effect of water absorption in the aggregates. But, as seen in the following section, the results shows that the method presents consistent results (hardened and mechanical properties) in each one of the castings. Fig. 3.6 presents the slump test performed in some of the studied mixes (after the water adjustement).

Table 3.7: Mixing water for the different castings

Cast	NA	RCA-10-DR	RCA-20-DR	RCA-40-DR	RCA-100-DR	RCA-40-SBR	RCA-100-SBR
Theoretical	175.0	175.0	175.0	175.0	175.0	172.0	168.0
Cast #1	192.5	188.1	179.4	188.1	175.0	197.8	193.2
Cast #2	179.4	-	-	183.8	192.5	-	184.8
Cast #3	179.4	-	-	-	179.4	-	193.2
Cast #4	192.5	-	-	-	196.9	-	

(a) NA (b) RCA-100-DR (c) RCA-100-SBR

Figure 3.6: Slump tests

3.4 Fresh and hardened properties

For each campaign, different fresh and hardened properties were measured. This section presents the results of the main properties related to mixture design, to evaluate the studied concretes and verify the repeatability of the proposed approaches. For fresh properties, the leading parameter was slump, measured following NF EN 12350-2 [17]. For hardened properties, compressive strength (NF EN 12390-3 [18]), elastic modulus (NF EN 12390-13 [19]), and splitting tensile strength (NF EN 12390-6 [20]) were measured. To this, cylindrical specimens (11 cm x 22 cm and 16 cm x 32 cm) were casted to determine mechanical properties at 28 days. Fig. 3.7 presents the fresh and hardened properties for all studied mixes, in relation to the replacement rate and the replacement method (DR or SBR). A different number of samples per mix are presented. For NA and RCA-100-DR, ten samples were presented; for RCA-100-SBR, eight samples; for

RCA-40-DR, five samples; and for remaining mixes (RCA-10-DR, RCA-20-DR and RCA-40-SBR), two samples were tested.

Fig. 3.7a presents the slump for all the studied mixes. Since it was a target value in our mixing method, the slump was kept inside the proposed range (180 mm and 190 mm) for most castings. Fig. 3.7b presents the compressive strength at 28 days for all castings. For DR samples, the compressive strength reduces as the replacement rate increases, as seen in previous works [21]. For the 100 % of replacement (RCA-100-DR), the reduction was about 23 % of initial compressive strength. For SBR, results show that the design method achieves the proposed objectives: the compressive strength is constant independent of the replacement rate.

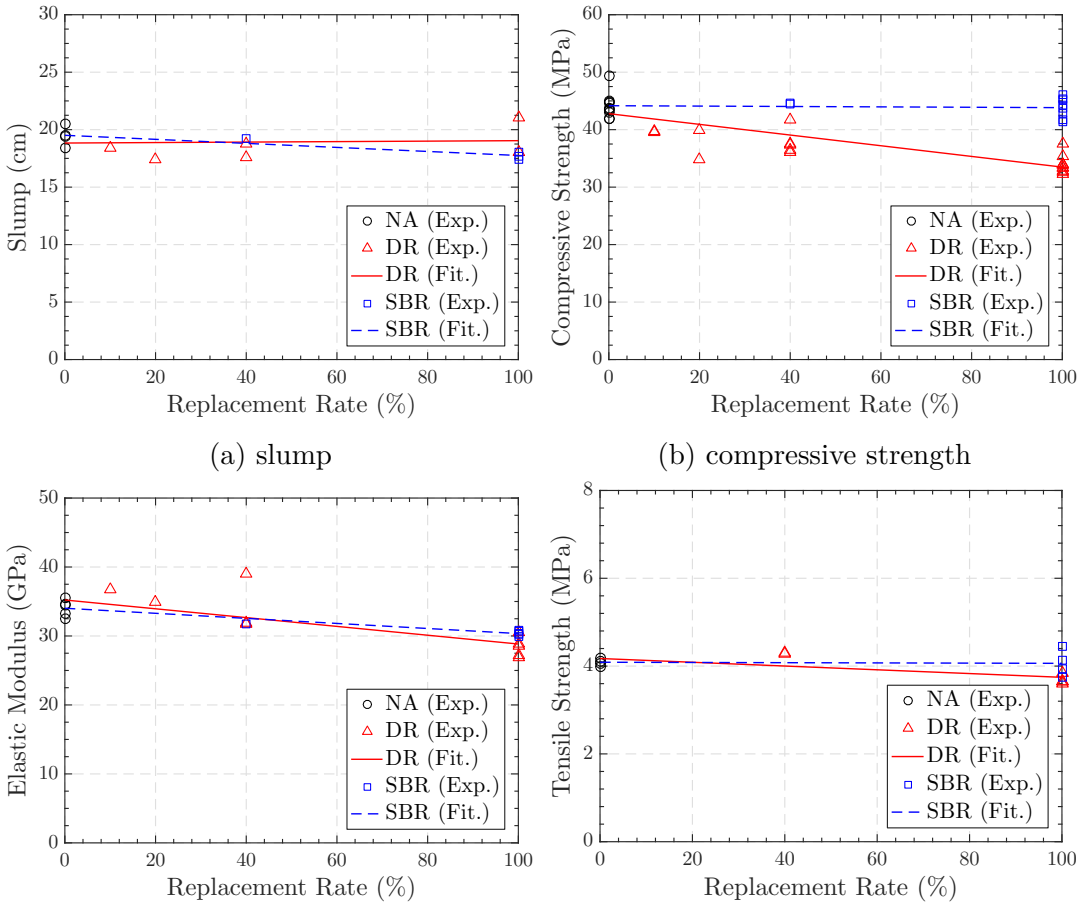

(a) slump (b) compressive strength

(c) elastic modulus (d) splitting tensile strength

Figure 3.7: Fresh and hardened properties of all studied mixes

For the elastic modulus (Fig. 3.7c), the behaviour is similar for DR mixes, with a decrease of about 17 % comparing to reference. For SBR, the elastic modulus is not constant with the replacement rate, and a similar reduction to DR mixes is observed (11 %). This reduction relies on the fact that SBR mixes contain more cement paste, which generally has a lower elastic modulus when compared to concrete made with NA [22]. For tensile strength (Fig. 3.7d), 20 % DR mixes presented a slight decrease of around 10 % comparing to reference.

This behaviour is also coherent with previous works [23], which show that tensile strength is decreased with replacement rate increase. For SBR, the tensile strength is not influenced by the replacement rate.

The results above show that the mixture design approaches presented similar results to previous works and are coherent with thesis objectives. Another point that can be evaluated is the repeatability of the mixture procedures. The fresh and hardened results were obtained from the same materials but fabricated at four different dates of the PhD lifespan. To evaluate the casting repeatability, Fig. 3.8 presents the results obtained for three mixes of the project (NA, RCA-100-DR and RCA-100-SBR) at four dates of fabrication. Results show the consistency of the method herein applied. With few exceptions, the variation between samples is slight, and they kept similar values during all the experimental phases.

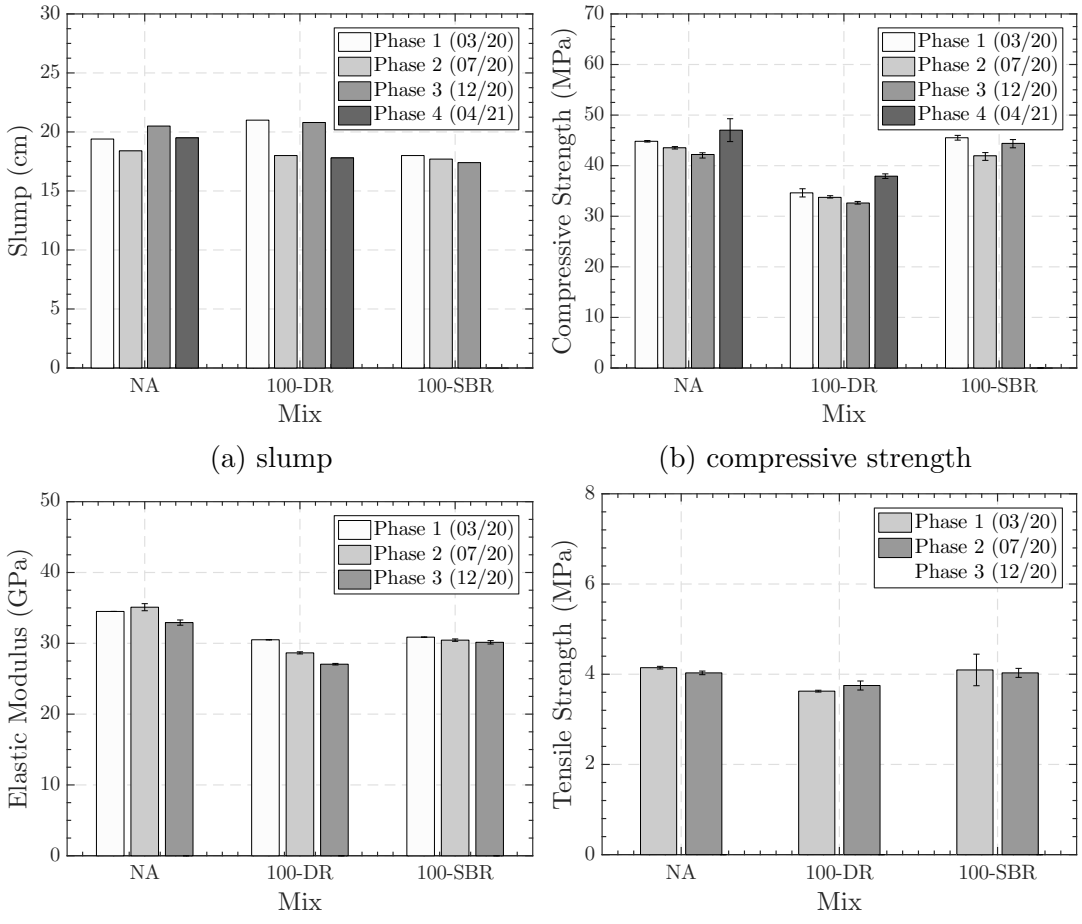

(a) slump (b) compressive strength

(c) elastic modulus (d) splitting tensile strength

Figure 3.8: Fresh and hardened properties of three mixes of the project in relation of casting date

3.5 Overview of tests and samples

As aforementioned, this thesis is divided into chapters structured as published or submitted papers. Hence, details about each experimental program will be given in each chapter. However, to obtain a global image of the testing program, this subsection presents an overview of all test samples (Tab. 3.8), including the experiments, evaluated mixes, testing variables, specimens size and heating parameters. The aforementioned experiments (fresh and hardened properties) are not specified in this table since they are presented again in each chapter. Lastly, the table also specifies the corresponding chapter/paper for each type of experiment.

Table 3.8: Experimental Program Overview

Chapter	Experiments	Speciment Type	Testing Variables	Mixes	High Temperature Parameters			
					Test Type	Rate/Curve (°C/min)	Temp. (°C)	Exposure Time (h)
4	Compressive Strength Elastic Modulus Splitting Tensile Strength Thermal Gradient	Cylinders (ø11x22 cm)	Replacement Rate and Temperature	NA, RCA-40-DR, RCA-100-DR and RCA-100-SBR	Residual	1	RT, 200, 400 and 600	2
	Thermal Conductivity Specific Heat Mass Loss	Disks (ø11x5 cm)				2		
	Density	1/4 of Disks (ø11x5 cm)						
	SEM/EDS Optical Microscopy	Prisms (4.5x3x2 cm)		NA and RCA-100-SBR				
5	Fire Spalling	Prisms (20x20x10 cm)	Replacement Rate and Load Level	NA, RCA-10-DR, RCA-20-DR, RCA-40-DR, RCA-100-DR, RCA-40-SBR and RCA-100-SBR	Fire	ISO 834-1	-	0.5
5	Fire Spalling	Prisms (20x20x10 cm)	Replacement Rate and Water Content	NA and RCA-100-DR	Fire	ISO 834-1	-	0.5
	Water Content	Small Cylinders (ø11x22 cm)			-	-	-	-
6	Water Porosity Permeability Capillary Water Absorption Carbonation	1/4 of Disks (ø11x5 cm) Disks (ø11x5 cm) Prisms (7x7x14 cm) Disks (ø11x6.5 cm)	Replacement Rate and Temperature	NA, RCA-100-DR and RCA-100-SBR	Residual	2	RT, 200, 400 and 600	2
	Chloride	Disks (ø11x5 cm)					RT and 200	

References

[1] *Tests for mechanical and physical properties of aggregates. Methods for the determination of resistance to fragmentation.* Comité Européen de Normalisation. Brussels, 2010.

[2] *Tests for mechanical and physical properties of aggregates. Determination of particle density and water absorption.* Comité Européen de Normalisation. Brussels, 2013.

[3] *Tests for geometrical properties of aggregates. Classification test for the constituents of coarse recycled aggregate.* Comité Européen de Normalisation. Brussels, 2009.

[4] *Essais pour déterminer les propriétés générales des granulats - Partie 1 : méthodes d'échantillonnage.* Comité Européen de Normalisation. Brussels, 1996.

[5] *Essais pour déterminer les propriétés générales des granulats - Partie 2 : méthodes de réduction d'un échantillon de laboratoire.* Comité Européen de Normalisation. Brussels, 1999.

[6] *Béton — Spécification, performance, production et conformité — Complément national à la norme NF EN 206.* Comité Européen de Normalisation. Brussels, 2014.

[7] IREX. *Comment Recycler Le Béton Dans Le Béton. Recommandations du Projet National Recybeton.* Institut pour la recherche appliquée et l'expérimentation en génie civil. Paris, 2019.

[8] F. de Larrard and T. Sedran. *BetonLab.* Version BetonLabFree. 2021.

[9] F. De Larrard. *Concrete mixture proportioning: a scientific approach.* CRC Press, 1999.

[10] M. Pepe. *A Conceptual Model for Designing Recycled Aggregate Concrete for Structural Applications.* 1st ed. Springer Theses. Springer International Publishing, 2015.

[11] M. Amario, C. S. Rangel, M. Pepe, and R. D. Toledo Filho. "Optimization of normal and high strength recycled aggregate concrete mixtures by using packing model". In: *Cement and Concrete Composites* 84 (2017), pp. 83–92. DOI: 10.1016/j.cemconcomp.2017.08.016.

[12] R. V. Silva, J. De Brito, and R. K. Dhir. "Properties and composition of recycled aggregates from construction and demolition waste suitable for concrete production". In: *Construction and Building Materials* 65 (2014), pp. 201–217. DOI: 10.1016/j.conbuildmat.2014.04.117.

[13] L. Butler. "Evaluation of Recycled Concrete Aggregate Performance in Structural Concrete". PhD thesis. University of Waterloo, 2012, p. 433.

[14] L. Ferreira, J. de Brito, and M. Barra. "Influence of the pre-saturation of recycled coarse concrete aggregates on concrete properties". In: *Magazine of Concrete Research* 63.8 (2011), pp. 617–627. DOI: 10.1680/macr.2011.63.8.617.

[15] *Essais pour déterminer les caractéristiques mécaniques et physiques des granulats - Partie 5 : détermination de la teneur en eau par séchage en étuve ventilée.* Comité Européen de Normalisation. Brussels, 2008.

[16] *Mise au point des formules de béton de référence.* RECYBETON. Nantes, 2017.

[17] *Testing fresh concrete - Part 2 : slump test.* Comité Européen de Normalisation. Brussels, 2019.

[18] *Testing hardened concrete - Part 3 : compressive strength of test specimens.* Comité Européen de Normalisation. Brussels, 2019.

[19] *Testing hardened concrete - Part 13 : determination of secant modulus of elasticity in compression.* Comité Européen de Normalisation. Brussels, 2021.

[20] *Testing hardened concrete - Part 6 : tensile splitting strength of test specimens.* Comité Européen de Normalisation. Brussels, 2012.

[21] R. V. Silva, J. De Brito, and R. K. Dhir. "The influence of the use of recycled aggregates on the compressive strength of concrete: A review". In: *European Journal of Environmental and Civil Engineering* 19.7 (2014), pp. 825–849. DOI: 10.1080/19648189.2014.974831.

[22] E. Ghorbel, T. Sedran, and G. Wardeh. "Instantaneous Mechanical Properties". In: *Concrete Recycling: Research and Practice*. Ed. by F. de Larrad and H. Colina. CRC Press, 2019, pp. 162–185.

[23] R. V. Silva, J. D. Brito, and R. K. Dhir. "Tensile strength behaviour of recycled aggregate concrete". In: *Construction and Building Materials* 83 (2015), pp. 108–118. DOI: 10.1016/j.conbuildmat.2015.03.034.

Chapter 04

Residual thermomechanical properties of concrete made with recycled concrete aggregates after exposure to high temperatures

This chapter is based on the paper *Residual thermomechanical properties of concrete made with recycled concrete aggregates after exposure to high temperatures*, a manuscript ready for submission. The literature review showed the importance of the mechanical and thermal properties of concrete made with RCA in assessing RAC fire behaviour. Hence, the first experimental campaign was designed to evaluate these properties. Four mixes were evaluated to study the replacement rate (0,40 and 100 %) and method (DR and SBR). Studied temperature levels were 200, 400 and 600 °C. After heating and cooling, concrete was evaluated in terms of mass loss, density, thermal and mechanical properties. In addition, microstructural analyses were made in two of the mixes. Lastly, an integrated comparative analysis of the residual thermomechanical behaviour was made.

Fernandes, B.; Carré, H.; Gaborieau, C.; Mindeguia, J-C.; Perlot, C.; Anguy, Y.; La Borderie, C. *Residual thermomechanical properties of concrete made with recycled concrete aggregates after exposure to high temperatures.* To be submitted.

4.1 Introduction

Concrete is the most widely used material in the construction industry [1]. Its popularity is related to its outstanding properties, versatility, cost-effectiveness, disponibility and ease of use [2, 3]. However, the massive use of concrete also represents a great aggressiveness to the environment: concrete represents a significant percentage of the global CO_2 emission [1]. In addition, concrete consumes substantial amounts of raw materials, water and energy [1, 4]. Lastly, construction demolition a high amount of waste, and the most common method of disposal is still landfilling [5–7].

Considering the amount of impact generated by the concrete industry, searching for solutions with less environmental impact is necessary. One of the approaches is using recycled concrete aggregates (RCA) as a replacement for natural aggregates. This approach can potentially reduce waste landfilling and the depletion of raw materials [2, 8, 9]. Several researchers have investigated the production of recycled aggregate concrete (RAC) in the last decades. In general, past works show that concrete made with RCA can present comparable properties to concrete made with NA, depending on aggregates' quality and replacement ratio of aggregates. [10, 11].

Even though its use is possible, the properties of concretes made with RCA differ from NA concrete due to the specific characteristics of the RCA itself. The main difference is associated with the fact that an RCA is composed of two materials: an old natural aggregate and attached (or adhered) mortar (AM). Due to AM, RCA usually presents higher porosity, higher water absorption and lower strength than NA [3, 8]. In addition, concrete made with RCA will also has particular characteristics, such as three different interfacial transition zones (ITZ) [8, 12]. All these aspects should be considered when using and assessing the performance of concrete made with RCA.

One of the most significant points when addressing the performance of concrete is the high-temperature behaviour. For concrete made with NA, the behaviour is quite well known. Exposure to high temperatures promotes physicochemical changes, the disintegration of hydration products, cracking, the release of vapour pressure, thermal mismatch and, in some cases, spalling [13–15]. All these phenomena will modify physical, mechanical, thermal, and transfer properties and they are directly linked with the concrete composition and properties [15, 16]. It is noteworthy that, since aggregates occupy a high volume of the concrete, their physical, mineralogical and, chemical composition play a key role in the behaviour of heated concrete [17–19]. In the case of concrete made with RCA, besides these properties, the higher porosity, high water absorption, and the new different ITZ may affect several crucial material parameters in the case of high-temperature exposure.

In the last years, different studies have been made to identify the behaviour of concrete made with RCA in these extreme conditions. Fernandes et al. [20] compiled different studies concerning the effect of elevated temperatures on concrete made with RCA. The authors highlight that the decrease of RCA concrete mechanical properties with temperature is similar to concrete made with NA.

They note that the compressive strength evolution with temperature presents two distinct phases.From room to 300 °C, the strength varies up to 20 % of its initial value, with individual results presenting both increase and decrease. Then, from this level and up to 800 °C, the relative strength significantly reduces until complete loss of strength. For elastic modulus and splitting tensile strength, the reduction is practically linear as temperature increases. Lastly, the authors point out that a minimal amount of past works evaluated the thermal properties of concrete made with RCA [13, 21]. It was verified that the thermal conductivity of concrete made with RCA decreases with temperature. No clear tendency was observed for the specific heat evolution with temperature.

Even though the compiled works present some general trends, it is not easy to establish the influence of the RCA and, more especially, the effect of replacement rate on thermal and mechanical properties. For example, different studies showed different trends concerning relative compressive strength (after exposure divided by room temperature). One group of authors observed an increase in strength as replacement rate increased, and it was attributed to the better compatibility of thermal expansion between RCA and the cement paste [22–27]. On the opposite, other authors observed weaker strength with increase in RCA [28–31]. This behaviour was attributed to different aspects, such as the higher porosity of RCA, the possible weaker and thicker ITZ, and possible microcracking.

Although relevant work has been done in previous years, the studies above demonstrate that the understanding of the effect of elevated temperature on concrete made with RCA is still far from being complete. To contribute to these knowledge gaps, this paper experimentally evaluates the thermo-mechanical residual properties of concretes made with RCA. Specimens with different coarse aggregates replacement rates (0, 40 and 100 %) were fabricated. For 100 % of substitution, a specific mix with comparable properties (28d compressive strength and slump) as concrete with NA was also studied. All the mixtures were then heated to three different temperatures (200, 400 and 600 °C). After cooling, a comprehensive program on residual thermomechanical properties was undertaken. Samples were evaluated for mass loss, density, thermal and mechanical properties, and scanning electro microscopy.

4.2 Experimental program

4.2.1 Materials and concrete mixes

Four different concrete mixes were studied. All of them had the same composition, except for coarse aggregates. The binder was z CEM II/A-L 42.5R cement, produced by Eqiom (La Rochelle, France). Filler was a limestone one (Betocarb HP-SC) made by Omya. A polycarboxylate-based superplasticizer (SIKA ViscoCrete Tempo-483) was used to improve workability. Lastly, alluvial sand was used in all mixes. Two types of coarse aggregates were used: natural aggregates (NA) and recycled concrete aggregates (RCA). Natural aggregates were diorite, coming from a quarry located in Genouillac (France). Recycled concrete aggregates were crushed and screened near Bordeaux (France) by a recycling company.

It is noteworthy that RCA presented some impurities (between 2.7 and 4.6 %) related to demolition wastes, such as wood, plastic, brick and bituminous materials. Table 4.1 present some of these materials properties.

Table 4.1: Raw materials properties

Property	Cement	Filler	Sand	NA 4/10	NA 10/20	RCA 4/10	RCA 10/20
Density (kg/m^3)	3010	2700	2650	2820	2840	2570	2590
Specific surface (cm^2/g)	4700	4330	-	-	-	-	-
Water absorption (%)	-	-	0.35	0.92	0.81	5.6	4.52
LA coefficient (%)	-	-	-	16	16	30	36
Fineness modulus	-	-	3.1	-	-	-	-

The four studied concrete types were: concrete with NA (used as a reference for the analysis), direct replacement (DR) mixes (RCA-40-DR and RCA-100-DR) and strength-based replacement (SBR) mixes (RCA-100-SBR). The concrete with NA was designed to achieve durability requirements (NF EN 206/CN:2014 [32]) according to the XD3 exposure class: water/cement (w/c) ratio of 0.5, C35/45 compressive strength class and cement content equal or higher than 350 kg/m^3. For DR mixes, NA were replaced by RCA (40 and 100 % of replacement in volume), without any changes in other constituents. In the SBR mix (made with 100 % coarse aggregates replacement), cement and water content were adjusted to achieve the same strength and workability as the reference mix. The SBR mix was pre-designed with BetonLab [33] software. Based on compressive strength results of reference and DR mixes, aggregates properties were calibrated. Then, the w/c ratio was adjusted to have the same compressive strength as the reference. Finally, water and cement contents were modified to achieve the same slump as the reference concrete. Table 4.2 presents the mixture proportions for the four studied concretes.

Table 4.2: Mix proportions (in kg/m^3, SP in % of cement mass)

Material	Mix			
	NA	RCA-40-DR	RCA-100-DR	RCA-100-SBR
Cement	350	350	350	420
Filler	60	60	60	60
Sand	804.3	804.3	804.3	799.8
NA 4/10	331.7	199.0	-	-
NA 10/20	711.1	426.7	-	-
RCA 4/10	-	120.9	302.3	291.5
RCA 10/20	-	259.4	648.5	630.3
Water	175	175	175	168
SP	0.9	0.9	0.9	0.9

Before casting, and due to water absorption issues, all aggregates (sand, NA and RCA) were pre-wetted for one hour using a soaker hose and then covered

with a plastic sheet for three hours. Working with wet aggregates instead of fully-saturated aggregates (common with RCA) was adopted to have a method that could be easily reproduced in an industrial concrete plant. Before casting, the aggregates' moisture content was measured to adjust the water content added to the mix.

Variations in fresh and hardened properties were observed in trial samples. To study this problem, reference mixes with dry aggregates were cast to determine the relationship between the slump and the compressive strength. These values were used as a reference for the final mixes. Then, in the final mixes, aggregates were pre-wetted, and water content was adjusted to achieve the same slump as the reference. In the end, the mixing procedure was the same for all mixes: first, aggregates and cement were mixed for 2 minutes. Then, water and superplasticizer were added. After two minutes of mixing, the first slump (following NF EN 12350-2 [34]) measurement was done. Extra water was added if the slump was not close to reference mixes (between 180 mm and 190 mm). If the slump reached the target consistency, the concrete specimens were produced. Different cylindrical specimens of 11 x 22 cm and prisms of 15 x 15 15 cm were cast. Samples for mechanical characterisation at 28 days were kept submerged in water at 20 °C. The other experimental samples were kept submerged for seven days and then placed into sealed plastic containers until test age (minimum of 90 days).

Different fresh and hardened properties were measured for concrete characterisation at room temperature. First, slump (NF EN 12350-2 [34]), fresh density (NF EN 12350-6 [35]) and air content (NF EN 12350-7 [36]) were measured. Then compressive strength (NF EN 12390-3 [37]) and water content (wc) were also measured. Table 4.3 presents the fresh and hardened properties for all studied mixes (average values and standard deviation in parenthesis).

Table 4.3: Fresh and hardened properties of studied mixes

Mix	Slump (mm)	Air Content (%)	Fresh Density (kg/m^3)	wc (%)	f_{c28} (MPa)
NA	184	4.2 (± 0.0)	2339.6 (± 0.9)	4.8 (± 0.4)	43.5 (± 0.3)
RCA-40-DR	188	4.1 (± 0.2)	2291.5 (± 21.5)	5.8 (± 0.5)	36.7 (± 0.8)
RCA-100-DR	180	3.9 (± 0.3)	2225.4 (± 4.1)	7.0 (± 0.4)	33.7 (± 0.3)
RCA-100-SBR	177	4.6 (± 0.3)	2211.2 (± 6.5)	6.9 (± 0.2)	42 (± 0.8)

Fig. 4.1 presents the compressive strength at 28 days in function of the coarse aggregates replacement rates. For DR samples, the compressive strength reduces as the replacement rate increases, as seen in previous works [38]. The reduction was about 22.5 % of the initial compressive strength when replacing all the coarse aggregates. For SBR, results show that the design method achieved the proposed objectives, i.e., the compressive strength of the concrete made with 100 % of RCA shows approximately the same compressive strength as the reference concrete.

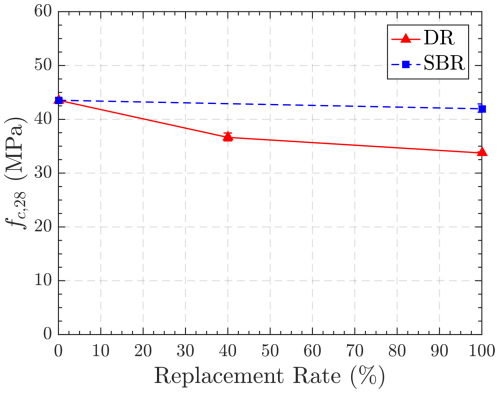

Figure 4.1: Effect of replacement rate on compressive strength

4.2.2 Heating procedure

Samples were heated in an electric furnace. This furnace has internal dimensions of 55 x 50 x 31 cm and a power of 4000 W. The electric resistance is at the walls of the furnace, and a fan is located at the top to homogenize temperature. The time-temperature parameters are controlled by an automated regulator connected to a thermocouple located inside the furnace.

The heating rate varies depending on the sample size (the samples' dimensions are specified in the sections describing the testing procedures). Low heating rates were chosen to guarantee homogenous temperature and avoid strong thermal gradients inside concrete cylinders. For smaller disks samples (⌀11 x 5 cm) a heating rate of 2 °C/min was applied. For cylindrical samples (⌀11 x 22 cm), a rate of 1 °C/min was adopted. This reduction was made after some trial tests, in which explosions were registered in cylinders heated at 2 °C/min. It is noteworthy that even though samples were more than 90 days older, they were kept inside sealed containers. Hence a high water content is expected inside the specimens, making them sensible to spalling during heating.

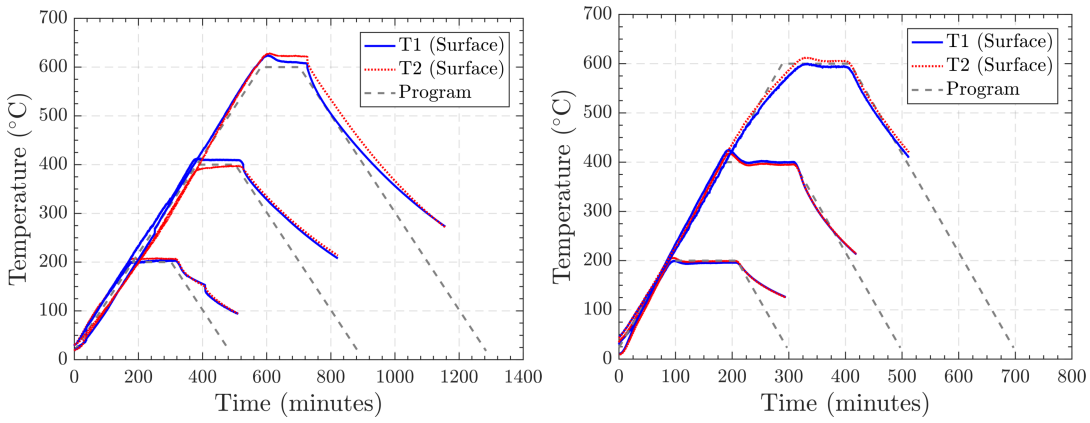

(a) heating rate of 1 °C/min (b) heating rate of 2 °C/min

Figure 4.2: Time-temperature curves

Samples were subjected to three different temperatures: 200 °C, 400 °C and

600 °C. The target temperature was maintained for 180 min, then naturally cooled to room temperature inside the furnace. Fig. 4.2 presents the time-temperature curves for all tested temperatures. T1 and T2 refer to type-K thermocouples installed at the surface of concrete samples. In addition, four ⌀11 x 22 cm cylinders were cast with internal thermocouples to measure the temperature diffusion in each mix. These thermocouples were placed at different depths: surface, 1/3 and 2/3 of the radius, and at the centre. After cooling, all samples were stored inside sealed containers with silica gel until test day. This conditioning was done to avoid any possible rehydration of heated concrete. The maximum duration between cooling and test was 24 h.

4.2.3 Testing procedures

4.2.3.1 Mass loss

For steady state mass loss, three ⌀11 x 5 cm disks were used for each mix. These specimens were weighted before and after heating to determine the mass loss induced by each temperature level.

4.2.3.2 Density

The hardened density (ρ_d) was measured based on NF EN 12390-7:2019 [39] and AFREM recommendations [40]. Three quarters of 11 x 5 cm disks were used for each mix and temperature. As determined by standard, samples at room temperature should be oven-dried before testing; hence, the first registered density refers to 80 °C.

4.2.3.3 Thermal properties

The thermal properties (thermal conductivity and specific heat) were measured using the Hot-Disk apparatus (TPS 1500). This apparatus is based on the Transient Plane Source (TPS) method, developed by Log and Gustafsson [41]. The specimen for this test was composed of two identical concrete disks (⌀11 x 5 cm), and between them, a flat sensor was placed. The probe is made of a double spiral nickel covered with two layers of Kapton. It has a radius of 9.868 mm and a thickness of 10 µm. The flat sensor acts simultaneously as the heat source and temperature sensor in this system. The apparatus has a built-in thermal analyzer, which calculates the thermal properties for each measurement.

Three specimens (6 disks) were tested for each mixture and each temperature level. The test was carried out at room temperature (23 °C, with water inside), at 80 °C (dried), and after each heating/cooling procedure (i.e., residual). In addition, three measurements were taken for each sample/state, with a 30 minutes interval between them - to reestablish thermal equilibrium and avoid any perturbations due to the previous measure.

4.2.3.4 Mechanical properties

The residual mechanical properties were determined on cylindrical ⌀11 x 22 cm samples. The tests were done on a hydraulic press (3R Syntech 700). Samples were first heated, following Section 4.2.2 procedures, and then subjected to residual mechanical properties. For compressive and elastic modulus tests, samples were between 8 and 15 months old. For splitting tensile strength tests, they were 4 months old.

For uniaxial compressive tests, two samples per mix and temperature were tested. The experimental procedure followed NF EN 12390-3 [37]. The cylinders were also used for elastic modulus determination. An extensometer composed of three LVDTs was attached to the sample for the displacement measurement, following NF EN 12390-13 [42] procedures. The specimen was subjected to three loading-unloading cycles, and the elastic modulus was determined from the last ascending branch, following RILEM TC 200-HTC recommendations [43]. For splitting tensile tests, three samples per mix and temperature were evaluated, and the test followed NF EN 12390-6 [44].

4.2.3.5 Microstructural analysis

The microstructural analysis was done with scanning electron microscopy (SEM). The aim was to evaluate the microstructure and the interfaces after exposure to elevated temperatures. For all the tests, the two mixes with similar strengths were evaluated: NA and RCA-100-SBR. A diamond saw was used to cut small prisms of 4.5 x 3 x 2 cm. These samples were dried at 80 °C for 24 hours and later they were polished. Samples were heated following Section 4.2.2 procedures to the different target temperatures. The same sample and the same regions were analysed to assess the crack evolution at the interface. After each of these thermal cycles, the microstructural analyses was carried using an environmental SEM (FEI Quanta FEG 250).

4.3 Results

4.3.1 Mass Loss

Fig. 4.3 presents the results of relative steady-state mass loss. As expected, mass loss increases with the rise in the temperature. The first branch of the curves, from room temperature to 200 °C, shows the higher mass loss rate. Up to this temperature, most of the mass loss is related to concrete drying [14, 45]. After this first branch, the mass loss rate reduces, and the curves flatten. Between 200 °C and 600 °C, most water is evaporated, and some of the hydration products of concrete (C-S-H and portalndite) decompose [14, 45, 46].

For all studied temperatures, concrete made with RCA loses more mass than concrete made with NA. Also, the loss is higher as the replacement increases. This phenomenon is mainly related to the fact that concrete made with RCA presents higher water content (see Table 4.3) due to the higher water absorption of RCA aggregates. Similar behaviour was observed in previous works [13, 47–

49]. Another influential factor was the presence of impurities, such as bituminous particles, wood and plastics, that burn and decompose at these temperatures level. Fig. 4.3 also shows that both mixes made with 100 % of RCA present a slight difference. The SBR mix showed a slightly higher mass decrease, especially after 200 °C. This difference can be explained because SBR mixes contain more cement paste, and this high paste volume induces the decomposition of more hydrated products.

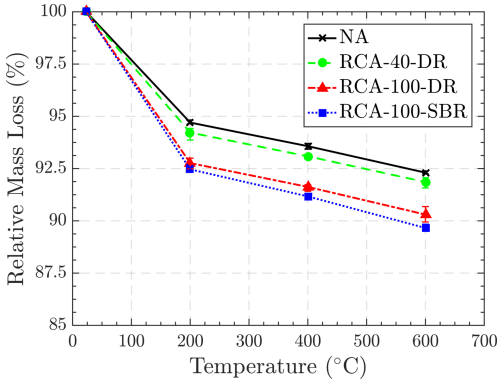

Figure 4.3: Steady state mass loss

4.3.2 Density

Fig. 4.4 presents the evolution of the density measurements according to temperature. First, at ambient temperature, the addition of recycled aggregates decreased the hardened density. This reduction is simply due to the lower density of RCA aggregates. When comparing 100 % DR and SBR, change in density is almost negligible, reinforcing the relative importance of aggregates in the overall density compared to the paste volume. After heating, density decreases for all concretes. This reduction is related to the physicochemical changes inside concrete when exposed to high temperatures.

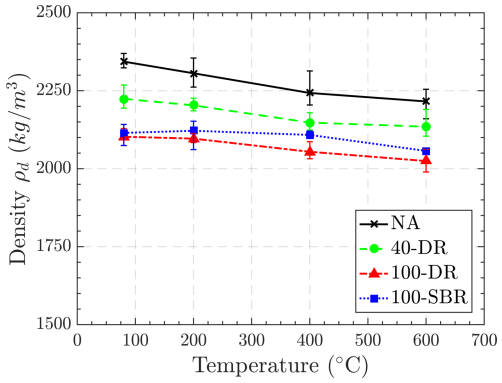

Figure 4.4: Density evolution with temperature

4.3.3 Thermal properties

Fig. 4.5a presents the temperature evolution of the residual thermal conductivity. At room temperature, the increase of replacement rate increases the thermal conductivity, the opposite as observed in previous works [21, 50]. Thermal conductivity is highly dependent on mix properties, such as moisture, porosity, type/volume of aggregates, and water/cement paste ratio [51, 52]. The increase herein observed could be explained by the higher quantity of moisture present in concrete made with RCA, which may overcome the porosity effect. However, measurements made in dried samples (80 °C) showed that the difference between RCA and NA keeps similar. When comparing 100-DR and 100-SBR mix, the latter present slightly less thermal conductivity since it has more paste, and in general, cement paste presents lower conductivity than aggregate [52]. In any case, the values herein measured are close to typical values observed in concrete made with NA (between 1.4 and 3.6 W/mK) [53] and concrete made with RCA (between 1.5 and 2.1 W/mK) [13, 21, 50].

As temperature increases, the conductivity starts to decrease with a trend similar for all mixes. Up to 200 °C, changes are linked to evaporation of free water at this range [21, 45, 54]. Further reductions are observed and related to further water loss (absorbed and bonded) and the increasing damage (cracks, porosity) [13, 21, 54]. After 600 °C, the difference between mixes is low, and residual thermal conductivity is close to 1 W/mK for all cases. These values are close to those observed in previous works [21, 50]. It is noteworthy that the results herein presented are evaluated after cooling; however, as seen in previous works [52, 55], as concrete cools, the residual conductivity stays approximately similar than the hot value.

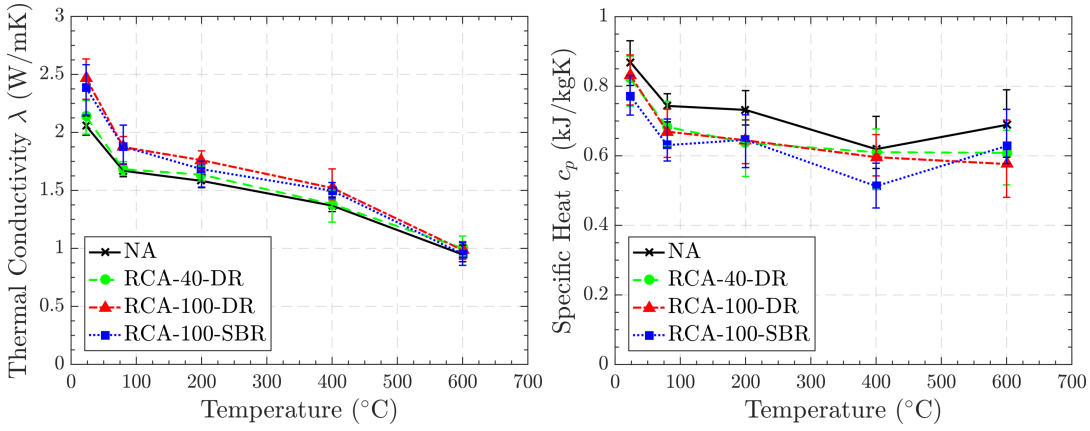

(a) thermal conductivity (b) specific heat

Figure 4.5: Evolution of thermal properties with temperature

The variation of specific heat with temperature is presented in Fig. 4.5b. At room temperature, concrete with NA presents a higher specific heat. The addition of recycled concrete aggregates slightly decreases the specific heat, as observed in previous work [13, 21, 50]. However, the value is not directly increasing with the replacement rate. Indeed, 100-DR and 40-DR present similar

values, whilst 100-SBR presents the lowest specific heat at ambient temperature. Specific heat is generally influenced by density, type of aggregates, moisture content, and w/b ratio [51, 56]. In any case, the values reported herein for NA and RCA are in good agreement with the range observed at ambient temperature in previous works (between 0.5 kJ/kgK and 1.3 kJ/kgK) [13, 21, 50].

Particular attention should be taken when observing the evolution of specific heat with temperature. Since the values herein are residual values (i.e., after cooling), the trend is not the usual as observed in previous works [13, 21, 50]. Typically, as temperature increases, specific heat will increase. However, this is a reversible phenomenon, and it strongly depends on the atomic vibration of solids: when temperature increases, vibration increases and higher values of specific heat are obtained [50]. Hence, residual measurements may not be an accurate representation of specific heat. However, the results herein are presented as an indicator for thermal and physical changes. The residual specific heat decreases for all mixes up to 400 °C. Then, for NA and RCA-100-SBR, an increase was observed, whilst a decrease was observed for RCA-100-DR and RCA-100-SBR.

4.3.4 Temperature diffusion

Temperature diffusion in ⌀11 x 22 cm concrete cylinders are presented in Fig. 4.6. First, the temperature registered in the centre of each specimen is presented (Fig. 4.6a), confirming that the target temperature is reached at the core during the plateau. Temperature slowdowns (orange lines) are observed at around 270 and 570 minutes (close to 200 °C and 550 °C at the sample surface, respectively). The first slowdown is usually linked with endothermic water evaporation and the initial decomposition of C-S-H. The second one is mainly related to portlandite decomposition [13, 50, 57].

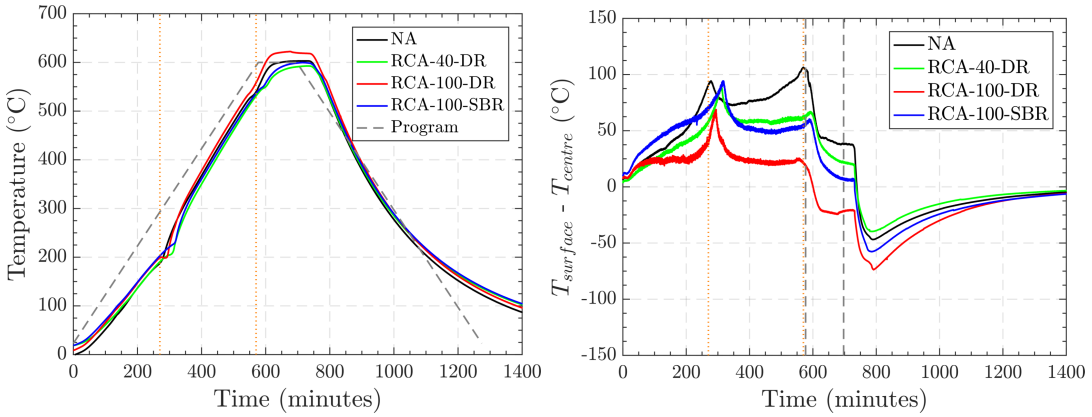

(a) core temperature (b) difference between surface and centre

Figure 4.6: Temperature diffusion into cylinders heated up to 600 °C

Fig. 4.6b presents the thermal difference between the surface and the centre of the sample for each tested concrete. The temperature slowdowns observed in the temperature rise at the centre of the sample results in two positive peaks in Fig. 4.6b. Besides these peaks, the temperature gradient is limited to 50 °C in

the samples. These two peaks diagrams were closer to those observed in previous works for NA and RCA [13, 50, 57]. The results herein presented agree with the measured thermal properties. Higher gradients were observed in concrete made with NA - mix with the lowest conductivity. Increasing RCA content slightly increases conductivity, and thermal gradients decrease in RCA-40-DR and RCA-100-DR. For RCA-100-SBR, the tendency is not the same since it presented relevant thermal gradients, but it is noteworthy that this behaviour will also depend on the other hot thermal properties (specific heat).

4.3.5 Mechanical properties

Fig. 4.7a presents compressive strength evolution with temperature in absolute values for all tested concretes. At room temperature, similar behaviour is observed compared to 28 days compressive strength - increasing the replacement rate decreases the compressive strength. Concrete made with NA and SBR mix presents closer values, as expected. However, the difference between NA and SBR is slightly higher in this test series (5 MPa) than those done at 28 days (1.5 MPa). The results here indicate that RCA may have a non-negligible effect on the late hardening process of concrete, i.e. after 28 days. However, for an exact explanation, an in-depth study of the long-term performance of concrete made with RCA should be made (out of focus on this paper).

The general behaviour with the increase of temperature is quite similar for all studied mixes. First, from room temperature up to 200 °C, a first decrease is observed, mainly associated with the decomposition of hydration products, water loss and microcracking [14, 45]. Then, from 200 °C to 400 °C, another reduction is observed, but the variation is lower than before. For example, the compressive strength of the SBR mix was almost constant. The last branch, from 400 °C to 600 °C, presents a significant decrease in strength. This decrease can be explained by the ongoing decomposition of portlandite and the microcracking induced by the thermal mismatch (i.e. the expansion of the aggregates while cement paste shrinks) inside the material [14, 15, 45].

Fig. 4.7b shows the temperature evolution of the relative compressive strength. The latter is defined as the ratio between compressive strength at elevated temperatures and strength at room temperature (${f_{cu}}^T/f_{cu}$). The behaviour is similar for all mixes: the relative strength decreases around 20 % at 400 °C, then significantly reduces until it reaches 40 % of the initial strength at 600 °C. This behaviour can be associated with the higher paste volume and the lower w/c, which may improve the interfaces between RCA and paste, possible reducing the cracks due to thermal mismatch inside the material. Similar behaviour was observed in previous works which evaluated the effect of different w/c ratio [22, 23]. The concrete with NA and RCA-100-DR have similar values, and the highest decrease was observed for RCA-40-DR (at each tested temperature.

The relative curves were compared to previous experimental results [13, 25, 28, 31, 48, 49, 58–60] compiled by Fernandes et al. [20]. These compiled experimental values refer to residual tests (after cooling), which are heated with low

heating rates. It can be seen that the obtained values fall within the observed range verified in previous works. The values were also compared to Eurocode 2 [61] prevision for siliceous and calcareous concrete. It is noticeable that results are pretty close to the Eurocode curves up to 400 °C but are lower at 600 °C.

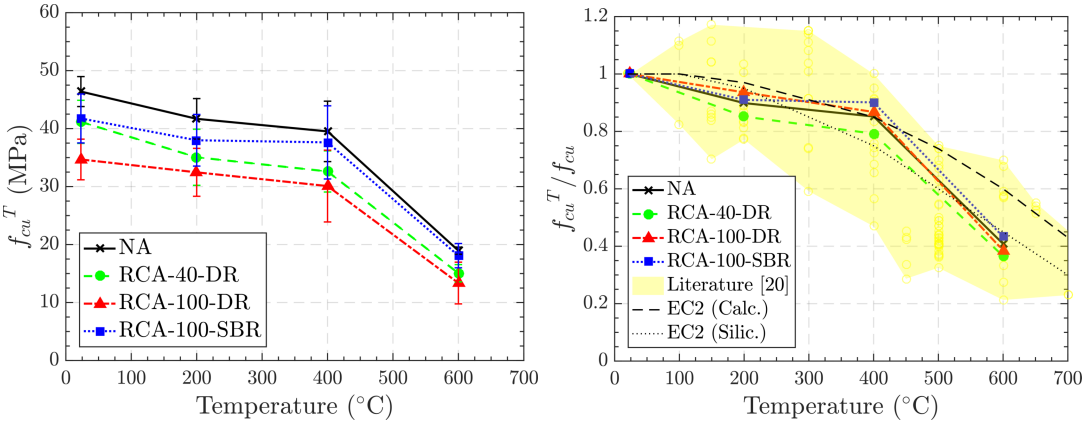

(a) absolute values (b) relative values

Figure 4.7: Evolution of compressive strength with temperature

Fig. 4.8a presents the evolution of the elastic modulus (absolute values) with temperature. At room temperature, the increase in replacement rate decreases the stiffness. Unlike the compressive strength, the higher paste volume in the RCA-100-SBR does not increase its elastic modulus when compared to the RCA-100-DR. This behaviour is likely due to the generally lower elastic modulus of cement paste (when compared to aggregates) [62]. With the increase of temperature, the elastic modulus linearly decreases, independently of the mix. This behaviour is similar to the classical observed behaviour of concrete made with NA [51, 63].

Fig. 4.8b present the evolution of the relative elastic modulus ($E_c{}^T/E_c$) with temperature. All curves present almost the same linear shape, with low variations between values. At 400 °C, the modulus reaches is 50 % of the initial value, and at 600 °C, it reaches only 20 % of the initial elastic modulus. As observed in literature [31, 59, 64, 65], the effect of high temperatures on relative elastic modulus is higher than for compressive strength. The relative values were also compared with previous works [31, 59, 64, 65], compiled by Fernandes et al. [20]. The experimental results refer to residual tests (after cooling). As in the case of compressive strength, the curves herein obtained are within the reported experimental range [20].

The evolution of the splitting tensile strength with temperature is presented in Fig. 4.9. Fig. 4.9a shows the absolute strength values. The results at room temperature show that the increase in replacement rate significantly decreases the tensile strength. The SBR mix recovered some of the tensile strength but not at the same level as concrete made with NA. The evolution of the tensile strength with temperature is similar for all tested concretes.

However, a peculiar behaviour was observed between 200 °C and 400 °C. Concrete made with NA slightly decreased, but concrete made with RCA maintained

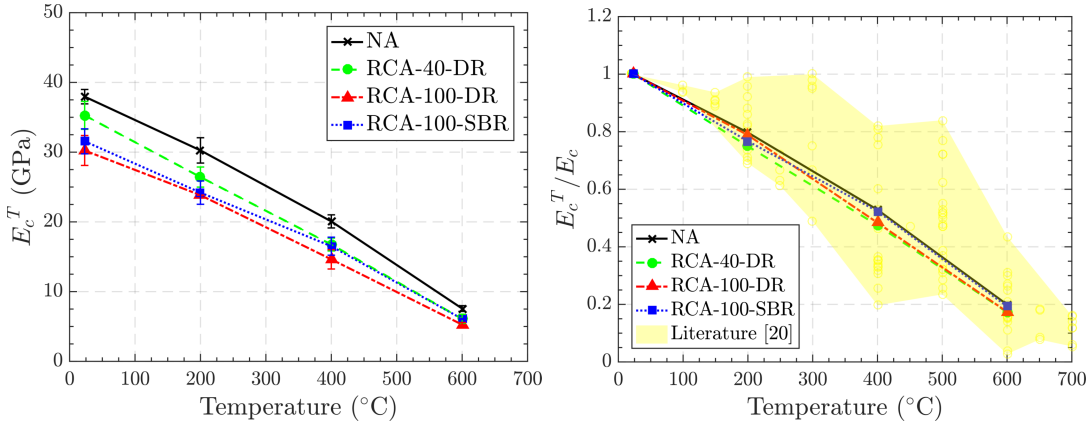

(a) absolute values (b) relative values

Figure 4.8: Evolution of elastic modulus with temperature

(RCA-40-DR) or even recovered a small amount of strength (RCA-100-DR and RCA-100-SBR). In previous works, similar behaviour was observed for concrete made with NA, and it was attributed to the drying process of the concrete, which may increase the tensile strength [66]. This was also verified in compressive strength, where the heating led to a movement of cement gel layers that increased van der Walls forces and finally increased strength [56, 67]. In the present work, this increase only happened in concrete with RCA and may be associated with the higher initial water content. Another possibility also relies on the less thermal mismatch with concrete made with RCA. Similar behaviour was observed in Kou et al. [25], which observed, at 300 °C, that mixes with 100 % of RCA exhibited an increase in their initial relative residual strength. After 400 °C and up to 600 °C, the splitting tensile strength decreases again.

Fig. 4.9b presents the evolution of the relative splitting tensile strength with temperature.The trend is similar for all concretes made with RCA, i.e. a first decrease, followed by a slight strength recovery, and then a decline up to 600 °C. The final decrease is lower than for compressive strength and elastic modulus. Relative values indicate better performance for RCA-100-DR. However, after 600 °C, all mixes present values lower than 50 % of the initial value. In the same figure, previous works [13, 24–26, 31, 48, 64, 68] and Eurocode 2 [61] prevision are shown. The presented results are coherent with prior studies. Eurocode 2 [61] prevision for NA aggregates presents a two branches prevision, with a plateau up to 100 °C. Similar behaviour can be observed, but this initial plateau is much higher in the present work: indeed, it can be seen that, up to 400 °C, all mixes maintain more than 80 % of their initial value.

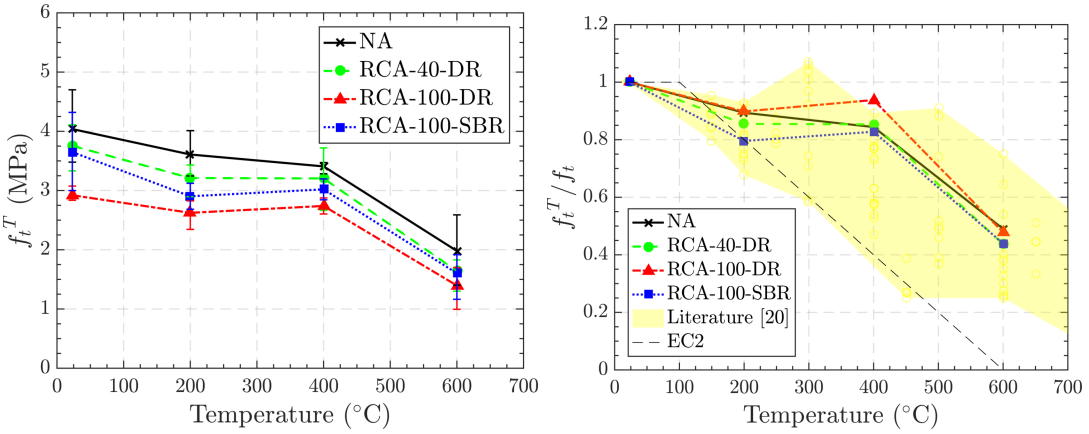

(a) absolute values (b) relative values

Figure 4.9: Evolution of splitting tensile strength with temperature

4.3.6 Microstructural analysis

Figs. 4.10 and 4.11 show SEM micrographs of the NA and RCA-100-SBR after exposure to elevated temperatures. In both cases, cracking evolves as the temperature increases, but the evolution has some particularities. Fig. 4.10 shows an interfacial zone between coarse NA, fine NA and cement paste. The first image (at 80 °C) already shows some cracks in the paste and the grain interface. At 200 °C, these cracks in the paste develop and start to distribute also at the Coarse NA. This phenomenon continues as the temperature increases, increasing width and distribution. At 600 °C, the crack width further develops, and a complete cracked microstructure is observed. Most of the paste compounds are already dehydrated at this temperature level, and the thermal mismatch has also started.

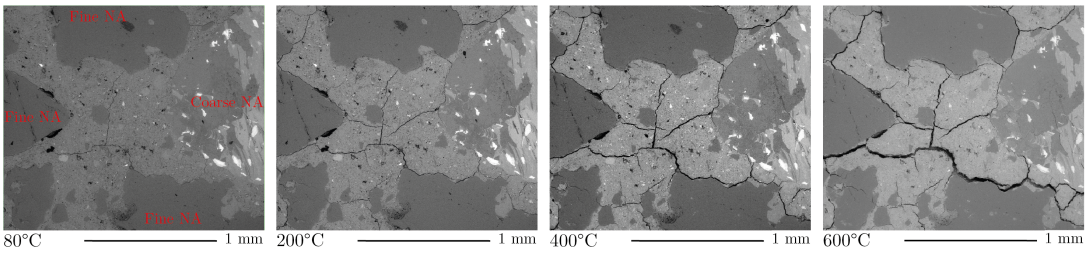

Figure 4.10: SEM micrographs of concrete made with NA (x150 magnification)

Fig. 4.11 shows the crack evolution in RCA-100-SBR. A zone with an RCA and the new cement paste is shown. In the RCA, the old NA and old paste are visible. At 80 °C, some cracks are visible in the new paste and in the old paste. Also, RCA showed different defects, such as voids. At 200 °C, cracks develop around sand grains, both in the new and old cement paste. These cracks are essentially perpendicular to the new paste/old paste interface. This can indicate a better match between paste. However, a further increase in the temperature leads to a higher connection between cracks. At 600 °C, crack opening increases,

with two big cracks at the new cement paste and the old cement paste. Comparatively, both at 400 °C and at 600 °C, the crack quantity and distribution seem slightly higher for concrete with RCA.

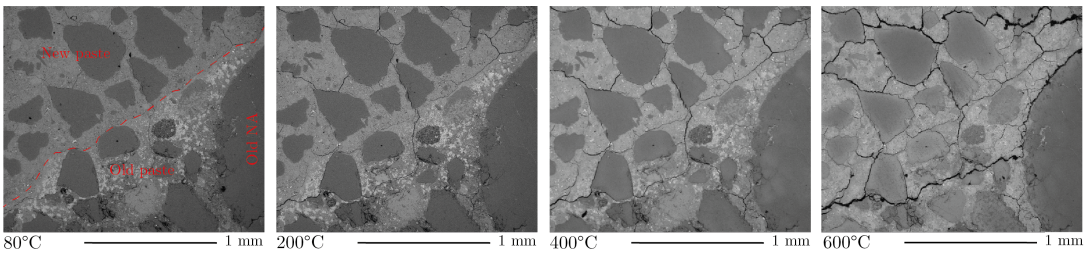

Figure 4.11: SEM micrographs of concrete made with RCA (x150 magnification)

4.3.7 Comparative analysis and discussion

As seen in the previous subsections, and similarly to concretes made with NA, the increase of temperature has a non-negligible influence on the residual thermomechanical properties of concrete made with RCA. To further depict this behaviour, a comparative analysis was made to have a broad view of the effect of RCA (Fig. 4.12 to Fig. 4.14). In these graphs, each mix is evaluated using the different relative values from compressive strength (f_{cu}), elastic modulus (E_c), splitting tensile strength (f_t), density (ρ_d), mass loss (ML), and thermal conductivity (λ). Residual specific heat was not used due to its low representativity to the actual specific heat (measured at hot state). The relative value is the ratio between the property at elevated temperature and the same property at room temperature. Each axis had different maximum and minimum values (values between 0 and 1), but the same gap between them (0.6) was kept. This strategy was adopted to improve visualisation and comparison between mixes - the main objective of this comparative analysis. For the analysis, 400 °C and 600 °C were selected, since the effect on properties is higher at this level.

Fig. 4.12 shows the effect of the replacement rate on the residual properties. The NA and the DR mixes (40 % and 100 %) are shown to see the effect of a simple direct replacement of coarse aggregates without modifying the mix. Density and mass loss values are close independently of temperature and replacement rate. On the opposite, the replacement rate has more influence on thermal properties, especially at 600 °C. For mechanical properties, the effect depends on the temperature and the replacement rate. At 400 °C, RCA-40-DR reduced all the properties, while RCA has different behaviour depending on the property. It positively affects the tensile and compressive ratio whilst reducing elasticity. This effect can be related to a lower thermal mismatch that reduces cracks in the material [22–25]. At 600 °C, the positive slightly better behaviour disappeared, and RCA's addition reduced all the relative mechanical properties. At the same time that some variation was observed, it can be said that the directly RCA addition did not change the general behaviour of concrete significantly after exposure to high temperatures.

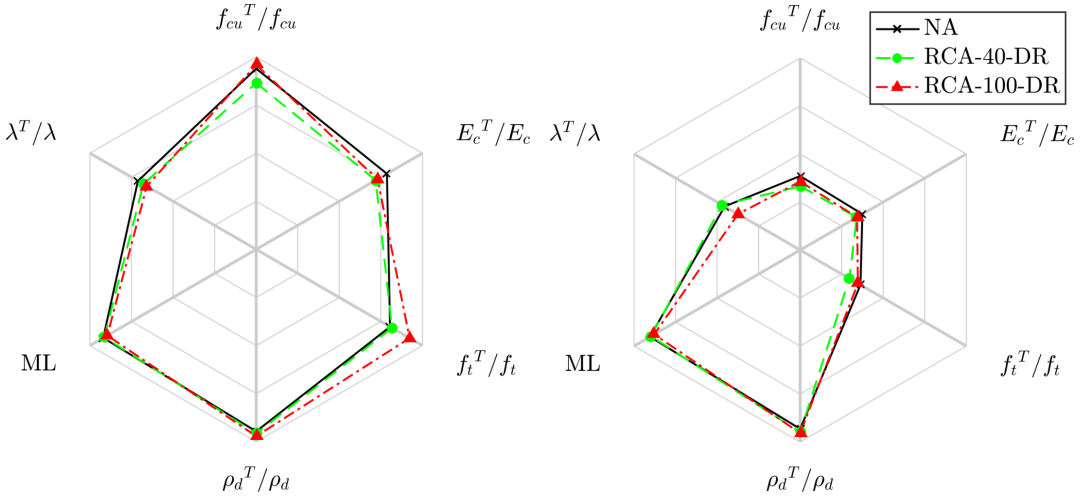

(a) 400 °C (b) 600 °C

Figure 4.12: Effect of direct replacement on the relative residual properties

The effect of recycled aggregates was also compared in the case of concretes with equivalent compressive strength at 28 days, i.e. NA and RCA-100-SBR (Fig. 4.13). Mass loss and density showed closer values between mixes: SBR showed less density loss but higher mass loss. This slightly higher mass loss is primarily due to high water content and water loss. The thermal conductivity is lower for concrete made with RCA, highlighting the verified behaviour when analysing replacement rate: the presence of RCA is a determinant in this property. Lastly, for mechanical, values were close, especially for modulus reduction, which was almost the same for both mixes and temperatures. Splitting and compressive had opposite behaviour: NA presented more loss of compressive, whilst it maintained more tensile strength. This trend was verified for both temperatures. It is noteworthy that this behaviour is challenging to associate with the cracks observed in SEM analysis. Both mixes presented relevant cracking, with apparently higher density for RCA, whilst NA showed a thicker crack. This analysis should be made at a larger scale for precise analysis.

Lastly, Fig. 4.14 shows the effect of the replacement method, i.e. the adjusting (SBR) or not (DR) of the concrete mix (cement paste volume and w/c ratio) when substituting all the coarse aggregates. This adjustement was done to reach, at room temperature, similar behaviour to a reference concrete. Density, mass loss and conductivity are not influenced by the replacement method. Both phenomenon indicate that cement paste does not substantially change these properties. In contrast, the higher quantity of paste slightly increases the residual compressive strength and elastic modulus. This increase was also observed in previous works that evaluated different w/c ratios [22, 23]. The authors related this to a better interface between old mortar and new mortar. However, the splitting tensile strength is better for concrete with less paste (DR), especially at 400 °C. Considering that thermal mismatch is similar and that most of the changes up to 400 °C are related to cement paste, the lowest value in the SBR mix can be connected to the higher cracks inside the cement paste at this

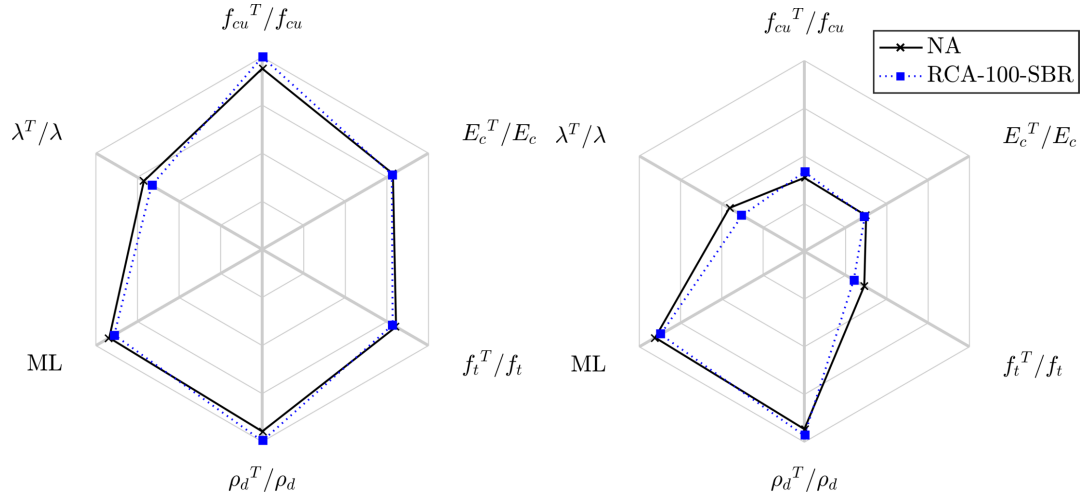

(a) 400 °C (b) 600 °C

Figure 4.13: Effect of a total replacement rate of coarse aggregates in the case of concretes designed to have similar performance at room temperature

temperature

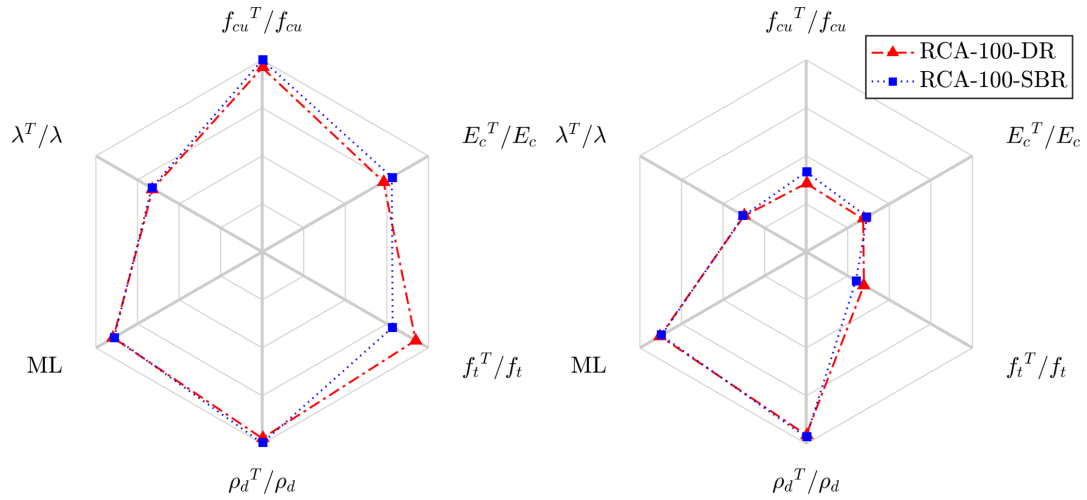

(a) 400 °C (b) 600 °C

Figure 4.14: Effect of replacement method

4.4 Conclusions

This paper presented an experimental investigation into thermomechanical behaviour of concrete made with recycled concrete aggregates. Based on the results, the following conclusions have been drawn:

- Mass loss measurements showed similar behaviour for all studied mixes. RCA mixes presented more mass loss than concrete with NA, and this is

mainly related to the higher quantity of water inside these mixes. The higher water content is directly linked with the higher water absorption of RCA. The aggregates also heavily influenced the density since mixes with a higher quantity of RCA presented lower density. When temperature increases, density is reduced similarly for all mixes.

- Thermal properties were evaluated in terms of conductivity and specific heat. In the case of conductivity, RCA content increased the conductivity of concrete. In addition, thermal gradients were also measured and showed that NA had higher thermal gradients - which can be associated with the measured thermal properties.

- The highest deteriorations were observed in mechanical properties. Compressive strength presented values within the typical values. A better retention on concrete made with 100 % of RCA was observed (DR and SBR), and could be linked with improved interfaces between RCA and new paste. Elastic modulus showed an almost linear decrease with temperature and was similar for all studied mixes. Tensile strength showed unique behaviour, with some increase in strength up to 400 °C. This could be associated with the drying process in the concretes with higher water content (RCA).

- Microstructural observations showed that cracks at RCA do not initiate new paste/old paste at the interface, reinforcing the good match between these phases. Crack development and crack density were similar for both concrete after high temperatures. Concrete made with RCA seems to present higher crack density, but crack width is higher for concrete made with NA.

- The comparative analysis of residual properties showed that the replacement affects some of the properties, especially in the case of mechanical properties. The mixes with 100 % recycled concrete aggregates showed potential to increase tensile strength and compressive strength retention but reduced elasticity. The differences in residual properties diminish if the mix is designed to achieve similar performance at 28 days.

- In general, this paper shows that, even though some differences were observed, RCA can be employed as aggregates and presents similar properties as NA, even in the case of exposure to elevated temperatures.

References

[1] G. Habert, S. Miller, V. John, J. Provis, A. Favier, A. Horvath, et al. "Environmental impacts and decarbonization strategies in the cement and concrete industries". In: *Nature Reviews Earth & Environment* 1.11 (2020), pp. 559–573.

[2] J. de Brito and N. Saikia. *Recycled Aggregate in Concrete*. Springer-Verlag London, 2013, p. 448. DOI: 10.1007/978-1-4471-4540-0.

[3] M. Behera, S. K. Bhattacharyya, A. K. Minocha, R. Deoliya, and S. Maiti. "Recycled aggregate from C&D waste & its use in concrete - A breakthrough towards sustainability in construction sector: A review". In: *Construction and Building Materials* 68 (2014), pp. 501–516. DOI: 10.1016/j.conbuildmat.2014.07.003.

[4] M. K. Dixit, J. L. Fernández-Solís, S. Lavy, and C. H. Culp. "Identification of parameters for embodied energy measurement: A literature review". In: *Energy and Buildings* 42.8 (2010), pp. 1238–1247. DOI: 10.1016/j.enbuild.2010.02.016.

[5] S. Böhmer, G. Moser, C. Neubauer, M. Peltoniemi, E. Schachermayer, M. Tesar, et al. *Aggregates case study*. Tech. rep. 2008, p. 282.

[6] F. de Larrard and H. Colina. "Introduction". In: *Concrete Recycling: Research and Practice*. Ed. by F. de Larrad and H. Colina. CRC Press, 2019, pp. 1–4.

[7] N. Tošić, S. Marinković, T. Dašić, and M. Stanić. "Multicriteria optimization of natural and recycled aggregate concrete for structural use". In: *Journal of Cleaner Production* 87.1 (2015), pp. 766–776. DOI: 10.1016/j.jclepro.2014.10.070.

[8] C. Shi, Y. Li, J. Zhang, W. Li, L. Chong, and Z. Xie. "Performance enhancement of recycled concrete aggregate–a review". In: *Journal of cleaner production* 112 (2016), pp. 466–472.

[9] M. Nedeljković, J. Visser, B. Šavija, S. Valcke, and E. Schlangen. "Use of fine recycled concrete aggregates in concrete: A critical review". In: *Journal of Building Engineering* 38 (2021), p. 102196.

[10] H.-b. Le and Q.-b. Bui. "Recycled aggregate concretes – A state-of-the-art from the microstructure to the structural performance". In: *Construction and Building Materials* 257 (2020), p. 119522. DOI: 10.1016/j.conbuildmat.2020.119522.

[11] F. de Larrard and H. Colina. "Conclusion". In: *Concrete Recycling: Research and Practice*. Ed. by F. de Larrad and H. Colina. CRC Press, 2019, pp. 544–545.

[12] R. Wang, N. Yu, and Y. Li. "Methods for improving the microstructure of recycled concrete aggregate : A review". In: *Construction and Building Materials* 242 (2020), p. 118164. DOI: 10.1016/j.conbuildmat.2020.118164.

[13] C. Laneyrie, A.-L. Beaucour, M. F. Green, R. L. Hebert, B. Ledesert, and A. Noumowe. "Influence of recycled coarse aggregates on normal and high performance concrete subjected to elevated temperatures". In: *Construction and Building Materials* 111 (2016), pp. 368–378.

[14] P. Pimienta, M. C. Alonso, R. Jansson McNamee, and J.-C. Mindeguia. "Behaviour of high-performance concrete at high temperatures: some highlights". In: *RILEM Technical Letters* 2.2017 (2017), p. 45. DOI: 10.21809/rilemtechlett.2017.53.

[15] G. A. Khoury. "Effect of fire on concrete and concrete structures". In: *Progress in Structural Engineering and Materials* 2.4 (2000), pp. 429–447. DOI: 10.1061/41016(314)299.

[16] *fib Bulletin 46: Fire design of concrete structures — structural behaviour and assessment*. Tech. rep. Lausanne, Swiss, 2008, p. 209.

[17] R. Niry, A.-l. Beaucour, R. L. Hebert, B. Ledesert, R. Bodet, and A. Noumowe. "High temperature behaviour of a wide petrographic range of siliceous and calcareous aggregates for concretes". In: *Construction and Building Materials* 123 (2016), pp. 261–273. DOI: 10.1016/j.conbuildmat.2016.06.097.

[18] R. Niry Razafinjato. "Comportement des bétons à haute température : influence de la nature du granulat". PhD thesis. Université de Cergy-Pontoise, 2015, p. 320.

[19] C. C. dos Santos and J. P. C. Rodrigues. "Calcareous and granite aggregate concretes after fire". In: *Journal of Building Engineering* 8 (2016), pp. 231–242.

[20] B. Fernandes, H. Carré, J.-C. Mindeguia, C. Perlot, and C. La Borderie. "Effect of elevated temperatures on concrete made with recycled concrete aggregates-An overview". In: *Journal of Building Engineering* (2021), p. 103235. DOI: 10.1016/j.jobe.2021.103235.

[21] H. Zhao, F. Liu, and H. Yang. "Thermal properties of coarse RCA concrete at elevated temperatures". In: *Applied Thermal Engineering* 140 (2018), pp. 180–189.

[22] C. Zega and A. Di Maio. "Recycled concrete exposed to high temperatures". In: *Magazine of Concrete Research* 58.10 (2006), pp. 675–682.

[23] C. J. Zega and A. A. Di Maio. "Recycled concrete made with different natural coarse aggregates exposed to high temperature". In: *Construction and building materials* 23.5 (2009), pp. 2047–2052.

[24] S. R. Sarhat and E. G. Sherwood. "Residual mechanical response of recycled aggregate concrete after exposure to elevated temperatures". In: *Journal of Materials in Civil Engineering* 25.11 (2013), pp. 1721–1730.

[25] S. C. Kou, C. S. Poon, and M. Etxeberria. "Residue strength, water absorption and pore size distributions of recycled aggregate concrete after exposure to elevated temperatures". In: *Cement and concrete composites* 53 (2014), pp. 73–82.

[26] Y. Wang, F. Liu, L. Xu, and H. Zhao. "Effect of elevated temperatures and cooling methods on strength of concrete made with coarse and fine recycled concrete aggregates". In: *Construction and Building Materials* 210 (2019), pp. 540–547. DOI: 10.1016/j.conbuildmat.2019.03.215.

[27] H. Zhao, F. Liu, and H. Yang. "Residual compressive response of concrete produced with both coarse and fine recycled concrete aggregates after thermal exposure". In: *Construction and Building Materials* 244 (2020), p. 118397. DOI: 10.1016/j.conbuildmat.2020.118397.

[28] G. Chen, Y. He, H. Yang, J. Chen, and Y. Guo. "Compressive behavior of steel fiber reinforced recycled aggregate concrete after exposure to elevated temperatures". In: *Construction and Building Materials* 71 (2014), pp. 1–15.

[29] J. Gales, T. Parker, D. Cree, and M. Green. "Fire performance of sustainable recycled concrete aggregates: mechanical properties at elevated temperatures and current research needs". In: *Fire Technology* 52.3 (2016), pp. 817–845.

[30] F. U. A. Shaikh. "Mechanical properties of concrete containing recycled coarse aggregate at and after exposure to elevated temperatures". In: *Structural Concrete* 19.2 (2018), pp. 400–410.

[31] J. B. da Silva, M. Pepe, and R. D. Toledo Filho. "High temperatures effect on mechanical and physical performance of normal and high strength recycled aggregate concrete". In: *Fire Safety Journal* 117.August (2020). DOI: 10.1016/j.firesaf.2020.103222.

[32] *Béton — Spécification, performance, production et conformité — Complément national à la norme NF EN 206*. Comité Européen de Normalisation. Brussels, 2014.

[33] F. de Larrard and T. Sedran. *BetonLab*. Version BetonLabFree. 2021.

[34] *Testing fresh concrete - Part 2 : slump test*. Comité Européen de Normalisation. Brussels, 2019.

[35] *Essais pour béton frais - Partie 6 : masse volumique*. Comité Européen de Normalisation. Brussels, 2019.

[36] *Essais pour béton frais - Partie 7 : teneur en air - Méthode de la compressibilité*. Comité Européen de Normalisation. Brussels, 2019.

[37] *Testing hardened concrete - Part 3 : compressive strength of test specimens*. Comité Européen de Normalisation. Brussels, 2019.

[38] R. V. Silva, J. De Brito, and R. K. Dhir. "The influence of the use of recycled aggregates on the compressive strength of concrete: A review". In: *European Journal of Environmental and Civil Engineering* 19.7 (2014), pp. 825–849. DOI: 10.1080/19648189.2014.974831.

[39] *Essais pour béton durci - Partie 7 : masse volumique du béton durci*. Comité Européen de Normalisation. Brussels, 2019.

[40] *Durabilité des Betons - Méthodes recommandés pour la mesure des granulats associées a la durabilité*. Association Française de recherches et d'essais sur les matériaux et constructions. Toulouse, 1997.

[41] T. Log and S. Gustafsson. "Transient plane source (TPS) technique for measuring thermal transport properties of building materials". In: *Fire and materials* 19.1 (1995), pp. 43–49.

[42] *Testing hardened concrete - Part 13 : determination of secant modulus of elasticity in compression*. Comité Européen de Normalisation. Brussels, 2021.

[43] R. T. Committee. "Recommendation of RILEM TC 200-HTC: mechanical concrete properties at high temperatures—modelling and applications: Part 1: Introduction—General presentation". In: *Materials and Structures* 40 (2007), pp. 841–853.

[44] *Testing hardened concrete - Part 6 : tensile splitting strength of test specimens*. Comité Européen de Normalisation. Brussels, 2012.

[45] M. C. Alonso and U. Schneider. "Degradation Reactions in Concretes Exposed to High Temperatures". In: *Physical Properties and Behaviour of High-Performance Concrete at High Temperature*. Springer, 2019, pp. 5–40.

[46] I. Hager. "Behaviour of cement concrete at high temperature". In: *Bulletin of the Polish Academy of Sciences: Technical Sciences* 61.1 (Jan. 2013), pp. 1–10. DOI: 10.2478/bpasts-2013-0013.

[47] Z. Chen, J. Chen, F. Ning, and Y. Li. "Residual properties of recycled concrete after exposure to high temperatures". In: *Magazine of Concrete Research* (2018), pp. 1–13.

[48] W. Khaliq et al. "Mechanical and physical response of recycled aggregates high-strength concrete at elevated temperatures". In: *Fire safety journal* 96 (2018), pp. 203–214.

[49] H. Salahuddin, A. Nawaz, A. Maqsoom, T. Mehmood, et al. "Effects of elevated temperature on performance of recycled coarse aggregate concrete". In: *Construction and Building Materials* 202 (2019), pp. 415–425.

[50] F. Robert, A.-L. Beaucour, and H. Colina. "Behavior Under Fire". In: *Concrete Recycling: Research and Practice*. Ed. by F. De Larrard and H. Colina. CRC Press, 2019. Chap. 13, p. 13.

[51] V. Kodur. "Properties of Concrete at Elevated Temperatures". In: *ISRN Civil Engineering* 2014 (2014), pp. 1–15. DOI: 10.1155/2014/468510.

[52] R. J. McNamee, P. Pimienta, and R. Felicetti. "Thermal Properties". In: *Physical properties and behaviour of high-performance concrete at high temperature : state-of-the-art report of the RILEM technical committee 227-HPB*. Ed. by P. Pimienta, R. J. McNamee, and J. Mindeguia. Springer, 2019, pp. 61–69.

[53] V. Kodur, S. Banerji, and R. Solhmirzaei. "Test methods for characterizing concrete properties at elevated temperature". In: *Fire and Materials* September (2019), pp. 1–15. DOI: 10.1002/fam.2777.

[54] V. Kodur, S. Banerji, and R. Solhmirzaei. "Effect of Temperature on Thermal Properties of Ultrahigh-Performance Concrete". In: *Journal of Materials in Civil Engineering* 32.8 (Aug. 2020), p. 04020210. DOI: 10.1061/(asce)mt.1943-5533.0003286.

[55] R. Jansson. *Measurement of thermal properties at elevated temperatures - Brandforsk project 328-031*. Tech. rep. 2004, p. 90.

[56] M. Malik, S. K. Bhattacharyya, and S. V. Barai. "Thermal and mechanical properties of concrete and its constituents at elevated temperatures : A review". In: *Construction and Building Materials* 270 (2021), p. 121398. DOI: 10.1016/j.conbuildmat.2020.121398.

[57] G. A. Khoury, P. J. Sullivan, and B. N. Grainger. "Radial temperature distributions within solid concrete cylinders under transient thermal states". In: *Magazine of Concrete Research* 36.128 (1984), pp. 146–156. DOI: 10.1680/macr.1984.36.128.146.

[58] Y. Liu, W. Wang, Y. F. Chen, and H. Ji. "Residual stress-strain relationship for thermal insulation concrete with recycled aggregate after high temperature exposure". In: *Construction and Building Materials* 129 (2016), pp. 37–47.

[59] N. K. Bui, T. Satomi, and H. Takahashi. "Effect of mineral admixtures on properties of recycled aggregate concrete at high temperature". In: *Construction and Building Materials* 184 (2018), pp. 361–373.

[60] J. Xie, Z. Zhang, Z. Lu, and M. Sun. "Coupling effects of silica fume and steel-fiber on the compressive behaviour of recycled aggregate concrete after exposure to elevated temperature". In: *Construction and Building Materials* 184 (2018), pp. 752–764.

[61] *Design of concrete structures - Part 1-2: General rules - Structural fire design*. Comité Européen de Normalisation. Brussels, 2004, p. 99.

[62] E. Ghorbel, T. Sedran, and G. Wardeh. "Instantaneous Mechanical Properties". In: *Concrete Recycling: Research and Practice*. Ed. by F. de Larrad and H. Colina. CRC Press, 2019, pp. 162–185.

[63] Q. Ma, R. Guo, Z. Zhao, Z. Lin, and K. He. "Mechanical properties of concrete at high temperature-A review". In: *Construction and Building Materials* 93 (2015), pp. 371–383. DOI: 10.1016/j.conbuildmat.2015.05.131.

[64] J. Vieira, J. Correia, and J. De Brito. "Post-fire residual mechanical properties of concrete made with recycled concrete coarse aggregates". In: *Cement and Concrete Research* 41.5 (2011), pp. 533–541.

[65] H. Yang, H. Zhao, and F. Liu. "Compressive Stress-Strain Relationship of Concrete Containing Coarse Recycled Concrete Aggregate at Elevated Temperatures". In: *Journal of Materials in Civil Engineering* 31.9 (2019), pp. 1–8. DOI: 10.1061/(ASCE)MT.1943-5533.0002851.

[66] P. Pimienta, J.-C. Mindeguia, G. Debicki, U. Diederichs, I. Hager, S. Huismann, et al. "Mechanical Properties". In: *Physical properties and behaviour of high-performance concrete at high temperature : state-of-the-art report of the RILEM technical committee 227-HPB*. Ed. by P. Pimienta, R. J. McNamee, and J. Mindeguia. Springer, 2019, pp. 71–124.

[67] D. J. Naus. *The effect of elevated temperature on concrete materials and structures - A literature review*. Tech. rep. 2005.

[68] H. Yang, H. Zhao, and F. Liu. "Residual cube strength of coarse RCA concrete after exposure to elevated temperatures". In: *Fire and Materials* 42.4 (2018), pp. 424–435.

Chapter 05

Spalling behaviour of concrete made with recycled concrete aggregates

This chapter is based on the paper *Spalling behaviour of concrete made with recycled concrete aggregates*, published in the *Construction and Building Materials*, and on the paper *Experimental investigation on the effect of water content profile on fire spalling*, submitted to the *7th International Workshop on Concrete Spalling due to Fire Exposure*. Both literature review and the first experimental campaign highlighted the influence of aggregate's properties on high temperature behaviour of concrete made with RCA. Even though some similar behaviour between concrete made with NA and RCA was observed, some particularities (porosity and water content, for example) are relevant, especially in the case of spalling. The first part of this chapter presents a comprehensive fire spalling screening test on several mixes of concrete made with RCA (0 %, 10 %, 20 %, 40 %, and 100 %). In the spalling tests, samples were subjected to fire (ISO 834-1) and constant uniaxial loading (2.5 and 5 MPa). For postfire assessment, digital photogrammetry was used. In the second part, the mechanisms behind the spalling were further investigated, especially the water content profile's effect on concrete's spalling behaviour (NA and RCA). To this, spalling samples were dried for different drying periods (from 12 h to 7 d) to obtain different water content profiles throughout the sample thickness. Small concrete cylinders underwent the same drying procedure to determine water content at different depths. After the different drying periods, fire spalling tests were made in spalling samples, as also the postfire assessment.

Fernandes, B.; Carré, H.; Mindeguia, J-C.; Perlot, C.; La Borderie, C. *Spalling behaviour of concrete made with recycled concrete aggregates*. Construction and Building Materials. (`https://doi.org/10.1016/j.conbuildmat.2022.128124`)

Fernandes, B.; Carré, H.; Mindeguia, J-C.; Perlot, C.; La Borderie, C. *Experimental investigation on the effect of water content profile on fire spalling*. Submitted to the 7th International Workshop on Concrete Spalling due to Fire Exposure, Berlin, Germany.

5.1 Introduction

One of the main concerns when evaluating the fire behaviour of concrete structures is spalling. This phenomenon consists of violent or nonviolent detachment of concrete fragments from the surface of a concrete member [1, 2]. Depending on the severity of the damage, fire spalling can seriously affect the structural performance because it reduces the cross section and may even expose steel rebars directly to the fire. This can lead to a reduction in fire resistance, thermal insulation, and load-bearing capacity [3–5]. Despite extensive research in recent years, uncertainties regarding the phenomenon remain, and current models cannot predict spalling events [4, 6, 7].

Concrete behaviour under fire is a coupled thermo-hygro-chemo-mechanical problem, and all these mechanisms can contribute to the spalling phenomenon [2]. Spalling is usually explained by one of two theories, (i) pore pressure build-up and (ii) thermal stresses, which may occur individually or jointly [2, 8]. The first, pore pressure build-up, is a thermo-hygral process driven by water vaporisation and transport. During heating, the vapour moves towards the exposed surface and into the inner part of the concrete (nonheated). Owing to thermal gradients, the vapour may condense in the inner core, creating a saturated layer a few centimetres from the exposed side (the so-called 'moisture clog'). This zone blocks further vapour movement, leading to an increase in pore pressure. When stresses resulting from pore pressure exceed the tensile strength of concrete, spalling may occur [2, 4, 9–11].

The second theory is a thermo-mechanical process driven by thermal-gradient-induced thermal stresses and/or restrained thermal dilation [2]. When these high stresses (compressive ones), localized in the first centimetres of the concrete surface, exceed concrete strength, spalling may occur [4, 8, 11]. Usually, spalling is also attributed to the coupled action of these mechanisms (thermo-hygral and thermo-mechanical), i.e., a combination of pore pressure, compression stresses (induced by thermal action and loading), and cracking [1]. In addition, a thermo-chemical spalling mechanism was proposed, in which the phenomenon is related to the decomposition of calcium hydroxide and the rehydration of calcium oxide [2].

The complexity of the spalling problem is highlighted by the several parameters that may influence the occurrence of spalling. These parameters can be classified into material (e.g., permeability, porosity, and water content), geometry (e.g., shape and size of elements), and environmental (e.g., heating rate, heating profile, and external mechanical load) factors [1]. In addition, spalling can occur in different forms, such as aggregate, surface, explosive, and corner spalling [1, 11].

Little is known about the susceptibility of concrete made with recycled concrete aggregates (RCA) to spalling, and the prediction of its sensitivity to spalling is generally not trivial. On the one hand, because RCAs are more porous than natural aggregates (NA), the use of this type of aggregate may contribute to vapour migration, reducing the pore pressure and spalling risk [12]. On the other hand, RCAs have higher water absorption, which may lead to concrete

with higher water content, i.e., a key parameter for spalling risk [13, 14]. Finally, more interfacial transition zones are observed in concrete made with RCA (old paste/new paste, old aggregate/new paste), which may lead to distinct behaviour under high temperatures.

Few studies have verified the occurrence of fire spalling in recycled concrete aggregate (RAC) [15]. Robert et al. [16] studied the spalling behaviour of concrete slabs made with RCA. They tested two reference slabs and two slabs of concrete made with RCA (one with 30 % coarse RCA and the other with 30 % both fine and coarse RCA). All the elements were tested under the ISO 834-1 [17] fire curve for 60 min. Superficial and localised spalling was observed in all slabs containing RCA, whereas slabs with NA did not exhibit any spalling. This phenomenon was attributed to the high moisture content of RAC slabs - between 4.4 % and 5.5 % at the element surface, whereas reference slabs had a moisture content of 4.0 %. However, the extent of damage in RAC slabs was not detrimental to their stability. Chen et al. [18] evaluated the mechanical properties of reinforced concrete and steel-reinforced concrete (i.e., composite) short columns and beams after exposure to elevated temperatures. Samples prepared with different replacement rates were heated in an electric furnace. Spalling in samples heated to 800 °C was reported, but no further details or explanations were provided

Spalling was also observed by Pliya et al. [12, 19]. In the first study [12], they tested the spalling sensitivity of high-strength concrete made with NA and RCA (0 %, 15 %, and 30 % replacement rates). Concrete cylinder samples were heated in an electric furnace at a rate of 10 °C/min. All mixes (with or without RCA) showed progressive and explosive spalling, characterised by the sudden disintegration of all samples. A similar phenomenon was observed in another study [19], in which spalling was found in samples subjected to preloading and when the surface temperature reached 150 °C. For samples made with NA spalling happened at 450 °C.

The aforementioned experimental studies demonstrated that spalling could occur in concrete made with RCA. However, a systematic evaluation of the spalling risk of concrete made with RCA has not been performed. This lack of information prevents the robust design of concrete made with RCA regarding its fire behaviour. In this chapter, the fire spalling sensitivity of concrete made with RCA was investigated experimentally. This investigation was made in two different campaigns. In the first one, a material screening test was made to provide a qualitative and comparative evaluation of the spalling behaviour of concrete made with RCA. In the second one, an investigation on the mechanisms behind spalling was made, especially on the influence of different water content profiles on spalling.

For the first campaign, fire tests on uniaxially loaded samples were performed. Ordinary concrete mixes containing different replacement rates of coarse aggregates (10 %, 20 %, 40 %, and 100 %) were subjected to the ISO 834-1[17] fire curve. In addition to the replacement rate, the effect of the external mechanical load and replacement method were studied. Spalling events were registered during the fire tests. For postfire spalling assessment, a method based on digital

photogrammetry was used. Finally, the spalling behaviour of the specimens and the influence of RCA were examined in light of common spalling theories.

For the second campaign, fire tests were carried out on concrete made with natural aggregate (NA) and on samples made with 100 % of coarse RCA. Before fire tests, samples were dried at 80 °C for different drying periods (from 12 hours to 7 days) to induce different water content profiles throughout the sample thickness, especially along the first centimetres of the exposed surface. After the drying period, concrete prisms were subjected to the uniaxial fire spalling test. Small concrete cylinders underwent the same drying procedure to determine the water content at different depths of the samples. Once again, spalling volume and depths were evaluated through digital photogrammetry. Lastly, spalling was examined in light of the different water content profiles.

5.2 Experimental program

5.2.1 Materials

Concrete mixes were prepared using cement CEM II/A-L 42.5R (Eqiom). This cement has a density of 3010 kg/m^3 and a specific surface area of 4700 cm^2/g. To achieve the desired workability, limestone filler (Omya Betocarb HP-SC) was used. This filler has a density of 2700 kg/m^3 and a specific surface area of 4330 cm^2/g. A polycarboxylate-based superplasticiser (SIKA ViscoCrete Tempo-483) was used in the mixes.

Alluvial sand with a fineness modulus of 3.10 was used. Two types of coarse aggregates were used: NA and RCA. Natural aggregates were made from diorite (Genouillac, France) and divided into two fractions: 4/10 and 10/20. The recycled concrete aggregates were crushed and screened by a recycling company near Bordeaux (France). They were divided into the same fractions as the NA. The physical properties (density, water absorption, and LA coefficient), measured according to EN 1097-2:2010 [20] and EN 1097-6:2013 [21], are presented in Table 5.1. As expected, RCA had higher water absorption and a lower LA coefficient owing to the presence of the adhered mortar.

Table 5.1: Aggregate properties

Property	Sand	Natural aggregate		Recycled aggregate	
Grading size	0/4	4/10	10/20	4/10	10/20
Density (kg/m^3)	2650	2820	2840	2570	2590
Water absorption (%)	0.35	0.92	0.81	5.60	4.52
LA coefficient (%)	-	16	16	30	36

Because RCAs were obtained from a recycling plant, they also presented some impurities related to demolition wastes, such as wood, plastic, brick, and bituminous materials. To quantify these impurities, manual sorting was performed following EN 933-11:2009 [22] guidelines. The results of this classification are listed in Table 5.2.

Table 5.2: RCA constituents

Aggregate Fraction	Constituents (% of mass)*					
	Rc	Ru	Rb	Ra	Rg	X
RCA 4/10	73.31	23.97	0.53	2.14	-	0.05
RCA 10/20	76.77	18.59	0.50	3.87	0.07	0.19

*Rc: concrete grains, Ru: natural stones, Rb: ceramic elements, Ra: bituminous grains, Rg: glass, X: other materials (wood, plastic,steel, paper, etc.)

5.2.2 Mixture design and casting

To investigate the fire spalling behaviour of concrete made with RCA, a comprehensive test program was undertaken on seven mixes divided into three categories: reference, direct replacement (DR), and strength-based replacement (SBR). Table 5.3 presents the mixture proportions for all the mixes. The reference samples are concrete made with NA, designed to meet the NF EN 206/CN:2014 [23] durability requirements for the XD3 exposure class. This class determines a maximum water/cement (w/c) ratio of 0.5, a compressive strength class of C35/45, and a minimum cement content of 350 kg/m^3. In DR mixes, NA was replaced by RCA in volume without any changes in the other constituents. Replacement rates for this mix were chosen based on the RECYBETON [24] French project recommendations, which, for XD3 exposure classes, allow maximum replacement rates of 20 % and 40 %. Additional replacement rates of 10 % and 100 % were also studied for the DR mixes.

In SBR mixes, in addition to aggregate replacement, the cement and water contents were adjusted to achieve the same strength as the reference mix. To adjust mixes, BetonLab [25] software was used. Based on the compressive strength results of the reference and DR mixes, the properties of the aggregates (p and q coefficients, which describe the aggregate contribution to the compressive strength) were calibrated. Then, new mixes were designed. The w/c ratio was adjusted to achieve the same compressive strength as that of the reference mix. The water and cement contents were adjusted to achieve the target consistency. For the SBR mixes, replacement rates of 40 % and 100 % were studied.

Table 5.3: Mix proportions (in kg/m^3, SP in percentage of cement mass)

Material	Mix						
	NA	RCA-10-DR	RCA-20-DR	RCA-40-DR	RCA-100-DR	RCA-40-SBR	RCA-100-SBR
Cement	350	350	350	350	350	368	420
Filler	60	60	60	60	60	60	60
Sand	804.3	804.3	804.3	804.3	804.3	787.1	799.8
NA 4/10	331.7	298.5	265.3	199.0	-	207.2	-
NA 10/20	711.1	640.0	568.9	426.7	-	447.5	-
RCA 4/10	-	30.2	60.5	120.9	302.3	114.7	291.5
RCA 10/20	-	64.9	129.7	259.4	648.5	248.1	630.3
Water	175	175	175	175	175	172	168
SP	0.9	0.9	0.9	0.9	0.9	0.9	0.9

One concern when using RCA stems from its higher water absorption. This

property can affect the workability of concrete, even when moisture adjustments are made to the mixes [26]. To develop a method that can be easily reproduced in a concrete plant, all the aggregates (sand, NA, and RCA) were prewetted for 1 h using a soaker hose and then covered with a plastic sheet for 3 h. Before casting, the moisture content of the aggregates was measured and the water quantity of the mix was corrected.

Preliminary studies showed some variations in workability and compressive strength, even for the same mixes. Because the ratio between the slump and compressive strength was constant in the preliminary mixes, mixes with dried aggregates were cast to verify the reference slump and its corresponding compressive strength. These values were used as a reference for the final mixes (slump between 180 and 190 mm). In the final mixes, the aggregates were prewetted, and the water content was adjusted to achieve the same slump as the reference. The same mixing procedure was used for all the concrete mixes. The slump was measured after mixing following NF EN 12350-2 [27].

For each mix, cylindrical specimens (11 x 22 cm and 16 x 32 cm) were cast to determine the mechanical properties at 28 days and at the fire test age. These samples kept submerged in water at 20 °C until the testing day. For the fire tests, prisms with dimensions of 20 x 20 x 10 cm (height x length x width) were cast. In addition, prisms of 15 x 15 x 10 cm (height x length x width) were cast for the water content study. Curing was slightly different for each one of the campaigns. For the first one (screening), samples were first kept submerged for seven days and then placed in sealed plastic bags until the test (between 88 and 125 days). For the second campaign (water content analysis), samples were then kept submerged in water until the drying process (between 70 and 90 days). In both campaigns, the curing process induced a high water content (when compared with air curing), thus inducing a high probability of spalling for all the mixes. At the test age, the water content (wc), density (ρd), and water-accessible porosity (η) were measured following the NF EN 12390-7:2019 [28] and AFREM recommendations [29]. The slump, mechanical and physical properties of all the studied mixes are listed in 5.4.

Table 5.4: Fresh, mechanical, and physical properties of studied mixes

Mix	Campaign	Slump (mm)	f_{c28} (MPa)	j (days)	$f_{c,j}$ (MPa)	$E_{c,j}$ (GPa)	WC (%)	ρd (g/cm3)	η (%)
NA	1	194	44.8	94	46.6	34.5	4.9	2.3	23.3
	2	195	47	-	-	-	-	-	-
RCA-10-DR	1	184	39.7	116	44.5	36.8	5.0	2.2	13.8
RCA-20-DR	1	174	37.4	88	50.8	34.9	5.1	2.2	16.0
RCA-40-DR	1	176	39.7	88	49.6	39	5.4	2.2	15.2
RCA-100-DR	1	210	34.6	125	39.1	30.5	7.1	2.1	18.1
	2	178	37.9	-	-	-	-	-	-
RCA-40-SBR	1	192	44.6	94	46.8	31.8	5.7	2.2	15.3
RCA-100-SBR	1	180	45.5	94	46	30.9	6.9	2.1	17.9

*j is fire test age

5.2.3 Water content analysis

In the second campaign, a specific workflow was proposed to estimate the water content profile in concrete made with NA and RCA-100-DR. From the saturated prisms of 15 x 15 x 10 cm, small concrete cylinders of ⌀1 x 10 cm were cored (Fig. 5.1a). Then, the curved face of the cylinders was wrapped with aluminium tape and placed in the oven for drying (Fig. 5.1b). They were dried at 80 °C and 3 % RH during different drying periods (Table 5.5). Six cylinders per drying condition were evaluated. After this period, cylinders were removed from the oven. Then, they were sliced into small pieces of approximately 1 cm (Fig. 5.1c) using dried sawing.

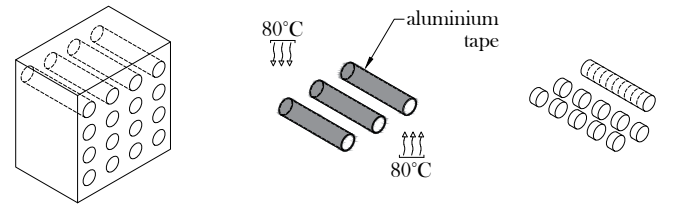

Figure 5.1: Water content analysis process

Table 5.5: Drying conditions

Mix	Drying duration (80 °C and 3 % RH)						
	Sat.	12 h	1 d	2 d	3 d	4 d	7 d
NA	X	X	X	X	X	X	X
RCA-100-DR	X	-	X	X	-	-	X

Each small piece was measured and then dried (80 °C and 3 % RH) until mass stabilisation (mass variation less than 0.05 %) to determine the water content in each one of the slices. The position of each slice was calculated based on piece thickness and the total height of the small cylinders. This method was done to take into account the thickness of the saw cut. With these two measures, the water content profile for each mix/condition was estimated. Since the drying was symmetrical, half of the cylinder was mirrored to obtain a denser cloud of data, and better estimate the profile. Then, a regression analysis was done for each case to estimate the water profile curve.

Fig. 5.2 presents the water content profile for two different conditions. Fig. 5.2a shows the profile in the saturated RCA-100-DR sample. The scatter values of each piece were plotted together with the average value from all the pieces. The value is close to the water content measured in bigger samples (1/4 of 11 x 22 cm), indicating that this approach can reasonably estimate the water content inside the concrete. Fig. 5.2b shows the water content profile in RCA-100-DR after 1 d of drying. In this case, for the regression, a second-degree polynomial

was used for the fit. Some variations from the individual values were observed, but they were expected given the small size of the cylindrical sample. In any case, the method seems to be an appropriate estimation of the water content profile. The same procedure was done for all the studied conditions.

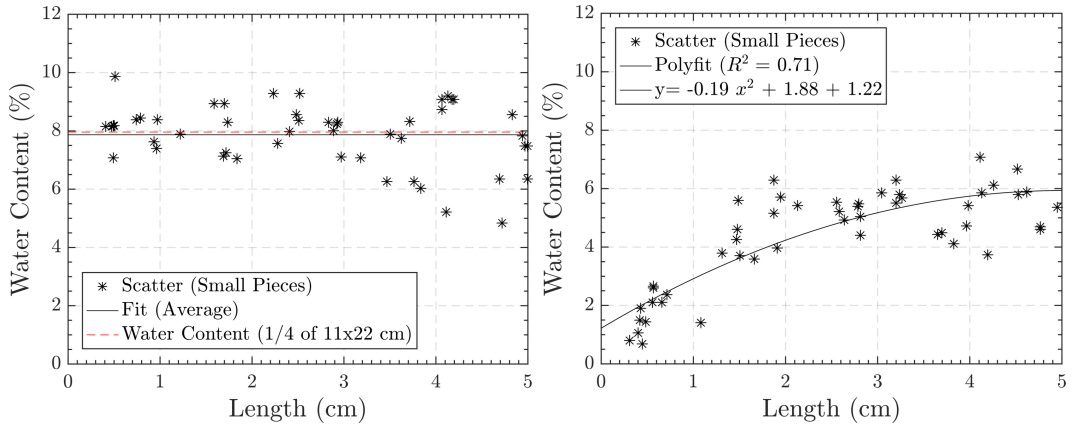

(a) RCA-100-DR (Saturated) (b) RCA-100-DR (1 d of drying)

Figure 5.2: Water content profiles examples

5.2.4 Fire tests

5.2.4.1 Test setup

The spalling behaviour was evaluated by testing 72 concrete prisms subjected to a standard fire and uniaxial mechanical loading. In the first campaign, 39 samples were evaluated. With the exception of the 10 % replacement rate, six prisms were evaluated for each mix. From these six samples, two load levels were evaluated: 2.5 and 5 MPa. In the second campaign, spalling was evaluated by testing 33 concrete prisms subjected to a standard fire and uniaxial mechanical loading (5 MPa). Three prisms were evaluated for each mix and each drying condition (Table 5.5).

The pre-conditioning before the test was also different for each campaign. For the first one, two days before the spalling tests, the four lateral sides (20 x 10 cm) of the prisms were sealed with aluminium foil tape, which was glued using refractory glue resistant up to 1200 °C. In the second campaign, saturated samples were removed from the water curing and also sealed with aluminium foil tape on the four lateral sides (20 x 10 cm). Then, they were placed in the drying oven at the same conditions (80 °C and 3 % RH) and exposure days as the small cylinders (Table 5.5). After the referred drying period, samples were removed from the oven and went to spalling tests. Before the tests, the samples were insulated with 12 cm of rock wool from both sides in both campaigns. The combination of aluminium foil and rock wool was used to provide quasi-unidirectional transport of heat and moisture.

An intermediate-scale furnace powered by a linear propane gas burner was used for heating. This furnace was used in similar experimental studies [30–32]. The gas pressure was controlled during the test according to the ISO 834-1:1999

[17]/NF EN 1363-1:2020 [33] fire curve. The furnace has an opening of 20 x 20 cm. Three type K jacketed thermocouples were used to measure the heating curve; they were placed in front of the furnace 1 cm from the heated face of the sample. The thermocouples were placed at heights of 4, 10, and 16 cm from the bottom of the furnace opening. The details of the furnace are shown in Fig.5.3.

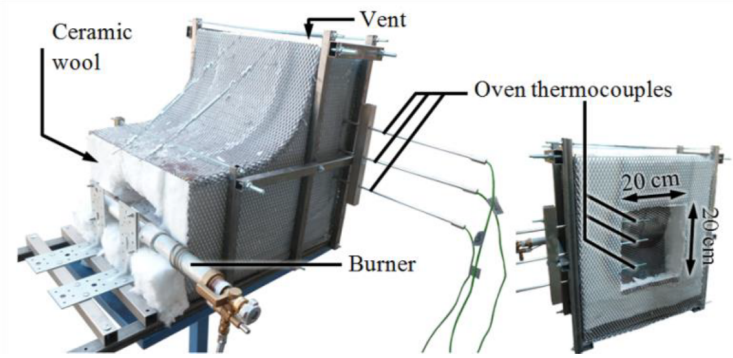

Figure 5.3: Furnace details

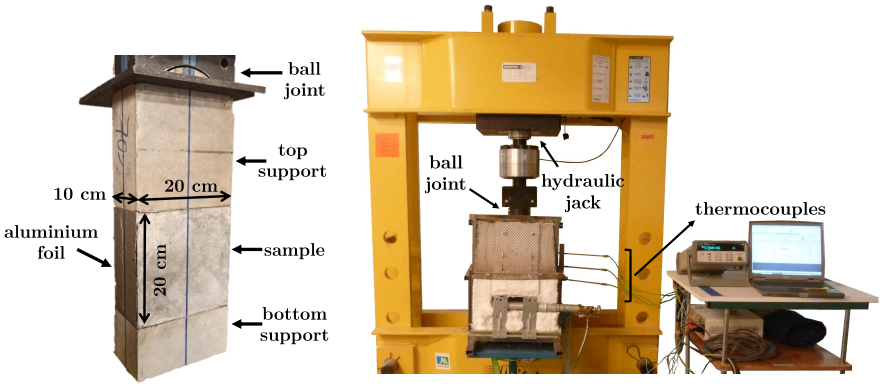

(a) sample and supports (b) furnace and press

Figure 5.4: Overview of test setup

A hydraulic press was used to apply the uniaxial loading. To ensure the load distribution, the tested specimen was placed between two concrete blocks (top and bottom supports). The sides of the tested specimen and support blocks were insulated with rock wool, as well as the hydraulic jack. Some details of the test setup and sample positions are shown in Fig.5.4. The load was applied first. After stabilisation, the heating process was initiated. After 30 min, the heating was turned off, and, after another 5 min, the sample was discharged. During the tests, the time of occurrence of each spalling event was recorded.

Fig. 5.5 presents the time-temperature curves from all tests (average of the three thermocouples). The x marks indicate the time of the first spalling event for each sample. Most of the curves, up to the first spalling event, closely followed the ISO 834-1:1999 [17]/NF EN 1363-1:2020 [33] prescription. After the first

spalling time, perturbations were observed at the recorded temperatures. The main criterion adopted for test validation was whether the curve followed the tolerances up to the first spalling event. For the first campaign (Fig. 5.5a) only two fire tests did not consider the tolerance (RCA-10-DR and RCA-20-DR). For the second campaign, only one mix (sample 2 from NA-1D) did not reach the criteria. These three samples were excluded from further analysis.

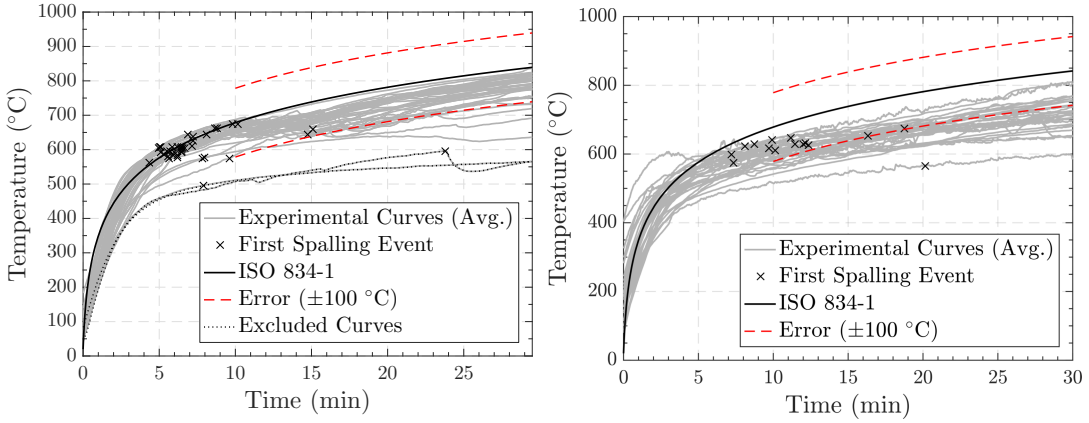

(a) first campaign (b) second campaign

Figure 5.5: Developed fire curves

5.2.4.2 Postfire analysis

After heating, a postfire analysis was conducted on all samples. First, mass measurements were performed before and after the fire tests. Digital photogrammetry was then used to quantify the spalling (volume and depth). This method makes it possible to construct 3D models from digital photographs. It has been previously used for different *in situ* and laboratory measurements [34, 35]. This method follows an approach that involves image acquisition and processing, 3D reconstruction, mesh generation, and post-processing [35].

A digital single-lens mirrorless camera (Panasonic DMC-GX80) with a zoom lens (G Vario 14-42 mm f/3.5-5.6 ASPH) was used. This camera has a sensor of 17.3 x 13.3 mm and resolution of 16 megapixels. For image acquisition, the samples were placed in a rotating table with marks on the surface to orient the 3D reconstruction. The camera was fixed on a tripod, and photographs were taken with ISO 400, an aperture of f/14, and a shutter speed of 1/3 seconds. These settings were selected to have an appropriate exposure with a larger depth of field such that all the exposed surfaces of the sample were in focus. Between shots, the rotating table was turned 10° to overlap consecutive images, which is a necessary procedure for 3D reconstruction. Thirty-six images were obtained for each sample; an example of the image taken is shown in Fig.5.6a.

The image processing and 3D reconstruction were done with Meshroom [36] software. The 3D model of each model was processed using CloudCompare software [37]. Using this software, the 3D model was cleaned and scaled utilizing the reference marks on the rotating table. Fig.5.6b presents an example of a cleaned and scaled 3D model. A binary mesh of the 3D model was imported in

a Cast3m [38] algorithm, which postprocessed the model to obtain the spalling volume and depths. A depth colour map generated in Cast3m [38] is presented in Fig.5.6c.

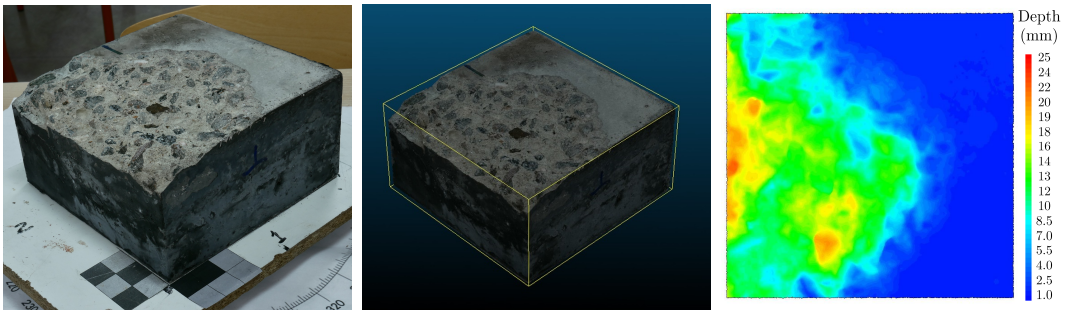

(a) digital photograph (b) 3D model (c) depth colour map

Figure 5.6: Steps in the photogrammetry analysis

An accuracy assessment was performed to estimate the error in the photogrammetry measurements. The experiment was conducted using small pieces of (Lego® pieces). A Lego® piece was placed on the surface of a concrete sample, and photogrammetry analysis was performed with this configuration. From this analysis, the dimensions of the Lego® pieces were measured, and the values were compared with the dimensions obtained using a calliper. The difference between the dimensions measured by photogrammetry analysis and the caliper range from 1.06 % to 2.07 %, showing good agreement between the measurements in all experiments. In addition, the results are within the range of different experimental programs that used digital photogrammetry methods (0.11 to 8.63 %) [34, 35].

Table 5.6: Accuracy assessment of photogrammetry measurements

Lego® Dimension	Calliper	3D Model	Difference (%)
Height (mm)	17.68	17.87	1.06
Width (mm)	15.78	15.55	1.50
Length (mm)	31.8	31.16	2.07

5.3 Results and discussion

5.3.1 First Campaign

This section presents the results obtained in the first campaign. This campaign evaluated different parameters: applied load, replacement method (DR vs SBR) and replacement rate. In the end, the spalling behaviour of the specimens and the influence of RCA were examined in light of common spalling theories.

5.3.1.1 Spalling events during fire tests

The spalling event time was recorded during the fire tests. Fig. 5.7a shows the time of the first spalling event for all the tests. Except for one test on RCA-10-

DR and one on RCA-100-SBR, the first spalling event occurred between 5 and 10 min. In general, no specific relationship was observed between the time of the first event and load or replacement rate. This range of time to the first spalling falls within the range observed in previous tests [7, 39, 40]. Fig. 5.7b shows the total number of spalling events for each test. No clear relationship was observed. The data were highly scattered, highlighting the random nature of the spalling phenomenon [41].

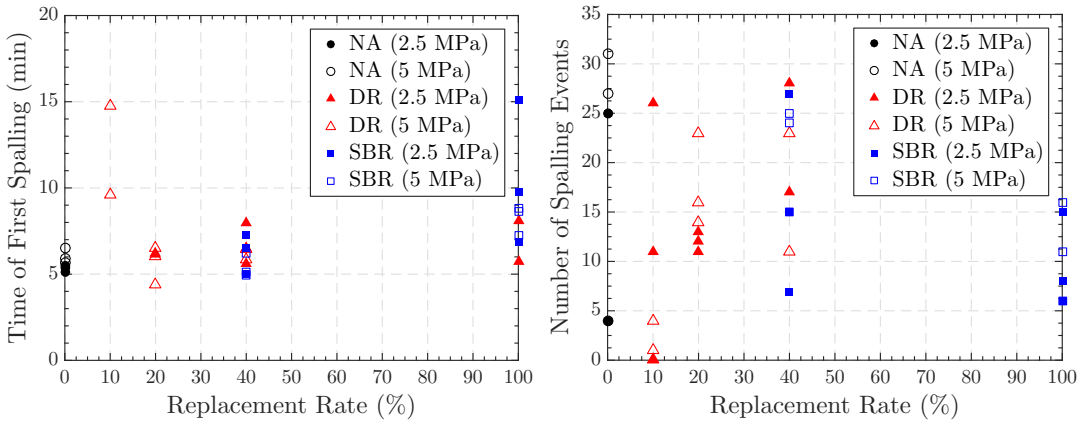

(a) time to first spalling (b) total spalling events

Figure 5.7: Spalling events

5.3.1.2 Inspection of samples after fire tests

Based on visual inspection, NA mixes showed less spalling than RCA mixes, regardless of RCA content, compressive strength, or applied load. As an example, Fig. 5.8 shows four samples after the fire test, together with the depth colour maps generated by the photogrammetry process. The NA mixes almost did not spall, with only some localised spalling. With 20 % RCA (RCA-20-DR), the concrete already had a higher degree of spalling than NA. Finally, both 100 % replacement rate mixes (RCA-100-DR and RCA-100-SBR) had the highest spalling degree, with no significant visual difference between them.

The samples with a high replacement rate presented some burned impurities, mainly bituminous products. Fig. 5.9a shows that the area around the bituminous particle is black, denoting the burning and melting of this kind of particle. Fig.5.9b presents a zoom-in of these particles, where it can be seen that the aggregates remain, but the bituminous material disintegrated. The presence of these impurities locally reduced the strength of concrete made with RCA at high temperatures, as observed by Laneyrie et al. [42]. However, it was not possible to establish a link between spalling and impurities in recycled aggregates.

5.3.1.3 Postfire assessment of spalling

The postfire assessment of spalling was performed using four different indicators: total weight loss of the sample (percentage of the initial mass of the sample),

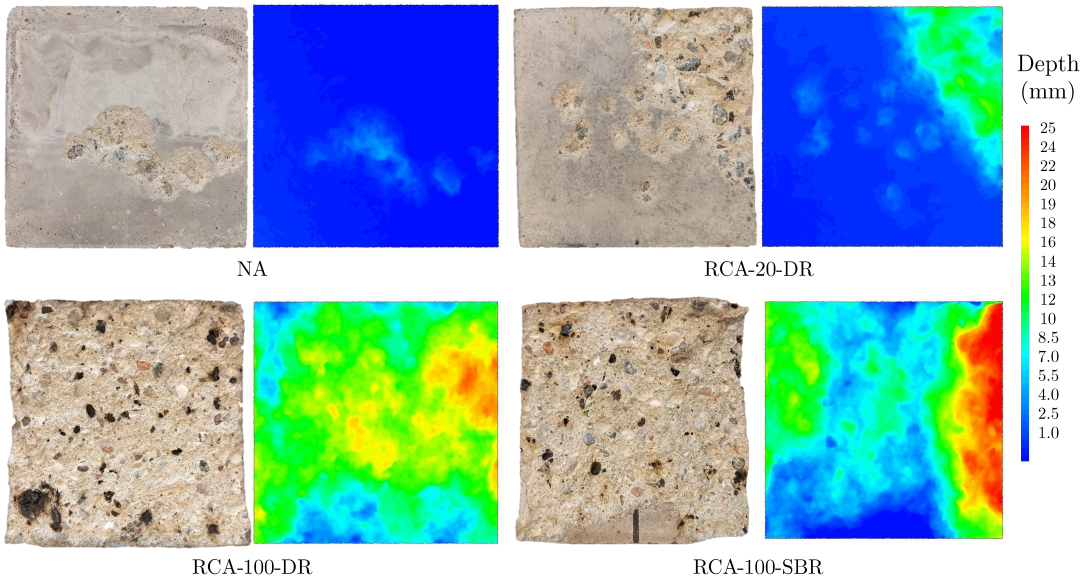

Figure 5.8: Four samples after fire test and spalling depths maps

(a) global view (b) burned impurity

Figure 5.9: RCA-40-DR sample after fire test

spalled volume (percentage of the initial volume of the sample), mean spalling depth (mm) and maximum spalling depth (mm). The last three were obtained using photogrammetry. Fig.5.10 shows some of the relationships between these indicators. Because the spalled volume is the integral of the mean spalling depth, the relationship these two indicators is not presented.

First, the relationship between the spalled volume and maximum spalling depth is presented at the top left. This relationship relatively linear, with a strong correlation between both indicators, even though they are not directly linked. At the top right, weight loss and spalled volume show a strong correlation. The linearity is expected because a higher spalled volume indicates higher mass loss. Some differences may be associated with the fact that weight loss comprises both the spalled volume and loss resulting from water evaporation. Finally, at

the bottom left, the weight loss is compared with the maximum spalling depth. The correlation is lower because a higher maximum spalling depth does not always mean a higher weight loss. Considering all the relationships between the indicators, further analysis will be performed by considering only the spalled volume and maximum spalling depth.

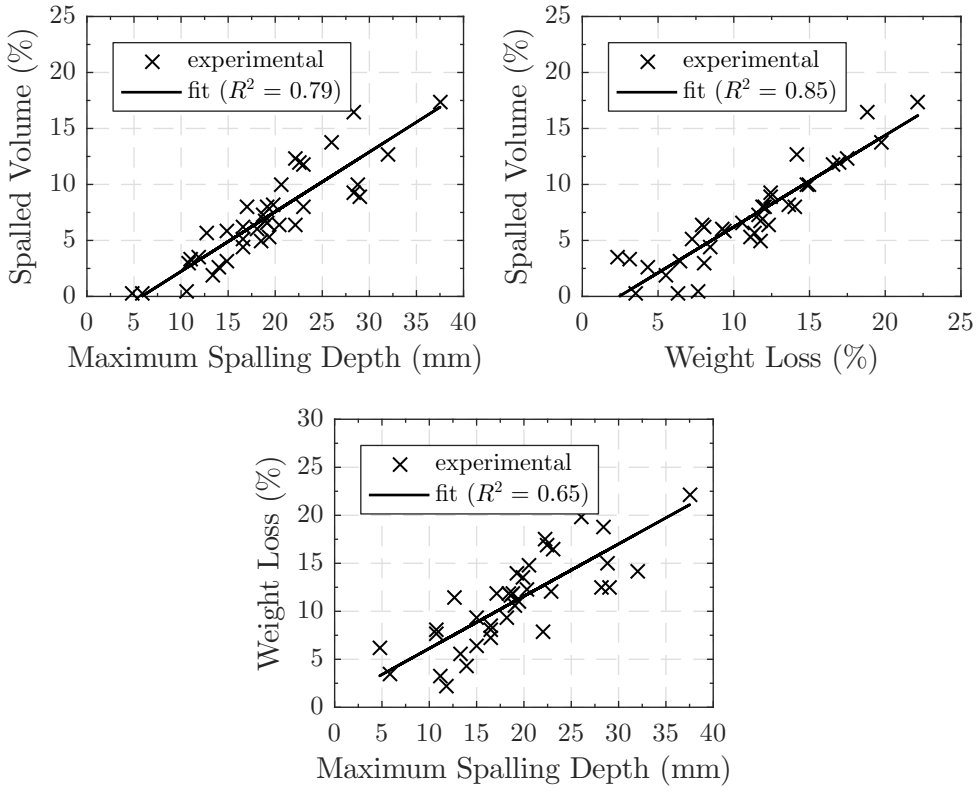

Figure 5.10: Relation between spalling indicators

The effect of uniaxial loading on the fire spalling behaviour is presented in Fig.5.11, both in terms of the spalled volume (Fig.5.11a) and maximum spalling depth (Fig.5.11b). The graphs show each of the mixes analysed with both applied mechanical loads. Even though the variation in the individual tests was high, both results indicate that the increase in the loading level led to an increase in spalling, except for RCA-100-DR. Scattering was more significant for concrete made with RCA than for concrete made with NA. However, no direct link to the replacement rate was identified.

The effect of loading was particularly observed for the RCA-40-DR mix, which presented more than twice the spalled volume with a load increase of 3.5 % for 2.5 MPa and 10.1 % for 5 MPa. By contrast, the lowest difference was observed for concrete made with NA, with spalled volumes of 2.05 % and 2.90 % for loadings of 2.5 MPa and 5 MPa, respectively. An increase in the spalled volume with the load was not observed for the RCA-100-DR mix, presenting a higher spalled volume of 2.5 MPa. This was one of the mixes that presented a higher dispersion of results.

Similar observations were made regarding the maximum spalling depth but with an even less clear tendency between the load and spalling depth. For example, NA, RCA-40-SBR, and RCA-100-SBR presented, had the same maximum spalling depth (average value), regardless of the applied load. The largest difference was observed for RCA-40-DR, with a variation of 9 mm between the two loads. In the case of the spalled volume, the RCA-100-DR mix also had a higher maximum spalling depth with a loading of 2.5 MPa.

The key influence of the load on spalling was previously verified in different experimental setups and concrete mixes [43, 44]. However, only a few studies [30, 45, 46] have evaluated the effect of different load levels on concrete. All of this previous studies were made in concrete made with NA. In general, their conclusions agree with the general behaviour observed herein: spalling severity may increase with external load.

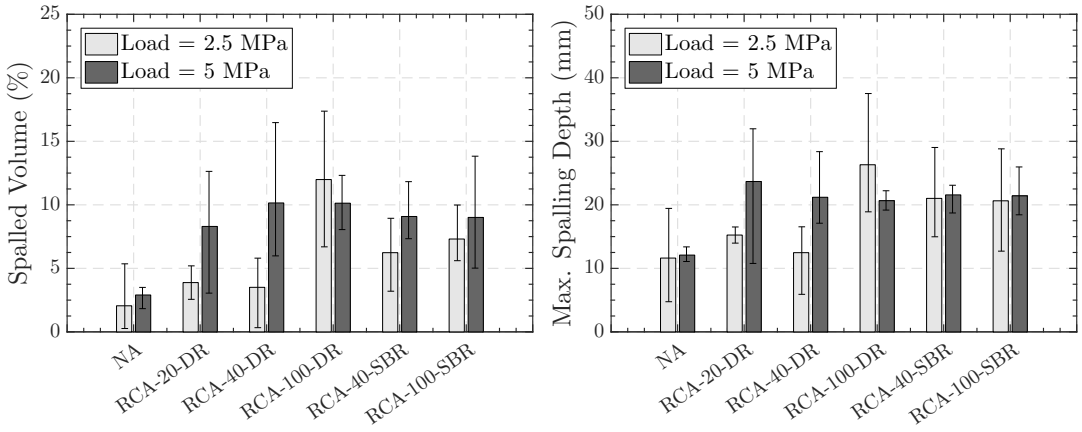

(a) spalled Volume (b) maximum Spalling Depth

Figure 5.11: effect of compressive axial loading on spalling indicators

Figs. 5.12 and 5.13 show the effect of replacement rate and the replacement method (DR/SBR) on the spalling behaviour. The replacement method affects the cement paste volume and, consequently, the concrete compressive strength. SBR mixes have denser and stronger pastes and a higher quantity of cement paste. In these graphs, the spalling indicators (volume and depth) are plotted against the replacement rate. In each graph, the individual experimental values and average are plotted. The data are scattered, highlightingthe random nature of spalling. However, some trends can be verified. As observed in the visual inspection, concrete made with RCA exhibited a higher spalling degree than that made with NA. The spalled volume showed a similar behaviour in most cases: an increase up to a certain replacement rate, followed by a constant value.This was more evident in the DR and SBR samples subjected to 5 MPa. In these curves, the spalled volume increases as the replacement rate increases from 0 % to 40 %. Then, from 40 % to 100 % of the replacement rate, the spalling indicators remain relatively constant, approximately 10 % of the volume loss for DR and 9 % for SBR. This difference also highlights the fact that the type of replacement method does not appear to influence the general spalling behaviour, especially for a loading of 5 MPa.

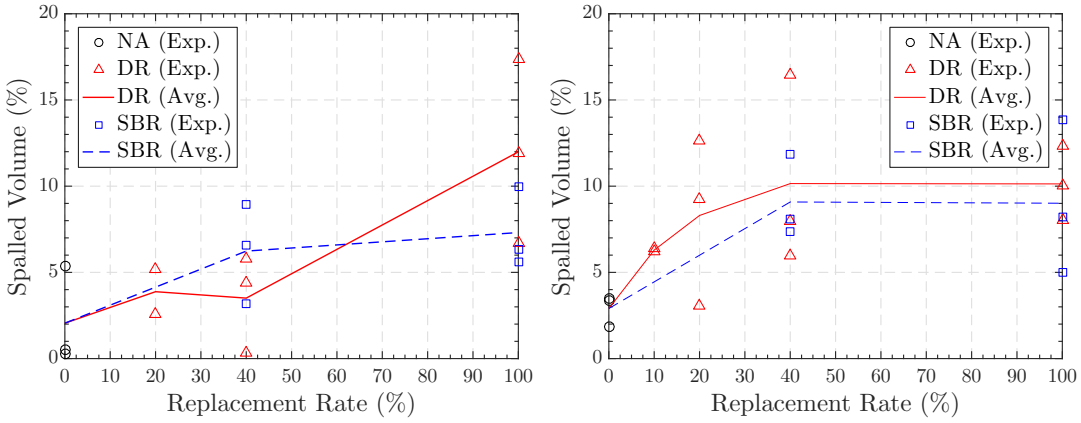

(a) 2.5 MPa (b) 5 MPa

Figure 5.12: Effect of replacement on the spalled volume

The evolution of the maximum spalling depth with the replacement rate exhibited the same general trend. However, differences were observed with the DR mixes subjected to a loading of 5 MPa. For these mixes, a higher maximum spalling depth (23.7 mm) was observed at a replacement rate of 20 %. However, for replacement rates from 40 % to 100 %, the values also remained comparatively constant, from 21.2 mm to 20.7 mm, respectively. This behaviour reinforces the fact that the RCA replacement rate does not change the spalling degree after a certain percentage (after 40 % in this study). Again, the type of replacement method does not influence the maximum spalling depth.

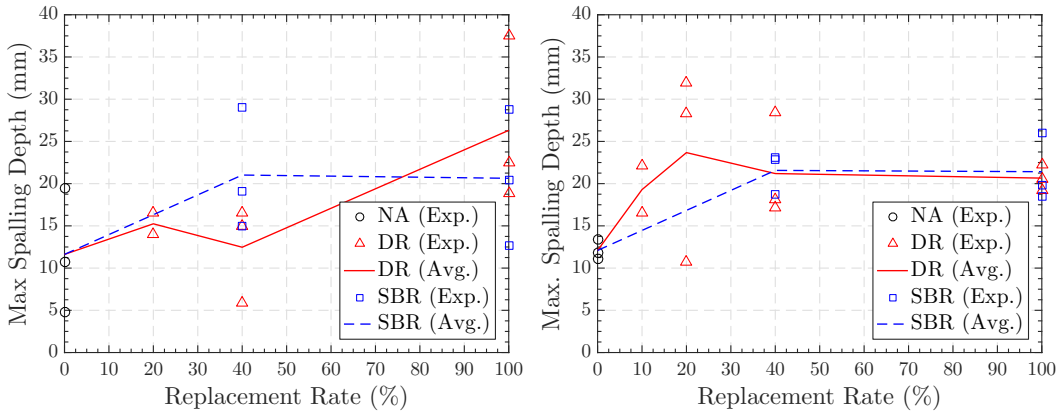

(a) 2.5 MPa (b) 5 MPa

Figure 5.13: Effect of replacement on the maximum spalling depth

5.3.1.4 Discussion of the influence of RCA on fire spalling mechanisms in concrete

The general trend observed in the spalled volume and maximum spalling depth indicates that the replacement rate has a contradictory effect on the spalling behaviour. First, up to a 40 % of replacement rate, the spalling degree increased

with the presence of RCA. Further addition of RCA did not substantially change the spalling severity. After a replacement level threshold, the presence of RCA kept the spalling degree constant. However, the replacement rate influences several physical properties of concrete that usually play a crucial role in spalling sensitivity. Two of these, compressive strength and water content, are discussed in this section.

Usually, high compressive strength leads to high compacity and low permeability [2, 47]. These properties may induce the build-up of pore pressure, possibly increasing the spalling risk according to different studies [2, 48]. Fig.5.14 shows the spalling results against the compressive strength measured at the test age for each of the studied mixes. Even if the results are slightly scattered, one can observe that both the spalled volume and the maximum spalling depth tend to decrease as the compressive strength increases. Hence, the trend of spalling risk increasing as the compressive strength increases was not identified for the studied mixes. One mix (RCA-100-DR), which presented a higher average spalled volume (12.0 %) and depth (26.3 mm), had a lower compressive strength. This behaviour indicates that, in this experimental evaluation, compressive strength does not seem to be a factor affecting spalling depth.

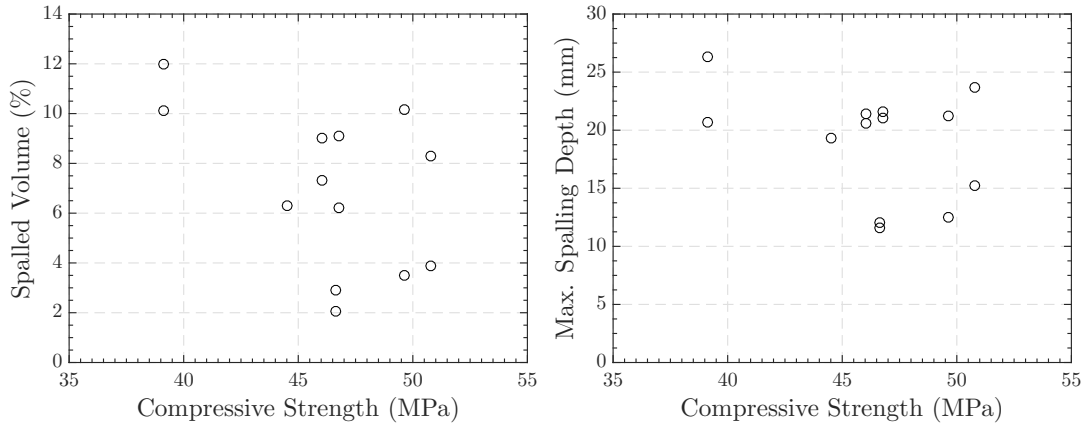

(a) spalled volume (b) maximum spalling depth

Figure 5.14: Effect of compressive strength on spalling indicators

The effect of water content on concrete spalling is also related to the build-up of pore pressure [48] and, according to some researchers, can have play a major role in the mechanical properties of concrete at high temperatures [49]. For both cases, and as observed in numerous experimental studies [4, 48, 50], spalling risk is concluded to be higher for high water content.

Fig.5.15 presents the spalling results against the water content (measured at the test age) for each studied mix. In the present study, the highest average spalled volume (12.0 %) and depth (26.3 mm) were observed for the mix with the higher water content (RCA-100-DR, wc=7.6 %), agreeing with the tendency reported in the literature. The results also indicated that spalling is very sensitive to water content. For example, between 5.2 % (NA) and 6.1 % (RCA-40-SBR) water content, the spalled volume increased more than three times (under a mechanical load of 5 MPa). This type of sensitivity was also identified by Maier

et al. [14], who verified a higher increase in damage within a small range of initial water content. At the same time, the results presented herein show some cases where the difference in water content was relatively high (6.1 % for RCA-40-SBR and 7.3 % for RCA-100-SBR). However, the maximum spalling depths were quite similar (21.6 mm and 24.4 mm, respectively). After 6.1 %, the spalling parameters remained almost constant.

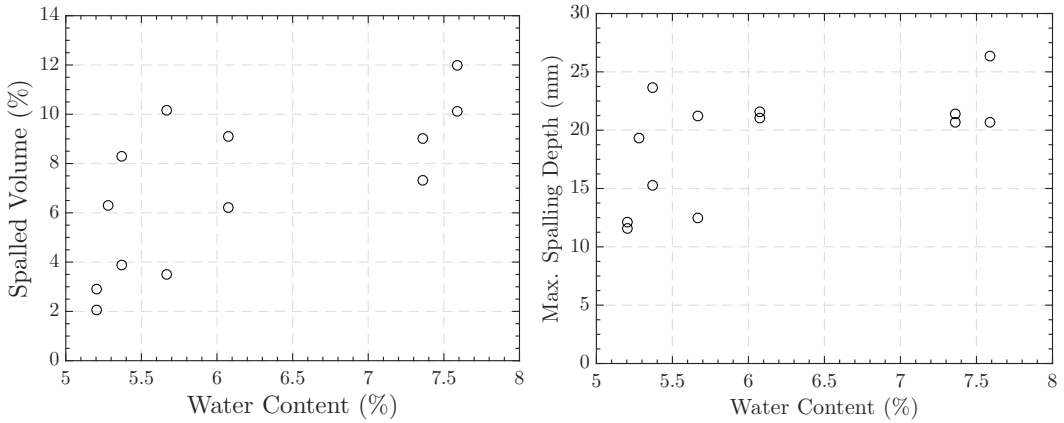

(a) spalled volume (b) maximum spalling depth

Figure 5.15: Effect of water content on spalling indicators

In short, compressive strength did not seem to affect the risk of spalling, and the water content appears to be a critical parameter. A higher RCA replacement rate leads to higher water content and spalling risk. However, its effect is insufficient to explain why the extent of spalling of the concrete made with RCA did not evolve from a replacement rate threshold of 40 % in this study. This particular behaviour of concrete made with RCA concerning the risk of spalling should involve other phenomena.

Two hypotheses are highlighted. The first one is related to a lower thermal mismatch between aggregate and paste. For concrete made with RCA, the higher the replacement rate, the more the old-paste–new-paste interfaces become the majority of the paste–aggregate interfaces. Consequently, increasing the replacement rate may decrease the thermal mismatch, leading to a lower cracking density. This reduction may improve the local mechanical properties of the concrete (mainly in the vicinity of the heated surfaces) . For example, this can be observed by comparing the mechanical properties of concretes where the thermal mismatch is different (e.g., concrete made with different aggregates [51, 52]). Finally, this improvement can reduce the risk of spalling in contrast to the previous effect.

The second theory is related to cracking. As verified experimentally in previous works [12], the use of saturated/wet RCA may lead to an excess of water surrounding aggregates. This extra water may reduce the bond in interfaces, inducing cracks and increasing permeability. In addition, the higher initial porosity of RCA also may cause higher permeability in the concrete mixes. This increase in permeability can favour the transport of fluids (liquid water and vapour) in the sensitive spalling zone, decreasing the pore pressure and the risk of spalling.

These effects, which may happen jointly, are some of the phenomena that could explain the results of this study. First, up to a certain replacement rate threshold (40 % in this study), the increase in spalling risk can be explained by the increase in water content. Above this threshold, the highlighted phenomena can counterbalance the effect of the water content and stabilise the spalling characteristics. Further analysis of permeability and microscopic observations of thermal cracking could help to clarify this point.

5.3.2 Second Campaign

This section presents the results obtained in the second campaign. The discussion above highlighted the importance of the water content in the spalling risk. Hence, this second campaign further investigates the effect of different water content profiles on spalling.

5.3.2.1 Water content profiles

The water content profiles estimated from the measurements of the small pieces are presented in Fig. 5.16. As expected, the values obtained in concrete made with RCA are higher than those obtained with NA. This higher water content is mainly related to RCA higher porosity and water absorption.

As expected, Fig. 5.16 shows the progressively drying of the sample. Values were similar for both cases, but the drying in concrete made with RCA was faster than in the case of NA. For example, after 2 days of drying, the NA samples showed 1.6 % water content at 1 cm, while concrete with RCA showed around 1.9 % water content. After 7 days of drying, the water content at 1 cm is lower in both cases, close to 0.5 %, but still higher in concrete with NA (0.7 %). Possible explanations are related to the higher porosity and the crack network in RCA. Previous works monitoring moisture migration in concrete made with NA showed that a more pervasive crack network induces a faster drying process [53].

The differences in drying kinetics are also depicted in Fig. 5.16b, which shows in grey the NA curves with the same drying periods as RCA. First, for 1 day of drying, RCA had higher water content at any length. However, for 2 days of drying, the water content curves cross at the initial centimetres (0.45 cm). Finally, for 7 days of drying, RCA had lower water content at any length.

A high gap between the saturated samples and the first drying period (12 hours for NA) was observed. One hypothesis for this was the water on the surface of the small cylinders. When evaluating saturated samples, they were directly removed from the water, cut and measured. During this operation, and despite having wiped the samples, extra water can still be present on the surfaces of the sample. To estimate the contribution of this superficial water, saturated cylinders were directly removed from the water and dried in the oven for 3 minutes to remove the surface water. Then, the usual process of water content determination (cut, measure and drying) was made for all samples. Fig. 5.16 shows the water content after 3 minutes of drying (dashed lines). It can be seen that the gap between saturated and the first drying period was lower, more

coherent with the observed water content. This value of saturated water content was adopted for further analysis.

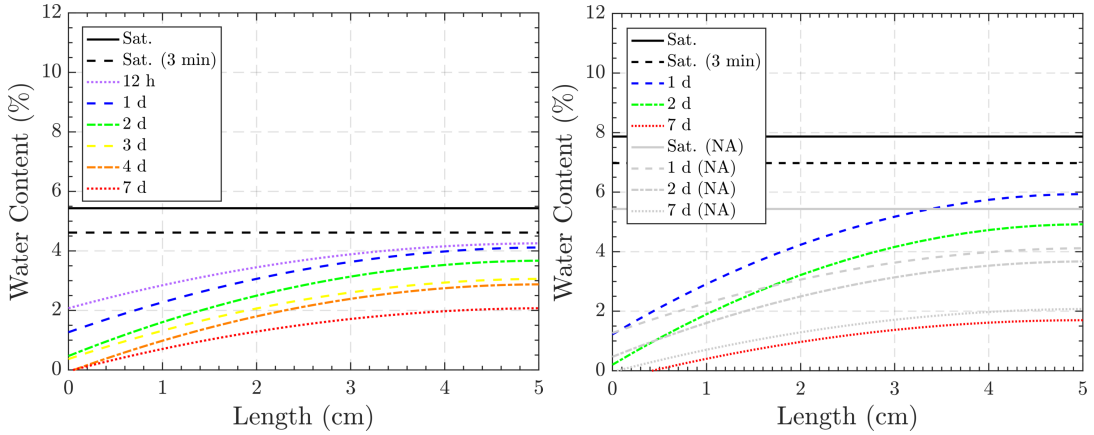

(a) concrete made with NA (b) concrete made with RCA

Figure 5.16: Water content profiles after different drying processes - curves are a regression (second-degree polynomial) of measured points

5.3.2.2 Postfire assessment of spalling

From the photogrammetry, two indicators were chosen to evaluate spalling: the mean spalling depth and the spalled volume. Fig. 5.17a shows the variation of spalled volume with drying period for both mixes. First, at the saturated state, both mixes showed a high spalling volume. It is noteworthy that the results are closer to the ones obtained in previous works with similar conditions and the same test setup [54].

However, drying changed the observed behaviour. First, NA samples presented higher spalled volume after 12 hours. It went from 2.4 % saturation to 4.7 % after 12 hours of drying. Further drying led to reduced spalling after 1 and 2 days of drying. The latter already shown relevant variations in spalling risk, given that, out of four samples tested at this drying condition, two did not spall, one presented small located spalling (0.1 %), and one had high spalled volume (6.8 %). Starting from 3 days of drying, no spalling was registered for all samples. Fewer conditions were tested for RCA, but a similar trend was observed. At saturation, average spalled volume was 11.4 %. An increase after the saturation was not observed, but after 1 day of drying, a high spalled volume was still registered (2.9 %). After 2 days no spalling was registered.

Similar observations can be drawn from the evaluation of mean spalling depth (Fig. 5.17b). Again, similar values from previous works were obtained at a saturated state [54]: 5.5 mm for concrete made with NA and 14.5 mm for concrete made with RCA. Then, even after 1 day, drying reduces significantly the mean spalling depth. It is noteworthy that for both cases, the average curves of spalling indicators cross between 1 and 2 days of drying. It was seen that after 2 days of drying, the curves of water content by length (Fig. 5.16b) cross at 0.45 cm,

indicating that NA has more water content at these first centimetres than RCA-100-DR.

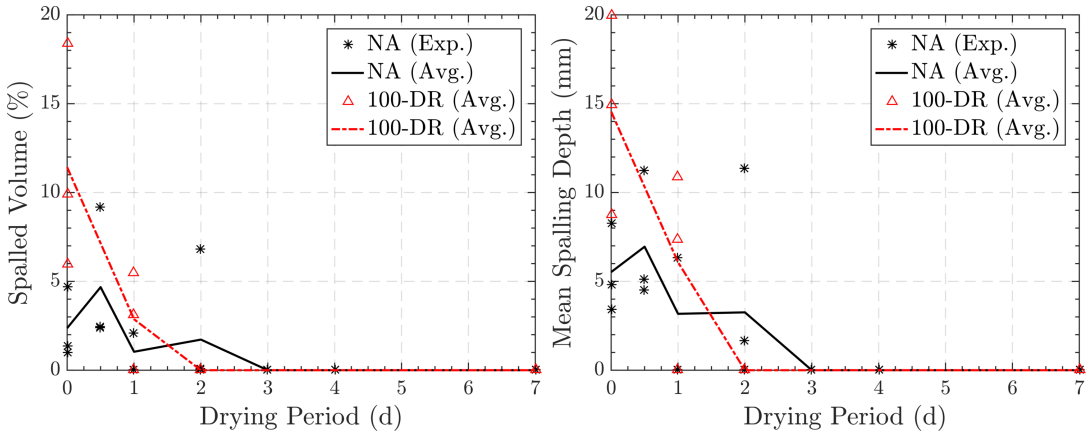

(a) spalled volume (b) mean spalling depth

Figure 5.17: Evolution of spalling indicators for studied mixes

To further evaluate the effect of the water content on the spalling behaviour, the water content was calculated at different depths using the regression curves. Fig. 5.18 shows mean spalling depth versus water content (W_c) at 1, 1.5 and 2 cm from the exposed surface for both mix types (NA and RCA). The trends for all depths indicate the same: an increase of the mean spalling depth with the rise in water content. These graphs also give an idea of the minimal water content needed in the 2 first centimetres for possible trigger spalling. For NA, spalling was observed when water content was higher than 1.3 % and 2.1 % at 1 cm and 2 cm, respectively. For RCA, spalling was verified when water content was higher than 1.9 % and 3.2 % for the same depths.

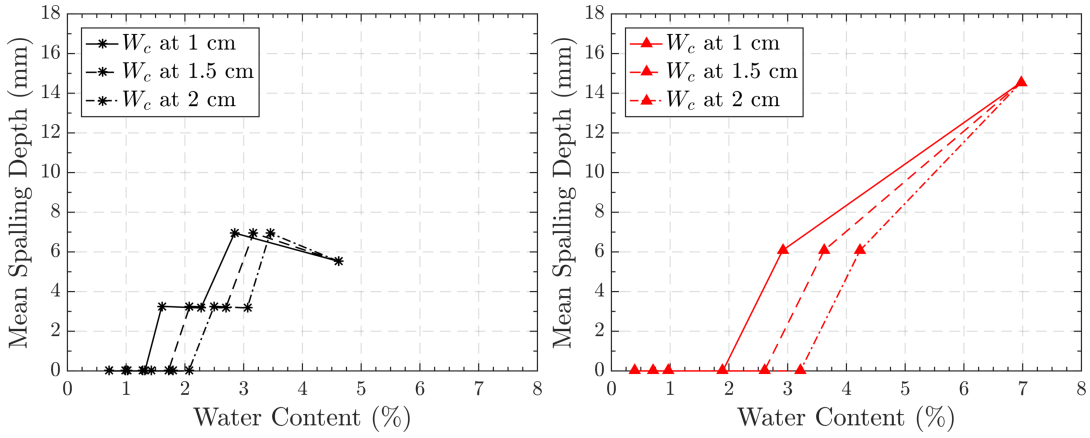

(a) Concrete made with NA (b) Concrete made with RCA

Figure 5.18: Mean spalling depth versus water content at different depths

The results herein showed the influence of the water content profile in the spalling risk evaluation. However, evaluating the water content or the amount of water needed to trigger spalling is complex. When analysing the first centimetres,

part of the water evaporates, and another moves towards the centre to form the so-called 'moisture clog'. To further investigate the triggering water content, three different graphs are presented in Fig. 5.19.

First, Fig. 5.19a plots the mean spalling depth versus the water content calculated at this mean depth. For this first case, except for one spalled sample (out of 14), water content at the mean spalling depth was higher than 1.5 % for NA, and more than 2 % for RCA. Fig. 5.19b plots the mean spalling depth versus the mean of water content between the surface and the mean spalling depth. As expected, this average water content is lower. In this case, the critical critical water content was around 1 % for NA and more than 1.5 % for RCA. In the last case, Fig. 5.19c, the mean spalling depth is plotted against the mean water content in all the first 5 centimetres (half cylinder). For this case, spalling happened with a water content of 2.6 % for NA and 4.4 % for RCA-100-DR.

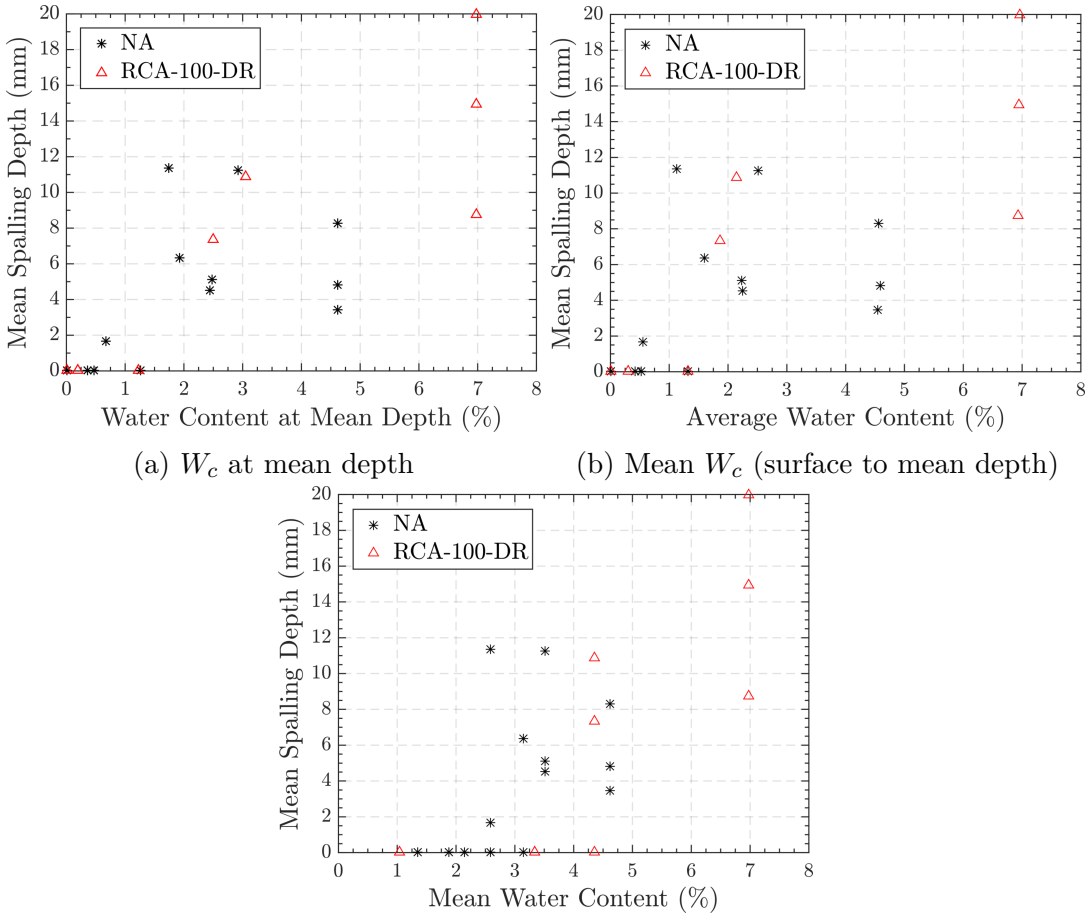

(a) W_c at mean depth

(b) Mean W_c (surface to mean depth)

(c) Mean W_c (half cylinder - 5 cm)

Figure 5.19: Mean spalling depth versus water content

It is noteworthy that this analysis shows a difference between the 'triggering' water content. The first two approaches are more conservative. These water contents agree with the ones obtained by Maier et al. [14]. They observed that concrete spalling is likely to occur for more than 1 % of water content, and this is also valid for concrete with high permeability - as in the case here of

concrete made with RCA. The last approach indicates a higher water content for both mixes. It is noteworthy that the value is close to the Eurocode 2 [55] recommendations, which states that explosive spalling is unlikely to happen if the moisture content is lower than 3 % by weight.

5.4 Conclusions

The spalling behaviour of concrete made with recycled concrete aggregates was investigated experimentally. The experiments comprised two phases: the first campaign, a material screening test, and the second campaign, in which the effect of water content profile on spalling risk was investigated. Based on the results, the following conclusions were drawn:

- Digital photogrammetry shows potential for postfire assessment. All spalling measurements showed a good relationship and can serve as appropriate indicators of the degree of damage when assessing the fire risk susceptibility of concrete mixes.

- In general, concrete made with RCA exhibited a higher spalling degree than concrete made with NA. An increase in the compressive axial load led to a slight increase in the spalling degree. Concerning the replacement rate, spalling indicators (volume and maximum depth) exhibited peculiar behaviour. First, the spalling volume and depth increased from 0 % to 40 %. From 40 % to 100 %, the spalling indicators remained constant. The replacement method (direct replacement or strength-based replacement) did not substantially change the general behaviour.

- The presence of RCA affects different properties that may influence spalling risks, such as the water content and compressive strength. Compressive strength did not affect the spalling risk of concrete made with RCA because concrete mixes with relatively low strength presented a noticeably higher spalling. The water content influenced the spalling damage because mixing with high water content resulted in higher spalling depths and volumes.

- Different hypotheses were proposed about the effect of replacement rate on spalling risk. The increase in spalling risk could be associated with higher water content and lower thermal cracking. At the same time, the possible reduction of spalling risk could be related to the cracking behaviour and the improvement of the mechanical properties of the concrete owing to the lower thermal mismatch.

- The water content measurement through a small cylinder showed potential to correctly estimate the water content profile along the thickness of samples before the fire test. Concrete made with RCA presented higher water content; however, the drying was faster in this mix. After 7 days of drying, both mixes showed low water content in the first centimetres.

- Drying significantly reduced the spalling risk of concrete. After only 3 days of drying at 80 °C, no spalling was registered for concrete made with NA. For concrete made with RCA, no spalling was registered after 2 days of drying.
- Mostly of the spalled samples showed a water content higher than 1.5 % at the mean spalling depth for NA and higher than 2 % for RCA. This values were even lower in the case of average water content at the first centimetres - between surface and spalling depth. This possible threshold is closer to previous works. At the same time, when evaluating the mean water content through all the depth, the critical value is close to 2.6 % for NA and 4.4 % to RCA. These values are closer to what is currently specified in Eurocode 2 [55].

Finally, it is essential to emphasise that these conclusions are drawn based for a specific type of aggregate (for both NA and RCA), from a specific region, with specific properties and nature. Full-scale fire tests on structural elements should be performed to analyse the spalling risk of concrete made with RCA and to verify the influence of possible spalling damage on structural performance (fire resistance).

References

[1] G. A. Khoury. "Effect of fire on concrete and concrete structures". In: *Progress in Structural Engineering and Materials* 2.4 (2000), pp. 429–447. DOI: 10.1061/41016(314)299.

[2] J.-C. Liu, K. H. Tan, and Y. Yao. "A new perspective on nature of fire-induced spalling in concrete". In: *Construction and Building Materials* 184 (2018), pp. 581–590. DOI: 10.1016/j.conbuildmat.2018.06.204.

[3] J. C. Mindeguia, P. Pimienta, A. Noumowé, and M. Kanema. "Temperature, pore pressure and mass variation of concrete subjected to high temperature - Experimental and numerical discussion on spalling risk". In: *Cement and Concrete Research* 40.3 (2010), pp. 477–487. DOI: 10.1016/j.cemconres.2009.10.011.

[4] J.-C. Mindeguia, H. Carré, P. Pimienta, and C. La Borderie. "Experimental discussion on the mechanisms behind the fire spalling of concrete". In: *Fire and Materials* 39.7 (2014), pp. 619–635. DOI: 10.1002/fam.2254.

[5] B. Lottman, A. Snel, F. Kaalberg, C. Blom, and E. Koenders. "Spalling Mechanism: Key for Structural Fire Resistance of Tunnels". In: *Structural Engineering International* 31.2 (2021), pp. 233–240. DOI: 10.1080/10168664.2020.1796556.

[6] F. L. Monte, R. Felicetti, and C. Rossino. "Fire spalling sensitivity of high-performance concrete in heated slabs under biaxial compressive loading". In: *Materials and Structures* 52.1 (2019), pp. 1–11.

[7] N. Hua, A. Tessari, and N. E. Khorasani. "Characterizing damage to a concrete liner during a tunnel fire". In: *Tunnelling and Underground Space Technology incorporating Trenchless Technology Research* 109.October 2020 (2021), p. 103761. DOI: 10.1016/j.tust.2020.103761.

[8] E. W. H. Klingsch. "Explosive spalling of concrete in fire". PhD thesis. ETH Zurich, 2014, p. 252.

[9] G. Shorter and T. Harmathy. "Discussion on the fire resistance of prestressed concrete beams". In: *Proceedings of the Institution of Civil Engineers* 20.2 (1961), pp. 313–315.

[10] T. Harmathy. "Effect of moisture on the fire endurance of building elements". In: *Moisture in materials in relation to fire tests*. ASTM International, 1965, pp. 74–95.

[11] Q. Ma, R. Guo, Z. Zhao, Z. Lin, and K. He. "Mechanical properties of concrete at high temperature-A review". In: *Construction and Building Materials* 93 (2015), pp. 371–383. DOI: 10.1016/j.conbuildmat.2015.05.131.

[12] P. Pliya, D. Cree, H. Hajiloo, A.-L. Beaucour, M. Green, and A. Noumowé. "High-Strength Concrete Containing Recycled Coarse Aggregate Subjected to Elevated Temperatures". In: *Fire Technology* (2019), pp. 1–18.

[13] M. Maier, A. Saxer, K. Bergmeister, and R. Lackner. "An experimental fire-spalling assessment procedure for concrete mixtures". In: *Construction and Building Materials* 232 (2020), p. 117172. DOI: 10.1016/j.conbuildmat.2019.117172.

[14] M. Maier, M. Zeiml, and R. Lackner. "On the effect of pore-space properties and water saturation on explosive spalling of fire-loaded concrete". In: *Construction and Building Materials* 231 (2020), p. 117150. DOI: 10.1016/j.conbuildmat.2019.117150.

[15] B. Fernandes, H. Carré, J.-C. Mindeguia, C. Perlot, and C. La Borderie. "Effect of elevated temperatures on concrete made with recycled concrete aggregates-An overview". In: *Journal of Building Engineering* (2021), p. 103235. DOI: 10.1016/j.jobe.2021.103235.

[16] F. Robert, A.-L. Beaucour, and H. Colina. "Behavior Under Fire". In: *Concrete Recycling: Research and Practice*. Ed. by F. De Larrard and H. Colina. CRC Press, 2019. Chap. 13, p. 13.

[17] *Fire-resistance tests — Elements of building construction — Part 1: General requirements*. International Organization for Standardization. Geneva, 1999.

[18] Z. Chen, J. Zhou, P. Ye, and Y. Liang. "Analysis on Mechanical Properties of Recycled Aggregate Concrete Members after Exposure to High Temperatures". In: *Applied Sciences* (2019). DOI: 10.3390/app9102057.

[19] P. Pliya, H. Hajiloo, S. Romagnosi, D. Cree, S. Sarhat, and M. F. Green. "The compressive behaviour of natural and recycled aggregate concrete during and after exposure to elevated temperatures". In: *Journal of Building Engineering* 38.June 2020 (2021), p. 102214. DOI: 10.1016/j.jobe.2021.102214.

[20] *Tests for mechanical and physical properties of aggregates. Methods for the determination of resistance to fragmentation.* Comité Européen de Normalisation. Brussels, 2010.

[21] *Tests for mechanical and physical properties of aggregates. Determination of particle density and water absorption.* Comité Européen de Normalisation. Brussels, 2013.

[22] *Tests for geometrical properties of aggregates. Classification test for the constituents of coarse recycled aggregate.* Comité Européen de Normalisation. Brussels, 2009.

[23] *Béton — Spécification, performance, production et conformité — Complément national à la norme NF EN 206.* Comité Européen de Normalisation. Brussels, 2014.

[24] IREX. *Comment Recycler Le Béton Dans Le Béton. Recommandations du Projet National Recybeton.* Institut pour la recherche appliquée et l'expérimentation en génie civil. Paris, 2019.

[25] F. de Larrard and T. Sedran. *BetonLab.* Version BetonLabFree. 2021.

[26] L. Butler. "Evaluation of Recycled Concrete Aggregate Performance in Structural Concrete". PhD thesis. University of Waterloo, 2012, p. 433.

[27] *Testing fresh concrete - Part 2 : slump test.* Comité Européen de Normalisation. Brussels, 2019.

[28] *Essais pour béton durci - Partie 7 : masse volumique du béton durci.* Comité Européen de Normalisation. Brussels, 2019.

[29] *Durabilité des Betons - Méthodes recommandés pour la mesure des granulats associées a la durabilité.* Association Française de recherches et d'essais sur les matériaux et constructions. Toulouse, 1997.

[30] M. J. Miah, F. Lo Monte, R. Felicetti, H. Carré, P. Pimienta, and C. La Borderie. "Fire spalling behaviour of concrete: role of mechanical loading (uniaxial and biaxial) and cement type". In: *Key Engineering Materials.* Vol. 711. Trans Tech Publ. 2016, pp. 549–555.

[31] M. J. Miah. "The Effect of Compressive Loading and Cement Type on the Fire Spalling Behaviour of Concrete". PhD thesis. Université de Pau et des Pays de l'Adour, 2017.

[32] F. Sultangaliyeva. "Formulation of fluid fire-resistant fiber-reinforced cementitious composite : Application to radioactive waste disposal". PhD thesis. Université de Pau et des Pays de l'Adour, 2017.

[33] *Essais de résistance au feu - Partie 1 : exigences générales.* Comité Européen de Normalisation. Brussels, 2020.

[34] A. E. Kenarsari, S. J. Vitton, and J. E. Beard. "Creating 3D models of tractor tire footprints using close-range digital photogrammetry". In: *Journal of Terramechanics* 74 (2017), pp. 1–11. DOI: 10.1016/j.jterra.2017.06.001.

[35] E. Cavaco, R. Pimenta, and J. Valença. "A new method for corrosion assessment of reinforcing bars based on close-range photogrammetry: Experimental validation". In: *Structural Concrete* 20.3 (2019), pp. 996–1009.

[36] AliceVision. *Meshroom: A 3D reconstruction software.* 2018.

[37] G. Software. *Cloud Compare.* Version Cloud Compare 2.12. 2021.

[38] CEA. *Cast3m.* Version Cast3m 19. 2021.

[39] L. Boström, R. McNamee, J. Albrektsson, and P. Johansson. *Screening test methods for determination of fire spalling of concrete*. Tech. rep. RISE, 2018, p. 2000.

[40] S. Mohaine, F. Robert, L. Boström, M. Lion, and R. Mcnamee. "Cross-comparison of screening tests for fire spalling of concrete". In: *Fire and Materials* November 2019 (2021), pp. 1–14. DOI: 10.1002/fam.2946.

[41] C. Maluk, L. Bisby, and G. P. Terrasi. "Effects of polypropylene fibre type and dose on the propensity for heat-induced concrete spalling". In: *Engineering Structures* 141 (2017), pp. 584–595.

[42] C. Laneyrie, A.-L. Beaucour, M. F. Green, R. L. Hebert, B. Ledesert, and A. Noumowe. "Influence of recycled coarse aggregates on normal and high performance concrete subjected to elevated temperatures". In: *Construction and Building Materials* 111 (2016), pp. 368–378.

[43] L. Boström, U. Wickström, and B. Adl-Zarrabi. "Effect of specimen size and loading conditions on spalling of concrete". In: *Fire and Materials: An International Journal* 31.3 (2007), pp. 173–186.

[44] M. Guerrieri, C. Sanabria, W. M. Lee, E. Pazmino, and R. Patel. "Design of the metro tunnel project tunnel linings for fire testing". In: *Structural Concrete* 21.6 (2020), pp. 2452–2480.

[45] H. Carré, P. Pimienta, C. La Borderie, F. Pereira, and J.-C. Mindeguia. "Effect of compressive loading on the risk of spalling". In: *MATEC Web of Conferences*. Vol. 6. EDP Sciences. 2013, p. 01007.

[46] F. Lo Monte and R. Felicetti. "Heated slabs under biaxial compressive loading : a test set-up for the assessment of concrete sensitivity to spalling". In: *Materials and Structures* 50.4 (2017), pp. 1–12. DOI: 10.1617/s11527-017-1055-1.

[47] V. Kodur and L. Phan. "Critical factors governing the fire performance of high strength concrete systems". In: *Fire safety journal* 42.6-7 (2007), pp. 482–488.

[48] Y. Li, E.-H. Yang, A. Zhou, and T. Liu. "Pore pressure build-up and explosive spalling in concrete at elevated temperature: A review". In: *Construction and Building Materials* 284 (2021), p. 122818.

[49] R. Jansson. "Fire spalling of concrete: theoretical and experimental studies". PhD thesis. KTH Royal Institute of Technology, 2013, p. 134.

[50] L. T. Phan. "Pore pressure and explosive spalling in concrete". In: *Materials and structures* 41.10 (2008), pp. 1623–1632.

[51] J.-C. Mindeguia, P. Pimienta, H. Carré, and C. La Borderie. "On the influence of aggregate nature on concrete behaviour at high temperature". In: *European Journal of Environmental and Civil Engineering* 16.2 (2012), pp. 236–253. DOI: 10.1080/19648189.2012.667682.

[52] Z. Xing, A.-L. Beaucour, R. Hebert, A. Noumowe, and B. Ledesert. "Influence of the nature of aggregates on the behaviour of concrete subjected to elevated temperature". In: *Cement and concrete research* 41.4 (2011), pp. 392–402.

[53] D. Dauti, A. Tengattini, S. Dal Pont, N. Toropovs, M. Briffaut, and B. Weber. "Analysis of moisture migration in concrete at high temperature through in-situ neutron tomography". In: *Cement and Concrete Research* 111 (2018), pp. 41–55.

[54] B. Fernandes, H. Carré, J.-C. Mindeguia, C. Perlot, and C. La Borderie. "Effect of elevated temperatures on concrete made with recycled concrete aggregates-An overview (Under Review)". In: *Construction and Building Materials* (2022), p. 128124. DOI: 10.1016/j.conbuildmat.2022.128124.

[55] *Design of concrete structures - Part 1-2: General rules - Structural fire design*. Comité Européen de Normalisation. Brussels, 2004, p. 99.

Chapter 06

Durability of concrete made with recycled concrete aggregates after exposure to elevated temperatures

This chapter is an extended version of the paper *Durability of concrete made with recycled concrete aggregates after exposure to elevated temperatures*, a manuscript ready for submission. The previous chapters showed that fire damages concrete structures, independently of the concrete mix or type. It also indicates that its fundamental to evaluate the behaviour in high-temperature situations, from fire tests to residual tests. In the case of post-fire situations, one of the properties that still lacks studies is durability. This evaluation is fundamental for assessing the remaining service life. This chapter evaluates the post-heating durability of concrete made with NA and with RCA (100-DR and 100-SBR). Mixes were exposed to elevated temperatures (200 °C, 400 °C and 600 °C) and, after cooling, evaluated through water porosity, capillary water absorption, permeability, chloride diffusion and accelerated carbonation tests. In addition, performance-based approaches were applied to evaluate the durability and post-heating durability of concrete made with RCA.

Fernandes, B.; Khodeir, M.; Perlot, C.; Carré, H.; Mindeguia, J-C.; La Borderie, C. *Durability of concrete made with recycled concrete aggregates after exposure to elevated temperatures.* To be submitted.

6.1 Introduction

The use of recycled coarse aggregate (RCA) as a replacement for natural aggregates has proven to be a possible solution to make sustainable concrete. This solution showed potential to minimize the consumption of raw materials and also reduce waste landfilling [1–3]. The production of recycled aggregate concrete (RAC) has been the aim of study for the last decades. In general, concrete made with RCA shows comparable properties to ordinary concrete, depending on RCA's quality and replacement rate [4, 5].

Although its use has been proven to be feasible, RCA will severely affect the properties of the concrete. First, related to the aggregate itself, RCA usually presents higher porosity, higher water absorption and lower strength than NA [2, 6], due to the attached (or adhered) mortar. Also, incorporating RCAs on concrete will result in a peculiar microstructure, with three different transition zones [2, 7]. These changes affect the behaviour of this sustainable concretes. Extensive research has been done in the last years to characterize the RAC concrete behaviour. However, some topics still need to be addressed, primarily related to exposure to extreme conditions, such as fire and post-fire durability.

Indeed, these properties have been studied before in literature [8, 9], but limited attention was given to durability-loss due to exposure to elevated temperatures. Kou et al. [10] evaluated water absorption and porosity of RAC after exposure to elevated temperatures. The authors state that after exposure to 500 °C, water absorption was higher for concrete made with RCA, and this behaviour inverses after 800 °C. Mercury Intrusion Porosimetry (MIP) results demonstrated that the concrete with RCA presented a lesser increase in total porosity and smaller average pore diameter. The authors state that this behaviour is associated with better thermal compatibility between new and old paste.

Xuan et al. [11] also evaluated porosity through MIP and found RAC after 600 °C are more porous than concrete made with NA and carbonated RCA. They attributed this behaviour to the decomposition of hydration products from the cement mortar in RAC. Laneyrie et al. [12] evaluated the effect of high temperature on the water accessible porosity. They pointed out that water porosity did not change significantly up to 300 °C. Finally, Ma et al. [13, 14] evaluated the residual chloride permeability of RCA after exposure to high temperatures. They state that substituting NA with RCA increased the chloride diffusion coefficient, and this value increases as RCA content increases.

There is a lack of knowledge about the post-heating durability of concrete made with RCA. Several crucial parameters, such as permeability and carbonation ingress, were not evaluated after exposure to elevated temperatures. Moreover, even for ordinary concrete made with NA, the durability of fire-damaged concrete is little know and often ignored in standards and guidelines [15]. It is noteworthy that the post-heating durability should be assessed after extreme events such as fire. Moreover, to be in use again, structures should meet the requirements of serviceability, strength and stability during all the remaining service life. The remaining durability properties should be assessed, and only

after this evaluation, the strategies for repair, strengthening, and maintenance can be made.

To contribute to these knowledge gaps, this paper experimentally evaluates the residual durability of concrete made with RCA subjected to elevated temperature. Concretes made with NA and with 100 % of RCA were produced. For 100 % of substitution, a specific mix with comparable strength as concrete with NA was also designed. The mixes were heated to three different temperatures (200 °C, 400 °C and 600 °C). A comprehensive range of durability tests was done before and after exposure to high temperatures: water porosity, capillary water absorption, gas permeability, chloride diffusion and accelerated carbonation. Lastly, the concrete durability was evaluated using performance-based approach.

6.2 Experimental program

6.2.1 Materials and concrete mixes

All materials were the same for the tested concretes except for coarse aggregate in this study. The cement was CEM II/A-L 42.5R (produced by Eqiom). The limestone filler was Betocarb HP-SC (produced by Omya). The superplasticizer was SIKA ViscoCrete Tempo-483. Alluvial sand was the fine aggregate chosen for the mixes. The two coarse aggregates were natural (NA) and recycled concrete aggregates (RCA). The NA was made from diorite, obtained from a quarry located in Genouillac (France). The RCA were crushed and screened near Bordeaux (France) by a recycling company. Table 6.1 present materials properties.

Table 6.1: Materials properties

Property	Cement	Filler	Sand	NA 4/10	NA 10/20	RCA 4/10	RCA 10/20
Density (kg/m^3)	3010	2700	2650	2820	2840	2570	2590
Specific surface (cm^2/g)	4700	4330	-	-	-	-	-
Water absorption (%)	-	-	0.35	0.92	0.81	5.6	4.52
LA coefficient (%)	-	-	-	16	16	30	36
Fineness modulus	-	-	3.1	-	-	-	-

Three concrete mixes were studied: concrete with NA (reference), 100 % direct replacement (DR) mix (RCA-100-DR) and 100 % strength-based replacement (SBR) mix (RCA-100-SBR). The concrete with NA was initially designed to meet durability requirements (NF EN 206/CN:2014 [16]) for the XD3 exposure class: water/cement (w/c) ratio of 0.5, C35/45 compressive strength class and cement content of 350 kg/m^3. This was done considering the most used concrete mix in the partner company. In RCA-100-DR, NA were replaced by RCA in volume, without any changes in other constituents. In RCA-100-SBR, cement and water content were also adjusted to achieve the same strength and slump as the reference mix. The SBR mix was designed with BetonLab [17] software. Based on compressive strength results of reference and DR mixes, aggregates properties were calibrated. Then, the w/c ratio was adjusted to have the

same compressive strength as the reference. Finally, water and cement content were modified (maintaining the same w/c) to achieve the same slump. Table 6.2 present mixture proportions. Compressive strength results of NA and DR mixes were used to calibrate the software's aggregate properties. Then, the w/c ratio and cement paste content were adjusted to achieve the same strength and workability as reference concrete. Table 6.2 present mixture proportions.

Table 6.2: Mix proportions (in kg/m^3, SP in % of cement mass)

Material	Mix		
	NA	RCA-100-DR	RCA-100-SBR
Cement	350	350	420
Filler	60	60	60
Sand	804.3	804.3	799.8
NA 4/10	331.7	-	-
NA 10/20	711.1	-	-
RCA 4/10	-	302.3	291.5
RCA 10/20	-	648.5	630.3
Water	175	175	168
SP	0.9	0.9	0.9

Working with wet aggregates instead of fully-saturated aggregates (soaked) was adopted thinking in a method that can be easily reproduced in the concrete plant from the partner company of the project. The aggregates (sand, NA and RCA) were pre-wetted for one hour using a soaker hose and then covered with a plastic sheet for three hours. The aggregates (sand, NA and RCA) were pre-wetted for one hour using a soaker hose and then covered with a plastic sheet for three hours. Before casting, moisture content was measured, and the mix water was adjusted to reach the same slump. Additional water corrections were done due to variations in initial mixes. More details are given in previous works [18, 19].

The mixing procedure was the same for all mixes. First, aggregates, cement and filler were mixed for 2 minutes. Then, water and SP were added and mixed for two minutes. The slump was measured following NF EN 12350-2 [20]. Concrete with NA presented slump of 205 mm, RCA-100-DR was 208 mm and RCA-100-SBR was 174 mm. Cylindrical specimens of 11 cm x 22 cm and prisms of 7 cm x 7 cm x 28 cm were cast. The samples for mechanical characterization at 28 days were kept submerged in water at 20 °C. The remaining experimental samples were kept submerged for seven days and then placed into sealed plastic containers until test age: approximately 6 months for all tests, with the exception of carbonation samples, which aged 12 months. For concrete mechanical characterization, compressive strength (NF EN 12390-3 [21]), splitting tensile strength (NF EN 12390-6 [22]) and elastic modulus(NF EN 12390-13 [23]) were determined (Table 6.3).

Table 6.3: Mechanical properties of studied mixes (average values and standard deviation)

Mix	f_{c28} (MPa)	f_{t28} (MPa)	E_{c28} (GPa)
NA	42.2 (± 0.6)	4.0 (± 0.1)	32.9 (± 0.5)
RCA-100-DR	32.6 (± 0.3)	3.8 (± 0.1)	27.1 (± 0.2)
RCA-100-SBR	44.4 (± 0.8)	4.0 (± 0.1)	30.1 (± 0.3)

6.2.2 Elevated temperature exposure

The heating process was done using an electric furnace of internal dimensions of 55 cm x 50 cm x 31 cm. The time-temperature parameters are controlled by an automated regulator connected to a thermocouple located inside the furnace. The furnace has electric resistance located in the back and a fan at the top to homogenize temperature properly. A low heating rate of 2 °C/min was chosen to avoid significant thermal gradients inside the concrete sample. Three temperatures were considered: 200 °C, 400 °C and 600 °C. The temperature was kept for 180 min at the target temperature, then naturally cooled to room temperature inside the furnace. After cooling, samples were stored inside sealed containers with silica gel until testing.

6.2.3 Determination of durability procedures

6.2.3.1 Water accessible porosity

The water porosity was measured based on AFREM recommendations [24]. Three 1/4 of 11 cm x 5 cm disks, removed from the middle of cylinders, were used for each mix and temperature. For room temperature measurements, samples were oven-dried at 80 °C until constant mass (mass variation less than 0.05 % in one day) before testing. Eq.6.1 presents the equation for water porosity (η, in %) calculation.

$$\eta = \left(\frac{m_{ssd} - m_{dry}}{m_{ssd} - m_{hyd}} \right) \cdot 100 \tag{6.1}$$

In these equations, m_{ssd} (kg) is the saturated superficially dried mass, m_{dry} (kg) is the dried mass, and m_{hyd} (kg) is the hydrostatic mass.

6.2.3.2 Gas permeability

Axial gas permeability was measured using the RILEM-CEMBUREAU method [25, 26], based on the Klinkenberg approach [27]. The test was carried out at room temperature and after each heating/cooling procedure described above. Three samples (⌀11 cm x 5 cm) per mix and temperature were evaluated. These disks were cut from ⌀11 cm x 22 cm cylinders using a diamond saw. The extremities (2 cm) of the ⌀11 cm x 22 cm cylinders were discarded to avoid any possible edge effect on the permeability measurements. Before testing, samples

were oven-dried at 80 °C. Then, the curved face of the cylinders was wrapped with aluminium tape to seal the sample, avoid any leakage and induce unidirectional flow.

The sample was placed in the permeameter cell, encased by a polyurethane ring and an inflated rubber tube. Once the sample was set, the rubber tube was inflated to apply lateral pressure on the specimen. The lateral pressure applied was 0.3 MPa, determined in trial tests with different confining pressures. These trial tests were done to verify the minimum value without any gas leakage on the setup. The reduction in lateral pressure was made based on Miah et al. [28], which showed that confining pressure strongly affects permeability measurements due to the closure of heat-induced microcracks. In any case, injected pressures were limited to half of the confining pressure.

The test principle consists of applying a inert gas (nitrogen in this work) at constant pressure and, after stabilization, measuring the flow rate at the inlet. Three inlet gas pressure levels were used for each sample. For each pressure, the apparent permeability (K_a) was first determined according to Eq. 6.2 (based on Darcy's Law). The intrinsic permeability (K_{int}), which is independent of inlet pressure, was determined from the three apparent permeability measurements using the Klinkenberg correction for gas slippage [27]. For this, experimental data is fitted to the Eq. 6.3 to determine the intrinsic permeability of the material. Also, apparent permeability at 0.2 MPa, used for the performance-based approach (Section 6.4), was determined from the fitting.

$$K_a = \frac{2P_{atm}Q_iL\mu}{A({P_i}^2 - {P_{atm}}^2)} \tag{6.2}$$

$$K_a = K_{int}\left(1 + \frac{\beta}{P_m}\right) \tag{6.3}$$

In these equations, K_a (m^2) is the apparent permeability, K_{int} (m^2) is the intrinsic permeability, P_i (Pa) is the inlet pressure , P_{atm} (Pa) is the atmospheric pressure, Q_i (m^3/s) is the gas flow, L (m) is the sample thickness, μ (Pa/s) is dynamic viscosity of the inlet gas at the temperature measured during the test, A (m^2) is the cross-section sample area, and β (Pa) is the klinkenberg's coefficient.

6.2.3.3 Capillary water absorption

The capillary water absorption was measured based on AFREM recommendations [24]. From the 28 cm x 7 cm x 7 cm prisms, two samples of 14 cm x 7 cm x 7 cm (height x length x width) were obtained and used for each mix and each temperature level. The height of the specimen was chosen based on a previous work [29] which showed a high capillary rise of samples heated up to 600 °C. For room temperature measurements, samples were oven-dried at 80 °C before testing, until constant mass (mass variation less than 0.05 % in one day). The lateral surface (7 cm x 14 cm) were coated with epoxy resin to ensure one-dimensional water transport. After resin drying, one of the uncoated sides (14 cm x 14 cm) was placed inside a covered recipient with water. Small metallic supports were

used to provide 3 mm of immersed depth. The mass of each sample was measured at different time intervals (from 0.25 and up to 72 hours). Capillary water absorption was calculated using Eq.6.4.

$$C_{wa} = \frac{m_t - m_0}{A} \tag{6.4}$$

Where C_{wa} (kg/m^2) is the capillary absorption, m_t (kg) is mass at time t, m_0 (kg) is initial mass and A (m^2) is the cross-section sample area in contact with water.

6.2.3.4 Chloride diffusion

The effective chloride diffusion coefficient was measured based on the accelerated migration test in steady-state conditions proposed by LMDC [30]. In this test, an electrical field is applied to a saturated concrete specimen placed between two compartments, upstream (a solution rich in chlorides) and downstream (solution without chlorides). The chloride diffusion coefficient is determined from the chloride ion flux between compartments [30–32]. For this, concrete disks of ⌀11 cm x 5 cm were sawn from ⌀11 cm x 22 cm cylinders. Two samples per mix and temperature were evaluated. Measurements were limited to 200 °C, since the crack state of samples after 400°C did not allowedproper determination of the chloride coefficient with the proposed method.

After vacuum saturation with a support solution (demineralised water, 1 g/l of $NaOH$, and 4.65 g/l of KOH), samples were placed in the migration cell. A constant potential of 30 V was applied between the electrodes to provide an electric field (E = 600 V/m) between downstream and upstream compartments. The upstream compartment contained a solution of $NaCl$ (12 g/l), $NaOH$ (1 g/l), KOH (4.65 g/l) and demineralised water, while the downstream compartment was filled with the the support solution. The concentration of chloride ions in the upstream was determined by $AgNO_3$ titration. This measurement was done before the start of the test and at regular intervals: two times per day for five days. For the calculation, first, the ionic flux of chlorides (J, in mol/m^{3}s) was determined (Eq.6.5) using the slope of the curve of the variation between the cumulative quantity of chlorides leaving the upstream versus time. Then, the effective chloride diffusion coefficient (D_{eff}, in m^2/s) was calculated, following Eq.6.6.

$$J = \frac{C_{up,1} - C_{up,2}}{t} \cdot \frac{V}{S} \tag{6.5}$$

$$D_{eff} = \frac{RTJ}{C_{up}FE} \tag{6.6}$$

Where $C_{up,1}$ and $C_{up,1}$ (mol/m^3) are the concentration of chlorides at upstream in the start and at the moment of the test, t (s) is test duration, V (m^3) is the volume of the upstream solution, S (m^2) is surface area of test specimen exposed to chloride, R (8.314 J/molK) is the perfect gas constant, T (K) is temperature during chloride test, C_{up} (mol/m^3) is chloride concentration of upstream

solution, F (96 487 C/mol) is Faraday constant and E (V/m) is the electric field applied.

6.2.3.5 Accelerated carbonation

The carbonation was evaluated by accelerated testing. The test protocol was based on French Standard XP P18-458 [33], with some differences described below. Concrete disks of ⌀11 cm x 6.5 cm were sawn from ⌀11 cm x 22 cm cylinders using a diamond saw. The pre-conditioning involved different steps. First samples were dried in a ventilated oven at 45 °C for 14 days. Then, samples were placed in a climatic chamber at 20 °C and 65 % HR for 14 days. For heated samples, the pre-conditioning involved an additional step. Since they were fully dried after heating, samples were immersed in water for 48 hours. This process was done to re-saturate the sample and recover the necessary humidity (usually between 50 % and 80 % [34]) for the carbonation phenomenon. Then, samples underwent the same procedure described before (drying for 14 days followed by 14 days inside the climatic chamber). Just before the test, the curved face of each cylinder was wrapped with aluminium tape to ensure a unidirectional carbonation flow.

The samples were then placed inside the carbonation chamber with 3±0.5 % of CO_2, relative humidity of 65±5 % and temperature of 20±3 °C. It is noteworthy that the CO_2 content used was much lower than the 50 % specified in the XP P18-458 [33] standard. The value was chosen based on previous studies, which showed that 3 % is suitable and representative of long-term carbonation in natural conditions [35, 36]. After 0, 2, 7, 14, 21 and 28 days of exposure, one disk per mix and temperature was removed and split into two parts through splitting tests. Phenolphthalein was sprayed in the fractures surfaces, and carbonation depth was measured using a calliper. Five depth measurements were taken from each side (top/bottom) of each part, and, in total, 20 values were taken per mix/condition. In addition to carbonation depth, the carbonation rate was calculated using Eq.6.7, based on square root theory and in accord with the second law of Fick [37].

$$X_c = k_{acc}\sqrt{t} \tag{6.7}$$

Where X_c (mm) is the carbonation depth, k_{acc} (mm/year$^{1/2}$) is accelerated carbonation rate and t (year) is time.

6.3 Results

6.3.1 Water accessible porosity

The evolution of water porosity with temperature is presented in absolute (Fig. 6.1a) and relative values (Fig. 6.1b). First, at room temperature, concrete with NA showed a porosity of 11.4 %, and the direct substitution of coarse NA by RCA resulted in a porosity increase to 16.2 %. The results and as well the increase in water porosity are coherent with previous works [38]. For the SBR

mix, the porosity remains close to the DR mix, 15.7 %. This behaviour shows that water porosity, in the case of concrete made with RCA, is mainly driven by RCA porosity.

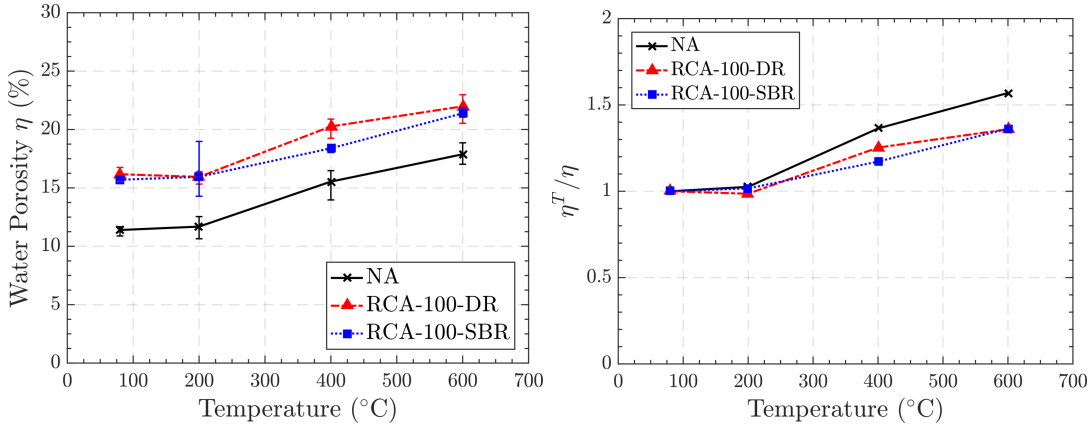

(a) absolute values (b) relative values

Figure 6.1: Evolution of water porosity with temperature

The evolution of water accessible porosity with temperature was similar for all tested concrete (Fig. 6.1a). First, up to 200 °C, the porosity almost did not change for studied mixes. Similar behaviour has been registered in previous works that studied NA, and RCA concretes [12, 39]. From 200 °C to 400 °C, the porosity starts to increase significantly, and it is mainly related to intense water loss and decomposition of C-S-H [40]. In the last branch, from 400 °C to 600 °C, water porosity increases again at a higher rate and is mainly associated with portlandite decomposition.

In general, concrete with NA presents the lowest water porosity values for all tested temperatures. The difference between NA and RCA is close to 3 % and 4 % at all temperatures. Both RCA mixes (DR and SBR) show similar values, execpt for 400°C, when difference reaches 1.8 %. This behaviour highlights again that aggregate plays a crucial role in the water accessible porosity. Reducing w/c and increasing the cement paste did not change the water porosity significantly. In terms of relative porosity evolution, concrete with NA presented higher values than the mixes with RCA. This higher rate is probably related to the higher thermal mismatch in the NA mix that promotes microcracks. The evolution observed in concrete made with RCA is lower probably due to the better match between new cement paste and old cement paste.

6.3.2 Gas permeability

Gas permeability results are presented in Fig. 6.2a and 6.2b. For room temperature (first points on Fig. 6.2a), the direct addition of coarse RCA appears to increase the gas permeability, as observed in previous works [38, 41]. However, contrary to the phenomenon observed in the water porosity, the strength-based replacement mix shows intrinsic permeability closer to concrete with NA. This

result shows that the cement matrix plays a key role in permeability. It is noteworthy also that the changes in permeability were observed within the same exponent (around 10^{-16}); hence, care should be taken when interpreting the results. In any case, similar findings were observed in previous studies [38, 42] that verified that the difference between k_{int} in concrete with NA and RCA is lower when the matrix quality is improved.

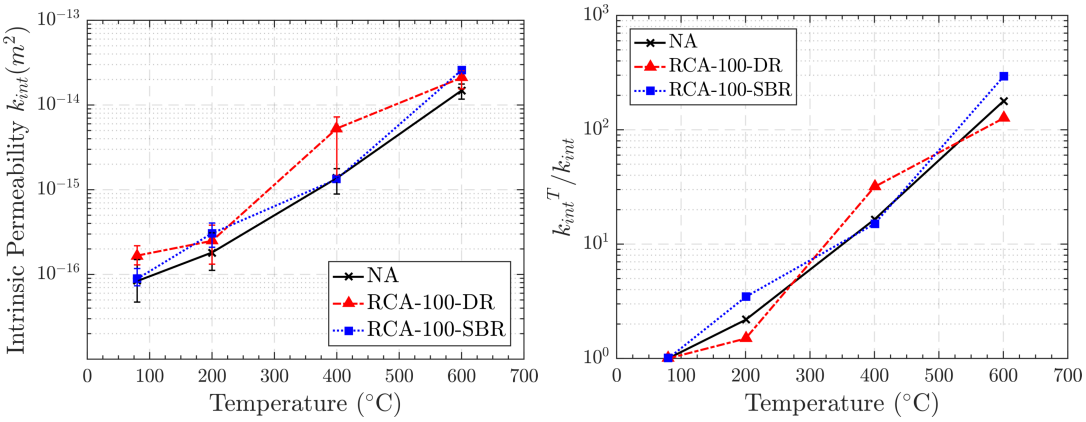

(a) absolute values (b) relative values

Figure 6.2: Evolution of permeability with temperature

Fig. 6.2a presents the evolution of permeability (absolute values in log scale) with all tested temperatures. Concrete with NA presented lower permeability for any given temperature, again highlighting the primary effect of initial aggregate properties. Both DR and SBR shows differential behaviour depending on the temperature level. At 200 °C, SBR and DR permeability were almost the same. This behaviour can be associated with the cracking and porosity due to water evaporation in cement paste. However, at 400 °C, the DR mix is almost four times more permeable than SBR, even though dispersion is high. Given that RCA porosity is the same, a probable reason is related to the cracking at cement paste and interfaces. The stronger cement paste in the SBR mix possibly reduces general cracking in the paste and reduces thermal mismatch between RCA and paste. At 600 °C, values approach again, with both mixes having similar behaviour.

Fig. 6.2b presents the evolution of permeability relative values (in log scale) with temperature. The same variation observed in absolute is also shown in relative values: concrete with NA presents a steady growth in permeability, while DR and SBR mix varies depending on temperature. The graph reveals the significant increase in DR permeability between 200 °C and 400 °C, highlighting the probable damage of cement paste and interface at this temperature level. Finally, from 400 °C to 600 °C, the growth is higher in the SBR mix, probably related to the degradation in portlandite and sand quartz transformation at this temperature level [40].

6.3.3 Capillary water absorption

The effect of RCA on the capillary water absorption is presented in Fig. 6.3a. This figure illustrates the evolution of water absorption with the square root of time (each curve is the average of two samples) for samples at room temperature. The RCA-100-DR presents higher absorption than the other two mixes at any given time. This behaviour is the same as reported in previous works and directly linked to the higher absorption and porosity of RCA [41, 43]. In the SBR mix, the changes in w/c and cement paste decreases the capillary water absorption curves: they get closer to what is observed in concrete made with NA. This improvement isrelated to the improvement in the cement matrix of RCA-100-SBR, which presents higher compacity than RCA-100-DR.

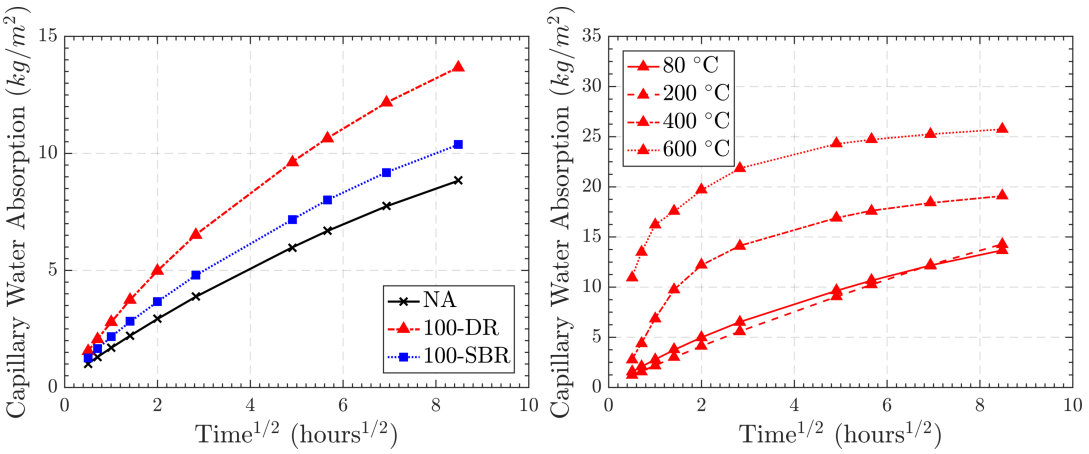

(a) room temperature (b) elevated temperatures (RCA-100-DR)

Figure 6.3: Evolution of capillary water absorption with time

The evolution of capillary water absorption with the square root of time varies significantly depending on the temperature level (example is given at Fig. 6.3b). Up to 200 °C, the behaviour is quite linear, as seen in typical absorption curves. However, from 400 °C to 600 °C, the curves present a different evolution, with two distinct phases: a first one, with a higher absorption rate, followed by a flattened phase. The behaviour is similar to what was observed in previous works [44, 45], which evaluated the effect of damage on absorption. The cracks act as a preferential flow and provide access to air-filled pores, usually filled only later in un-damaged concrete. In the second phase, with the lower rate, the air-filled voids had already been filled, explaining the behaviour in this second period. Given this behaviour, to analyze the results with temperature, it was chosen to evaluate the water absorbed at 72 hours as the primary indicator.

Fig. 6.4a presents the evolution of 72-hour capillary water absorption versus temperature. From room to 200 °C, the absorption was almost constant for all mixes, showing that the crack state is not relevant to induce higher absorption at this temperature. From 200 °C to 600 °C, a linear increase is observed, and it is due to crack development and dehydration. In general, concrete with RCA presented higher absorption than concrete made with NA. The same behaviour was verified in Kou et al. [10]. This behaviour is mainly attributed to RCA's

higher porosity and mortar content, which drive the capillary water rise in these concretes. The SBR mix presented lower values than DR, showing that paste improvement reduced the capillary pores. If the RCA-100-DR presented higher absolute values, this mix presented a lower evolution (Fig. 6.4) in terms of relative values. NA and RCA-100-SBR showed close growth. The highest evolution of concrete made NA could be related to the worst thermal mismatch in this type of concrete. However, this is not the case of RCA-100-SBR, which presents an equal mismatch as RCA-100-DR. In this case, the evolution can be related to the higher deterioration of hydration products of cement paste as temperature increases.

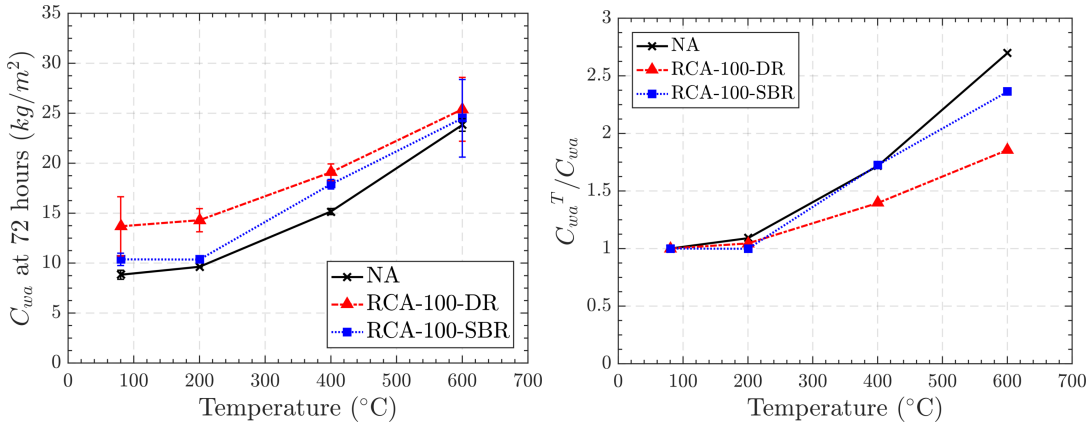

(a) absolute values (b) relative values

Figure 6.4: Evolution of capillary water absorption with temperature

6.3.4 Chloride diffusion

Fig. 6.5 presents the evolution of chloride diffusion coefficient (in log scale) with temperature. At room temperature, the direct addition of RCA increases almost by seven the chloride diffusion coefficient. The lower resistance of RAC to chloride penetration has been verified in previous works [38, 43, 46]. It is noteworthy that RCA-100-DR presented a relevant variation in measurements (relevant error bar), but the mix presented higher diffusion than NA in all samples. The increase in chloride diffusion for SBR was lower than in the DR mix, but the average value did not return to the reference concrete level. Indeed, the chloride evolution behaves similarly to water porosity behaviour: the reduction of w/c and increase in cement paste did not overcome the higher RCA porosity. The influence of RCA porosity on chloride behaviour is also reported in some previous work [46, 47].

For high temperature evolution, as explained in the methodology, the coefficient was not possible to measure after 200 °C, due to the crack state of samples. In any case, it is seen that concrete with NA presents the lowest chloride diffusion for the two tested temperatures. However, the difference between concrete with NA and RCA mixes is lower than at 200 °C. From room temperature to 200 °C, both NA and RCA-100-SBR increased significantly, probably due to the

development of microcracks in the material. It is noteworthy that the evolution in RCA-100-DR is much lower than in the other mixes. This is coherent with permeability and porosity evolution, which was lower for RCA-100-DR. The worst behaviour in concrete made with RCA for chloride was also reported in Ma et al. [13]. They verified that increase in RCA content increased the chloride permeability.

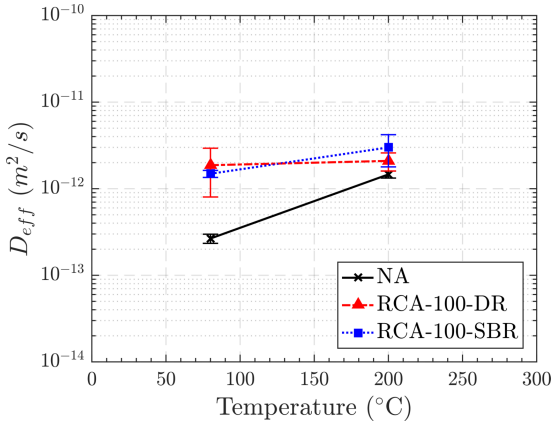

Figure 6.5: Evolution of chloride diffusion coefficient with temperatures

6.3.5 Accelerated carbonation

Table 6.4 presents an overview of all the results from accelerated carbonation tests. The carbonation rate was calculated using Fick Law's and each graph of carbonation depth versus test duration. The high r^2 of the regression curves shows that this model is appropriate even for the case of high-temperature exposure.

Table 6.4: Carbonation results after exposure to elevated temperature (average values and standard deviation)

Mix	Parameters	Temperature			
		23°C	200°C	400°C	600°C
NA	Depth at 28 days (mm)	6.42 (1.02)	8.04 (1.08)	9.84 (0.89)	12.20 (1.21)
	Carbonation rate (mm/year$^{1/2}$)	1.14	1.49	1.79	2.51
	r^2	0.93	0.97	0.97	0.97
RCA-100-DR	Depth at 28 days (mm)	10.37 (1.85)	11.49 (0.85)	11.62 (0.81)	20.49 (1.66)
	Carbonation rate (mm/year$^{1/2}$)	1.93	2.15	2.29	3.72
	r^2	0.99	0.98	0.97	0.98
RCA-100-SBR	Depth at 28 days (mm)	6.24 (0.93)	6.76 (0.81)	8.90 (0.87)	13.87 (2.16)
	Carbonation rate (mm/year$^{1/2}$)	1.14	1.32	1.77	2.69
	r^2	0.96	0.97	0.95	0.97

For room temperature, the carbonation depth at 28 days of RCA-100-DR was 1.6 times greater than reference mix. This is coherent with previous works [48], which verified that relative carbonation depth increases with RCA due to higher porosity and absorption of RCA aggregates. Silva et al. [48], with a statistical approach in a literature compilation, showed that RCA usually presents

a carbonation depth 2.5 times higher than ordinary concrete. The adjustment of cement paste in the SBR mix improved the carbonation resistance of RAC mixes, and the depth was even slightly lower than concrete with NA. This behaviour is also verified in previous works, which adjusted the w/c ratio to obtain the same target strength [48, 49]. The same behaviour was identified using the accelerated carbonation rate. The evolution was equal for NA and RCA-100-SBR, highlighting that improving cement paste can result in similar carbonation performance.

To compare the effect of temperature in each mix, carbonation rate versus temperature was plotted in Fig. 6.6. Fig. 6.6a presents the evolution of carbonation rate with temperature in absolute values. The behaviour seen in room temperature keeps similar for all tested temperatures. The direct addition of RCA increased the carbonation rate, while the SBR mix showed similar performance to concrete made with NA. After exposure to 600 °C, the rate in RCA-100-DR was almost 1.5 more elevated than in concrete made with NA. The difference in carbonation depth after 28 days was more than 8 cm higher, as seen in Table 6.4. The same table and figure show that concrete made with NA and RCA-100-SBR presented minor differences in rate and carbonation depth. This indicates that the paste enhancement for SBR was also helpful for carbonation performance.

For absolute values, the evolution of carbonation rate with temperature is quite similar in all studied mixes. From 23 °C to 400 °C, the evolution rate was relatively low, especially for RCA-100-DR. In this case, the carbonation rate varied from only 0.36 mm/year$^{1/2}$. At this temperature, the changes are related to the increase of porosity and permeability due to water loss and first C-S-H dehydration. From 400 °C to 600 °C, the increase in carbonation rate was substantial. At 600 °C, concrete suffers from deterioration due to portlandite dehydration and thermal mismatch. When analyzing the relative values (Fig. 6.6b), a similar behaviour to the other indicators is observed. Concrete with NA and RCA-100-SBR presents higher evolution. And, even though the increase from 400 °C to 600 °C is relevant, the growth in RCA-100-DR is lower than the other two.

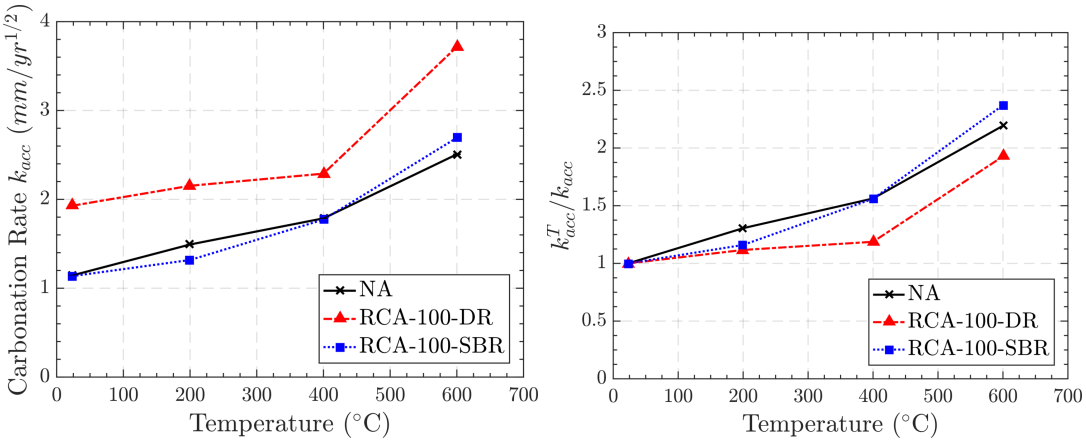

(a) absolute values (b) relative values

Figure 6.6: Evolution of carbonation rate with temperature

6.4 Towards a performance-based approach

Different analyses were proposed to evaluate the durability performance of concrete made with RCA. They were divided into two sections concerning temperature exposure: at room temperature and after elevated temperatures. In the first case, the objective was to evaluate the effect of replacement rate on concrete durability. The second case refers to the effect of temperature on concrete durability.

Two different performance-based approaches were proposed at room temperature to evaluate the durability of concrete made with RCA. The first is the equivalent performance concept, based on NF EN 206-1/CN:2014 [16] prescription. In this method, the new concrete should have an equal or better performance than the concrete designed according to the durability requirements from NF EN 206-1/CN:2014 [16]. In this project, both RCA-100-DR and RCA-100-SBR are compared to the concrete made with NA. An index of equivalent performance (EP^R) was calculated for each property. These indexes are the ratio between the property of concrete made with NA (X_{NA}) and concrete made with RCA (X_{RCA}). If the ratio is lower than 1, the concrete has deteriorated. If it is higher or equal to 1, concrete has improved or kept the performance of the reference. For permeability and chloride diffusion, the index calculated using the log values, and the final value was inversed to compatibilize with the proposed scale. Eqs. 6.8 and 6.9 shows the index calculation. All values were plotted in a spider-plot type of graph (Fig. 6.7a). Similar approaches were made in previous studies [50–53].

$$EP^R{}_i = \frac{X_{NA}}{X_{RCA}} \tag{6.8}$$

$$EP^R{}_i = \frac{1}{\frac{\log X_{RCA}}{\log X_{NA}}} \tag{6.9}$$

In these equations, $EP^R{}_i$ is the equivalent performance index for replacement rate. The index i varies from 1 to 5, where 1 is water porosity, 2 is intrinsic permeability, 3 is chloride diffusion coefficient, 4 is accelerated carbonation rate, and 5 is capillary water absorption at 72-hours.

The second approach for room temperature evaluation was the analysis based on the potential durability established by the AFGC guide for durability [54]. Selected (water porosity, permeability and chloride) were used to classify the concrete according to five classes: very low (VL), low (L), medium (M), high (H) and very high (VH). Table 6.5 presents the limits associated with each one of the evaluated properties. To a comparative analysis, the values were normalized from 0 to 1, using Eq. 6.10. The 0 was defined as the very low limit (X_{vl}). It was chosen a value lower than the threshold presented in the table (18 for water porosity; 30 for chloride and 3000 for permeability). The 1 was the very high limit (X_{vh}) indicated in the table (in the case of water porosity, 9 was the adopted as threshold value). It is noteworthy that gas permeability and chloride diffusion were calculated also using base-ten logarithms. Using Eq. 6.10 and

Table 6.5, the scale presented in Fig. 6.7b was proposed. In this figure, all the potential durability zones are indicated. Eq. 6.10 was also used to calculate the potential durability indicator for each of the studied mixes.

$$DI^R{}_i = \frac{X_i - X_{vl}}{X_{vh} - X_{vl}} \tag{6.10}$$

In these equations, $DI^R{}_i$ is the potential durability indicators for each mix. The index i varies from 1 to 3, where 1 is water porosity, 2 is gas permeability at $P_i = 0.2\,\text{MPa}$, and 3 is chloride diffusion coefficient. The X_i correspond to the property to be normalized, X_{vl} is very low limit and X_{vh} is very high limit.

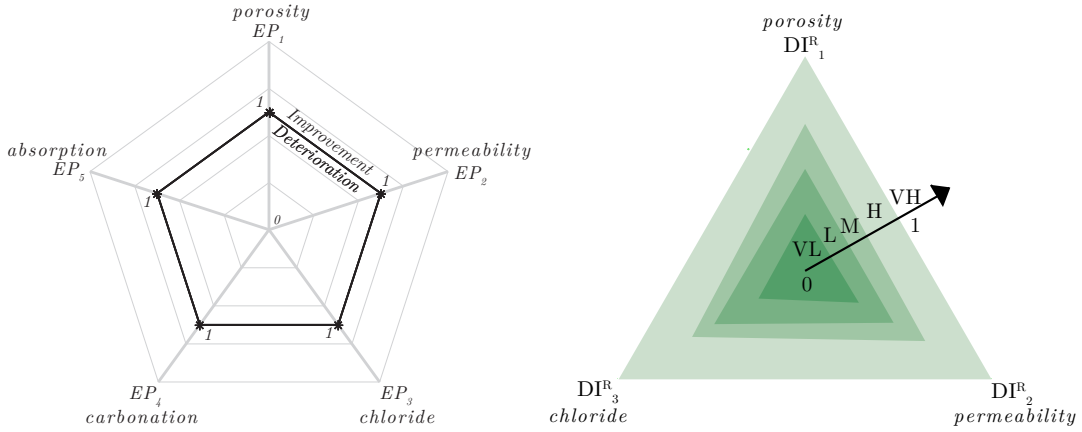

(a) Equivalent Performance (b) Potential Durability

Figure 6.7: Scale used in performance approaches

Table 6.5: Durability indicators (adapted from [54])

Property	Classes and limit values				
	Very Low	Low	Medium	High	Very High
Water Porosity η (%)	>16	14 to 16	12 to 14	9 to 12	9 to 6
Effective chloride coefficient D_{eff} ($10^{-12}m^2/s$)	>8	2 to 8	1 to 2	0.1 to 1	<0.1
Gas permeability at ($P_i = 0.2\,\text{MPa}$) k_{gaz} ($10^{-18}m^2$)	>1000	300 to 10000	100 to 300	10 to 100	<10
Compressive strength class (indicative)	-	C25 to C40	C30 to C60	C55 to C80	>C80

For concrete after exposure to elevated temperatures, similar approaches were applied, but they were adapted considering the objective of the analysis. For the first approach, an equivalent concept was also proposed. But this time, the equivalence of each heated concrete was compared with its respective value at room temperature. In a post-fire scenario, the interest is in how much from the initial durability remains. Hence, an index of equivalent performance at high temperature (EP^T) was calculated for each property. In this case, these indexes are the ratio between the property of concrete at room temperature and concrete at high temperature. The same principle of deterioration and improvement is

applied. Since the chloride diffusion coefficient was determined only up to 200 °C, the analysis was done only in the four remaining parameters.

The potential durability approach following AFGC criteria was also applied for high-temperature evaluation. The method, including limits and normalization procedure, was the same as that used at room temperature. Since the chloride diffusion coefficient was determined only up to 200 °C, the analysis was done this time considering room temperature and 200 °C.

6.4.1 Room temperature

Fig. 6.8 presents the equivalent performance for the three studied mixes. When analyzing the DR mix, it can be seen that the substitution of NA with RCA worsened all durability indicators. An improvement in the durability was achieved when optimizing the w/c and the cement paste content to obtain the same strength as reference concrete. Even though the water porosity remains high, due to the high porosity of the RCA, the RCA-100-SBR showed reduced deterioration in some indicators. This is especially highlighted for the accelerated carbonation rate. These results also highlight that water accessible porosity may not be the most appropriate indicator to evaluate durability.

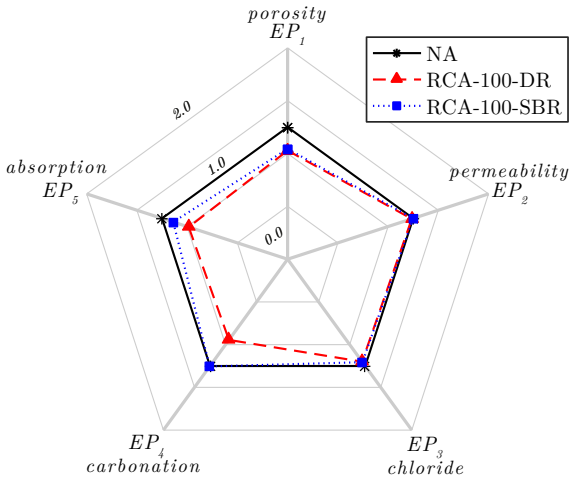

Figure 6.8: Equivalent performance for mixes at room temperature

Fig. 6.9 presents the potential durability evaluation for the three studied mixes. Concrete with NA had different potential according to the different parameters. Water porosity and chloride indicates that the mix has high (H) durability, while permeability indicates that concrete has medium (M) durability. As the case of the equivalent comparison, the DR mix worsened all the performances. Water porosity and permeability were classified as very low (VL), and chloride showed medium potential durability. For the SBR mix, even though it has improved from the DR mix, this mix did not recover the same potential as the concrete made with NA. Gas permeability and chloride diffusion presented the same potential (medium). Still, water porosity was classified as low (L). It's

noteworthy that, in this document, carbonation was not defined as a parameter for potential durability indicator. Hence, if only this approach were used, the improvement in carbonation resistance would not be verified. This highlights the necessity of precaution when evaluating durability through a similar approach.

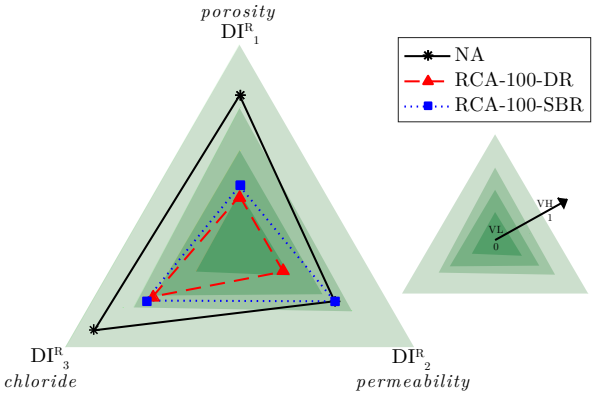

Figure 6.9: Potential durability for mixes at room temperature

6.4.2 Elevated temperatures exposure

Fig. 6.10 presents the equivalent performance analysis for exposure to elevated temperatures. A different mix is evaluated in each plot, and a curve for each temperature level is presented. For all mixes, it is seen that up to 200 °C, the performance is close to the room temperature. This shows that the concrete can retain some initial durability if heated only up to this temperature level. After 400 °C, the deterioration gets high, and the increase is more prominent in concrete with NA and RCA-100-SBR. This indicates that these mixes undergo higher damage up to this temperature, mainly associated with cracks due to water loss and paste hydrates deterioration. The lower evolution of RCA-100-DR can also be associated with the fact that the initial durability of this concrete is lower. Hence, the transformations at this level do not deteriorate indicators as much as the other mixes.

Fig. 6.11 presents the potential durability evaluation for the mixes after exposure to 200 °C. A similar trend observed in equivalent durability is also verified here: the RCA-100-DR degrades less than the other mixes. However, concrete with NA presents a better performance, even after exposure to high temperatures. The porosity keeps in the high zone potential, but permeability and chloride degrade one class: permeability enter to low durability zone, and chloride enters the medium durability zone. This behaviour reinforces that this concrete can retain some of its durability properties and may still be functional after exposure to this level. For RCA-100-DR, the values kept almost the same after exposure to 200 °C. However, it's noteworthy that the durability of this mix is already low at room temperature. Lastly, for RCA-100-SBR, porosity and chloride kept similar, with both staying in the same potential after exposure to 200 °C (low and medium, respectively). However, the permeability moved

from medium to low potential, indicating a reduction in the performance of this concrete. In general, this methodology seems a good approach for evaluating post-fire durability.

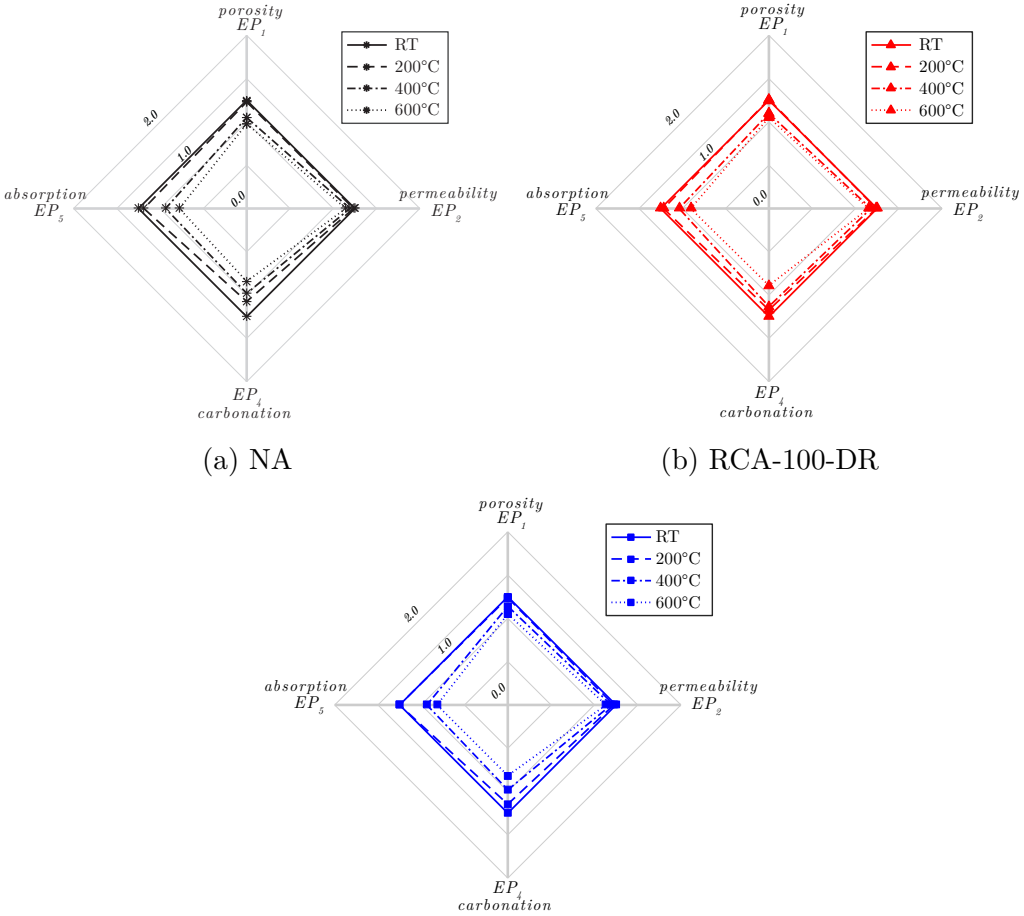

(a) NA

(b) RCA-100-DR

(c) RCA-100-SBR

Figure 6.10: Equivalent performance for mixes at after exposure to high temperature

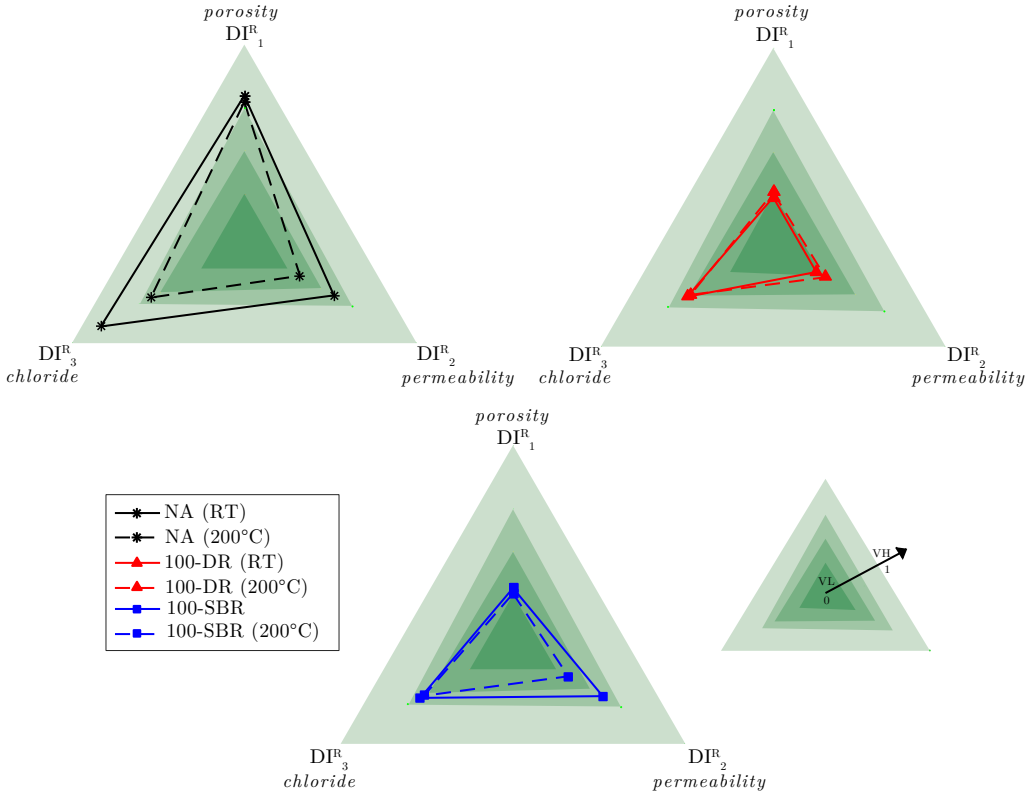

Figure 6.11: Potential durability for mixes after exposure to elevated temperatures

6.5 Conclusions

This paper presented an experimental investigation into the post-heating durability of concrete made with recycled concrete aggregates. Based on the results, the following conclusions have been drawn:

- The direct addition of RCA in DR mixes reduced the durability of ordinary strength concrete. The reduction was prominent on all durability indicators. The reduction of w/c and increase in cement paste in SBR mix contributed to the recovery of some durability parameters. Even though water porosity kept high for SBR mix, permeability and accelerated carbonation showed the same performance as reference concrete. The chloride diffusion coefficient and capillary water absorption were better than DR but not at the same level as concrete with NA. This behaviour highlights that the same compressive strength is not enough to guarantee the exact same durability, and these parameters should be evaluated.

- Exposure to high temperatures deteriorated the durability of all studied mixes, and the extent is greater as temperature increases. In general, the relative increase is lower for the DR mix and similar in the case of the NA and SBR mix. Capillary water absorption and water porosity evolved

similarly, with almost constant values up to 200 °C, followed by a significant increase at 400 °C and 600 °C. Accelerate carbonation rate increased in a low rate up to 400 °C, then a remarkable increase was observed after 600 °C. Permeability showed a different behaviour depending on the temperature level - with slight variations between all mixes. For chloride, NA presented lower values than RCA mixes, but the increase was higher.

- The proposed performance-based approaches showed potential to evaluate durability indicators. The equivalent performance concept showed potential, but some indicators (e.g. water porosity) should be considered with precaution. The potential durability concept was an excellent method to evaluate the durability, including the high-temperature scenario. However, this method should be updated and extended for different indicators (accelerated carbonation, for example).

- This paper shows that the addition of RCA reduces the ambient and post-fire durability of concrete made with RCA. However, with proper mix optimization, the durability can be recovered to some extent.

References

[1] J. de Brito and N. Saikia. *Recycled Aggregate in Concrete*. Springer-Verlag London, 2013, p. 448. DOI: 10.1007/978-1-4471-4540-0.

[2] C. Shi, Y. Li, J. Zhang, W. Li, L. Chong, and Z. Xie. "Performance enhancement of recycled concrete aggregate–a review". In: *Journal of cleaner production* 112 (2016), pp. 466–472.

[3] M. Nedeljković, J. Visser, B. Šavija, S. Valcke, and E. Schlangen. "Use of fine recycled concrete aggregates in concrete: A critical review". In: *Journal of Building Engineering* 38 (2021), p. 102196.

[4] H.-b. Le and Q.-b. Bui. "Recycled aggregate concretes – A state-of-the-art from the microstructure to the structural performance". In: *Construction and Building Materials* 257 (2020), p. 119522. DOI: 10.1016/j.conbuildmat.2020.119522.

[5] F. de Larrard and H. Colina. "Conclusion". In: *Concrete Recycling: Research and Practice*. Ed. by F. de Larrad and H. Colina. CRC Press, 2019, pp. 544–545.

[6] M. Behera, S. K. Bhattacharyya, A. K. Minocha, R. Deoliya, and S. Maiti. "Recycled aggregate from C&D waste & its use in concrete - A breakthrough towards sustainability in construction sector: A review". In: *Construction and Building Materials* 68 (2014), pp. 501–516. DOI: 10.1016/j.conbuildmat.2014.07.003.

[7] R. Wang, N. Yu, and Y. Li. "Methods for improving the microstructure of recycled concrete aggregate : A review". In: *Construction and Building Materials* 242 (2020), p. 118164. DOI: 10.1016/j.conbuildmat.2020.118164.

[8] H. Guo, C. Shi, X. Guan, J. Zhu, Y. Ding, T. C. Ling, et al. "Durability of recycled aggregate concrete – A review". In: *Cement and Concrete Composites* 89 (2018), pp. 251–259. DOI: 10.1016/j.cemconcomp.2018.03.008.

[9] B. Fernandes, H. Carré, J.-C. Mindeguia, C. Perlot, and C. La Borderie. "Effect of elevated temperatures on concrete made with recycled concrete aggregates-An overview". In: *Journal of Building Engineering* (2021), p. 103235. DOI: 10.1016/j.jobe.2021.103235.

[10] S. C. Kou, C. S. Poon, and M. Etxeberria. "Residue strength, water absorption and pore size distributions of recycled aggregate concrete after exposure to elevated temperatures". In: *Cement and concrete composites* 53 (2014), pp. 73–82.

[11] D. Xuan, B. Zhan, and C. S. Poon. "Thermal and residual mechanical profile of recycled aggregate concrete prepared with carbonated concrete aggregates after exposure to elevated temperatures". In: *Fire and Materials* 42.1 (2017), pp. 134–142.

[12] C. Laneyrie, A.-L. Beaucour, M. F. Green, R. L. Hebert, B. Ledesert, and A. Noumowe. "Influence of recycled coarse aggregates on normal and high performance concrete subjected to elevated temperatures". In: *Construction and Building Materials* 111 (2016), pp. 368–378.

[13] Z. Ma, G. Ba, and Z. Duan. "Effects of High Temperature and Cooling Pattern on the Chloride Permeability of Concrete". In: *Advances in Civil Engineering* 2019 (2019).

[14] Z. Ma, M. Liu, Q. Tang, C. Liang, and Z. Duan. "Chloride permeability of recycled aggregate concrete under the coupling effect of freezing-thawing, elevated temperature or mechanical damage". In: *Construction and Building Materials* 237 (2020), p. 117648. DOI: 10.1016/j.conbuildmat.2019.117648.

[15] A. Valente Monteiro and M. Vieira. "Effect of elevated temperatures on the residual durability-related performance of concrete". In: *Materials and Structures/Materiaux et Constructions* 54.6 (2021), pp. 13–15. DOI: 10.1617/s11527-021-01824-5.

[16] *Béton — Spécification, performance, production et conformité — Complément national à la norme NF EN*

206. Comité Européen de Normalisation. Brussels, 2014.

[17] F. de Larrard and T. Sedran. *BetonLab*. Version BetonLabFree. 2021.

[18] B. Fernandes, H. Carré, J.-C. Mindeguia, C. Perlot, and C. La Borderie. "Effect of elevated temperatures on concrete made with recycled concrete aggregates-An overview (Under Review)". In: *Construction and Building Materials* (2022), p. 128124. DOI: 10.1016/j.conbuildmat.2022.128124.

[19] B. Fernandes, H. Carré, J.-C. Mindeguia, C. Perlot, and C. La Borderie. "Residual thermomechanical properties of concrete made with recycled concrete aggregates after exposure to high temperatures (Under Review)". In: *European Journal of Civil Engineering* (2022).

[20] *Testing fresh concrete - Part 2 : slump test*. Comité Européen de Normalisation. Brussels, 2019.

[21] *Testing hardened concrete - Part 3 : compressive strength of test specimens*. Comité Européen de Normalisation. Brussels, 2019.

[22] *Testing hardened concrete - Part 6 : tensile splitting strength of test specimens*. Comité Européen de Normalisation. Brussels, 2012.

[23] *Testing hardened concrete - Part 13 : determination of secant modulus of elasticity in compression*. Comité Européen de Normalisation. Brussels, 2021.

[24] *Durabilité des Betons - Méthodes recommandés pour la mesure des granulats associées a la durabilité*. Association Française de recherches et d'essais sur les matériaux et constructions. Toulouse, 1997.

[25] J. J. Kollek. "The determination of the permeability of concrete to oxygen by the Cembureau method-a recommendation". In: *Materials and Structures* 22.3 (1989), pp. 225–230. DOI: 10.1007/BF02472192.

[26] R. T. 116-PCD. "RILEM TC 116-PCD: Permeability of Concrete as a Criterion of its Durability". In: *Materials and Structures* 32 (1999), pp. 174–179.

[27] L. Klinkenberg. "The permeability of porous media to liquids and gases". In: *Drilling and production practice*. American Petroleum Institute. 1941, pp. 200–214.

[28] M. J. Miah, H. Kallel, H. Carré, P. Pimienta, and C. La Borderie. "The effect of compressive loading on the residual gas permeability of concrete". In: *Construction and Building Materials* 217 (2019), pp. 12–19.

[29] H. Carré, C. Perlot, A. Daoud, M. J. Miah, and B. Aidi. "Durability of ordinary concrete after heating at high temperature". In: *Key Engineering Materials*. Vol. 711. Trans Tech Publ. 2016, pp. 428–435.

[30] O. Truc, J. Ollivier, and M. Carcassès. "A new way for determining the chloride diffusion coefficient in concrete from steady state migration test". In: *Cement and Concrete Research* 30.2 (2000), pp. 217–226.

[31] "Influence of cement type on transport properties and chemical degradation: Application to nuclear waste storage". In: *Materials and Structures/Materiaux et Constructions* 39.5 (2006), pp. 511–523.

[32] E. Roziere, A. Loukili, and F. Cussigh. "A performance based approach for durability of concrete exposed to carbonation". In: *Construction and Building Materials* 23.1 (2009), pp. 190–199.

[33] *Essai pour béton durci - Essai de carbonatation accélérée - Mesure de l'épaisseur de béton carbonaté*. Association Française de Normalization. 2008.

[34] H. Beushausen, M. Alexander, M. Basheer, V. Baroghel-Bouny, R. d'Andréa, A. Gonçalves, et al. "Principles of the Performance-Based Approach for Concrete Durability". In: *Performance-Based Specification and Control of Concrete Durability: Specifications State-of-the-Art Report RILEM TC 230-PSC*. Ed. by H. Beushausen and L. Luco. Springer, 2016, pp. 107–131.

[35] M. Auroy, S. Poyet, P. Le Bescop, J. M. Torrenti, T. Charpentier, M. Moskura, et al. "Comparison between natural and accelerated carbonation (3% CO2): Impact on mineralogy, microstructure, water retention and cracking". In: *Cement and Concrete Research* 109.February (2018), pp. 64–80. DOI: 10.1016/j.cemconres.2018.04.012.

[36] M. Castellote, L. Fernandez, C. Andrade, and C. Alonso. "Chemical changes and phase analysis of OPC pastes carbonated at different CO2 concentrations". In: *Materials and Structures/Materiaux et Constructions* 42.4 (2009), pp. 515–525. DOI: 10.1617/s11527-008-9399-1.

[37] K. Sisomphon and L. Franke. "Carbonation rates of concretes containing high volume of pozzolanic materials". In: *Cement and Concrete Research* 37.12 (2007), pp. 1647–1653. DOI: 10.1016/j.cemconres.2007.08.014.

[38] P. Rougeau, L. Schmitt, J. Mai-Nhu, A. Djerbi, M. Sailio, E. Ghorbel, et al. "Durability-Related Properties". In: *Concrete Recycling: Research and Practice*. Ed. by F. de Larrad and H. Colina. CRC Press, 2019, pp. 214–250.

[39] J.-C. Mindeguia, P. Pimienta, H. Carré, and C. La Borderie. "On the influence of aggregate nature on concrete behaviour at high temperature". In: *European Journal of Environmental and Civil Engineering* 16.2 (2012), pp. 236–253. DOI: 10.1080/19648189.2012.667682.

[40] P. Pimienta, M. C. Alonso, R. Jansson McNamee, and J.-C. Mindeguia. "Behaviour of high-performance concrete at high temperatures: some highlights". In: *RILEM Technical Letters* 2.2017 (2017), p. 45. DOI: 10.21809/rilemtechlett.2017.53.

[41] W. H. Kwan, M. Ramli, K. J. Kam, and M. Z. Sulieman. "Influence of the amount of recycled coarse aggregate in concrete design and durability properties". In: *Construction and Building Materials* 26.1 (2012), pp. 565–573. DOI: 10.1016/j.conbuildmat.2011.06.059.

[42] A. Gonçalves, A. Esteves, and M. Vieira. "Influence of recycled concrete aggregates on concrete durability". In: *International RILEM Conference on the Use of Recycled Materials in Buildings and Structures*. RILEM Publications SARL. 2004, pp. 554–562.

[43] S. C. Kou and C. S. Poon. "Enhancing the durability properties of concrete prepared with coarse recycled aggregate". In: *Construction and Building Materials* 35 (2012), pp. 69–76. DOI: 10.1016/j.conbuildmat.2012.02.032.

[44] F. Ghasemzadeh and M. Pour-Ghaz. "Effect of Damage on Moisture Transport in Concrete". In: *Journal of Materials in Civil Engineering* 27.9 (2015), p. 04014242. DOI: 10.1061/(asce)mt.1943-5533.0001211.

[45] L. Wang and Q. Zhang. "Investigation on water absorption in concrete after subjected to compressive fatigue loading". In: *Construction and Building Materials* 299 (2021), p. 123897. DOI: 10.1016/j.conbuildmat.2021.123897.

[46] L. Evangelista and J. de Brito. "Durability performance of concrete made with fine recycled concrete aggregates". In: *Cement and Concrete Composites* 32.1 (2010), pp. 9–14. DOI: 10.1016/j.cemconcomp.2009.09.005.

[47] M. Gomes and J. De Brito. "Structural concrete with incorporation of coarse recycled concrete and ceramic aggregates: Durability performance". In: *Materials and Structures/Materiaux et Constructions* 42.5 (2009), pp. 663–675. DOI: 10.1617/s11527-008-9411-9.

[48] R. V. Silva, R. Neves, J. De Brito, and R. K. Dhir. "Carbonation behaviour of recycled aggregate concrete". In: *Cement and Concrete Composites* 62 (2015), pp. 22–32. DOI: 10.1016/j.cemconcomp.2015.04.017.

[49] R. Dhir, M. Limbachiya, and T. Leelawat. "Suitability of recycled concrete aggregate for use in BS 5328 designated mixes". In: *Proceedings of the Institution of Civil Engineers-Structures and buildings* 134.3 (1999), pp. 257–274.

[50] N. Kaid, M. Cyr, S. Julien, and H. Khelafi. "Durability of concrete containing a natural pozzolan as defined by a performance-based approach". In: *Construction and Building Materials* 23.12 (2009), pp. 3457–3467. DOI: 10.1016/j.conbuildmat.2009.08.002.

[51] R. San Nicolas, M. Cyr, and G. Escadeillas. "Performance-based approach to durability of concrete containing flash-calcined metakaolin as cement replacement". In: *Construction and Building Materials* 55 (2014), pp. 313–322. DOI: 10.1016/j.conbuildmat.2014.01.063.

[52] R. Idir, M. Cyr, and A. Pavoine. "Investigations on the durability of alkali-activated recycled glass". In: *Construction and Building Materials* 236 (2020), p. 117477. DOI: 10.1016/j.conbuildmat.2019.117477.

[53] R. Bucher, M. Cyr, and G. Escadeillas. "Performance-based evaluation of flash-metakaolin as cement replacement in marine structures – Case of chloride migration and corrosion". In: *Construction and Building Materials* 267 (2021). DOI: 10.1016/j.conbuildmat.2020.120926.

[54] *Conception des bétons pour une durée de vie donnée des ouvrages – Maîtrise de la durabilité vis-à-vis de la corrosion des armatures et de l'alcali-réaction.* Association Française de Génie Civil. Paris, 2004.

Chapter 07

Conclusion and Perspectives

The present chapter summarizes the main contributions of this thesis and gives perspectives for future works.

7.1 Conclusion

This research aimed to study the spalling risk and the high temperature behaviour of concrete made with recycled concrete aggregates (RCA). An extensive experimental program was performed on several mixes with and without coarse RCA. Based on the results, conclusions were drawn and divided into four sections: design of concrete made with RCA, thermomechanical properties of concrete made with RCA, fire spalling behaviour of concrete made with RCA, and post-heating durability of concrete made with RCA.

7.1.1 Design of concrete made with RCA

The study on mix design and the properties of concrete made with RCA at room temperature was presented in Chapter 03. Based on the results, the following conclusions have been drawn:

- The direct substitution of coarse NA by RCA reduces all mechanical properties. For mixes with 100 % of RCA, compressive strength reduced around 23 %, elastic modulus around 17 % and splitting tensile strength around 10 % (in relation to concrete made with NA).
- The application of a strength-based replacement approach led to a recovery in concrete performance. In this project, water/cement and paste volume were adjusted to achieve the same compressive strength (at 28 days) as concrete made with NA. The strategy has proven successful for the two studied mixes (40 % and 100 %), with the compressive strength keeping the same level as the reference. The tensile strength also kept similar values with SBR, but this is not translated to the elastic modulus. The SBR mix presented a reduction of 11 % in the Elastic Modulus.

7.1.2 Residual thermomechanical properties of concrete made with RCA

The thermomechanical properties of concrete made with RCA were studied in Chapter 04 (Paper II). Residual thermal, mechanical and microstructural properties were evaluated. Based on the results, the following conclusions have been drawn:

- Two different thermal properties were evaluated: thermal conductivity and specific heat. The addition of RCA directly increased conductivity at the room temperature (up to 20 % of the reference mix). Still, after exposure to elevated temperatures, this difference diminishes (up to 4 % at 400°C). Specific heat had peculiar behaviour but indicated the thermal damage in concrete after exposure to elevated temperatures. In addition, temperature diffusion inside concrete was measured and concrete with RCA presented lower thermal gradients than reference concrete.

- Mechanical properties had significant degradations (for both NA and RAC), but the reductions were within the traditional range observed in concrete previous works.

- For the evolution of relative compressive strength with temperature, concrete made with 100 % of RCA showed less relative deterioration. For example, after 400 °C, RCA-100-DR and RCA-100-SBR decreased 13 % and 10 %, respectively, while NA reduced 15 %. This better behaviour is possibly linked to the interfaces between RCA and cement paste. Elastic modulus showed similar behaviour independently of the RCA content, with an almost linear decrease with temperature evolution. After 400 °C, around 50 % of initial modulus was lost. Tensile strength showed a particular increase in strength when exposed to 400 °C. This behaviour is possibly associated with the concretes' drying process. The phenomenon was registered in concrete made with RCA, which had higher water content.

- Microstructural observations showed that the first cracks started perpendicular to the interface new paste - old paste (RCA). This indicates a better match between cement paste and aggregates in concrete made with RCA when compared to concrete made with NA. Concrete made with RCA seems to present a higher crack density, but crack width is higher for concrete made with NA.

7.1.3 Fire spalling of concrete made with RCA

The spalling of concrete made with RCA was investigated in Chapters 05 and 06 (Papers III and IV). A fire spalling screening test was used to evaluate the spalling risk of concrete made with coarse RCA. Samples with different replacement rates (0 % to 100 %) and the replacement method (DR versus SBR) were exposed to standard fire and load. Based on the results, the following conclusions have been drawn:

- The digital photogrammetry was successfully used for the postfire assessment of spalled concrete. The spalling properties (depth and volume) obtained with this method can be used as indicators of the spalling risk of different concrete mixes.

- In this work, concrete made with RCA showed more spalling damage than concrete made with NA. The spalling indicators (volume and maximum depth) exhibited a peculiar behaviour when the quantity of RCA increased. For example, spalled volume went from 3 % to 10 %, when replacement rate increases from 0 % to 40 % of RCA. For further additions of RCA (100 % of RCA), the spalled volume remained almost constant. The replacement method (DR or SBR) did not substantially change the general behaviour.

- The presence of RCA affected the water content of concrete made with RCA, which was one of the triggers of spalling. In general, mixes with high water content showed a higher risk of spalling.

- The influence was further studied by evaluating the spalling risk of different water content profiles. The drying of the samples reduced the spalling risk of concrete. After 3 days of drying at 80 °C, no spalling was registered for concrete made with NA, while after 2 days of drying, no spalling was registered for concrete made with RCA.

- Spalled samples showed a water content higher than 1.5 % for NA and higher than 2 % for RCA. This possible threshold is closer to previous works but lower than what is currently specified in Eurocode 2. At the same time, when evaluating the mean water content through all the half depth (5 cm), the critical value is close to 2.6 % for NA and 4.4 % to RCA. These two values are closer to the 3 % what is currently specified in Eurocode 2.

7.1.4 Post-heating durability of concrete made with RCA

The post-heating properties of concrete made with RCA was studied in Chapter 07 (Paper V). Residual water porosity, capillary water absorption, permeability, chloride diffusion and carbonation were evaluated. In addition, a performance-based approach was performed for post-heating durability. Based on the results, the following conclusions have been drawn:

- According to all durability indicators, the addition of RCA reduced the durability of the mixes. The improvement in the mix (SBR) recovered some of the performance, but it was not enough to reach the same level as concrete made with NA. Exposure to high temperatures deteriorated the durability of all studied mixes, and the extent is greater as temperature increases. Absolute values were lower for RCA-100-DR, but the relative values showed a smaller reduction than the others.

- In relation to transport properties, water porosity showed almost constant values up to 200 °C, followed by a significant increase at 400 °C and 600 °C. For the latter (600 °C) concrete made with NA showed an increase of 57 % of its value at room temperature, while DR and SBR mixes showed similar damage (an increase around 36 %). Capillary water absorption showed similar evolution as water porosity, but the two mixes made with RCA showed distinct behaviour. After 600°C, the 72 hours capillary absorption of DR was 1.9 times higher than the room temperature, while SBR was 2.4 times higher. For NA, the increase was around 2.7 times. Permeability showed a peculiar behaviour depending on the temperature level - with slight variations between all mixes.

- In relation to the penetration of aggressive agents, accelerate carbonation rate increased in a low rate up to 400 °C, then a remarkable increase was observed after exposure to 600 °C. Concrete made with NA and 100 % SBR showed an increase of 2.2 and 2.4 times their values at room temperature. DR mix showed lesser rate, with and increase of 1.9 times the value at room temperature. For chloride, NA presented lower values than RCA

mixes, but the relative increase after exposure to elevated temperatures was higher.

- The performance-based approaches showed potential to evaluate durability of concrete made with RCA - both before and after exposure to elevated temperatures. The potential durability concept was an excellent method to evaluate the durability, including the high-temperature scenario. However, this method should be updated and extended for different indicators (carbonation, for example).

7.1.5 Final remarks

This study provided a comprehensive overview of the behaviour of concrete made with RCA after exposure to elevated temperatures. Even though it was seen that results show that high temperature behaviour of concrete made with RCA has some similarities to the behaviour of concrete made with NA, novel aspects were highlighted.

The comprehensive evaluation of residual thermomechanical properties gave new insights into the study of concrete made with RCA, especially related to the assessment of mixes with 100 % of RCA and equivalent performance as concrete made with NA. Indeed, this study showed that the concrete behaviour can be improved with mix optimisation, even for post-heating thermomechanical properties.

Also, this study did a comprehensive fire spalling screening test on concrete made with RCA. Moreover, it indicates that spalling of concrete made with RCA should not be fully ignored. Even though a critical situation, prone to spalling, was considered, the results showed a risk of spalling, especially if the concrete has high water content. The study also indicated that this water content threshold is close to 1.5 % at the mean spalling depth.

The comprehensive evaluation of the post-heating durability of concrete made with RCA was also an innovative aspect. The behaviour was close to the residual thermomechanical properties: temperature reduced all the studied properties, from porosity to carbonation, but the mix optimisation slightly improved the behaviour of concrete made with RCA. Performance-based approaches were also applied for the first time in heated concrete.

This work gives novel insights and contributions to the behaviour of concrete made with RCA after exposure to elevated temperatures. These contributions will allow for the design and use of concrete structures made with RAC, increasing performance and safety while reducing environmental impact.

7.2 Perspectives

Even though several aspects of the high temperature behaviour of RAC were studied, some topics still need to be addressed. Hence, based on our research results, the following research needs and recommendations are proposed:

- Concerning thermomechanical properties, the measurement of mechanical properties at a hot state (under thermal and mechanical stress) is needed for an accurate estimative of the mechanical and thermal behaviour of concrete made with RCA under fire.
- Deformation properties also should be studied, including the free thermal strain, the elastic strain, and the transient thermal strain. Understanding the total strain of concrete made with RCA during heating is crucial to develop realistic computations.
- A full microstructural investigation of heat-damaged concrete made with RCA is needed. X-ray diffraction (XRD), differential thermal analysis (DTA), and X-ray computed tomography could improve the knowledge regarding the behaviour and the differences between concrete made with RCA and NA at high temperatures.
- Different post-heating durability parameters (e.g., freeze/thaw cycles, water permeability, and resistance to chemical attacks) should be evaluated. The applicability of different durability test methods to the case of heated concretes should also be studied.
- Specific parameters for the performance-based approach should be defined. A unified approach must be proposed. In addition, these parameters should be extended for the case of post-heating/post-fire durability.
- Intermediate-scale screening tests (e.g. slabs and walls) are also a necessity in the field. They represent a more precise scenario in terms of boundary and loading conditions. In the same way, full-scale fire resistance tests are also needed. The loadbearing capacity, integrity and insulation of structural concrete made with RCA should be verified.
- Lastly, numerical models, including the different phases of concrete made with RCA, should be used for thermo-mechanical simulations. This will help to understand and develop realistic simulations.